JSCSEN 88(11)1065–1188(2023)

ISSN 1820-7421(Online)

Journal of the Serbian Chemical Society

Electronic version

VOLUME 88

No 11

BELGRADE 2023

Available on line at

www.shd.org.rs/JSCS/

The full search of JSCS is available through

DOAJ DIRECTORY OF OPEN ACCESS JOURNALS

www.doaj.org

The **Journal of the Serbian Chemical Society** (formerly Glasnik Hemijskog društva Beograd), one volume (12 issues) per year, publishes articles from the fields of chemistry. The **Journal** is financially supported by the **Ministry of Education, Science and Technological Development of the Republic of Serbia.**

Articles published in the **Journal** are indexed in **Clarivate Analytics products: Science Citation Index-Expanded™** – accessed *via* **Web of Science®** and **Journal Citation Reports®**.

Impact Factor announced on 28 June, 2023: **1.000; 5-year Impact Factor**: **1.100**.

Articles appearing in the **Journal** are also abstracted by: **Scopus, Chemical Abstracts Plus (CAplus℠), Directory of Open Access Journals, Referativnii Zhurnal (VINITI), RSC Analytical Abstracts, EuroPub, Pro Quest** and **Asian Digital Library.**

Publisher:	**Serbian Chemical Society**, Karnegijeva 4/III, P. O. Box 36, 1120 Belgrade 35, Serbia tel./fax: +381–11–3370–467, E-mails: **Society** – shd@shd.org.rs; **Journal** – jscs@shd.org.rs Home Pages: **Society** – http://www.shd.org.rs/, **Journal** – http://www.shd.org.rs/JSCS/
Internet Service:	Contents, Abstracts and full papers (from Vol 64, No. 1, 1999) are available in the electronic form at the Web Site of the **Journal** (http://www.shd.org.rs/JSCS/).
Former Editors:	**Nikola A. Pušin** (1930–1947), **Aleksandar M. Leko** (1948–1954), **Panta S. Tutundžić** (1955–1961), **Miloš K. Mladenović** (1962–1964), **Đorđe M. Dimitrijević** (1965–1969), **Aleksandar R. Despić** (1969–1975), **Slobodan V. Ribnikar** (1975–1985), **Dragutin M. Dražić** (1986–2006).
Editor-in-Chief:	BRANISLAV Ž. **NIKOLIĆ**, Serbian Chemical Society (E-mail: jscs-ed@shd.org.rs)
Deputy Editor:	DUŠAN **SLADIĆ**, Faculty of Chemistry, University of Belgrade
Sub editors:	
Organic Chemistry	DEJAN **OPSENICA**, Institute of Chemistry, Technology and Metallurgy, University of Belgrade JÁNOS **CSANÁDI**, Faculty of Science, University of Novi Sad
Biochemistry and Biotechnology	OLGICA **NEDIĆ**, INEP – Institute for the Application of Nuclear Energy, University of Belgrade
Inorganic Chemistry	MILOŠ **ĐURAN**, Serbian Chemical Society
Theoretical Chemistry	IVAN **JURANIĆ**, Serbian Chemical Society
Physical Chemistry	LJILJANA **DAMJANOVIĆ-VASILIĆ**, Faculty of Physical Chemistry, University of Belgrade
Electrochemistry	SNEŽANA **GOJKOVIĆ**, Faculty of Technology and Metallurgy, University of Belgrade
Analytical Chemistry	RADA **BAOŠIĆ**, Faculty of Chemistry, University of Belgrade
Polymers	BRANKO **DUNJIĆ**, Faculty of Technology and Metallurgy, University of Belgrade
Thermodynamics	MIRJANA **KIJEVČANIN**, Faculty of Technology and Metallurgy, University of Belgrade
Chemical Engineering	TATJANA **KALUĐEROVIĆ RADOIČIĆ**, Faculty of Technology and Metallurgy, University of Belgrade
Materials	RADA **PETROVIĆ**, Faculty of Technology and Metallurgy, University of Belgrade
Metallic Materials and Metallurgy	ANA **KOSTOV**, Mining and Metallurgy Institute Bor, University of Belgrade
Environmental and Geochemistry	VESNA **ANTIĆ**, Faculty of Agriculture, University of Belgrade
History of and Education in Chemistry	DRAGICA **TRIVIĆ**, Faculty of Chemistry, University of Belgrade
English Language Editors:	LYNNE **KATSIKAS**, Serbian Chemical Society VLATKA **VAJS**, Serbian Chemical Society JASMINA **NIKOLIĆ**, Faculty of Technology and Metallurgy, University of Belgrade
Technical Editors:	VLADIMIR **PANIĆ**, Institute of Chemistry, Technology and Metallurgy, University of Belgrade, MARIO **ZLATOVIĆ**, Faculty of Chemistry, University of Belgrade
Journal Manager & Web Master:	MARIO **ZLATOVIĆ**, Faculty of Chemistry, University of Belgrade
Office:	VERA **ĆUŠIĆ**, Serbian Chemical Society

Editorial Board

From abroad: **R. Adžić**, Brookhaven National Laboratory (USA); **A. Casini**, University of Groningen (The Netherlands); **G. Cobb**, Baylor University (USA); **D. Douglas**, University of British Columbia (Canada); **G. Inzelt**, Etvos Lorand University (Hungary); **J. Kenny**, University of Perugia (Italy); **Ya. I. Korenman**, Voronezh Academy of Technology (Russian Federation); **M. D. Lechner**, University of Osnabrueck (Germany); **S. Macura**, Mayo Clinic (USA); **M. Spiteller**, INFU, Technical University Dortmund (Germany); **M. Stratakis**, University of Crete (Grecce); **M. Swart**, University de Girona (Cataluna, Spain); **G. Vunjak-Novaković**, Columbia University (USA); **P. Worsfold**, University of Plymouth (UK); **J. Zagal**, Universidad de Santiago de Chile (Chile).

From Serbia: **B. Abramović**, **V. Antić**, **R. Baošić**, **V. Beškoski**, **J. Csanadi**, **Lj. Damjanović-Vasilić**, **A. Dekanski**, **V. Dondur**, **B. Dunjić**, **M. Đuran, S. Gojković**, **I. Gutman**, **B. Jovančićević**, **I. Juranić**, **T. Kaluđerović Radoičić**, **L. Katsikas**, **M. Kijevčanin**, **A. Kostov**, **V. Leovac**, **S. Milonjić**, **V.B. Mišković-Stanković**, **O. Nedić**, **B. Nikolić**, **J. Nikolić**, **D. Opsenica**, **V. Panić**, **M. Petkovska**, **R. Petrović**, **I. Popović**, **B. Radak**, **S. Ražić**, **D. Sladić**, **S. Sovilj**, **S. Šerbanović**, **B. Šolaja**, **Ž. Tešić**, **D. Trivić**, **V. Vajs, M. Zlatović**.

Subscription: The annual subscription rate is **150.00 €** including postage (surface mail) and handling. For Society members from abroad rate is **50.00 €**. For the proforma invoice with the instruction for bank payment contact the Society Office (E-mail: shd@shd.org.rs) or see JSCS Web Site: http://www.shd.org.rs/JSCS/, option Subscription.

Godišnja pretplata: Za članove SHD: **2.500,00 RSD**, za penzionere i studente: **1000,00 RSD**, a za ostale: **3.500,00 RSD**:za organizacije i ustanove: **16.000,00 RSD**. Uplate se vrše na tekući račun Društva: **205-13815-62**, poziv na broj **320**, sa naznakom "pretplata za JSCS".

Nota: Radovi čiji su svi autori članovi SHD prioritetno se publikuju.

Odlukom Odbora za hemiju Republičkog fonda za nauku Srbije, br. 66788/1 od 22.11.1990. godine, koja je kasnije potvrđena odlukom Saveta Fonda, časopis je uvršten u kategoriju međunarodnih časopisa (**M-23**). Takođe, aktom Ministarstva za nauku i tehnologiju Republike Srbije, 413-00-247/2000-01 od 15.06.2000. godine, ovaj časopis je proglašen za publikaciju od posebnog interesa za nauku. **Impact Factor** časopisa objavljen 28. juna 2023. godine je **1,000**, a petogodišnji **Impact Factor 1,100**.

Journal of the Serbian Chemical Society
JSCS-info@shd.org.rs • www.shd.org.rs/JSCS

J. Serb. Chem. Soc. Vol. 88, No. 11 (2023)

CONTENTS*

Published by the Serbian Chemical Society
Karnegijeva 4/III, P.O. Box 36, 11120 Belgrade, Serbia
Printed by the Faculty of Technology and Metallurgy
Karnegijeva 4, P.O. Box 35-03, 11120 Belgrade, Serbia

* For colored figures in this issue please see electronic version at the Journal Home Page: http://www.shd.org.rs/JSCS/

Journal of the Serbian Chemical Society
JSCS-info@shd.org.rs • www.shd.org.rs/JSCS
J. Serb. Chem. Soc. *88* (11) 1065–1087 (2023)
JSCS–5681
Review
Published 10 November 2023

REVIEW

Chemically-assisted DNA transfection methods – An overview

SOFIJA S. BEKIĆ*# and SUZANA S. JOVANOVIĆ-ŠANTA#

University of Novi Sad, Faculty of Sciences, Department of Chemistry, Biochemistry and Environmental Protection, Trg Dositeja Obradovića 3, 21000 Novi Sad, Serbia

(Received 21 December 2022, revised 21 January, accepted 9 April 2023)

Abstract: Non-viral chemical-based methods for *in vitro* cell transfection are commonly used to incorporate foreign gene of interest into mammalian cells due to numerous benefits – high efficiency, low cost and simple methodology. These powerful transfection methods generally do not possess safety risks as virus-based, and cell toxicity is significantly reduced. To obtain transfectants, host cells are usually treated with biocompatible DNA carriers such as calcium phosphate, cationic lipids, DEAE-dextran, polyethylenimine or dendrimers, classifying these methods based on chemical reagents used. All these different approaches are based on the similar principle, namely formation of encapsulated amphiphilic complexes between DNA and various particles, following cell uptake, most likely mediated by endocytosis. Depending on the aim and design of experiment, the choice of appropriate method is made. This review article outlines strategies of the most widely used chemical transfection techniques, pointing out advantages and limitations of different DNA carriers, also findings of researchers as how to optimize and enhance efficiency of gene delivery procedure. With methodology constantly being improved, transfection methods described here find their main, biomedical application in gene therapy, a promising way to introduce functional copy of exogenous gene to genetically defective target cells.

Keywords: calcium phosphate; cationic polymers; gene delivery; lipofection; non-viral transfection.

CONTENTS

* Corresponding author. E-mail: sofija.bekic@dh.uns.ac.rs
# Serbian Chemical Society member.
https://doi.org/10.2298/JSC221222019B

1. INTRODUCTION

A widely used laboratory technique called transfection underlies the introduction of foreign nucleic acids into host cells and the study of gene and protein expression in cellular environment. Chemically-assisted transfection methods catalyze intracellular trafficking of nucleic acids through the use of various compounds and serve as chemical tool that enables advancement in drug discovery research.[1] The basis of this chemical method is interaction between negatively charged nucleic acids and positively charged ions of chemical reagents.[2]

Exogenous DNA must cross different barriers prior to nuclear uptake and gene expression. Unprotected plasmid DNA would be degraded inside the cell by nucleases in a very short period of time, so it has to be encapsulated with appropriate carriers/particles or condensed with high packing density polycationic particles.[3] Avoiding enzymatic degradation depends on the stability of the complex between DNA and transfection agent, as well as the cell type. Upon entering the cell by endocytosis, the endosome matures and vesicle fusion between matured late endosome and lysosome occurs. As a result of increased osmotic pressure and destabilization of lysosomal membrane, endosome escapes in the next step. After bursting, vesiclular content is released into the cytoplasm.[4] Following burst of endolysosome, complexes further enter the nucleus by not fully understood mechanism and plasmid DNA is released into the nucleus, resulting in transcription of gene of interest.[5,6] On the other side, destiny of complexes that did not successfully leave the endolysosome is degradation by lysosomal enzymes.[4]

Expression of the functional eukaryotic protein in bacteria is often a problematic task. Protein expression is significantly improved by using eukaryotic cell cultures due to possibility of post-translational modifications and correct protein folding in this system.[7,8] Introduction of foreign nucleic acids into cultured mammalian cells, enabled by a powerful transfection technique, also known as gene delivery, has revolutionized the study of gene function and expression of specific proteins.[9,10] Furthermore, this technique is promising in the prevention and treatment of genetic disorders and diseases such as cystic fibrosis,[11] hemophilia,[12] dystrophy[13] and cancer,[14] through an innovative approach in biomedicine, namely gene therapy.[15] This up-to-date therapy, where genetically defective target cells are modified by the introduction of an exogenous functional gene, greatly attracts the attention of the scientific community.[11–15] Except repair of genetic damage, with gene therapy treatments it is also possible to treat infectious diseases[16] by inhibiting life cycle stages, as well as malignancies.[14] Although

this type of therapy promises a lot, development of new, effective and safe therapeutics in this field is very slow and demanding.[17]

There are two types of transfection – stable and transient, with the main difference in long-term integration of foreign DNA into the host genome in stable transfection, whereas in transient type transfected gene is not integrated, so expression lasts for only a limited period of time.[18,19] Depending on the purpose and scope of research, choice between creating stable or transient cell lines is made. When required to examine effects of short-term expression of a gene or protein product on a small scale, transient transfection is mainly method of choice as well as in the assays that precede creation of stable cell lines. On the other side, although stable transfection is a complex process, it plays an unavoidable role in revealing mechanism of gene regulation, large scale protein production or pharmacological studies.[20,21] Experimental methods used to create recombinant cell lines can be classified as direct, when the gene of interest is introduced in nucleus directly by microinjection, and indirect, where the transfer of genetic material occurs indirectly through complex formation between DNA and various chemical agents, using viral vectors or by physical force-mediated cell uptake. In addition to this classification, there is another one that classifies transfection methods to biological (use of viral vectors), physical (sonoporation, electroporation, magnetofection, phototransfection) and chemical (use of calcium phosphate, cationic polymers, cationic lipids).[10,19,22]

The main goal of transfection process is to efficiently deliver gene of interest into cells without safety risks. Non-viral carriers are developed as an alternative to viral ones, not only due to their straightforward manipulation, but also due to reduced cell toxicity and absence of immune response or potential mutagenicity.[23] Much effort is put into developing vectors that are not toxic for cells. Motivated by the significance of chemically-assisted transfection methods in biomedicine and importance of availability of summarized information related to their methodology and efficiency improvement, we provide in this paper an overview of currently available and the most commonly used methods for DNA transfection of mammalian cells based on the use of chemical reagents. Short description of the chemically-based transfection methods and their advantages and disadvantages are summarized in the Table I.

2. CALCIUM PHOSPHATE-MEDIATED TRANSFECTION

Among chemical methods, calcium phosphate (CaP) precipitation is one of the most commonly used due to its numerous advantages.[24] The first method developed for mammalian cell transfection was actually CaP based method initially performed in 1973 by Graham and van der Eb for the introduction of adenoviral DNA into mammalian cells.[25] Adenovirus type 5 DNA was successfully adsorbed by human KB cells in monolayer culture.[25] Widespread use of this transfection method in biomedical research was demonstrated through the gener-

TABLE I. Overview of chemically-based transfection methods

Type of transfection	Description	Advantages	Disadvantages
Calcium phosphate--mediated transfection	Widely used method for introducing foreign DNA into cells that includes mixing DNA with calcium chloride and phosphate ions, formation of coprecipitates and cell uptake.	-Use in biomedical research -Simplicity -Cost-effective -Applicability to large number of cell lines -Biocompatibility -Suitable for stable and transient transfection -Safe use	-low efficiency -Sensitive to changes in pH and salt concentration -Low reproducibility -Phosphate-free medium required -Serum-supplemented medium required -Low efficiency in most primary cell lines
Lipofection	This commonly used transfection method is based on the use of cationic lipids to deliver DNA to eukaryotic cells in the form of vesicles called liposomes.	-High efficiency -The most extensively studied types of DNA carriers -Simplicity -Commercially available reagents -High reproducibility -Suitable for stable and transient transfection -Large scale use -Safe use -Induction of anti-inf-lammatory response	-Cytotoxicity -Inactivation in the presence of serum proteins -Expensive
Cationic polymer--mediated transfection	This method uses cationic polymers such as DEAE--dextran, PEI and dendrimers to form complexes with DNA and introduce nucleic acids into cells of interest via electrostatic interactions.	-Simplicity -Cost-effective -Applicability to large number of cell lines -Structural versatility of cationic polymers -Biocompatibility -Large scale use -Efficient cell recovery after transfection	-Low efficiency (for stable transfection) -Limited to short-term transient transfection -Inactivation in the presence of serum proteins -Expensive synthetic procedures -Cytotoxicity

ation of numerous highly productive recombinant cell lines.[26] Benefits of divalent calcium cations, as DNA carriers in the transfection process, are related to their natural presence in many cells in the organism and physiological acceptability.[27] Principle of this method includes mixing DNA with calcium chloride in phosphate buffer and adherence of resulting DNA-CaP coprecipitates on the surface of the cell membrane.[9]

Endocytosis (Fig. 1) and direct penetration through the membrane are most likely the primary mechanisms of CaP–DNA complex cellular entry.[3,28] One of

the potential mechanisms of endocytotic uptake at the intracellular level is described in the work of Neuhaus *et al.*[4] Using specific inhibitors, Olton *et al.* demonstrated that uptake of NanoCaPs–DNA complexes into the cell and subsequent gene expression were mediated by both endocytosis types, clathrin- and caveolae-dependent, whereas the former one was more highlighted prior to this study.[29]

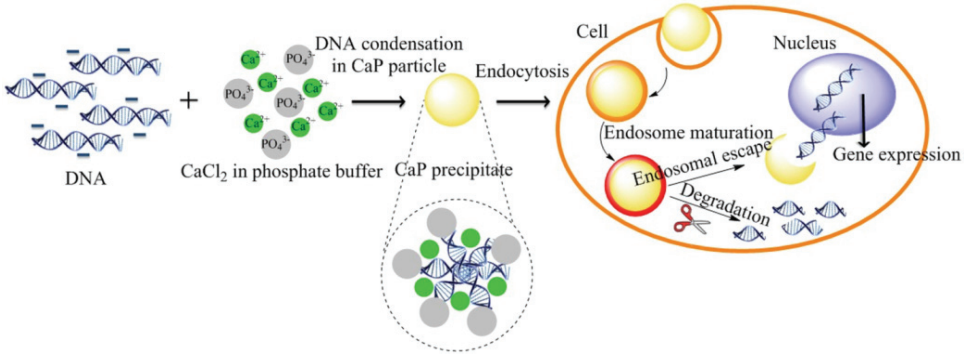

Fig. 1. Proposed endocytotic mechanism of CaP-mediated cell transfection.

This method is characterized by high efficiency, simplicity, low cost, applicability to a large number of cell lines, biocompatibility and it is suitable for both, transient and stable transfection.[27] It is also method of choice when co-transfecting multiple plasmids.[27] Disadvantages include significant changes in transfection efficiency due to small variations in pH and difficulty in reproducing conditions for creating coprecipitates of adequate size and quality.[26] Furthermore, a medium with already high amount of phosphates is undesirable for this type of transfection procedure and this gene delivery method is effective only on highly differentiated cells but not on primary cell lines or animals.[30] Potential difficulties related to transfection of high copy number plasmids by CaP precipitation method are requirements for serum-supplemented medium, often avoided during recombinant protein production in cell lines and low efficiency.[24] The highest efficiency of exogenous DNA uptake was achieved in 80–90 % confluent cells that divide quickly, as well as in those growing in monolayer due to uniform precipitation.[2] Moreover, glycerol and dimethyl sulfoxide (DMSO) are shown to increase efficiency of DNA delivery into some cell lines, however, exposure time to these agents is limited since they may exhibit cytotoxicity.[20,21]

In order to examine optimal conditions and achieve the highest efficiency, the original CaP method has undergone numerous modifications and optimizations since it was published. In the original protocol HEPES buffer (*N*-(2-hydroxyethyl)piperazine-*N*′-(2-ethanesulfonic acid)) was used.[25] However, many variations in buffer composition were subsequently tested and conditions were individually optimized for specific cell lines. Chen and coworkers significantly

improved effectiveness of this method by replacing HEPES with lower pH buffer, BES (*N*,*N*-bis(2-hydroxyethyl)-2-aminoethane sulfonic acid).[31] During cell growth in 3 % CO_2 atmosphere at lower pH (6.95), DNA–CaP precipitates are formed gradually and uniformly on the cell surface, resulting in reduced cytotoxicity and increased transfection efficiency, most likely due to uptake of precipitates by a larger number of cells. Furthermore, transfection efficiency was reported by Chen *et al.* to be enhanced with the use of circular plasmids instead of linear ones, that are easily degraded by nucleases from culture medium.[31]

In the paper of Jordan *et al.* it was stated that formation of CaP–DNA coprecipitates for successful transfection is possible only in a narrow range of conditions and is mostly dependent on the concentration of calcium and phosphate ions and other physicochemical factors – DNA concentration, temperature and reaction time.[32] Optimized procedures were applied to both, transient and stable transfection, and, using them, greater efficacy than in previous protocols was achieved.[32] Study of Ling *et al.* posed the same question.[30] Key parameters responsible for high transfection efficiency of highly differentiated cells were estimated to be primarily characteristics of the buffer, suggesting HBS buffer with pH 7.10 as an optimal, then presence of fetal bovine serum in the medium, vortexing cells with precipitant particles and glycerol shock, whereas replacement of the consumed medium with fresh before transfecting cells had no effect on transfection potency.[30] Sun *et al.* demonstrated that, with optimization of this method, it is possible to transfect cell types such as primary neurons, a popular target in neural cell biology.[33] Moreover, study of Sariyer provides a high-efficiency protocol for transfection of primary neuronal cultures.[34]

Due to many factors that affect efficiency including pH, salt and DNA content, the period between precipitation and transfection, type of the cell line and the researcher's skills, it is very challenging to standardize the CaP transfection technique.[15] These conditions must be optimized for each cell line and laboratory. Transfection has to be performed shortly after precipitation, otherwise CaP will lose activity when it reaches microcrystal size.[27,28] In order to maintain appropriate size of calcium phopshate particles and inhibit their further growth, functionalization with various organic molecules is preferred.[14] To overcome this problem, several strategies for controlled growth of CaP nanoparticles have been developed, including polymer stabilization or lipid coating.[35] DNA may be adsorbed onto CaP nanoparticles with added additives to maintain their size.[27] Obtaining particle size in submicrometer range facilitates penetration of DNA––CaP complexes through the cell membrane. Additionally, it is of great importance to focus on enhancing stability of nanoparticle-DNA complexes, as well as on biodegradable properties of carrier, especially useful in gene therapy. Working in the field of cancer gene therapy, Liu and coworkers developed modified

formulations of CaP nanoparticles as vectors for efficient DNA delivery into cancer cells.[14,36]

3. LIPOFECTION

Cationic lipid mediated transfection (lipofection) is a bright spot in the field of gene therapy and significantly superior in clinical trials compared to other transfection methods.[37] Therapeutic potential of cationic liposomes was tested many times in clinical trials in patients with cystic fibrosis.[38] In the late 1970s Felgner *et al.* first demonstrated procedure for cell transfection using a positively charged cationic lipid, *N*-[1-(2,3-dioleyloxy)propyl]-*N*,*N*,*N*-trimethylammonium chloride (DOTMA), which forms spherical vesicles in aqueous solution with one (unilamellar) or more (multilamerllar) concentric phospholipid bilayers, called liposomes.[39] Cationic lipids are actually the largest and the most extensively studied group of non-viral DNA carriers widely used today. Currently, there is a growing interest in the development of new reagents for successful lipofection and some of them have already found their way to the market. Numerous commercially available cationic lipid transfection reagents from different manufacturers (lipofectamine 3000 or 2000, lipofectin, cellfectin, effectene, FuGENE 6, and DOTAP) vary in price, efficiency and application in different cell types.[40]

Cationic lipids are amphiphilic molecules generally built of three structural domains – positively charged polar heads, hydrophobic domain and linker between them, and even small changes in the structure of any of them can significantly affect transfection efficiency. Cationic head is usually composed of primary, secondary or tertiary amines, but can also contain imidazole and guanidino groups.[40] Byk *et al.* described synthesis of novel cationic lipids as gene delivery agents and conducted structure–activity relationship (SAR) studies to explain differences in transfection potential of geometrically different, asymmetric polyamine groups in cationic heads.[41] Hydrophobic moiety generally represents doubly saturated or unsaturated hydrocarbon chain of varying lengths, which does not have to be symmetrical in structure, whereas linkers are usually esters, ethers, amides or carbamates.[40] A wide range of different linkers, building elements of cationic lipids, is described in detail in review article of Zhi *et al*.[42] Within the liposomes, hydrophobic components of cationic lipids are facing inside of the vesicle and they are protected from aqueous solution by the presence of polar heads on the surface of the molecule. In the central part of the liposome there is a cavity where DNA of interest is packed for delivery and protected from degradation by various enzymes after cell uptake. Review article of Niculescu-Duvaz *et al.* covers SAR studies of cationic lipid domains and helps understanding mechanism of liposome formation and action providing an excellent basis for the rational design of new improved transfection vectors.[40]

Briefly, the mechanism of cationic lipid mediated transfection is divided into several steps: lipoplex formation, membrane binding, entry into the cell, endosomal escape and finally nuclear entry and expression of gene of interest.[40] Electrostatic interactions are formed between liposomes, due to polar heads with overall net positive charge, and negatively charged phosphate groups of transfecting nucleic acids. Penetration of lipid-associated DNA through the hydrophobic cell membrane is facilitated by neutralization of anionic groups and entry into the target cell in the form of lipoplex is probably mediated via endocytosis or fusion (Fig. 2).[38,39] Total charge of lipoplexes is positive enabling them to bind to negatively charged surface of the cell membrane.[39] Following nonspecific electrostatic interaction with the cell membrane lipoplexes are introduced into intracellular compartments dominantly by endocytotic mechanism and this whole process of internalization is mostly influenced by the size of lipoplex. Next phase of lipofection involves endosomal escape which is mediated by flip-flop mechanism due to lipid nature of both, lipoplex and endosomal membrane. In response to the phase behavior of these lipid bilayers, DNA is released after complete neutralization of cationic lipids,[43] which was also investigated and described by Xu and Szoka.[44] Their conclusion was that lipoplexes destabilize endosomal membrane, reducing the intensity of electrostatic interactions between DNA and cationic lipids and releasing DNA to the cytoplasm.[44] There are two theories about the entry of released DNA into the nucleus-by passive transport during cell division, when nuclear membrane is temporarily ruptured, or by active transport through the nuclear pores.[43] Besides endocytosis, dominant pathway for DNA delivery inside the cell – fusion of cationic liposome with the cell membrane is also possible mechanism. Which mechanism of these two will take place depends on the liposomal formulation itself.[38]

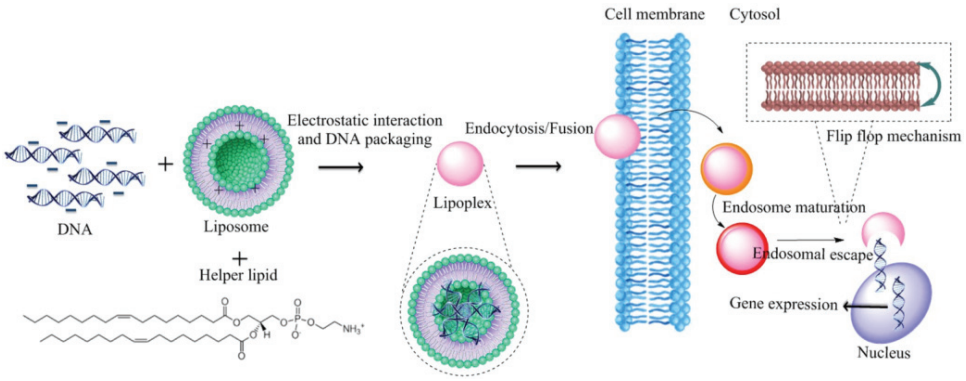

Fig. 2. Proposed mechanism of cationic lipid-mediated transfection.

Key features of this cationic lipid-mediated transfection process are simplicity, high efficiency (especially in adherent cell lines), reproducibility and

applicability to both, transient and stable transfection types, as well as to *in vivo* models, where it has shown lower efficacy indeed.[39,45] Genetic material owes protection from degradation to stability and structural properties of liposomes, but in order to avoid possible cell toxicity, it is necessary to find balance between optimal conditions, crucial for transfection efficiency and potential toxic effect on cells.[46] As expected, when considering the principle of this method, one of the essential factors for successful lipofection is optimal ratio between liposomal and DNA component. However, if this ratio moves in favor of the first component, cytotoxicity may occur.[45] Liposomes are suitable for large-scale production, their use is safe [47] and, significantly, there are no limitations to the size of the DNA molecules that can be transfected.[48]

Depending on the cell type, this technique has proven to be up to 100 times more effective than transfection using CaP or cationic polymers.[39] Routinely for performing this procedure, cells are grown in serum-free media. It is likely that negatively charged serum proteins interact with cationic liposomes and destabilize them, dramatically reducing efficiency of transfection process. Yang and Huang separated serum proteins by chromatography and tested efficacy of lipofection in the presence of both fractions.[49] Except introducing serum-free media, that is impossible in *in vivo* conditions, they suggested overcoming this problem by increasing the charge ratio between cationic lipid reagent and DNA molecule or by adding positively charged polylysine to neutralize multiply negatively charged serum proteins.[49] Ross *et al.* attempted to overcome reduced transfection potential in the presence of serum by controlled growth of lipoplexes and concluded that key parameter for successful transfection is appropriate size of lipoplex, crucial for association with the cell membrane.[50] Since it was shown that inhibition of lipoplex formation by serum proteins is actually the cause of lower efficiency of lipofection-mediated gene transfer, they developed a protocol for fine regulation of lipoplex growth in polyanion-containing medium that stopped at a crucial moment by serum supplementation.[50]

Higher transfection efficiency achieved by combining cationic liposome with “helper” neutral lipid was discussed in many published studies.[51–53] The most commonly used helper lipids for enhancement of cationic liposomes transfection potency are unsaturated phosphatidylethanolamines (PE), such as dioleoyl-PE (DOPE). This molecule is believed to facilitate fusion of cationic liposomes from lipoplexes with endosomal membrane, followed by release of DNA into the cytoplasm. The efficiency of fusogenic lipid is believed to be result of its ability to form structural forms similar to membrane fusion intermediates and destabilize it.[53] Hui *et al.* attempted to explain complex role of helper lipids comparing efficiency of PE and phosphatidylcholine (PC) in transfection of CHO cells.[53] According to their results, former lipid led to rapid and premature aggregation of complexes in the medium resulting in formation of too large granules

to enter the cell, while transfection efficiency was higher in the presence of PC as helper lipid. Gradual formation of PC agregates was directed at the cell surface and after reaching appropriate size, granules were introduced into the cell. They also pointed out that endocytosis together with all other factors affecting this process is crucial for successful transfection, while fusion of cationic liposomes with the cell membrane is secondary and insufficient for entry of DNA complexes into the cell in the absence of endocytosis.[53]

Opposite results of efficiency of neutral helper lipids, DOPE and DOPC, in the lipofection approach were identified by Du *et al.* in the study about design of novel lipopolyplex formulations using combination of plasmid DNA, cationic liposomes and peptide component.[51] Increased transfection efficiency was reported in the presence of neutral lipid DOPE instead of DOPC, as claimed above. Peptides are thought to participate in DNA packaging and directing complex to membrane receptors, whereas liposomal component, stabilized by electrostatic interactions between cationic lipid and DNA, presumably causes fusion with endosomal membrane, endosomal escape and release of genetic content into the cytoplasmic region.[51] After cellular uptake of lipo(poly)plexes by clathrin-dependent endocytosis, release of nucleic acids from endosome to cytosol is required in order to avoid endosomolysis, degradation of genetic material by lysosomal enzymes, suggesting the need to promote destabilization of the endosomal membrane and increase lipoplex stability after entering the cell.[54] It has also been noticed that, due to its nature, DOPE promotes formation of inverted hexagonal lipid structures that fuse with lipid bilayer of endosome leading to endosomal escape, DNA release into the cytoplasm and accumulation in the nucleus, whereas non-fusogenic DOPC promotes more stable laminar forms of lipid bilayer leaving lipoplexes trapped within the late endolysosomes.[51,54]

Besides DOPE, effect of cholesterol, as helper lipid molecule, has also been recognized in enhancing transfection efficiency of cationic liposomes.[55] Biological importance of cholesterol is widely known. This molecule is essential building block of membranes, participant in many metabolic and biochemical processes, as well as highly involved in endocytosis.[56] Group led by Safinya explained impact of cholesterol on enhancing transfection efficiency by inducing structural changes in lipoplexes.[48] Increase in cholesterol concentration will lead to a decrease in hydration layer of the lipoplex cationic part that, due to repulsions, acts as a barrier for endosomal fusion. In this manner not only fusion between lipoplex and endosomal membrane is facilitated, but also endosomal release of the complex.[48] Importance of cholesterol in enhancing efficiency of cationic polymer transfection has also been reported. Replacement of poly(allylamine) primary amino group with cholesterol significantly reduced cytotoxicity of this agent and enabled hydrophobic interaction with the cell membrane.[52]

Interestingly, cationic lipids have not only been shown to function as carriers of hydrophilic molecules (DNA), but also interacting with the cell, they can modify different signaling pathways, stimulating immune and anti-inflammatory response.[57] However, there is a lack of information on this topic. Combination of immunostimulating and carrier properties of these molecules is highly recommended in the vaccine field.[58] During their interaction with the main target, cell membrane, physiology of the cell changes, especially at the level of membrane proteins involved in numerous signaling cascades, such as MAPK kinases.[59] Considering large number of synthesized cationic lipids of different structures and various targets of their action, it is obvious that only a small part of their possible activities has been identified to date.

4. CATIONIC POLYMER-MEDIATED CELL TRANSFECTION

Cationic polymer-mediated transfection is a technique used in biochemistry and molecular biology to introduce nucleic acids into cells with many applications in gene therapy,[60] drug delivery and recombinant protein production.[61] Its methodology is relatively straightforward, cost-effective, and can be applicable to a wide range of cell types. Cationic polymers are classified based on their chemical structure, molecular weight, morphologies and charge density to linear, branched, hybrid and amphipathic.[62] Unlike cationic lipids, cationic polymers are water-soluble molecules that create polyplexes by complexation with DNA. Principle of cationic polymer based transfection for the most commonly used reagents is shown in Fig. 3. Resulting complexes are smaller in the size and DNA is more compactly packed than by previously described methods, implying that these advantages may be the key for efficiency.[63,64]Cationic polymers are very flexible molecules that can be prepared as linear or branched form and due to structural versatility it is easy to manipulate with their molecular weight and geometry.[64] Molecular weight of cationic polymers was found to be inversely proportional to their cytotoxicity along with the distance between charged atoms in polymer.[65]

Naturally occurring carbohydrates, such as dextrans, are characterized by biocompatibility and ability to directly bind nanoparticles from polyplex formulations to receptors on the cell membrane.[66] Except biocompatibility, sugar-based nanoparticles, as an alternative to non-viral vectors, exhibit low toxicity, low cost and structural modifications to improve their biological potential also are easily obtained.[67] In addition to dextran, chitosan and gelatin are natural polymers commonly used in biomedicine, whereas structures of synthetic gene delivery carriers are based on polyethyleneamine (PEI) [68], poly-L-lysine (PLL), polyprene and dendrimers.[67] Use of cationic polysaccharides in non-viral transfection procedures, with a focus on chitosan and its derivatives, has been recognized and extensively studied by Liu *et al.*[69]

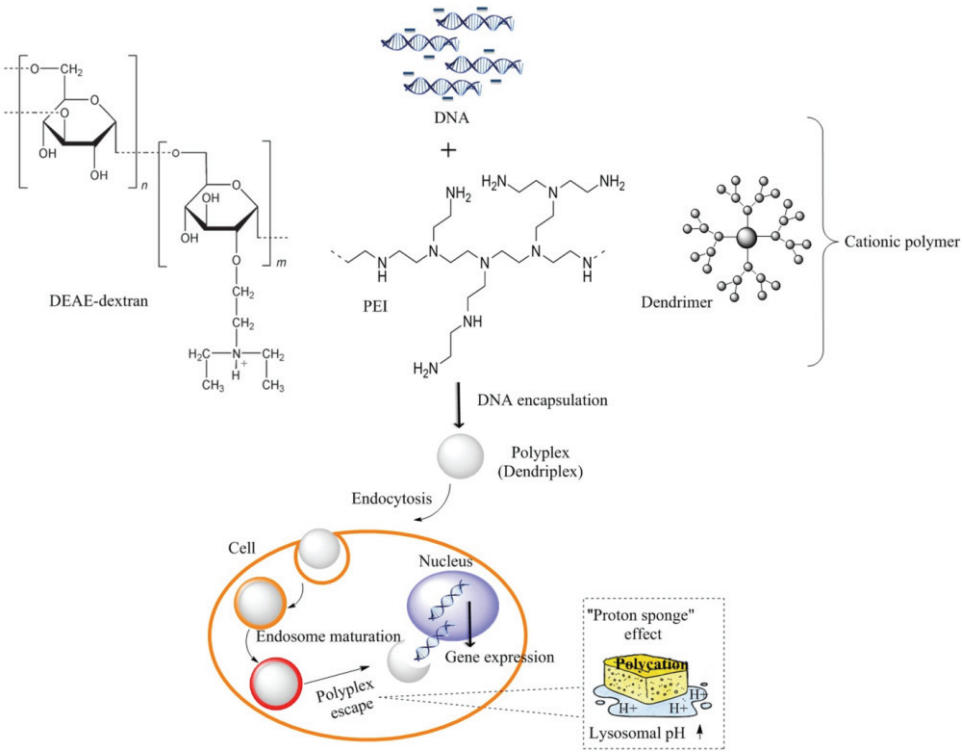

Fig. 3. Cationic polymer based transfection with the most commonly used reagents.

In this review more details are discussed on three the most prominent types of cationic polymers with superior efficiency compared to others, commonly used as transfection vectors due to their wide range of applications, high charge density, low cytotoxicity and immunogenicity.

5. DEAE-DEXTRAN-MEDIATED CELL TRANSFECTION

Diethylaminoethyl (DEAE)-dextran was among the first reagents used to deliver exogenous nucleic acids (poliovirus RNA) to mammalian cells (primary rhesus monkey kidney cells) over 50 years ago.[70] DEAE-dextran is cationic polysaccharide polymer of bacterial origin. Positively charged DEAE moiety electrostatically binds to DNA of total negative charge, resulting in formation of compact particles, polyplexes.

Due to the presence of three basic groups of different pKa values in the structure, specific association between DEAE-dextran and DNA is dependent on pH and solution ionic strength.[71] As a result of excess positive charge, this soluble complex associates with negatively charged cell membrane and is probably introduced into the cell by a process of nonspecific endocytosis, osmotic shock and change of membrane permeability either assisted by glycerol or DMSO.

Method for transfection of lymphocyte cell lines, described by Smale, is based on an initial incubation with a mixture of DEAE-dextran and DNA, followed by a secondary one in the presence of chloroquine.[63] Chloroquine participates in the neutralization of lysosomal enzymes, prevents acidification in endosomes and thereby inhibits intracellular degradation of plasmid DNA.[63] The increase in transfection efficiency with chloroquine treatment was investigated by Luthman and Magnusson.[72] They assumed that, except increasing pH in lysosomes, this molecule can strongly bind to DNA and protect it from degradation.[72]

Osmotic shock probably facilitates DNA uptake into the cell and prevents its breakdown by action of nucleases from lysozyme, causing pinocytotic vesicles burst due to osmotic imbalance.[73] Takai *et al.* applied combination of DEAE--dextran and osmotic shock, by treating cells with high osmolality buffer, for transient and stable transfection of lymphocyte cell line, with less efficiency and lower gene expression observed in the latter one.[73] DEAE-dextran-mediated DNA uptake is generally limited to a short-term transient transfection, whereas in the case of stable transfection, except low number of successfully transfected cells, toxicity may represent another drawback.[63] In addition to its biocompatibility, beneficial effects of dextran on the lipid status of the organism make it an attractive candidate in drug delivery and gene therapy.[71,74] Examining effect of polysaccharide dextran polymers of wide molecular weights range on transfection efficiency, it was concluded that efficiency positively correlates with increase in molecular weight, without impact on cell viability.[74] Furthermore, DEAE-dextran found its use in lipofection in the design of appropriate delivery carrier systems by stabilizing liposomal vesicles.[75]

Modified cell transfection protocol with DEAE-dextran, published by Shovel and coworkers in the early 1980s, introduced a step of "shocking" cells by exposure to DMSO or glycerol, which significantly increased expression of transfected gene, up to 50 fold.[76] Traditional protocol was also improved by Sussman *et al.* by treating mouse Ltk cells with DMSO at higher pH during initial incubation, resulting in 80 % of cells successfully transfected with thymidine kinase gene from simplex virus.[77] Mack *et al.* published reproducible method for transfecting sensitive adherent human primary macrophages using DEAE-dextran.[78] In this study three critical parameters for successful DEAE-dextran mediated transfection were identified and described: amount of added DNA per transfection, concentration of cationic polymer DEAE-dextran and time of incubating cells in transfection medium. [78]

Due to its great biomedical potential, Onishi *et al.* chose DEAE-dextran as a basis for the development of non-viral carriers for *in vivo* gene delivery.[79] This polymer can be autoclaved, it exhibits low cytotoxic and high transfection activity, and plays protective role against DNases. They performed graft polymer-

ization of methyl methacrylate on DEAE-dextran generating stable and efficient vector in the form of copolymer with significant therapeutic potential.[79]

6. PEI-MEDIATED CELL TRANSFECTION

Among leading and highly diverse group of non-viral carriers in the gene delivery field, PEI attracts attention as cationic polymer with easily modifiable structure that allows fine regulation of its physicochemical potential.[80] PEI is polymer of aziridine, with amino nitrogen atoms (at every third position) available for protonation, contributing to significant cationic potential of this organic molecule and buffering properties in wide pH range.[81] PEI does not have defined center of symmetry.[82] This molecule is easy to handle, low-cost and effective even in the treatment of cells growing in suspension.[5] It can be prepared in two forms, linear and branched, with the latter proven to be more effective in DNA condensation and transfection of mammalian cells and, unless otherwise stated in the literature, it refers to a branched type.[6] Due to branched structure and high density of positive charge, DNA is certainly more easily trapped within this polymer than with linear structures such as PLL and, thus, protected for safe gene transfer to target eukaryotic cell.[81] PLL alone does not show significant transfection efficiency *in vitro* and it mostly requires binding to molecules that will facilitate either cell entry or endolysosomal escape.[82]

PEI/DNA complexes enter most of the cells, but only a small number will express protein of interest.[83] Investigating destiny of these polyplexes inside the cell may explain why this occurs and answer a number of other important questions related to the mechanism of action. After endosome formation, polyplexes are released into the cytoplasm, destabilizing the endosomal membrane by "proton sponge" effect.[81] This phenomenon is associated with buffering capacity of PEI molecule and its ability to bind free protons within endosomes.[63] By binding protons PEI leads to an increase in endolysosomal pH that may affect folding of enzymes involved in DNA degradation, whose inactivation leads to release of functional, undegraded nucleic acids. One of the speculations is that surface of these complexes, due to cationic character, adheres to negatively charged phospholipids from nuclear membrane or from membrane fragments of bursted endolysosomes and being introduced into the nucleus by fusion.[5,6]

Optimal PEI/DNA ratio is essential for successful transfection. It has been documented that treating cells by complexes with low ratio showed no significant transfection efficiency, whereas too high ratio resulted in altered cellular morphology and reduced growth.[81] Accordingly, to optimize this method, it is crucial to find optimal ratio between these two components. On the other hand, entering large number of polyplexes by endocytosis may lead to cytotoxicity due to increased concentration of components from damaged endosomal membrane parts, upon endosomal escape.[81] Cytotoxicity of PEI polyplexes may be related to their

charge,[84] especially formation of non-specific interactions in the cell, so modification of their structure is popular strategy to avoid undesirable binding. Circulating serum proteins can bind to PEI/DNA complexes and inactivate them. For these reasons, their surface is modified by non-ionic molecules such as PEG,[85] as well as by various polysaccharides, which also play a role in targeting cells via receptors on the membrane. Patnaik *et al.* performed complexation of PEI with alginic acid and optimized appropriate ratio of these two components to achieve high mammalian cell transfection efficiency and viability.[80] Unmodified PEI molecule showed approximately 2–16 fold lower transfection efficiency compared to PEI-alginate complex against all tested cell lines. Beside reducing polyplex cytotoxicity, this inserted polysaccharide molecule increases transfection efficiency by participating in endosome damage.[80]

Godbey *et al.* provide an overview of physicochemical characteristics of PEI, its complexes and role in transfection of cell lines.[6] The protonability of this nucleic acid carrier was demonstrated to correlate with transfection efficiency. Also, it has been shown that manipulation of balance of components in PEI/DNA complex is essential to overcome attenuation of transfection efficiency caused by off-target interactions with interfering proteins. Although this undesirable binding can be bypassed by modifying complex surface with PEG, polystyrene, ethoxylated glycerol, poloxamer and polylactic acid,[86] significant improvement of transfection efficiency was made by attaching PEI to different transport proteins, such as transferrin.[6] In addition to concentration of H^+, formation of DNA/PEI polyplexes depends on the time of incubation, temperature, medium characteristics and amount of ions and various salts in solution.[83] PEI/DNA polyplexes occur in different forms, including rods and toroids. These two structures determine the uptake efficiency and therefore overall transfection efficiency.[6] Taking into account the fact that all these factors affect transfection efficiency, methods that provide insight into physicochemical characteristics of these complexes are of great importance. Scanning force microscopy was used to determine morphological properties and dimensions of PEI/DNA condensates, as well as to visualize way of DNA packaging and compactness under physiological conditions.[87] On the other hand, using particle tracking techniques (nanoparticle tracking analysis (NTA), dynamic light scattering (DLS)) and electron microscopy and varying incubation time of polyplex formation Dominguez *et al.* found a strong correlation between rate of polyplex aggregation and success of transfection.[5] Together with previously mentioned factors, transfection efficiency is affected by concentration of DNA, as well as by the type of cell being transfected and its environment.[5]

In comparison to CaP method, where presence of serum in the medium is mandatory and complex formation time-consuming, PEI transfection is more suitable for large scale use since it can be performed in serum-free medium and

does not require formation of pre-complexes between PEI and DNA.[88] Comparing transfection efficiency of CHO cells with PEI or CaP, Chenuet *et al.* emphasized higher efficiency of the first method in terms of cell recovery and the latter one related to cell-specific productivity and copy number of integrated plasmids in stable transfection system.[24] Cell recovery after PEI-mediated transfection is more efficient than in the case of CaP, although it was believed that interaction of this polymer with genomic DNA in the nucleus can lead to destabilization of chromosomes and reduced recovery.[24] On the other side, when considering costs of performing on a large scale, this method requires lower budget than lipofection.[88]

7. DENDRIMERS IN CELL TRANSFECTION

Dendrimers represent another gene delivery system of unique structure and will be briefly described here. These molecules are highly branched synthetic polymers of spherical geometry composed of monomeric subunits arranged around central core.[89] Owing to different synthetic strategies, functional groups, monomer units, as well as structure of central dendrimer core and number of concentric layers around it differs.[90] Layer number around central nucleus increases molecular weight of dendritic molecules, reaching values of protein molecular weights,[91] which is important for transfection process because structurally more complex vectors are able to carry and deliver more DNA.

More than 100 types of dendrimers have been synthesized and classified into several families – peptide, polyamidoamine, PAMAM, polypropyleneimine, PPI, phosphorus, carbosilane and polylysine or polyornithine dendrimers.[92] Characteristics of listed dendrimer groups have been extensively reviewed in the article of Pedziwiatr-Werbicka *et al*.[92] Binding affinity and stability of peptide dendrimer–DNA complex, and thus transfection efficiency, can be influenced by the type of interactions (covalent or non-covalent) between peptide and non-peptide components in this dendritic molecule.[93,94] Structure of one of the most commonly used peptide dendrimers is based on polylysine.[93] PAMAM is among the most common commercially available cores for dendrimer formation.[93] Core of PAMAM dendrimers contains ammonia or ethylenediamine, where nitrogen is tri- or tetravalent.[91] Controlled polymerization around this central molecule in PAMAM dendrimers leads to gradual formation of structure with spherical molecular architecture and large number of repeating amidoamine units. High density positive charge of primary amino groups on the surface, protonated at neutral pH, enables interaction with biological molecules of polyanionic character, such as DNA.[91]

These molecules, of usually radial symmetry, generally exhibit: low cytotoxicity, good biocompatibility and water solubility making them vectors of choice in transfection process.[95] However, due to high density charge, dendrimers may

become cytotoxic, and to overcome this barrier, they undergo functionalization and coating. In terms of costs, synthetic procedures with these compounds can be expensive.[93] Nature of dendrimer surface affects stability of encapsulatied complexes with DNA, cellular uptake and gene delivery. Dendrimers showed great biomedical potential as drug delivery carriers and transfection agents in both, nucleic acid and protein transfection, as well as in gene therapy.[92] Functional role of these molecules in biomedicine has been described comprehensively in recent work of Mirakabad *et al.*[93]

In the article of Tang and Szoka interaction of dendrimers and other cationic polymer structures with DNA was examined, as well as morphology of resulting complexes.[82] It was observed by electron microscopy that DNA condensation occurs in compact toroidal form. Complexes with degraded polyamidoamine dendrimers were observed as single units, while intact ones were clustered with almost 100 times larger diameter, suggesting that degree of aggregation is dependent on properties of individual polymers.[82,96] Unexpectedly, compared to intact, degraded dendrimers were more successful in transfection, most likely due to increased flexibility.[82] Wang and coworkers modified surface of dendrimer by fluorination introducing fluorine atom into aromatic ring of benzoic acid conjugated with dendrimer.[95] Transfection efficiency was estimated to increase with the degree of dendrimer fluorination.[95] Kwok *et al.* developed new hybrid transfection concept by studying synergistic action of peptide dendrimers and lipids as transfection reagents.[97] Combination of different transfection agents affects increase in their individual efficacy probably due to multiple interactions with DNA and membrane on their way to the cell nucleus. This field has not yet been extensively studied because dendrimer structure modifications are very challenging.[97]

8. CONCLUSION

Transfer of exogenous genes into cultured mammalian cells is a very powerful tool for manipulating DNA and represents an essential step in understanding function and regulation of genes and their products, proteins. Testing using this model system precedes *in vivo* studies and clinical trials converging towards the same milestone – therapeutic use in humans. Gene therapy, designed to introduce exogenous functional copies of genes into cells with damaged protein function represents a real revolution in medicine. Mammalian cell transfection methods are developing exponentially. New generations of transfection technologies are sophisticated and easily amenable to further improvement, such as automation with minimal operator input. In order to become commercially available products, gene delivery carriers have to meet certain criteria and overcome a lot of barriers. Undesirable characteristics of these vectors are induction of immunogenicity and cytotoxicity, whereas it is preferable to be biocompatible, stable,

available for structural modifications and to exhibit significant potential for cargo delivery of molecules of various types and sizes in the cell.

Due to simple handling procedure and reduced costs there is a great interest for developing non-viral methods, especially those based on the use of various chemical agents-inorganic amphiphilic aggregates, cationic polymers or cationic lipids. Their chemical design is constantly undergoing modifications in order to increase transfection efficiency and reduce side effects. Generally, transfection by chemical methods is based on electrostatic interactions between polycationic core of chemical agent and oppositely charged DNA followed by entry of resulting complexes into the cell, most likely via endocytosis. Chemically-assisted approaches described here have their own advantages and disadvantages and choice of the optimal one depends on the purpose of planned experiment. Furthermore, remarkable transfection success is achieved by combination of individual methods and transfection agents, with promising potential in biomedicine. Synergistic action leads to overcoming disadvantages of individual methods and improves their activity. Transfection efficiency may also be increased by removing nonspecifically binding serum proteins from the medium, optimizing size of complexes formed between chemical reagent and DNA, then modifying charge on their surface, inhibiting degradation within the lysozymes, increasing cell permeability, etc. To sum up, *in vitro* non-viral gene delivery to cells by chemical methods represents promising area in biomedical research with methodology constantly being improved.

Acknowledgement. The authors gratefully acknowledge the financial support of the Ministry of Science, Technological Development and Innovation of the Republic of Serbia (Grant No. 451-03-47/2023-01/200125).

И З В О Д

ПРЕГЛЕД ХЕМИЈСКИХ МЕТОДА ЗА ДНК ТРАНСФЕКЦИЈУ

СОФИЈА С. БЕКИЋ и СУЗАНА С. ЈОВАНОВИЋ-ШАНТА

Универзитет у Новом Саду, Природно–математички факултет, Департман за хемију, биохемију и заштиту животне средине, Трг Доситеја Обрадовића 3, 21000 Нови Сад

За *in vitro* уношење жељеног гена у ћелије сисара обично се користе невирусне хемијске методе за трансфекцију с обзиром на то да су веома ефикасне, јефтине и једноставне. Углавном немају безбедносне ризике као оне засноване на употреби вирусних вектора, а и токсичност према ћелијама је значајно смањена. Ове методе се класификују на основу хемијских реагенса који се користе за трансфекцију ћелија домаћина. Углавном су то биокомпатибилни носачи ДНК, као што су калцијум фосфат, катјонски липиди, DEAE-декстран, полиетиленимин или дендримери. Иако различити приступи, сви су засновани на формирању инкапсулираних амфифилних комплекса између ДНК и различитих честица, након чега следи улазак у ћелију, највероватније посредован ендоцитозом. У зависности од циља и дизајна експеримента, врши се избор одговарајуће методе. У овом прегледном раду описане су стратегије најчешће коришћених техника хемијске трансфекције. Поред тога, указано је на предности и ограничења различитих

носача ДНК, а наведени су и резултати истраживача добијени током оптимизације протокола у циљу повећања ефикасности испоруке гена. Главна биомедицинска примена овде описаних метода трансфекције је генска терапија, где се дефектни гени замењују функционалним.

(Примљено 22. децембра 2022, ревидирано 21. јануара, прихваћено 9. априла 2023)

REFERENCES

1. C. Hardee, L. Arévalo-Soliz, B. Hornstein, L. Zechiedrich, *Genes (Basel)* **8** (2017) 65 (https://doi.org/10.3390/genes8020065)
2. J. Valsalakumari, J. Baby, E. Bijin, I. Constantine, S. Manjila, K. Pramod, *Int. J. Pharm. Investig.* **3** (2013) 1 (https://doi.org/10.4103/2230-973X.108958)
3. R. Zhou, R. C. Geiger, D. A. Dean, *Expert Opin. Drug Deliv.* **1** (2004) 127 (https://doi.org/10.1517/17425247.1.1.127)
4. B. Neuhaus, B. Tosun, O. Rotan, A. Frede, A. M. Westendorf, M. Epple, *RSC Adv.* **6** (2016) 18102 (https://doi.org/10.1039/c5ra25333k)
5. I. González-Domínguez, N. Grimaldi, L. Cervera, N. Ventosa, F. Gòdia, *Nat. Biotechnol.* **49** (2019) 88 (https://doi.org/10.1016/j.nbt.2018.09.005)
6. W. T. Godbey, K. K. Wu, A. G. Mikos, *J. Control. Release* **60** (1999) 149 (https://doi.org/10.1016/s0168-3659(99)00090-5)
7. F. M. Wurm, *Nat. Biotechnol.* **22** (2004) 1393 (https://doi.org/10.1038/nbt1026)
8. E. Wells, A. S. Robinson, *Biotechnol. J.* **12** (2017) 1600105 (https://doi.org/10.1002/biot.201600105)
9. W. A. Keown, C. R. Campbell, R. S. Kucherlapati, in *Methods Enzymol.*, 1990, pp. 527–537 (https://doi.org/10.1016/0076-6879(90)85043-n)
10. A. Fus-Kujawa, P. Prus, K. Bajdak-Rusinek, P. Teper, K. Gawron, A. Kowalczuk, A. L. Sieron, *Front. Bioeng. Biotechnol.* **9** (2021) 701031 (https://doi.org/10.3389/fbioe.2021.701031)
11. J.A. Lee, A. Cho, E. N. Huang, Y. Xu, H. Quach, J. Hu, A. P. Wong, *J. Transl. Med.* **19** (2021) 452 (https://doi.org/10.1186/s12967-021-03099-4)
12. A. C. Nathwani, *Hematology* **2022** (2022) 569 (https://doi.org/10.1182/hematology.2022000388)
13. J. S. Chamberlain, *Hum. Mol. Gen.* **11** (2002) 2355 (https://doi.org/10.1093/hmg/11.20.2355)
14. D. Cross, J. K. Burmester, *Clin Med Res.* **4** (2006) 218 (https://doi.org/10.3121/cmr.4.3.218)
15. N. Sayed, P. Allawadhi, A. Khurana, V. Singh, U. Navik, S. K. Pasumarthi, I. Khurana, A. K. Banothu, R. Weiskirchen, K. K. Bharani, *Life Sci.* **294** (2022) 120375 (https://doi.org/10.1016/j.lfs.2022.120375)
16. T. I. Cornu, C. Mussolino, M. C. Müller, C. Wehr, W. V. Kern, T. Cathomen, *Hum. Gene Ther.* **32** (2021) 52 (https://doi.org/10.1089/hum.2020.159)
17. E. Hanna, C. Rémuzat, P. Auquier, M. Toumi, *J. Mark. Access Heal. Policy* **5** (2017) 1265293 (https://doi.org/10.1080/20016689.2017.1265293)
18. M. M. Lufino, P. A. Edser, R. Wade-Martins, *Mol. Ther.* **16** (2008) 1525 (https://doi.org/10.1038/mt.2008.156)
19. T. K. Kim, J. H. Eberwine, *Anal. Bioanal. Chem.* **397** (2010) 3173 (https://doi.org/10.1007/s00216-010-3821-6)

20. R. E. Kingston, C. A. Chen, H. Okayama, *Curr. Protoc. Mol. Biol.* **14** (1991) 9.1.1 (https://doi.org/10.1002/j.1934-3647.1991.tb00206.x)
21. G. S. Pari, Y. Xu, in *Gene Deliv. to Mamm. Cells*, Humana Press, Totowa, NJ, pp. 25–32 (https://doi.org/10.1385/1-59259-649-5:25)
22. A. A. Stepanenko, H. H. Heng, *Mutat. Res.* **773** (2017) 91 (https://doi.org/10.1016/j.mrrev.2017.05.002)
23. S. Patil, Y. Gao, X. Lin, Y. Li, K. Dang, Y. Tian, W. Zhang, S. Jiang, A. Qadir, A.-R. Qian, *Int. J. Mol. Sci.* **20** (2019) 5491 (https://doi.org/10.3390/ijms20215491)
24. S. Chenuet, D. Martinet, N. Besuchet-Schmutz, M. Wicht, N. Jaccard, A. Bon, M. Derouazi, D. L. Hacker, J. S. Beckmann, F. M. Wurm, *Biotechnol. Bioeng.* **101** (2008) 937 (https://doi.org/10.1002/bit.21972)
25. F. L. Graham, A. J. Van der Eb, *Virology* **52** (1973) 456 (https://doi.org/10.1016/0042-6822(73)90341-3)
26. P. Batard, M. Jordan, F. Wurm, *Gene* **270** (2001) 61 (https://doi.org/10.1016/S0378-1119(01)00467-X)
27. K. Khosravi-Darani, M. R. Mozafari, L. Rashidi, M. Mohammadi, *Acta Med. Iran.* **48** (2010) 133 (https://pubmed.ncbi.nlm.nih.gov/21137647)
28. T. Welzel, I. Radtke, W. Meyer-Zaika, R. Heumann, M. Epple, *J. Mater. Chem.* **14** (2004) 2213 (https://doi.org/10.1039/b401644k)
29. D. Olton, J. Close, C. Sfeir, P. N. Kumta, *Biomaterials* **32** (2011) 7662 (https://doi.org/10.1016/j.biomaterials.2011.01.043)
30. G. Ling, W. Liyang, Y. Ronghua, F. Rui, L. Zhongguang, M. Nishi, Z. Qi, W. Isaacs, J. Ma, X. Xuehong, *Saudi J. Biol. Sci.* **24** (2017) 622 (https://doi.org/10.1016/j.sjbs.2017.01.034)
31. C. Chen, H. Okayama, *Mol. Cell. Biol.* **7** (1987) 2745 (https://doi.org/10.1128/mcb.7.8.2745-2752.1987)
32. M. Jordan, A. Schallhorn, F. M. Wurm, *Nucleic Acids Res.* **24** (1996) 596 (https://doi.org/10.1093/nar/24.4.596)
33. M. Sun, L. P. Bernard, V. L. Dibona, Q. Wu, H. Zhang, *J. Vis. Exp.* **81** (2013) 1 (https://doi.org/10.3791/50808)
34. I. K. Sariyer, *Methods Mol Biol.* **1078** (20163) 133 (https://doi.org/10.1007/978-1-62703-640-5)
35. J. L. Huang, H. Chen, X. L. Gao, *J. Drug Target.* **26** (2018) 398 (https://doi.org/10.1080/1061186X.2017.1419360)
36. T. Liu, A. Tang, G. Zhang, Y. Chen, J. Zhang, S. Peng, Z. Cai, *Cancer Biother. Radiopharm.* **20** (2005) 141 (https://doi.org/10.1089/cbr.2005.20.141)
37. B. Ma, S. Zhang, H. Jiang, B. Zhao, H. Lv, *J. Control Release* **123** (2007) 184 (https://doi.org/10.1016/j.jconrel.2007.08.022)
38. T. W. R. Lee, D. A. Matthews, G. E. Blair, *Biochem. J.* **387** (2005) 1 (https://doi.org/10.1042/BJ20041923)
39. P. L. Felgner, T. R. Gadek, M. Holm, R. Roman, H. W. Chan, M. Wenz, J. P. Northrop, G. M. Ringold, M. Danielsen, *Proc. Natl. Acad. Sci.* **84** (1987) 7413 (https://doi.org/10.1073/pnas.84.21.7413)
40. D. Niculescu-Duvaz, J. Heyes, C. J. Springer, *Curr. Med. Chem.* **10** (2003) 1233 (https://doi.org/10.2174/0929867033457476)

41. G. Byk, C. Dubertret, V. Escriou, M. Frederic, G. Jaslin, R. Rangara, B. Pitard, J. Crouzet, P. Wils, B. Schwartz, D. Scherman, *J. Med. Chem*. **41** (1998) 224 (https://doi.org/10.1021/jm9704964)
42. D. Zhi, Y. Bai, J. Yang, S. Cui, Y. Zhao, H. Chen, S. Zhang, *Adv. Colloid Interface Sci.* **253** (2018) 117 (https://doi.org/10.1016/j.cis.2017.12.006)
43. P. Shende, N. Ture, R. S. Gaud, F. Trotta, *Int. J. Pharm.* **558** (2019) 250 (https://doi.org/10.1016/j.ijpharm.2018.12.085)
44. Y. Xu, F. C. Szoka, *Biochemistry* **35** (1996) 5616 (https://doi.org/10.1021/bi9602019)
45. F. Recillas-Targa, *Mol. Biotechnol.* **34** (2006) 337 (https://doi.org/10.1385/MB:34:3:337)
46. K. Romøren, B. J. Thu, N. C. Bols, Ø. Evensen, *Biochim. Biophys. Acta* **1663** (2004) 127 (https://doi.org/10.1016/j.bbamem.2004.02.007)
47. C. Charcosset, A. Juban, J. Valour, S. Urbaniak, H. Fessi, *Chem. Eng. Res. Des.* (2014) 1 (https://doi.org/10.1016/j.cherd.2014.09.008)
48. A. Zidovska, H. M. Evans, A. Ahmad, K. K. Ewert, C. R. Safinya, *J. Phys. Chem., B* **113** (2009) 5208 (https://doi.org/10.1021/jp809000e)
49. J. Yang, L. Huang, *Gene Ther.* **4** (1997) 950 (https://doi.org/10.1038/sj.gt.3300485)
50. P. C. Ross, S. W. Hui, *Gene Ther.* **6** (1999) 651 (https://doi.org/10.1038/sj.gt.3300863)
51. Z. Du, M. M. Munye, A. D. Tagalakis, M. D. I. Manunta, S. L. Hart, *Sci. Rep.* **4** (2014) 1 (https://doi.org/10.1038/srep07107)
52. R. K. Oskuee, M. Ramezanpour, L. Gholami, B. Malaekeh-Nikouei, *Brazilian J. Pharm. Sci.* **53** (2017) 1 (https://doi.org/10.1080/17458080.2013.771245)
53. S. W. Hui, M. Langner, Y. Zhao, P. Ross, E. Hurley, K. Chan, *Biophys. J.* **71** (1996) 590 (https://doi.org/10.1016/S0006-3495(96)79309-8)
54. D. Afonso, T. L. Gall, H. Couthon-Gourves, A. Grelard, S. Prakash, M. Berchel, N. Kervarec, E. J. Dufourc, *Soft Matter* **12** (2016) 4516 (https://doi.org/10.1039/c6sm00609d)
55. E. S. Hosseini, M. Nikkhah, S. Hosseinkhani, *Int. J. Nanomedicine* **14** (2019) 4353 (https://doi.org/10.2147/IJN.S199104)
56. J. Zhang, Q. Li, Y. Wu, D. Wang, L. Xu, Y. Zhang, S. Wang, T. Wang, F. Liu, M. Y. Zaky, S. Hou, S. Liu, K. Zou, H. Lei, L. Zou, Y. Zhang, H. Liu, *Cell Commun. Signal.* **17** (2019) 15 (https://doi.org/10.1186/s12964-019-0328-4)
57. M. C. Filion, N. C. Phillips, *Br. J. Pharmacol.* **122** (1997) 551 (https://doi.org/10.1038/sj.bjp.0701396)
58. D. Christensen, K. S. Korsholm, P. Andersen, E. M. Agger, *Expert Rev. Vaccines* **10** (2011) 513 (https://doi.org/10.1586/erv.11.17)
59. C. Lonez, M. F. Lensink, M. Vandenbranden, J.M. Ruysschaert, *Biochim. Biophys. Acta* **1790** (2009) 425 (https://doi.org/10.1016/j.bbagen.2009.02.015)
60. R. Rai, S. Alwani, I. Badea, *Polymers (Basel)* **11** (2019) 745 (https://doi.org/10.3390/polym11040745)
61. K. M. Luly, H. Yang, S. J. Lee, W. Wang, S. D. Ludwig, H. E. Tarbox, D. R. Wilson, J. J. Green, J. B. Spangler, *Int. J. Nanomed.* **17** (2022) 4469 (https://doi.org/10.2147/IJN.S377371)
62. S. Barua, J. Ramos, T. Potta, D. Taylor, H.-C. Huang, G. Montanez, K. Rege, *Comb. Chem. High Throughput Screen.* **14** (2011) 908 (https://doi.org/10.2174/138620711797537076)
63. S. T. Smale, *Cold Spring Harb Protoc* **2** (2010) 1 (https://doi.org/10.1101/pdb.prot5373)

64. H. Lv, S. Zhang, B. Wang, S. Cui, J. Yan, *J. Control. Release* **114** (2006) 100 (https://doi.org/10.1016/j.jconrel.2006.04.014)
65. M. E. Davis, *Curr. Opin. Biotechnol.* **13** (2002) 128 (https://doi.org/10.1016/s0958-1669(02)00294-x)
66. S. Pustylnikov, D. Sagar, P. Jain, Z. K. Khan, *J. Pharm. Pharm. Sci.* **17** (2014) 371 (https://doi.org/10.18433/J3N590)
67. S. J. Hong, M. H. Ahn, J. Sangshetti, P. H. Choung, R. B. Arote, *Carbohydr. Polym.* **181** (2018) 1180 (https://doi.org/10.1016/j.carbpol.2017.11.105)
68. P. A. Longo, J. M. Kavran, M. Kim, D. J. Leahy, *Methods Enzym.* (2013) 227 (https://doi.org/10.1016/B978-0-12-418687-3.00018-5)
69. W. G. Liu, K. De Yao, *J. Control. Release* **83** (2002) 1 (https://doi.org/10.1016/s0168-3659(02)00144-x)
70. A. Vaheri, J. S. Pagano, *Virol* **27** (1965) 434 (https://doi.org/10.1016/0042-6822(65)90126-1)
71. C. I. Cámara, N. Wilke, *Chem. Phys. Lipids* **204** (2017) 34 (https://doi.org/10.1016/j.chemphyslip.2017.03.005)
72. H. Luthman, G. Magnusson, *Nucleic Acids Res.* **11** (1983) 1295 (https://doi.org/10.1093/nar/11.5.1295)
73. T. Takai, H. Ohmori, *Biochim. Biophys. Acta* **1048** (1990) 105 (https://doi.org/10.1016/0167-4781(90)90029-2)
74. C. Wu, Y. Lu, *Cell Mol. Biol.* **53** (2010) 67 (www.ncbi.nlm.nih.gov/pmc/articles/PMC2830788)
75. P. Menon, T. Y. Yin, M. Misran, *Colloids Surfaces, A* **481** (2015) 345 (https://doi.org/10.1016/j.colsurfa.2015.05.036)
76. M. A. Lopata, D. W. Cleveland, B. Sollner-Webb, *Nucleic Acids Res.* **12** (1984) 5707 (https://doi.org/10.1093/nar/12.14.5707)
77. J. Sussman, G. Milman, *Mol. Cell. Biol.* **4** (1984) 1641 (https://doi.org/10.1128/mcb.4.8.1641-1643.1984)
78. K. D. Mack, R. Wei, A. Elbagarri, N. Abbey, M. S. McGrath, *J. Immunol. Methods* **211** (1998) 79 (https://doi.org/10.1016/s0022-1759(97)00194-4)
79. Y. Onishi, Y. Eshita, A. Murashita, M. Mizuno, J. Yoshida, *Nanomedicine* **3** (2007) 184 (https://doi.org/10.1016/j.nano.2007.07.002)
80. S. Patnaik, A. Aggarwal, S. Nimesh, A. Goel, M. Ganguli, N. Saini, Y. Singh, K. C. Gupta, *J. Control. Release* **114** (2006) 398 (https://doi.org/10.1016/j.jconrel.2006.06.025)
81. O. Boussif, F. Lezoualch, M. A. Zanta, M. D. Mergny, D. Schermant, B. Demeneixt, J. P. Behr, *Proc. Natl. Acad. Sci. USA* **92** (1995) 7297 (https://doi.org/10.1073/pnas.92.16.7297)
82. M. X. Tang, F. C. Szoka, *Gene Ther.* **4** (1997) 823 (https://doi.org/10.1038/sj.gt.3300454)
83. S. Gutiérrez-Granados, L. Cervera, A. A. Kamen, F. Gòdia, *Crit. Rev. Biotechnol.* **38** (2018) 918 (https://doi.org/10.1080/07388551.2017.1419459)
84. Z. Rezvani Amin, M. Rahimizadeh, H. Eshghi, A. Dehshahri, M. Ramezani, *Iran. J. Basic Med. Sci.* **16** (2013) 150 (https://doi.org/10.22038/ijbms.2013.295)
85. Y. H. Choi, F. Liu, J.-S. Kim, Y. K. Choi, Jong Sang Park, S. W. Kim, *J. Control. Release* **54** (1998) 39 (https://doi.org/10.1016/S0168-3659(97)00174-0)
86. G. Storm, S. O. Belliot, T. Daemen, D. D. Lasic, *Adv. Drug Deliv. Rev.* **17** (1995) 31 (https://doi.org/10.1016/0169-409X(95)00039-A)

87. D. D. Dunlap, A. Maggi, M. R. Soria, L. Monaco, *Nucleic Acids Res.* **25** (1997) 3095 (https://doi.org/10.1093/nar/25.15.3095)
88. D. L. Hacker, D. Kiseljak, Y. Rajendra, S. Thurnheer, L. Baldi, F. M. Wurm, *Protein Expr. Purif.* **92** (2013) 67 (https://doi.org/10.1016/j.pep.2013.09.001)
89. V. Viswanath, K. Santhakumar, *J. Photochem. Photobiol., B* **173** (2017) 61 (https://doi.org/10.1016/j.jphotobiol.2017.05.023)
90. D. G. Shcharbin, B. Klajnert, M. Bryszewska, *Biochem.* **74** (2009) 1070 (https://doi.org/10.1134/s0006297909100022)
91. J. F. Kukowska-Latallo, A. U. Bielinska, J. Johnson, R. Spindler, D. A. Tomalia, J. R. Baker, *Proc. Natl. Acad. Sci. USA* **93** (1996) 4897 (https://doi.org/10.1073/pnas.93.10.4897)
92. E. Pedziwiatr-Werbicka, K. Milowska, V. Dzmitruk, M. Ionov, D. Shcharbin, M. Bryszewska, *Eur. Polym. J.* **119** (2019) 61 (https://doi.org/10.1016/j.eurpolymj.2019.07.013)
93. F. S. T. Mirakabad, M. S. Khoramgah, K. Keshavarz F., M. Tabarzad, J. Ranjbari, *Life Sci.* **233** (2019) 1 (https://doi.org/10.1016/j.lfs.2019.116754)
94. F. Xie, R. Li, W. Shu, L. Zhao, J. Wan, *Mater. Today Biol.* **14** (2022) 100239 (https://doi.org/10.1016/j.mtbio.2022.100239)
95. M. Wang, Y. Cheng, *Biomaterials* **35** (2014) 6603 (https://doi.org/10.1016/j.biomaterials.2014.04.065)
96. M. X. Tang, C. T. Redemann, F. C. Szoka, *Bioconjug. Chem.* **7** (1996) 703 (https://doi.org/10.1021/bc9600630)
97. A. Kwok, G. A. Eggimann, J. Reymond, T. Darbre, F. Hollfelder, *ASC Nano* **7** (2013) 4668 (https://doi.org/10.1021/nn400343z).

Journal of the Serbian Chemical Society
JSCS@tmf.bg.ac.rs • www.shd.org.rs/JSCS
J. Serb. Chem. Soc. *88* (11) 1089–1102 (2023)
JSCS–5682
Original scientific paper
Published 10 November 2023

Antidiabetic potential of simple carbamate derivatives: Comparative experimental and computational study

RELJA V. SURUČIĆ[1], IVANA I. JEVTIĆ[2#], TATJANA P. STANOJKOVIĆ[3] and JELENA B. POPOVIĆ-DJORDJEVIĆ[4]*

[1]*University of Banja Luka, Faculty of Medicine, Save Mrkalja 14, 78000 Banja Luka, Bosnia and Herzegovina,* [2]*University of Belgrade-Institute of Chemistry, Technology and Metallurgy, Department of Chemistry, Njegoševa 12, 11000 Belgrade, Serbia,* [3]*University of Belgrade-Institute for Oncology and Radiology of Serbia, Pasterova 14,11000 Belgrade, Serbia and* [4]*University of Belgrade-Faculty of Agriculture, Department of Chemistry and Biochemistry, Nemanjina 6, 11080 Belgrade, Serbia*

(Received 23 September 2022, revised 16 February, accepted 8 September 2023)

Abstract: With the increasing global burden of diabetes mellitus type 2, the search for the new drugs, with better pharmacological profile is continued. As a part of this surge, the synthesis, pharmacological *in vitro* and computational evaluation of five, simple carbamate derivatives, against carbohydrate digestive enzyme *α*-glucosidase, is disclosed herein. Results of the experimental and computational assessment indicated that examined carbamates deterred the activity of *α*-glucosidase with acceptable IC_{50} values ranging from 65.34 to 79.89 μM compared to a standard drug acarbose (109.71 μM). Similarly, the studied compounds displayed *in silico* binding affinity for *α*-glucosidase enzyme with significant binding energies. Preliminary toxicity profiles of studied carbamates against three cancerous cell lines indicated their poor activity, suggesting that significant structural modifications have to be made to improve their anticancer efficiency. Results of the present study indicate that the examined carbamates were able to virtually or experimentally interact with an important target of diabetes mellitus type 2. Additionally, a new pharmacophore model is proposed featuring hydrogen bond donating carbamate –NH group, hydrogen bond accepting carbamate $–OCH_3$ group and hydrophobic stabilization of aromatic moieties.

Keywords: diabetes mellitus; Hofmann rearrangement; molecular docking; *α*-glucosidase; molecular dynamics simulation.

* Corresponding author. E-mail: jelenadj@agrif.bg.ac.rs
# Serbian Chemical Society member.
https://doi.org/10.2298/JSC220923058S

INTRODUCTION

Today, diabetes mellitus (DM) is one of the most important metabolic syndromes causing thousands of deaths worldwide and an efficient therapy to permanently postpone its pathogenesis and/or complications is not yet developed.[1] As a major form, DM type 2 represents for more than 95 % of all diabetic cases and is mainly associated with hyperglycemia and insulin resistance of peripheral tissues.[2] In contrast, DM type 1 is a genetic autoimmune disorder mainly represented for less than 5 % of all diabetic patients and associated with inflammation and pancreatic β-cells dysfunction.[2,3] Other subtypes of DM such as gestational diabetes, mild obesity-related diabetes, mild age-related diabetes and other forms, although occurred in low rates, can also cause physiological problems for affected individuals.[4,5]

Recent advances in synthetic methods, enabled researchers to contrive some new classes of synthetic anti-diabetic drugs which can alleviate the DM complications.[6] A majority of synthetic drugs, developed for the treatment of diabetes mainly target the inhibition of glycol-processing enzymes such as α-glucosidase (α-Glc) and α-amylase, as well as other targets such as sodium glucose co-transporter 2 (SGLT2) and dipeptidyl peptidase 4 (DPP-4) inhibitors. Despite the effectiveness of these artificial inhibitors for postponing the incidence of DM, several shortcomings including gastrointestinal pains, stomach gas, diarrhoea and even vomiting were reported for some of these synthetic drugs.[2,6–8] Therefore, searching for a new class of inhibitors with better pharmacological profile is the main goal of most of research conducted in this area. In that respect, versatile heterocyclic nitrogen containing compounds gained considerable attention as α-Glc inhibitors.[9,10]

The importance of carbamate derivatives in medicinal chemistry is widely studied, and the growing body of evidence indicates that carbamate moiety is a pivotal chemical structural attachment in a variety of approved therapeutic medications.[11] Carbamate moiety is basically generated from an unstable molecule, carbamic acid, by the alteration of amino and carboxyl groups with aryl-alkyl or alkyl-aryl moieties.[12] Studies suggested that carbamate moiety has the potential to interact with the active site of the target proteins forming donor (carbonyl oxygen) and/or acceptor (nitrogen) hydrogen bonds. Moreover, the metabolic stability and good membrane permeability are important features of this structural motif, interesting for medicinal chemistry.[11]

Presently, most of carbamate derivatives are used as potential agrochemical metabolites and intermediates in the organic synthesis of several types of chemical agents.[8,11,13] Carbamates are known to possess a wide range of biological activities including antimicrobial,[14] anti-HIV,[15–17] anticancer[18] and anti-Alzheimer properties.[19] The potential benefits of several carbamate derivatives to deter α-Glc *in vitro*, have been also reported.[8,20]

Over the past decades, computational methods such as docking and molecular dynamics simulations provided an in-depth insight into the biological mode of action of many chemical compounds.[21] In fact, these *in silico* techniques are the upper hands of molecular biologists and medicinal chemists to evaluate the effectiveness of chemical compounds before introducing them into experimental assays. Using these methods for both ligand- and structure-based drug design policies could support researchers to develop several classes of Food and Drug Administration (FDA) approved drugs.[21,22]

Therefore, this study demonstrates an improvement of the previously published procedure for carbamate synthesis,[23] and it briefly sets out to investigate the α-Glc binding mode and inhibitory activity of simple carbamate derivatives **1**-**5**, using both computational and experimental assays (Fig. 1).

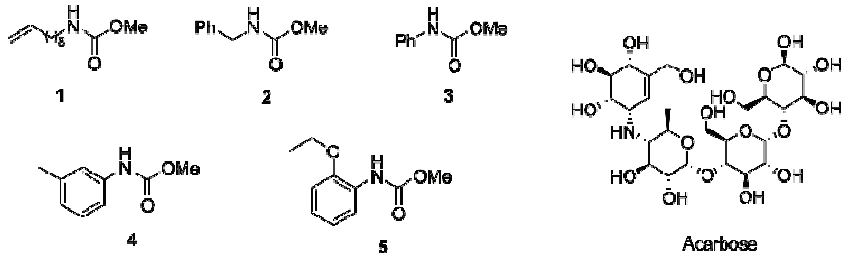

Fig. 1. Structures of the examined carbamates **1**–**5** and acarbose.

EXPERIMENTAL

General information

All reagents were purchased from a commercial vendor and used as supplied, except *N*-bromoacetamide (NBA) which was synthesized according to the literature procedure.[21] All reactions were monitored by thin layer chromatography (TLC). Dry-column flash chromatography was carried out using silica gel (10−18 or 18–32 μm, ICN-Woelm). Melting points were obtained at a heating rate of 4 °C/min, and are uncorrected. ^{1}H- and ^{13}C-NMR spectra were recorded on Bruker Avance III spectrometer, at 500 MHz for the proton (^{1}H) and at 126 MHz for the carbon (^{13}C) and Varian/Agilent, at 200 MHz for the proton (^{1}H) and at 50 MHz for the carbon (^{13}C). Chemical shifts are given in parts per million (ppm) from tetramethylsilane (TMS) as internal standard in deuterated chloroform ($CDCl_3$). Coupling constants (J) are reported in Hz. All spectra were recorded at 25 °C, unless stated otherwise. High resolution mass spectra (HRMS) were obtained with an ESI-ToF spectrometer. α-Glc from *Saccharomyces cerevisiae*, RPMI 1640 (product number R8755), *p*-nitrophenyl α-D-glucopyranoside (PNP-G), acarbose, fetal bovine serum (FCS), dimethyl sulfoxide (DMSO), hepes, ethidium bromide, sodium dodecyl sulfate (SDS), acridine orange, disodium hydrogen phosphate dihydrate, sodium dihydrogen phosphate dihydrate and thiazolyl blue tetrazolium bromide (MTT) were purchased from Sigma–Aldrich. Trypsin and phosphate buffered saline (PBS) were obtained from Institute of Virology, Vaccines and Sera “Torlak”, Belgrade, Serbia.

*General procedure for the synthesis of carbamates **1**–**5***

To a magnetically stirred solution of corresponding carboxamide (3.7 mmol, 1.0 equiv.) in MeOH (5 mL), $LiOH \cdot H_2O$ (5.0 equiv.) and NBA (1.5 equiv.) were added. The mixture was allowed to steer at 65 °C, in dark. Reaction was monitored by TLC, on SiO_2 plates, using the mixture of *n*-hexane/EtOAc = 1:1 and CH_2Cl_2/MeOH = 9:1, as eluent. After 5 min, the mixture was concentrated by rotary evaporator to give a residue which was mixed with 1 M solution of NaOH (20 mL). The mixture was extracted with 2×25 mL of CH_2Cl_2. The organic layers were combined and concentrated by rotary evaporator. The obtained crude product was purified by dry-column flash chromatography (SiO_2; petroleum ether/EtOAc, 8:2 to 1:1). The spectroscopic data for compounds **1**–**5** are given in Supplementary material to this paper and are in accordance with the previously published data.[23]

Enzymatic assay – Anti α*-glucosidase activity*

Anti *α*-Glc activity of compounds **1**–**5** was performed using *α*-glucosidase inhibitory activity test described by McCue *et al*. with some modification.[24] The final concentrations of the extracts in each well were 166.67, 83.33, 41.67, 20.83, 10.42 and 5.21 μM. Acarbose was used as a positive control. The percent of the enzyme inhibition was calculated as Inhibition = = 100(1-(*AS* at 15 min−*AS* at 0 min)/(*AC* at 15 min−*AC* at 0 min)), where *AS* is the absorbance readings of samples, *AC* is the absorbance readings of the control. The experiments were conducted in duplicate and IC_{50} value (estimated concentration of compounds that caused 50 % inhibition of *α*-Glc activity was determined using linear regression analysis. Measurements were done in triplicate.

MTT assay – Cytotoxic activity

The incubation of the cultures was performed according to literature procedure.[25] Target cells HeLa, cervix adenocarcinoma cell line (2000 cells per well), A549, non-small cell lung carcinoma cell line (5000 cells per well), and MDA-MB-453 human breast cancer cell line (3000 cells per well) were seeded into 96-well plate. The final concentrations range was 1––200 μM. The final concentration of DMSO solvent never exceeded 0.5 %, which was non--toxic to the cells. All concentrations were set up in triplicate. The cultures were incubated for 72 h.

Molecular docking simulation

To reveal the type of interaction of synthesized compounds against target receptor, the following procedures have been applied. First, using Biovia Draw academic version, the 2D structure of input ligands were generated and then converted to "*.pdb*" format using OpenBabel and Avogadro tools. Next, polar hydrogens were added to the structure of these ligands and 3D geometries were optimized using Hyperchem software. Crystal structure of human *α*-Glc (ID: 5NN8)[26] was taken up from the Protein Data Bank (PDB). Water molecules and other types of unwanted atoms were deleted from the structure of the obtained receptor and using Modeller 9.21 software, missing residues were fixed. AutoDock tools version 2.4.6 was applied for docking analysis. The coordination of grid box parameters including x = = 19.023, y = 23.328 and z = 23.3467 was fixed up based upon the location of target active site residues. Lamarckian genetic algorithm was applied for docking searches and other parameters of docking simulation were considered based on default options.[27] To enhance the reliability of docking outcomes, the applied docking procedure was repeated three times and no violation was observed for the prepared results.

Molecular dynamics (MD) simulation

In order to determine all dimensions of possible biological interactions between synthesized carbamate derivatives and human α-Glc enzyme, MD simulation using GROMACS 5.1.2 tool was performed using GPU support. All calculations including geometry optimization, minimization, NVT/NPT equilibration were performed for all docked complexes. GROMOS96 43A1 force field was applied for protein–ligand complexes. Enough water molecules were added to the predefined simulation box and sodium and chloride ions were used for neutralization of prepared systems. By setting the Langevin dynamics at 300 K, the whole system temperature was controlled. Default parameters were applied for performing the NVT/ /NPT ensemble simulations.[28] Overall, 50ns MD simulation was performed for all of the prepared ligand–protein complexes and for the evaluation of MD results; the generated MD trajectories were analysed to produce final graphs and interpretation of generated results.

RESULTS AND DISCUSSION

The mild and scalable method for Hofmann rearrangement of carboxamides that we previously published, is suitable for the synthesis of wide variety of carbamates.[23] Nevertheless, the important method drawbacks were relatively high amounts of reagents NBA and $LiOH \cdot H_2O$ and 24–48 h reaction time, especially in the case of complex carboxamides. Even though, these reagents can be considered as easy affordable, economizing in terms of quantity is always favourable, from both financial and ecological point of view. Furthermore, reducing the reaction time is with no doubt one of the ever-present goals in synthetic chemistry. Our attempts to make this procedure greener, cost and time more effective, led to a substantial improvement in the synthesis of complex carbamates.[29] Important changes included reducing the amount of reagents, but even more reaction time, *i.e.*, from 24–48 h to 5 min, by increasing the temperature from 25 to 65 °C. We then decided to extend the improved method on the production of simple carbamates for the purposes of this research. The amounts of reagents sufficient for the reaction completion were found to be comparable with our previously reported synthesis of simple carbamates, albeit all reactions were completed within the 5 min.[23] Thus, carbamates **1**–**5** (Fig. 1) were obtained in high yields starting from readily available carboxamides (Scheme 1). The products of Hofmann rearrangement of NBA itself, were not observed, regardless of the known temperature dependent stability of NBA under basic conditions.

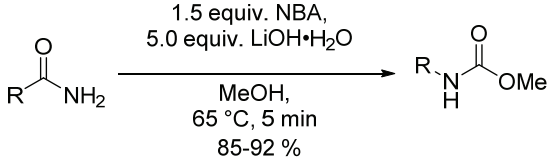

R = CH_2=CH_2(CH_2)$_8$, **1**; $PhCH_2$, **2**; Ph, **3**; 3-MePh, **4**; 2-EtOPh, **5**

Scheme 1. Synthetic procedure for carbamates **1**–**5**.

Previously, the antidiabetic potential of different carbamates, which expressed high *α*-Glc inhibitory activity was disclosed.[8] Encouraged by these results we decided to extend the research toward simpler carbamate derivatives that were part of our library of compounds (Fig. 1). Compounds **1**–**5** were examined for their *α*-Glc inhibitory activity, together with acarbose (Fig. 1), a commercial FDA-approved antidiabetic drug, which was used as a standard for the assays. According to the obtained results, all studied compounds expressed higher *α*-Glc inhibitory activity than acarbose (Table I). These results are consistent with our previously published data on carbamate derivatives and some imidazo[1,2-*a*]pyridines linked to carbamate group,[8,20] underlying the importance of carbamate moiety for *α*-Glc inhibitory activity.

Encouraged by the reported anti-cancer activities of some carbamate derivatives,[28] the compounds **1**–**5** were additionally examined for *in vitro* cytotoxic effect against HeLa, A549 and MDA-MB-453 human tumor cell lines, using MTT assay. The obtained results indicated that compounds **1**, **4** and **5** possess moderate anticancer activity, while compounds **2** and **3** did not show anticancer activity up to the tested concentration of 200 μM. The highest activities were observed for compounds **1** and **5** against A549 and MDA-MB-453 cell lines, respectively (Table I). This was in accordance with our previously published results suggesting that even though there is some anticancer potential in this kind of carbamate derivatives, some significant structural modifications have to be made to improve their anticancer efficiency.[8]

TABLE I. *In vitro* *α*-Glc inhibitory activity, cytotoxic effect and calculated binding affinities of compounds **1**–**5**; results are presented as a mean ± *SD*

Compd.	α-Glc inhibiton (IC_{50} / μM)[a]	Calc. bind. affinity kJ mol^{-1}	MTT assay (IC_{50} / μM)		
			HeLa	A549	MDA-MB-453
1	79.65±1.82	–33.47	132.27±1.91	111.64±29.54	136.53±5.39
2	65.34±1.64	–37.24	>200	>200	>200
3	68.55±0.09	–34.73	>200	>200	>200
4	69.26±2.71	–37.66	159.02±9.18	180.15±9.65	146.99±10.09
5	79.89±1.16	–42.68	167.49±13.23	162.68±6.41	118.96±17.54
Acarbose[a]	109.71±1.19	–41.84	–	–	–

[a]Acarbose was used as a standard drug in *α*-Glc inhibition assay

In order to obtain insight in the binding mode of the examined carbamates and *α*-Glc, molecular docking was performed. According to the docking analysis, the studied compounds established acceptable binding energies with the *α*-Glc active site, being surrounded by catalytic and binding amino acids of the active site (Table I). The crystallographic analysis of *α*-Glc active site, revealed several amino acid residues including Trp376, Asp404, Ile441, Trp516, Asp518, Met519, Arg600, Trp613, Asp616, Phe649 and His674, that play a quintessential

role in the catalytic process.[26] Accordingly, the interactions of inhibitors with these residues can cause conformational change in the α-glucosidase active site, thus preventing the biological function of the enzyme. All of the tested carbamates were stabilised by the conventional hydrogen bonds with some of the α-Glc active site residues (Fig. 2).

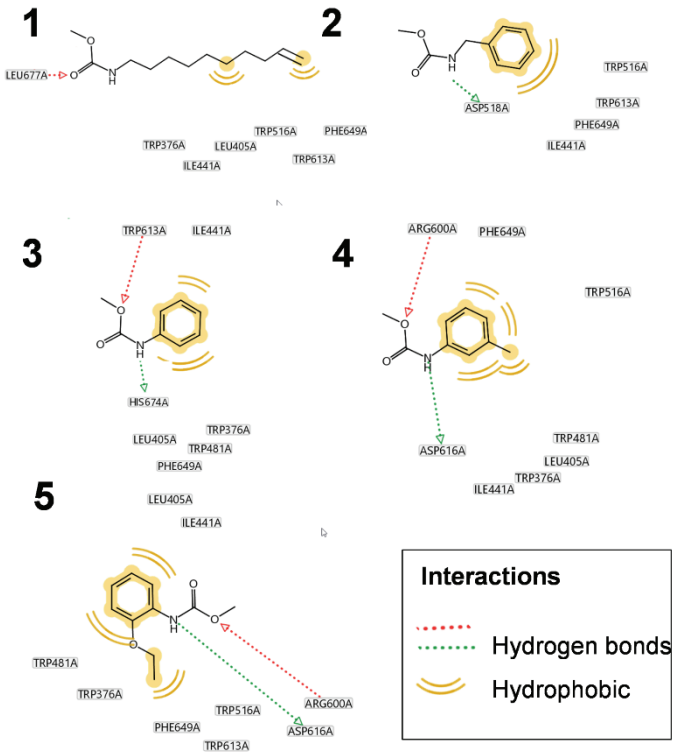

Fig. 2. Graphical presentation of interactions between α-Glc residues and carbamates **1**–**5** in their most stable conformations.

The hydrophobic interactions were also seen to contribute to binding stability. The highest calculated binding affinity was found for the compound **5** (Table I), afforded through the multiple interactions with α-Glc, including conventional hydrogen bonds with Asp616 and Arg600 residues. Compound **5** complexed with glucosidase was found to be more stable than α-Glc complexed with acarbose, a confirmed α-Glc inhibitor. The superimposition of these two molecules in Fig. 3 shows that they are close enough to create hydrogen bonds with the identical critical residues from the α-Glc active catalytic site, Asp616 and Arg600. The most stable conformation of compound **4** in complex with α-Glc was also stabilised by these residues, whereas compounds **1**–**3** maintained

significant stability in complex with *α*-Glc *via* hydrogen bonds with Leu677, Asp518, His674 and Trp613, respectively.

In comparison with **4** and **5**, the other tested carbamates lacked certain chemical features for a favourable mode of interaction in the active site of the *α*-Glc. These features were defined through the pharmacophore model presented in the Fig. 4, which shows that the carbamate –NH group acted as a hydrogen bond donor while the carbamate $–OCH_3$ served as a hydrogen bond acceptor. Furthermore, the aromatic rings additionally stabilised complexes through the hydrophobic interactions.

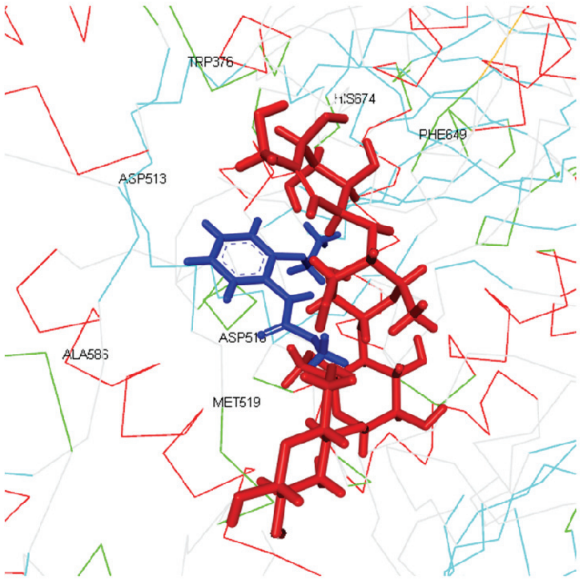

Fig. 3. Compound **5** (blue) and acarbose (red) structures superimposed at the *α*-Glc active site.

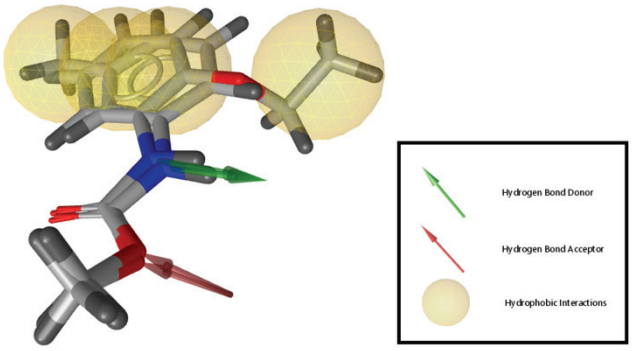

Fig. 4. Chemical features of superimposed carbamates **4** and **5** for favorable binding mode with α-Glc.

MD simulations were conducted in order to compare the structural changes of ligand–enzyme complexes. As depicted in Fig. 5, in comparison to the native, ligand free enzyme, significant structural changes were observed for ligand–protein complexes. Root mean square deviation (*RMSD*) plot of MD simulations indicated that the compounds **3**–**5** obviously decreased the *RMSD* value of protein–ligand complexes in comparison to the native protein. The highest decrease of *RMSD* value was observed for compound **3** while compounds **1** and **2** partially increased the *RMSD* value (Fig. 5A and B).

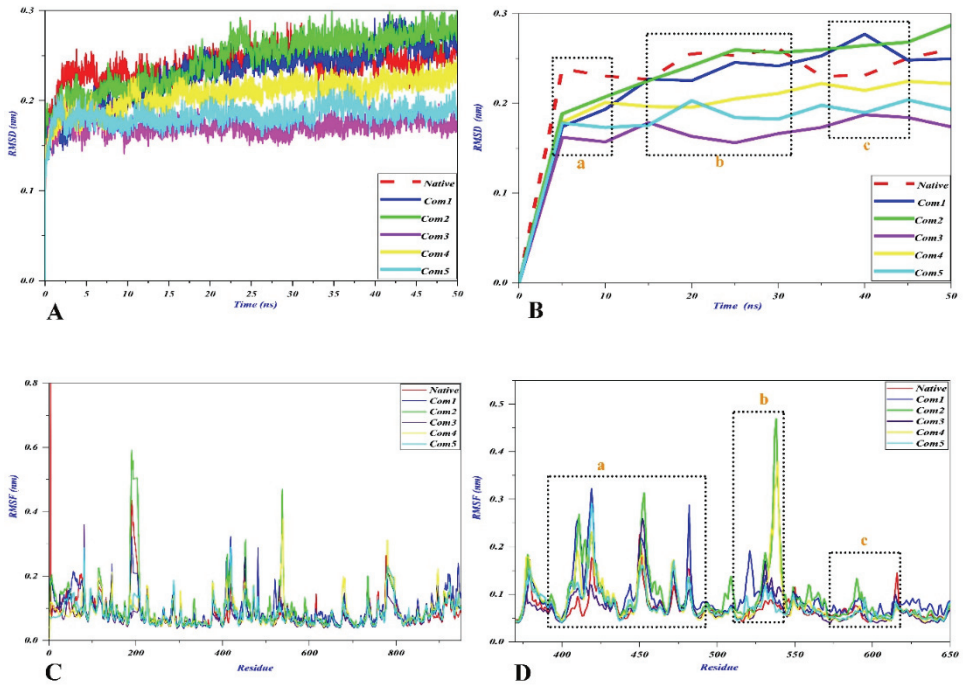

Fig. 5. *RMSD* and *RMSF* plots of studied carbamate derivatives: A) compressed view of *RMSD* curves for ligand–protein complexes vs. native protein; B) close view of *RMSD* curves of studied complexes; C) *RMSF* plot of entire protein residues; D) *RMSF* plot of active site residue.

As illustrated in Fig. 5B, the *RMSD* score has been changed in three regions namely a, b and c. In the first 10 ns of MD simulations, all docked compounds decreased *RMSD* curve with compound **3** causing the major changes for this time-period. Afterwards, between times the series of 15 and 33 ns, *RMSD* curves of each protein–ligand complex fairly changed and it seems that during this period of time the target complexes reached a primary stabilization phase.

After 40 ns (region c, Fig. 5B), the biggest changes of *RMSD* values were observed for the complexes **1** and **2** whereas in this time-period the protein and complexes **3**–**5** showed partial decrease in their *RMSD* curves. Overall, after 10 ns, all of the complexes reached a stabilised condition, though during the MD process several changes were observed for their *RMSD* values. Because *RMSD* plot quantitatively measures the average distances between backbone atoms of a protein (or a group of atoms), it can determine the possible conformational changes of either ligands or proteins, whenever they are bound to other types of macromolecules.[31] Based on the chemical essence of simulated bio-macromolecules, *RMSD* values can possess higher or lower scores. Indeed, the numerical values of *RMSD* plot also demonstrated how ligand–protein complexes may move between folded and unfolded states.[31]

Plots C and D of Fig. 5 indicated the root mean square fluctuation (*RMSF*) values changes for the protein backbone residues and the active site amino acids of *α*-Glc. As shown, all docked compounds violated the conformational pose of active site residues. Accordingly, these results have proven that the interacted carbamate derivatives were able to approach the active site residues and bind to their side chains atoms. Basically, the conformational changes in the side chain of amino acids after the interaction with inhibitor ligands can disrupt the biological activity of target enzyme. The numerical values of *RMSF* plot suggest the total flexibility (or fluctuation) of protein residues during MD simulation. The total fluctuation of protein residues towards backbone atoms or chemical moieties of nearby ligands may predict the tendency of target amino acids for further chemical interactions. *RMSF* per residue plot showed the enhanced active site residue flexibility for all tested compounds (Fig. 5D) compared to the native enzyme which is known to decrease enzyme kinetic stability.[32]

The solvent accessible surface area (*SASA*) plot is another output of MD simulation to determine how protein–ligand complexes may behave during MD process. Any change in *SASA* of proteins determines how much surface of a protein is exposed to the solvent. According to the Fig. 6A–D, carbamates **1**–**4** significantly changed the numerical values of *SASA* plot in comparison to the native protein. In the regions a1–a4, the fingerprinting of several changes can be followed. The compound **2**–*α*-Glc complex, which had the greatest *SASA* value, exemplifies these shifts the most. This suggests that the number of hydrophobic residues that can be solvent-accessible and the interaction with their molecules has increased significantly. In addition, the *SASA* values for the protein complexes containing carbamates **1**–**4** were unstable during MD. The instability was particularly noticeable in areas a1 and a2 (Fig. 6B and C), indicating that the *α*-Glc surface underwent considerable conformational changes while interacting with these carbamates. During MD simulation however, the compound **5** *SASA*

plot remained relatively stable, implying a mode of interaction with the α-Glc active site that prevented significant protein structural changes.

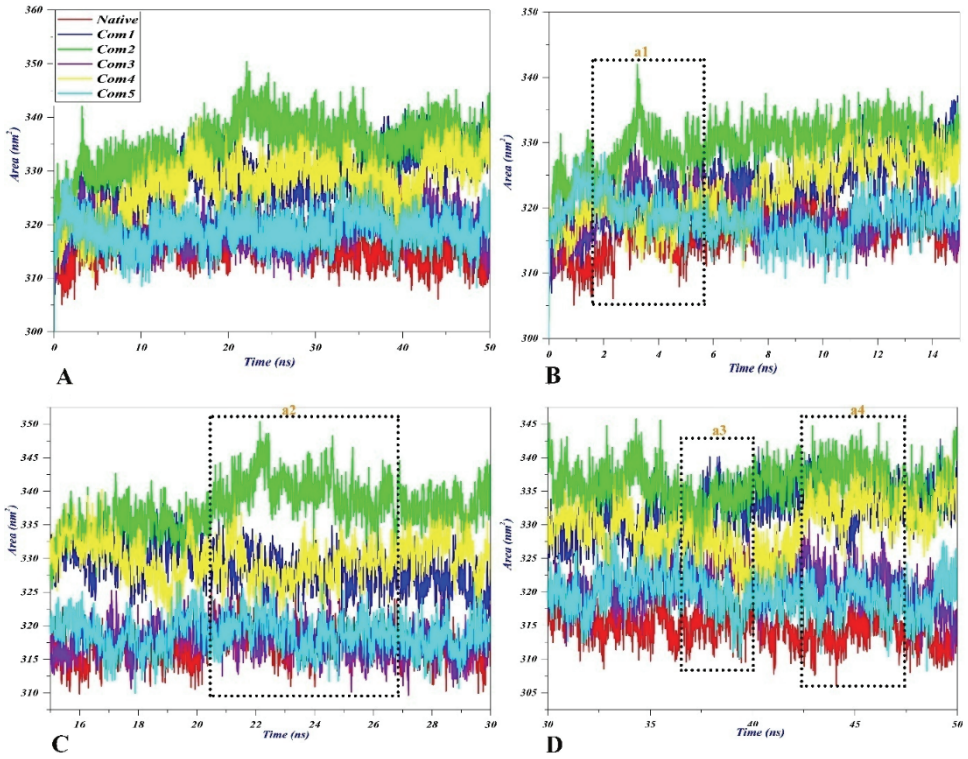

Fig. 6. *SASA* plots of studied complexes during time-period of 50 ns MD simulation: A) the total changes of *SASA* during the time from 0 to 50 ns; B) *SASA* changes between 0 and 15 ns; C) observed changes between 15 and 30 ns; D) changes between 30 and 50 ns.

CONCLUSION

The α-Glc inhibitory activity of five carbamate derivatives was investigated *in vitro* and according to the obtained results, the examined carbamates were able to inhibit the normal action of the enzyme, showing the IC_{50} values lower than the standard drug, acarbose. Computational analysis revealed that all tested compounds exhibited high binding affinities and had a considerable impact on the flexibility of the α-Glc active site residues. However, a favourable binding mode was confirmed only for compounds **4** and **5**, making their pharmacophore model, composed of two hydrophobic, one hydrogen acceptor and one hydrogen donor features, a potential model for the development of novel carbamate derivatives, glucosidase inhibitors with higher glucosidase IC_{50} values.

The preliminary toxicity profiles of studied derivatives against three cancerous cell lines indicated their poor activity, suggesting that some significant structural modifications have to be made to improve their anticancer efficiency.

The results of the present study indicate that the examined derivatives were able to virtually or experimentally interact with an important target of DM type 2. The current results corroborate well with the previously published data in the analysis of the potential of this class of compounds as potential new antidiabetic drugs. In spite of that, the additional examples of simple carbamate derivatives should be examined for efficient SAR analysis.

SUPPLEMENTARY MATERIAL

Additional data and information are available electronically at the pages of journal website: https://www.shd-pub.org.rs/index.php/JSCS/article/view/12085, or from the corresponding author on request.

Acknowledgements. This work was financially supported by the Ministry of Education, Science and Technological Development of the Republic of Serbia (Grants No. 451-03-68/ /2022-14/200026 and 451-03-68/2022-14/200043). Authors express their appreciation to MSc Hassan Rasouli for valuable help in performing computational studies and profound manuscript revision.

И З В О Д

АНТИДИЈАБЕТСКИ ПОТЕНЦИЈАЛ ЈЕДНОСТАВНИХ КАРБАМАТА: КОМПАРАТИВНА ЕКСПЕРИМЕНТАЛНА И РАЧУНАРСКА СТУДИЈА

РЕЉА В. СУРУЧИЋ[1], ИВАНА И. ЈЕВТИЋ[2], ТАТЈАНА П. СТАНОЈКОВИЋ[3] и ЈЕЛЕНА Б. ПОПОВИЋ-ЂОРЂЕВИЋ[4]

[1]Универзитет у Бања Луци-Медицински факултет, Саве Мркаља 14, 78000 Бања Лука, Босна и Херцеговина, [2]Универзитет у Београду-Институт за Хемију, Технологију и Металургију, Центар за Хемију, Његошева 12, 11000 Београд, [3]Универзитет у Београду-Институт за Онкологију и Радиологију Србије, Пастерова 14, 11000 Београд и [3]Универзитет у Београду-Пољопривредни факултет, Катедра за Хемију и Биохемију, Немањина 6, 11080 Београд

Са порастом појаве дијабетеса типа 2 у свету, јавља се потрага за новим лековима са што ефикаснијим фармаколошким профилом. Као део овог истраживања, приказана је синтеза, фармаколошко *in vitro* и рачунарско испитивање пет карбамата једноставне структуре, као инхибитора – глукозидазе, ензима који учествује у дигестивном разлагању шећера. Резултати експерименталног испитивања показали су да испитивани карбамати инхибирају активност – глукозидазе са задовољавајућим IC_{50} вредностима у опсегу од 65,34 до 79,89 μM, а у поређењу са стандардним леком, акарбозом (109,71 μM). Такође, *in silico* методом добијене су значајне енергије везивања за активно место – глукозидазе. У прелиминарном испитивању цитотксичности према три типа канцерозних ћелија, карбамати су показали лошу активност, сугеришући да су потребне значајне структурне промене за побољшање њиховог антиканцерозног дејства. Уопштено говорећи, резултати ове студије показали су да су испитивани карбамати успешно виртуелно и експериментално интераговали са важном метом код дијабетеса типа 2. Такође је предложен и нови фармакофорни модел за -глукозидазу, који укључује карбаматну –NH групу као донора водоничне везе, затим карбаматну $–OCH_3$ групу као акцептора водоничне везе, а такође и стабилизујуће хидрофобне интеракције ароматичних прстенова.

(Примљено 23. септембра 2022, ревидирано 16. фебруара, прихваћено 8. септембра 2023)

REFERENCES

1. X. Lin, Y. Xu, X. Pan, J. Xu, Y. Ding, X. Sun, X. Song, Y. Ren, P.-F. Shan, *Sci. Rep*. **10** (2020) 14790 (https://doi.org/10.1038/s41598-020-71908-9)
2. H. Rasouli, R. Yarani, F. Pociot, J. P. Popović-Djordjević, *Pharmacol. Res*. **155** (2020) 104723 (https://doi.org/10.1016/j.phrs.2020.104723)
3. J. Størling, F. Pociot, *Genes* **8** (2017) 72 (https://doi.org/10.3390/genes8020072)
4. R. V. Cohen, J. C. Pinheiro, C. A. Achiavon. J. E. Salles, B. L. Wajchenberg, D. E. Cummings, *Diabetes Care* **35** (2012) 1420 (https://doi.org/10.2337/dc11-2289)
5. N. S. Artzi, S. Shilo, E. Hadar, H. Rossman, S. Barbash-Hazan, A. Ben-Haroush, R. D. Balicer, B. Feldman, A. Wiznitzer, E. Segal, *Nat. Med.* **26** (2020) 71 (https://doi.org/10.1038/s41591-019-0724-8)
6. J. B. Popovic-Djordjevic, I. I. Jevtić, T. P. Stanojkovic, *Curr. Med. Chem.* **25** (2018) 2140 (https://doi.org/10.2174/0929867325666171205145309)
7. H. Rasouli, R. Khodarahmi, S. Mohammad, B. Hosseini Ghazvini, H. Adibi, *Food Funct.* **8** (2017) 1942 (https://doi.org/10.1039/C7FO00220C)
8. J. B. Popović-Djordjević, I. I. Jevtić, N. Dj. Grozdanić, S. B. Šegan, M. V. Zlatović, M. D. Ivanović, T. P. Stanojković, *J. Enz. Inhib. Med. Chem.* **32** (2017) 298 (https://doi.org/10.1080/14756366.2016.1250754)
9. J. N. Gorantla, S. Maniganda, S. Pengthaisong, L. Ngiwsara, P. Sawangareetrakul, S. Chokchaisiri, P. Kittakoop, J. Svasti, J. R. Ketudat Cairns, *ACS Omega* **6** (2021) 25710 (https://doi.org/10.1021/acsomega.1c03928)
10. N. Kausar, S. Ullah, M. Aqeel Khan, H. Zafar, A.-t.-Wahab, M. I. Choudhary, S. Yousuf, *Bioorg. Chem.* **106** (2021) 104499 (https://doi.org/10.1016/j.bioorg.2020.104499)
11. A. K. Ghosh, M. Brindisi, *J. Med. Chem.* **58** (2015) 2895 (https://doi.org/10.1021/jm501371s)
12. M. Chandrasekhar, G. S. Prasad, C. Venkataramaiah, C. Naga Raju, K. Seshaiah, W. Rajendra, *Mol. Divers.* **23** (2019) 723 (https://doi.org/10.1007/s11030-018-9906-4)
13. J. Ma, N. Lu, W. Quin, R. Xu, Y. Wang, X. Chen, *Ecotoxicol. Environ. Saf.* **63** (2006) 268 (https://doi.org/10.1016/j.ecoenv.2004.12.002)
14. M. D. Stephens, N. Yodsanit, C. Melander, *Org. Biomol. Chem.* **14** (2016) 6853 (https://doi.org/10.1039/C6OB00706F)
15. S. Clarke, F. Mulcahy, *HIV Medicine* **1** (2000) 15 (https://doi.org/10.1046/j.1468-1293.2000.00004.x)
16. C. Fortin, V. Joly, *Expert Rev. Anti Infec. Ther.* **2** (2004) 671 (https://doi.org/10.1586/14789072.2.5.671)
17. N. Y. Rakhmanina, J. N. Van den Anker, *Expert Opin. Drug Metab. Toxicol.* **6** (2010) 95 (https://doi.org/10.1517/17425250903483207)
18. N. Pathak, K. Fatima, S. Singh, D. Mishra, A. C. Gupta, Y. Kumar, D. Chanda, D. U. Bawankule, K. Shanker, F. Khan, A. Gupta, S. Luqman, A. S. Negi, *J. Steroid Bioch. Mol. Biol.* **194** (2019) 105457 (https://doi.org/10.1016/j.jsbmb.2019.105457)
19. U. Košak, N. Strašek, D. Knez, M. Jukič, S. Žakelj, A. Zahirović, A. Pišlar, X. Brazzlotto, F. Nachon, J. Kos, S. Gobec, *Eur. J. Med. Chem.* **197**(2020) 112282 (https://doi.org/10.1016/j.ejmech.2020.112282)
20. M. Saeedi, M. Raeeisi-Nafchi, S. Sobhani, S. S. Mirfazli, M. Zardkanlou, S. Mojtabavi, M. A. Faramarzi, T. Akbarzadeh, *Mol. Divers.* **25** (2021) 2399 (https://doi.org/10.1007/s11030-020-10137-8)
21. J. D. Durrant, J. A. McCammon, *BMC Biol.* **9** (2011) 1 (https://doi.org/10.1186/1741-7007-9-71)

22. J. E. Kerrigan, in *In Silico Models for Drug Discovery. Methods in Molecular Biology (Methods and Protocols)*, S. Kortagere, Ed., Humana Press, Totowa, NJ, 2013, p. 95 (https://doi.org/10.1007/978-1-62703-342-8_7)
23. I. I. Jevtić, Lj. Došen-Mićović, E. R. Ivanović, M. D. Ivanović, *Synthesis* **48** (2016) 1550 (https://doi.org/10.1055/s-0036-1588985)
24. P. Mccue, Y. I. Kwon, K. Shetty, *J. Food Biochem*. **29** (2005) 278 (https://doi.org/10.1111/j.1745-4514.2005.00020.x)
25. V. Marković, N. Debeljak, T. Stanojković, B. Kolundžija, D. Sladić, M. Vujčić, B. Janović, N. Tanić, M. Perović, V. Tešić, J. Antić, M. D. Joksović. *Eur. J. Med. Chem*. **89** (2015) 401 (https://doi.org/10.1016/j.ejmech.2014.10.055)
26. V. Roig-Zamboni, B. Cobucci-Ponzano, R. Iacono, M. Carmina Ferrara, S. Germany, Y. Bourne, G. Parenti, M. Moracci, G. Sulzenbacher, *Nat. Commun*. **8** (2017) 1 (https://dx.doi.org/10.1038%2Fs41467-017-01263-3)
27. H. R. Mohammadi-Motlagh, Y. Shokohina, M. Majarrab, H. Rasouli, A. Mostafaie, *Biomed. Pharmacother.* **93** (2017) 117 (https://doi.org/10.1016/j.biopha.2017.06.013)
28. H. Rasouli, M. Mehrabi, S. S. Arab, R. Khodarahmi, *J. Iran. Chem. Soc.* **14** (2017) 2023 (https://doi.org/10.1007/s13738-017-1140-y)
29. I. I. Jevtić, K. Savić Vujović, D. Srebro, S. Vučković, M. D. Ivanović, S. V. Kostić-Rajačić, *Pharmacol. Rep.* **72** (2020) 1069 (https://doi.org/10.1007/s43440-020-00121-2)
30. V. Janganati, N. Reddy Penthala, N. Reddy Madadi, Z. Chen, P.A. Crooks, *Bioorg. Med. Chem. Lett*. **24** (2014) 3499 (https://doi.org/10.1016/j.bmcl.2014.05.059)
31. I. Kufareva, R. Abagyan, *Methods of Protein Structure Comparison* in *Homology Modeling. Methods in Molecular Biology (Methods and Protocols)*, A. Orry, R. Abagyan, Eds., Humana Press, Totowa, NJ, 2011, p. 231 (https://doi.org/10.1007/978-1-61779-588-6_10)
32. Y. Xie, J. An, G. Yang, G. Wu, Y. Zhang, L. Cui, Y. Feng, *J. Biol. Chem*. **289** (2014) 7994 (https://doi.org/10.1074/jbc.M113.536045).

Journal of the Serbian Chemical Society
JSCS@tmf.bg.ac.rs • www.shd.org.rs/JSCS
J. Serb. Chem. Soc. 88 (11) S318–S325 (2023) *Supplementary material*

SUPPLEMENTARY MATERIAL TO

Antidiabetic potential of simple carbamate derivatives: Comparative experimental and computational study

RELJA V. SURUČIĆ[1], IVANA I. JEVTIĆ[2], TATJANA P. STANOJKOVIĆ[3] and JELENA B. POPOVIĆ-DJORDJEVIĆ[4]*

[1]*University of Banja Luka, Faculty of Medicine, Save Mrkalja 14, 78000 Banja Luka, Bosnia and Herzegovina,* [2]*University of Belgrade-Institute of Chemistry, Technology and Metallurgy, Department of Chemistry, Njegoševa 12, 11000 Belgrade, Serbia,* [3]*University of Belgrade-Institute for Oncology and Radiology of Serbia, Pasterova 14,11000 Belgrade, Serbia and* [4]*University of Belgrade-Faculty of Agriculture, Department of Chemistry and Biochemistry, Nemanjina 6, 11080 Belgrade, Serbia*

J. Serb. Chem. Soc. 88 (11) (2023) 1089–1102

SPECTROSCOPIC DATA AND YIELDS OF SYNTHESIZED COMPOUNDS 1-5

Methyl dec-9-en-1-ylcarbamate [**1**] Yield: 0.30 g (92 %); pale yellow oil. ^{1}H NMR (200 MHz, $CDCl_3$): δ= 5.81 (ddt, J = 16.9, 10.1, 6.6 Hz, 1H), 5.08 – 4.87 (m, 2H), 4.80 (br s, 1H), 3.66 (s, 3H), 3.16 (dd, J = 13.1, 6.5 Hz, 2H), 2.13 – 1.94 (m, 2H), 1.61 – 1.17 (m, 12H) ppm. ^{13}C NMR (50 MHz, $CDCl_3$): δ=157.1, 139.1, 114.1, 51.9, 41.0, 33.7, 29.9, 29.2, 29.1, 28.9, 28.8, 26.6 ppm. (+)ESI-ToF-HRMS m/z: calculated for [$C_{12}H_{23}NO_2$ + H+] 214.18016, observed 214.17992.

The spectra are in accordance with the previously reported data.[1]

Methyl benzylcarbamate [**2**] Yield: 0.25 g (86 %); white amorphous solid; mp: 65 °C. ^{1}H NMR (200 MHz, $CDCl_3$): δ= 7.46 – 7.10 (m, 5H), 5.19 (br s, 1H), 4.34 (d, J = 6.0 Hz, 2H), 3.67 (s, 3H) ppm. ^{13}C NMR (50 MHz, $CDCl_3$): δ= 157.1, 138.5, 128.5, 127.4, 52.0, 44.9 ppm. (+)ESI-ToF-HRMS m/z: calculated for [$C_9H_{11}NO_2$ + H+] 166.08626, observed 166.08596.

The spectra are in accordance with the previously reported data.[1]

Methyl phenylcarbamate [**3**] Yield 0.52 g (90 %); white powder; mp: 47 °C. ^{1}H NMR (200 MHz, $CDCl_3$): δ= 7.67 (br. s, 1H), 7.37 (ddd, J = 4.4, 3.3, 1.8 Hz, 2H), 7.30 – 7.12 (m, 2H), 7.03 – 6.90 (m, 1H), 3.63 (s, 3H) ppm. ^{13}C NMR (50 MHz, CD_3CN): δ= 155.6, 140.2, 130.2, 124.3, 119.9, 52.9 ppm. (+)ESI-ToF-HRMS m/z: calculated for [$C_8H_9NO_2$ + H+] 152.07060, observed 152.07036.

The spectra are in accordance with the previously reported data.[1]

Methyl m-tolylcarbamate [**4**] Yield 0.33 g (92 %); Yield: 0.33 g (89 %); pale yellow solid; mp: 57-58°C. ^{1}H NMR (500 MHz, CD_3CN) δ = 7.67 (d; J = 0.7 Hz; 1H); 7.29 – 7.21 (m, 2H); 7.17 (t; J = 7.8 Hz; 1H); 6.91 – 6.82 (m; 1H); 3.69 (s; 3H); 2.30 (s; 3H) ppm. ^{13}C NMR (126 MHz, CD_3CN) δ = 155.6 (C=O); 140.2 (C); 140.1 (C); 130.1 (CH); 125.0 (CH);

* Corresponding author. E-mail: jelenadj@agrif.bg.ac.rs

120.5 (CH); 117.1 (CH); 53.0 (CH_3); 21.9 (CH_3) ppm. (+)ESI-ToF-HRMS m/z: calculated for [$C_9H_{11}NO_2$ + H+] 166.08626, observed 166.08653.

The spectra are in accordance with the previously reported data.[1]

Methyl (2-ethoxyphenyl)carbamate [**5**] Yield: 0.08 g (85 %); colorless oil. ^{1}H NMR (200 MHz, $CDCl_3$) δ = 8.20 – 7.95 (m; 1H); 7.26 (d; J = 2.2 Hz; 1H); 7.07 – 6.70 (m; 3H); 4.06 (q; J = 7.0 Hz; 2H); 3.78 (s; 3H); 1.42 (t; J = 7.0 Hz; 3H) ppm. ^{13}C NMR (50 MHz, $CDCl_3$) δ = 153.9 (C=O); 146.8 (C), 127.6 (C); 122.6 (CH); 120.9 (CH); 118.0 (CH); 110.8 (CH); 64.0 (CH_2); 52.1 (CH_3); 14.7 (CH_3) ppm. (+)ESI-ToF-HRMS m/z: calculated for [$C_{10}H_{13}NO_3$ + H+] 196.09682, observed 196.09680.

The spectra are in accordance with the previously reported data.[1]

NMR SPECTRA OF COMPOUNDS **1**–**5**

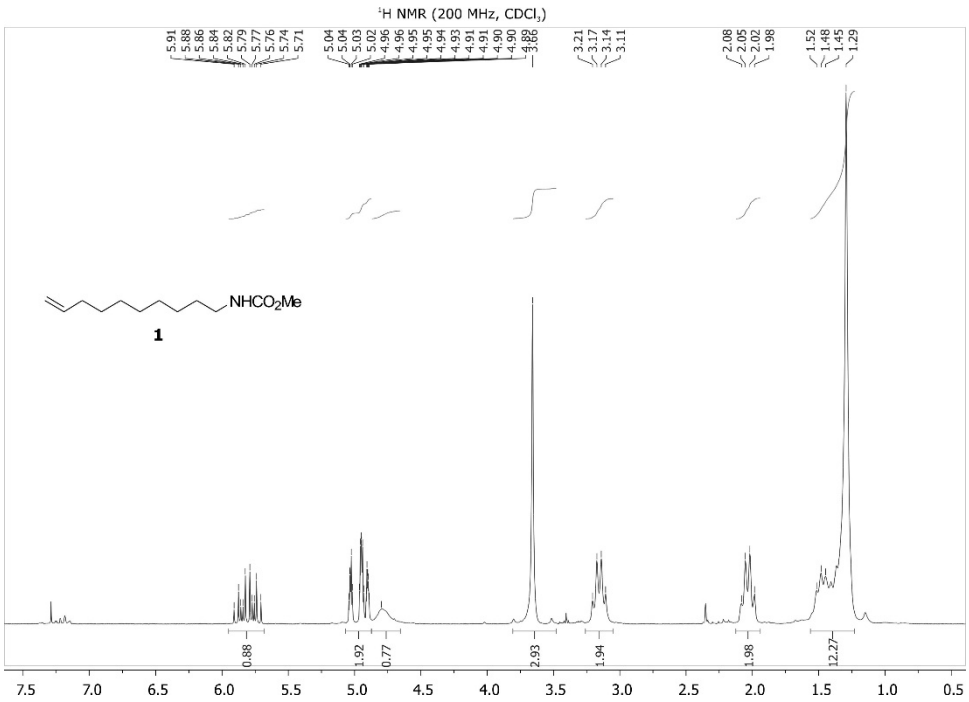

Figure S-1. ^{1}*H NMR of* methyl dec-9-en-1-ylcarbamate **[1]**

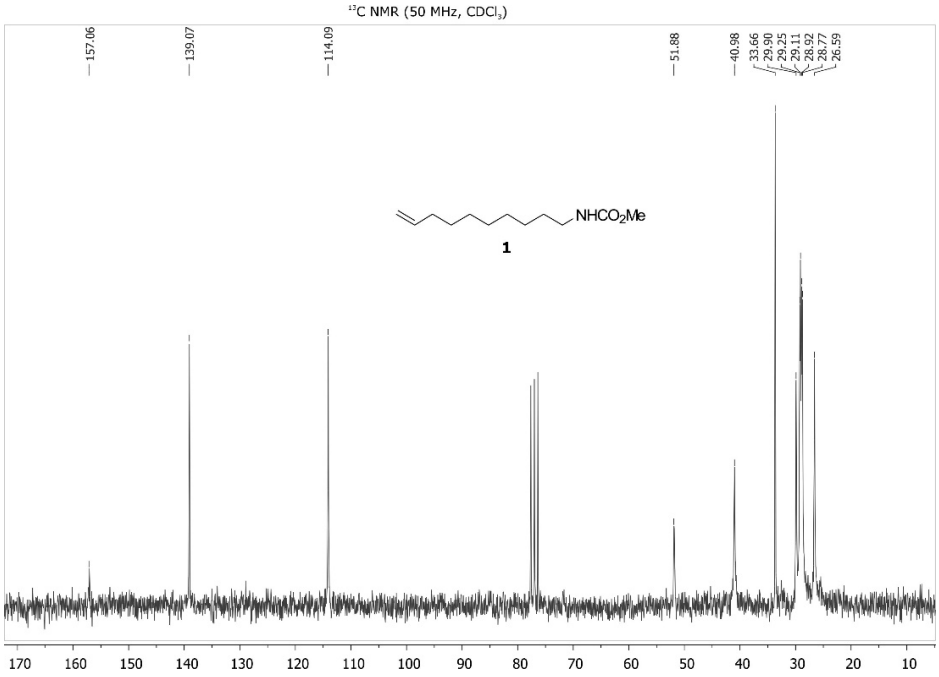

Figure S-2. ^{13}C NMR of methyl dec-9-en-1-ylcarbamate **[1]**

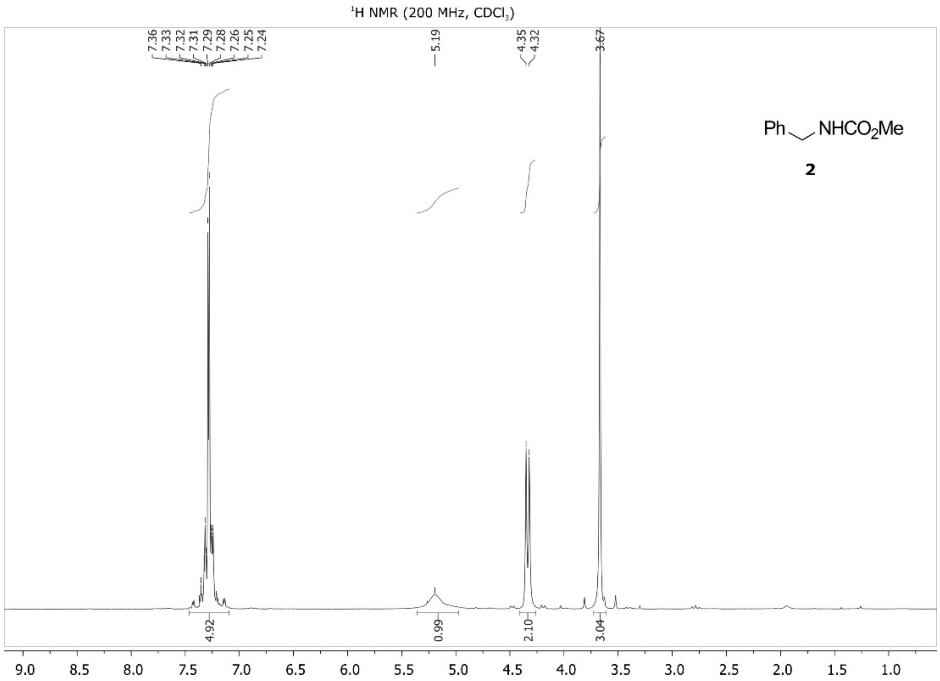

Figure S-3. ^{1}H NMR of methyl benzylcarbamate **[2]**

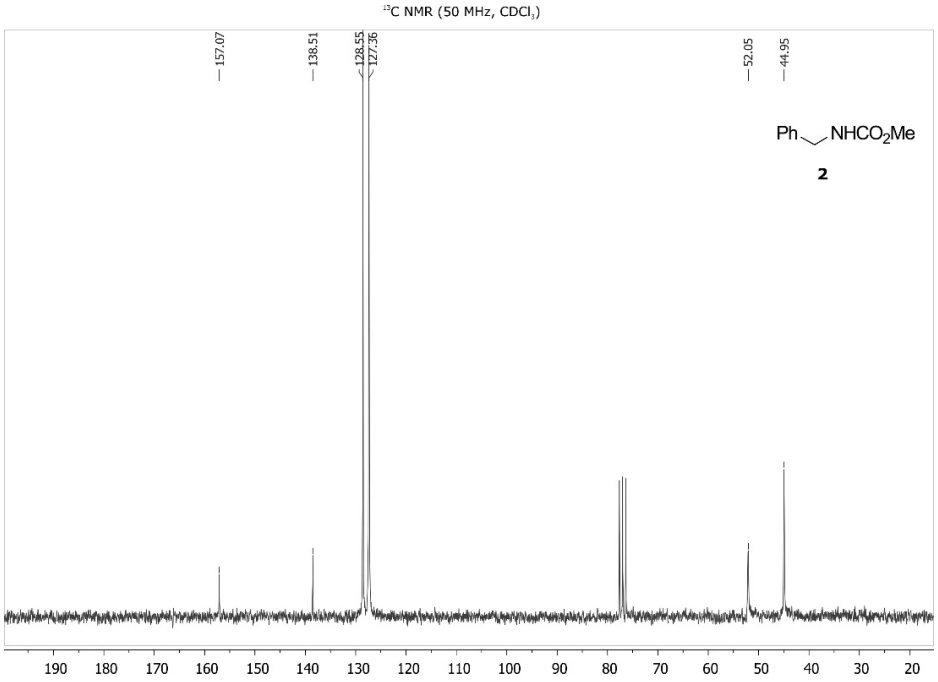

Figure S-4. ^{13}C NMR of methyl benzylcarbamate **[2]**

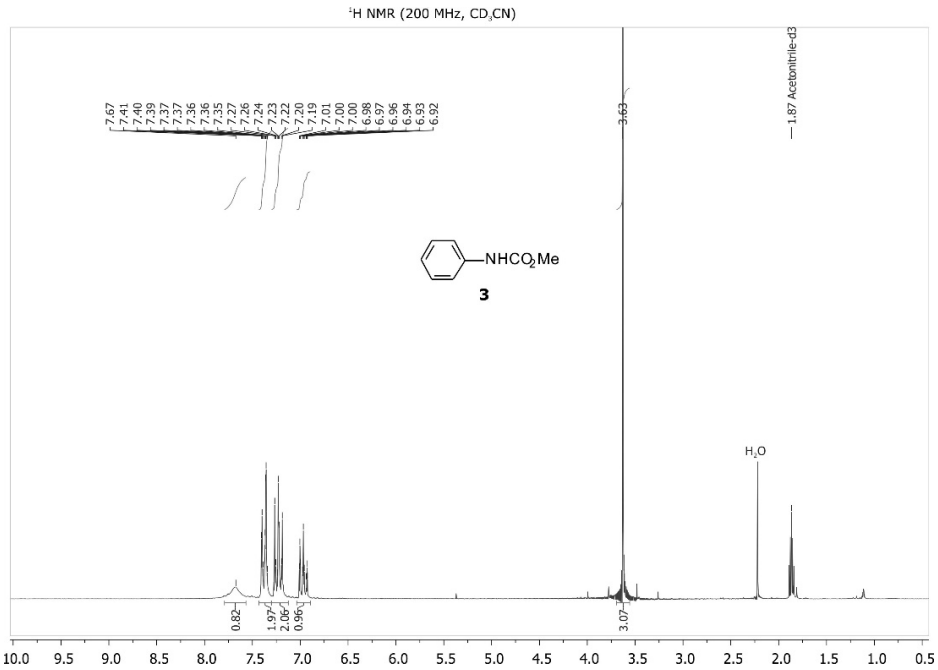

Figure S-5. ^{1}H NMR of methyl phenylcarbamate **[3]**

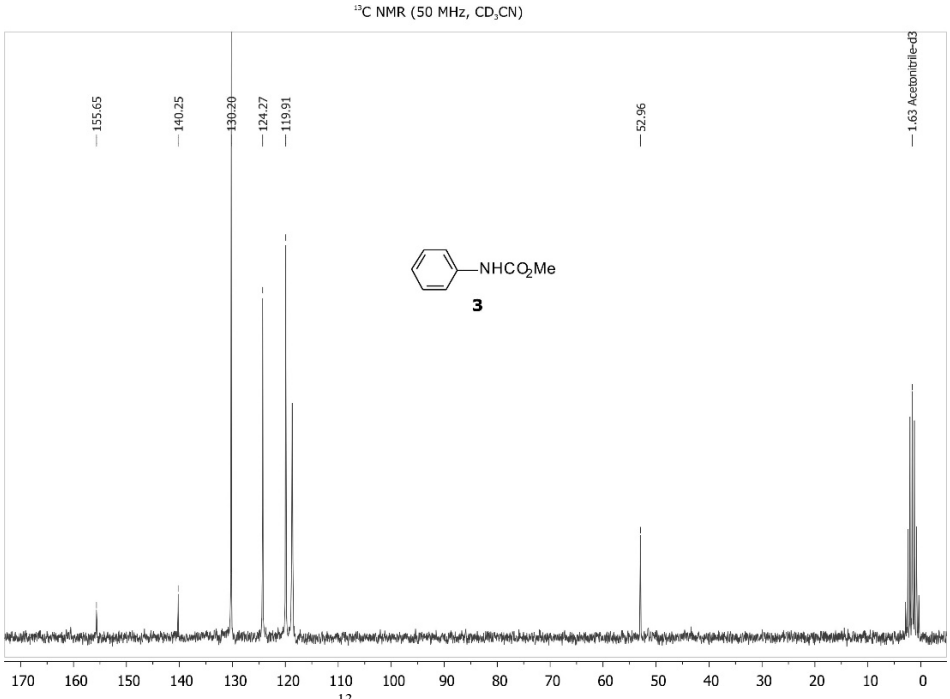

Figure S-6. ^{13}C NMR of methyl phenylcarbamate **[3]**

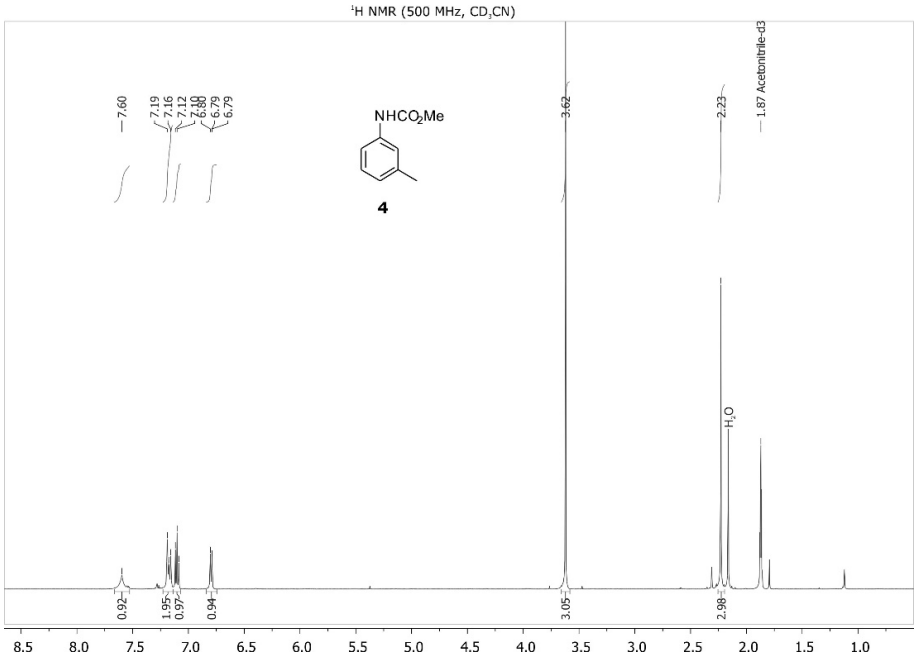

Figure S-7. ^{1}H NMR of methyl m-tolylcarbamate **[4]**

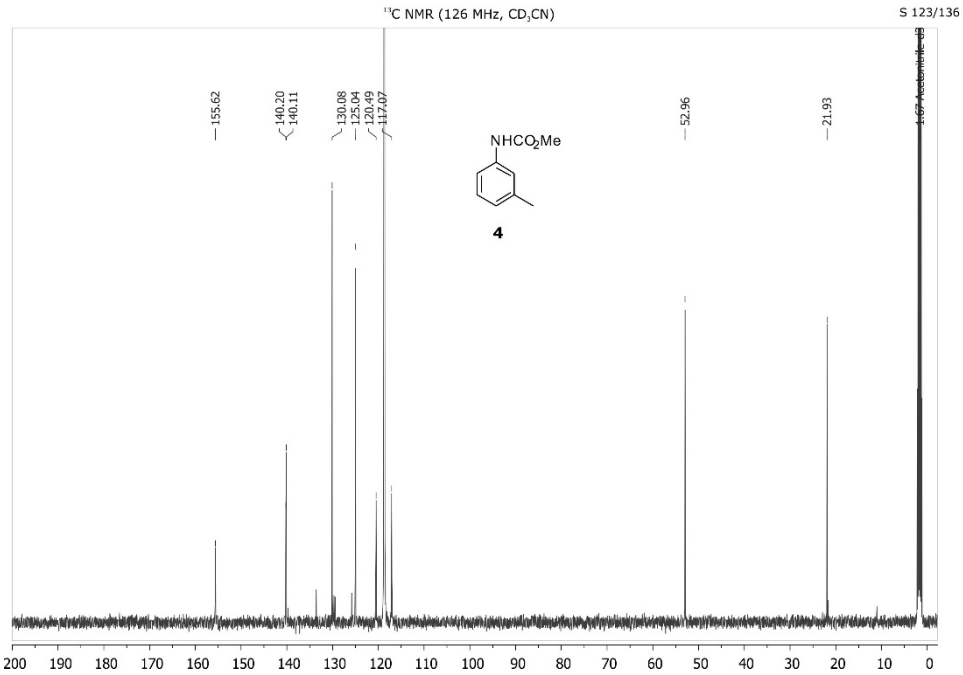

Figure S-8. ^{13}C NMR of methyl m-tolylcarbamate **[4]**

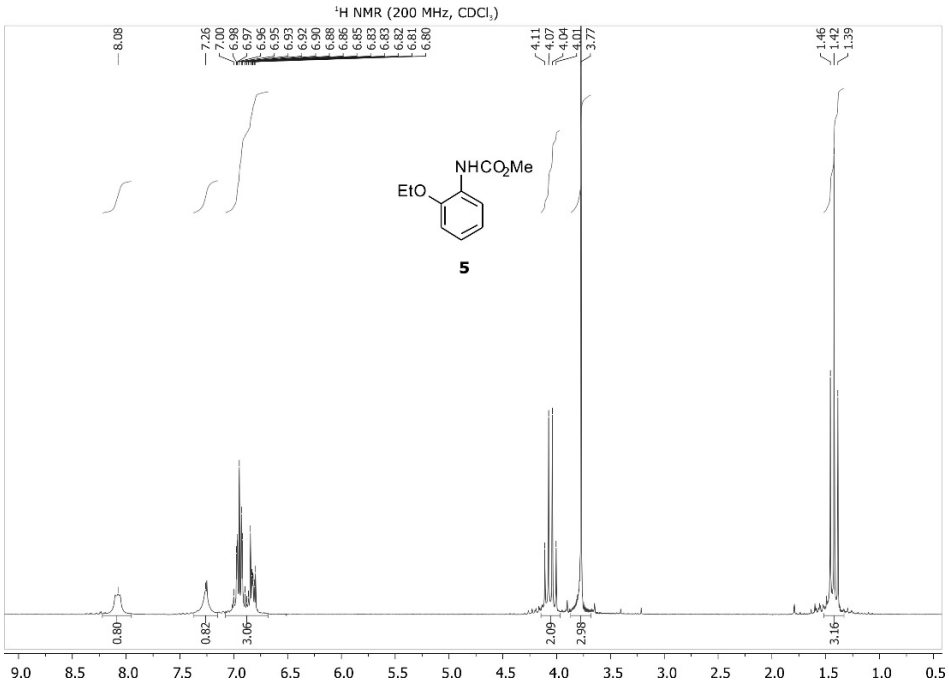

Figure S-9. ^{1}H NMR of methyl (2-ethoxyphenyl)carbamate **[5]**

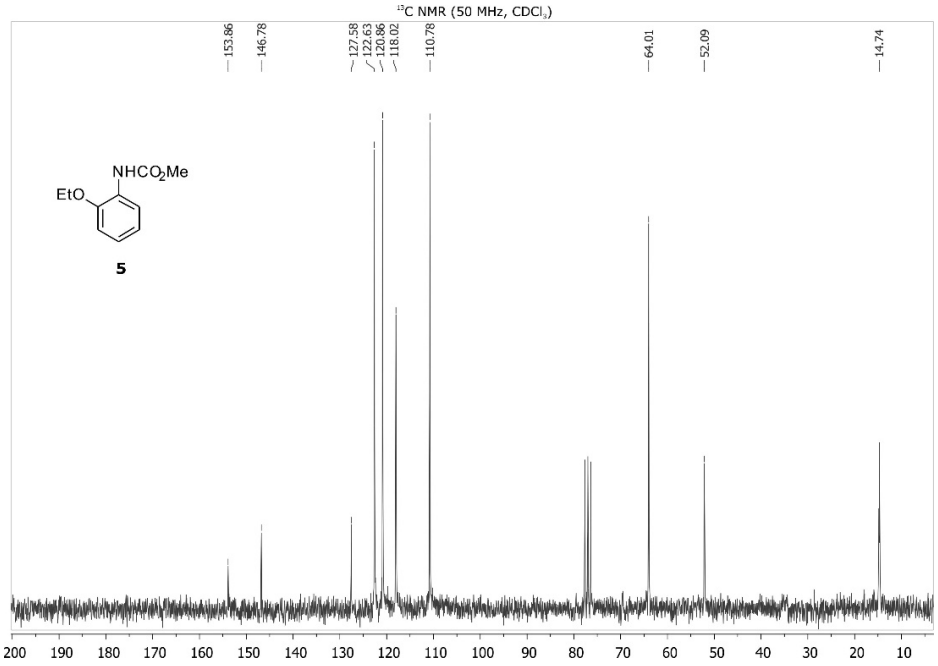

Figure S-10. ^{13}C NMR of methyl (2-ethoxyphenyl)carbamate **[5]**.

REFERENCES

1. I. I. Jevtić, Lj. Došen-Mićović, E. R. Ivanović, M. D. Ivanović, *Synthesis* **48** (2016) 1550 (https://doi.org/10.1055/s-0036-1588985).

Journal of the Serbian Chemical Society
JSCS@tmf.bg.ac.rs • www.shd.org.rs/JSCS
J. Serb. Chem. Soc. *88* (11) 1103–1117 (2023)
JSCS–5683
Original scientific paper
Published 10 November 2023

High cell density cultivation of *Bacillus subtilis* NCIM 2063: Modeling, optimization and a scale-up procedure

SANDRA STAMENKOVIĆ STOJANOVIĆ*, IVANA KARABEGOVIĆ, BOJANA DANILOVIĆ, STOJAN MANČIĆ and MIODRAG LAZIĆ

Faculty of Technology, University of Niš, Bulevar Oslobodjenja 124, 16000 Leskovac, Serbia

(Received 7 April, revised 3 May, accepted 8 July 2023)

Abstract: *Bacillus subtilis* is a non-pathogenic, sporulating, Gram-positive bacteria with pronounced antimicrobial and metabolic activity and great potential for wide application in various fields. The aim of this paper was to determine the optimum *B. subtilis* NCIM 2063 growth conditions and to scale up biomass production from shake flasks to a bioreactor level. The critical growth parameters and their interaction effects were studied using Box–Behnken experimental design and response surface methodology. Developed model equations were statistically significant with good prediction capability. It was found that during shake flask cultivation glucose should be added in concentration up to 5 g L^{-1} in DSM medium, *OTR* at 10 mol m^{-3} h^{-1} and temperature of 33 °C, to achieve the maximum number of viable cells and spores. To scale up the process from shake flasks to the bioreactor level k_La was used as a main criterion. Scale up effect was evaluated by comparing the growth kinetics in the shake flasks and in a laboratory bioreactor. The total number of cells obtained in the bioreactor was 4.57×10^9 CFU mL^{-1} which is 1.41 times higher than the number of cells in the shake flasks (3.24×10^9 CFU mL^{-1}), proving that the scale-up procedure was conducted successfully.

Keywords: shake flask; bioreactor; microbial biomass.

INTRODUCTION

Bacillus subtilis is a Gram-positive, rod-shaped bacterium with a unique ability to rapidly multiply and to form endospores, thus being resistant to adverse environmental conditions. This strain has the ability to produce industrially important metabolites such as antibiotics, polysaccharides and proteins[1–3] and to degrade different pollutants in the environment.[4] A great diversity of previously published papers has showen that *B. subtilis* is capable of producing various important biotechnological products, such as different enzymes[5,6] (Akcan 2012,

* Corresponding author. E-mail: sandra.stamenkovic@live.com
https://doi.org/10.2298/230407036S

Božić, 2011), polysaccharides[7] and surfactants.[7,8] Many of them, including iturin A and surfactin, have antibiotic, antiviral and immunomodulatory effect when applied on humans. Additionally, *B. subtilis* has wide application in the environmental protection, as it can degrade different trace organic compounds[9] and organochlorine insecticides.[10] It is also attributed to probiotic properties and "GRAS" (generally recognized as safe) status, which makes it safe for human use. These species are highly attractive for industrial applications and commercial biomass production due to its exceptional physiological characteristics, ability to easily adapt to new environmental conditions and capability to produce a wide range of metabolites.[3,11]

Microbial biomass production implies cultivation in bioreactors in liquid, semi-liquid or solid nutrient media. At the beginning of the research, cultivation is carried out in shake flasks of smaller volumes, in order to establish optimal production procedures at minimum costs. Different optimization techniques can be applied to determine the optimum medium composition, carbon and nitrogen source concentration, mixing speed, temperature, or pH value. Based on such experiments, valuable data are obtained about the microorganism, it's growth kinetics and nutrient requirements. If modern multifactorial optimization techniques are applied, experimental data are used to develop a predictive model that will describe the further behaviour of the system.[12] After that, the scale of the process is gradually increased to a laboratory bioreactor, and further on to bioreactors of larger volumes, to determine whether the same or similar results will be achieved on larger-scale equipment.[13,14] The transition from shake flask to laboratory bioreactor is a critical point of the highest importance in the whole scale-up process. If done properly, it ensures the smooth further continuation of the scale-up procedure from laboratory to pilot and industrial scale bioreactor.[15] When transitioning from a shake flask to laboratory bioreactor particular changes in the vessel geometry and size occur, which cause changes in mixing efficiency, affect oxygen supply, and increase the possibility of creating "dead zones" and uneven nutrient distribution. For that reason, the shake flask-bioreactor transition needs to be carefully optimized and designed. Modeling the complex hydrodynamic behaviour is one of the most difficult numerical problems that has fundamental importance in many aspects of engineering. The key parameters are related to mass and heat transfer, mixing and aeration.[16] In order to optimize the performance of the bioreactor, it is necessary to know the local fluid dynamics in the bioreactor, *i.e.*, the relation between hydrodynamics and the mass transfer coefficient.[17] Volumetric oxygen mass transfer coefficient ($k_L a$) and oxygen transfer rate (*OTR*) are the key parameters used to describe the efficiency of oxygen utilization. $k_L a$ is most commonly used as a scale-up criterion in aerobic processes used to estimate the efficiency of the bioreactor.[18,19] This practice is supported by the fact that the main problem in aerobic systems is the adequate sup-

ply of oxygen from the gas to the liquid phase. Dimensional analysis helps to develop correlations that will ensure a constant value of $k_L a$ corresponding to the desired *OTR*. The success of the scale-up process is confirmed experimentally when it is shown that the same or similar results can be achieved in a bioreactor under the same conditions as in shake flasks.[17] Therefore, the aim of this work was to produce good-quality biomass of desired high cell and spore density, and to:

– assess the individual and combined effect of critical *B. subtilis* NCIM 2063 growth parameters: oxygen transfer rate, mixing speed, temperature and glucose concentration;

– determine the optimum growth conditions for *B. subtilis* NCIM 2063 on a shake flasks level using response surface methodology (RSM);

– provide statistically significant model equations for the shake flasks level;

– scale-up the cultivation of *B. subtilis* NCIM 2063 from shake flasks to batch bioreactor using $k_L a$ as scale-up criterion;

– evaluate the success of the scale-up procedure by bioreactor cultivation with additional analysis of kinetic and stoichiometric parameters.

EXPERIMENTAL

Inoculum preparation

Sporogenic Gram-positive bacterium *B. subtilis* 2063 from the NCIM collection was provided by a private company Fertico d.o.o. located in Niš, Serbia. The bacterial culture was stored at –80 °C in vials and at 4 °C on agar plates. 300 ml Nutrient broth was inoculated with a single loop of *B. subtilis* NCIM 2063 and incubated at 37 °C for 24 h in shake flasks at 150 rpm. An 1 vol. % overnight culture was used as inoculum for further cultivation.

Shake flask cultivation study

To optimize the *B. subtilis* growth conditions in the shake-flasks, the Box–Behnken experimental design (BBD) was used (Table I). 1 % *B. subtilis* 2063 overnight culture was used to inoculate sterilized nutrient DSM medium (8 g nutrient broth, 10 mL 10 % KCl, 10 mL 1.2 % $MgSO_4$, 1 mL1 M $Ca(NO_3)_2$, 1 mL 0.01 M $MnCl_2$, 1 mL 1 mM $FeSO_4$) in a 500 ml Erlenmeyer vessel. DSM is a commonly used medium for *Bacillus* cultivation, owing its popularity to its simplicity, high biomass yield and sporulation efficiencies.[20-24] The three factors varied on three levels were: temperature (25–37 °C), *OTR* (2–10 mol m^{-3} h^{-1}) and glucose concentration (0–20 g l^{-1}). The factors and their levels were selected based on the preliminary experiments and available literature data.[22,25-27] Cultivation was performed for 24 h on a rotary shaker at 150 rpm according to the design matrix. The total number of viable vegetative cells and the number of spores were chosen as dependent variables. The viable cell count was determined using the spread plate method. Spores were counted using the same method, but the samples were previously heated at 80 °C for 10 min.

TABLE I. Coded and non-coded values of process factors according to BBD design

Symbol	Factor	Low level (-1)	Middle level (0)	High level (+1)
A	Temperature, °C	25	31	37
B	*OTR*, mol m^{-3} h^{-1}	2	6	10
C	Glucose concentration, g/L	0	10	20

Bioreactor cultivation

1 % *B. subtilis* NCIM 2063 inoculum was used to inoculate the laboratory bioreactor containing a sterile DSM medium. The cultivation was performed at the optimum conditions determined in the shake flasks and after the scale-up procedure. The bioreactor cultivation was performed in a bioreactor KLFM, BioEngineering, Wald, Switzerland (working volume: 2.5 L, total volume 3.7 L), equipped with two Rajasthan impellers with 6 blades (48 mm diameter) and 4 baffles. Sterile air supplied from an external compressor was used for aeration with a specific air flow of 0.3 v.v.m (volume of gas per volume of liquid per min). The bioreactor is equipped with a pH (BioEngineering 4695) and an oxygen electrode (Mettler Toledo 3420036) and connected to the BioScada software system, which monitors the process parameters.

k_La *and* OTR *determination*

k_La values in the bioreactor were determined using the absorption method, while the *OTR* values in shake flasks and in the bioreactor were calculated according to:[28]

$$OTR = 7.23\times10^{-4}\left(\frac{V_L}{V_F}\right)^{-0.845} CN \quad (1)$$

$$TR = k_La\left(C^* - C\right) \quad (2)$$

where: V_L is a liquid volume (mL), V_F is Erlenmeyer flask volume (mL), C is dissolved oxygen concentration (mg L^{-1}), N is shaking speed (s^{-1}), and C^* oxygen solubility in the medium at a given temperature.

Kinetic and stoichiometric parameters

The yield coefficients, $Y_{x/0}$ and $Y_{x/s}$ were calculated according to the following equations:

$$Y_{x/0} = \frac{X}{OTR\times t} \quad (4)$$

$$Y_{x/s} = \frac{s_0 - s}{x - x_0} \quad (5)$$

where s_0 is initial glucose concentration (g L^{-1}), s is final glucose concentration, x is final biomass concentration (g L^{-1}), x_0 is initial biomass concentration (g L^{-1}), X is the biomass concentration at the moment t, *OTR* is oxygen transfer rate (mol m^3 h^{-1}), and t is time (s). $Y_{x/0}$ was calculated under the assumption that all of the oxygen that was transferred to the medium was also consumed by the microorganism.

Specific growth rate, μ_m, and generation time, t_d, were calculated using the following equations:[29]

$$\ln\frac{x}{x_0} = \mu_m t \quad (6)$$

$$t_d = \frac{\ln 2}{\mu_m} \quad (7)$$

where x is the biomass concentration at the moment t, and x_0 is the initial biomass concentration (g L^{-1}).

Statistical analysis

Each experiment was run three times in parallel, and the findings were reported as the mean value of three repetitions ± standard deviation. The program Origin 6.0, Excel 2013 and

Expert Design 7.0 were used for the statistical processing of experimental data. RSM and Derringer's desirability function were used for modeling and optimization. The adequacy of the response surface model was assessed using the analysis of variance (ANOVA).

RESULTS AND DISCUSSION

The reliability and durability of microbial biomass formulation largely depend on the number of living cells, particularly the spores, which is why it is important to enabling the microorganism to reach a high cell density and to sporulate. Three independent factors (temperature, oxygen transfer rate and initial glucose concentration) were varied at three levels according to the Box–Behnken experimental design, and their effect on total vegetative cell and spore count after 24 h of cultivation is shown in Table S-I (Supplementary material to this paper). By applying the nonlinear regression method to the obtained experimental data the following mathematical models were proposed for the total number of *B. subtilis* vegetative cells and spores, respectively:

$$X = 9.04 + 0.01A - 0.29B + 0.02C + 6.04\times10^{-3}AB - 8.75\times10^{-4}AC + \\ +0.01BC - 81.87\times10^{-4}A^2 + 0.01B^2 - 5.36\times10^{-3}C^2 \quad (8)$$

$$Y = 7.05 + 0.06A - 0.18B + 0.105C + 0.02B^2 - 7.43\times10^{-3}C^2 \quad (9)$$

where X is vegetative cell count, Y is spore count, A is the temperature (°C), B is *OTR* (mol m^{-3} h^{-1}) and C is initial glucose concentration (g L^{-1}). The significance and reliability of the models were assessed by comparing the predicted and experimental values and by conducting ANOVA analysis (Table II). It can be observed that each of the individual factors in the model that predicts the number of viable vegetative cells is statistically significant with a degree of reliability of 99 %. The calculated p-value for the lack of fit (0.219) for this model is statistically insignificant and indicates a good fit of the experimental data for both of the models. The highest significance was recorded for initial glucose concentration and *OTR* (in both their individual and quadratic form). Individual temperature term, as well as temperature – *OTR* interaction term are also found to significantly influence the number of *B. subtilis* vegetative cells. Since *OTR* and the initial glucose concentration are significant on a quadratic level, a small variation in their values will greatly affect the growth rate and the final number of cells.[21]

On the other hand, sporulation was highly affected by initial glucose concentration (individual and quadratic term) which is the most significant factor. Apart from glucose, temperature, quadratic term of *OTR* and interaction between *OTR* and initial glucose concentration were also significant. The spore-predicting model was also statistically significant (with an F value of 21.01 and 0.0002 for the p-value), with an insignificant lack of fit. The reliability of the models was additionally assessed by analyzing the values of R^2, *Adj* R^2 and *Pred* R^2, which are in accordance with the requirements that R^2 and *Adj* R^2 should be reasonably

close to 1, and that the difference between *Adj* R^2 and *Pred* R^2 should not exceed 0.2.[30] Obtained values imply that both developed regression equations have a good fit and that they can successfully predict system responses.

TABLE II. ANOVA for the models obtained for *B. subtilis* NCIM 2063 viable cell and spore count; Values of *p* less than 0.05 indicate model terms are significant

Parameter	Viable cell count		Spore count	
	F value	*p*-value	*F* value	*p*-value
Model	41.32	< 0.0001	20.86	**< 0.0001**
A	13.62	0.0078	5.84	**0.0363**
B	109.04	<0.0001	0.99	0.3425
C	126.23	< 0.0001	91.22	**< 0.0001**
AB	5.03	0.0599	–	–
AC	0.66	0.4436	–	–
BC	40.2	0.0004	9.26	**0.0124**
A^2	0.011	0.9177	–	–
B^2	6.5	0.0381	4.13	**0.0696**
C^2	75.52	<0.0001	14.52	**0.0034**
Lack of fit	2.3	0.2186	3.59	0.1182
R^2	0.982		0.926	
Adj R^2	0.958		0.882	
Pred R^2	0.802		0.697	
C.V. / %	1.47		5.10	
PRESS	1.25		6.59	
MRPD / %	0.1		1.52	

The regression equation is also graphically represented in two-dimensional contours, visualizing the relationship between the response and each of the independent variables in the system (Fig. 1).

It can be concluded that at higher initial glucose concentrations, an increase in *OTR* has a positive effect on the total number of viable vegetative cells, while temperature has no significant effect. By reducing the concentration of glucose, the effect of temperature becomes more pronounced, with the largest number of cells being achieved in a medium with 10 g L^{-1} glucose. In contrast, in a glucose--free medium, increasing the *OTR* has little effect on the cell number. This effect is diminished by an increase in temperature. Such moderate interaction of *OTR* and temperature was also previously confirmed through the calculated *p*-value. Similarly, the significance of this interaction effect was observed in a study optimizing the growth of *Bacillus coagulans* using the RSM method, with maximum biomass yield obtained by a combination of high temperatures and specific airflow.[31] The graphic analysis confirmed the importance of oxygen availability, which is explained by the fact that lack of oxygen reduces the pH of the substrate, leading to rapid lysis of the cell and the initiation of new metabolic pathways.[32]

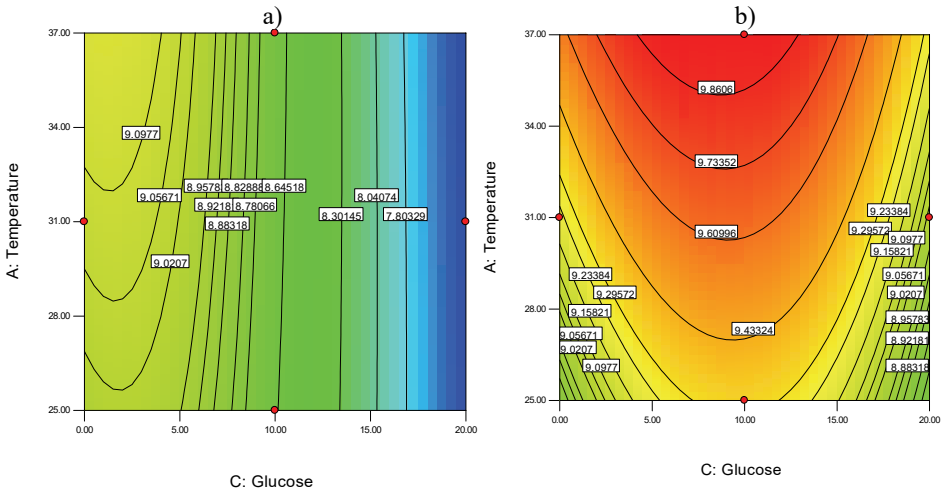

Fig. 1. Contour plots representing the total number of *B. subtilis* NCIM 2063 viable cells as a function of glucose concentration, g L^{-1}, temperature (°C), and *OTR* = 2 (a) and 10 mol m^{-3} h^{-1} (b).

Fig. 2 shows the visualized relationship between dependent and independent variables for the spore-predicting model. The maximum number of spores was obtained in a glucose-free medium at *OTR* = 10 mol m^{-3} h^{-1}, while the effect of temperature was negligible. As expected, nutrient deprivation initiated sporulation, which allows *B. subtilis* to enter a dormant state, preserving its genetic material and resistance to harsh conditions until favourable growth conditions are restored.[24] The effect of temperatures higher than 30 °C is most pronounced at the maximum concentration of the initial glucose applied. In a glucose-free medium, increasing the *OTR* increases the number of sporulated cells. As the initial glucose concentration increases, the influence of *OTR* on the sporulation is reduced with the increase in the initial glucose concentration in the medium, although cultivation at higher temperatures reduces the effect of glucose. It can be explained by the fact that increasing the initial glucose concentration increases the viscosity of the medium, which creates greater resistance of the liquid film and thus reduces the real *OTR* value. Increasing the temperature increases the solubility of the components of the nutrient medium, which diminishes the negative effect of glucose in this interaction. The literature data agree with the experimental results achieved here. It was found that the maximum yield of spores is achieved at low initial glucose concentrations and that bacterial culture begins to sporulate when the cell density is about 10^8 CFU mL^{-1}.[33] The reason for this is the characteristic of cells to sporulate in unfavorable environmental conditions, ie. in conditions when nutrients are not available in excess.[34] As a result of that, the microorganism can undergo metabolic shifts, activating alternative metabolic

pathways, or employing strategies such as gluconeogenesis to sustain growth using non-carbohydrate carbon sources. The gluconeogenesis pathway involves a series of enzymatic reactions that convert non-carbohydrate precursors into glucose-6-phosphate, which are metabolized through glycolysis for energy production or used as a precursor for biosynthesis.[35]

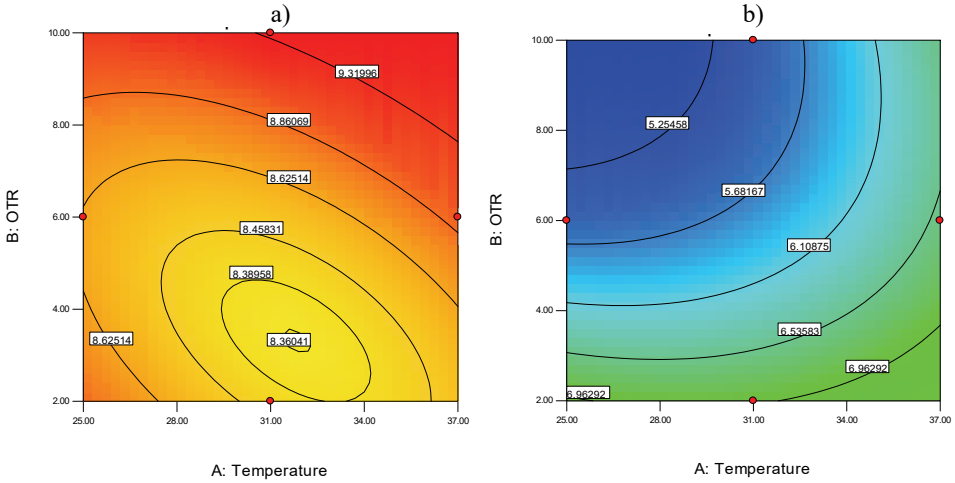

Fig. 2. Contour plots for the number of *B. subtilis* NCIM 2063 spores as a function of *OTR*, temperature and initial glucose concentration: 0 (a) and 20 g L^{-1} (b).

Multicriteria optimization using Derringer's desirability function

Derringer's desirability function is used in complex multivariate processes in which variables that need to be optimized are influenced by multiple factors simultaneously. Based on multicriteria optimization (Table S-II, Supplementary material), several combinations of process conditions have been proposed to obtain the maximum value of the desirability function as well as of both response variables. Taking into account the response surface analysis and knowing that the increase in temperature does not decisively affect the increase in the total number of viable cells, it was decided to maximize the cell growth and provide the necessary conditions for sporulation, while achieving energy savings. According to that, the following optimum conditions for the cultivation of *B. subtilis* NCIM 2063 were proposed: t = 33 °C, *OTR* =10 mol m^{-3} h^{-1} and initial glucose concentration 4.89 g l^{-1}. Under these conditions, the model predicts a maximum viable vegetative cell concentration of 9.66 log (CFU ml^{-1}) and spores of 9.19 log (CFU ml^{-1}) with a high desirability function value (0.931). The experimental cell density for the total number of cells and spores obtained under the given conditions was 9.51±0.09 and 9.08±0.06 log (CFU mL^{-1}), respectively. The experiment was performed in triplicate, and the relative error between predicted and

obtained values for vegetative cells and spores was 1.5 and 1.2 %, respectively, which confirms that there is a good agreement between predicted and experimental values.

A scarce number of previously published studies is dedicated to the topic of multicriteria optimization of *B. subtilis* growth conditions. Most of the available research deals with optimizing the media composition,[36–40] while a small number of them optimize growth conditions. A group of authors conducted a screening of the influence of volumetric airflow and mixing rate on cell density and sporulation of *B. subtilis* EA-CB0575 using a central composite experimental design.[31] As optimal conditions, a mixing speed of 432 rpm and a volumetric airflow of 12 L/min at a temperature of 30 °C are given.[41] The same experimental design was used to optimize the sporulation of *B. subtilis* in a solid medium. It was found that temperature and volumetric air flow have an impact on sporulation, with 27 °C and 1.2 L min^{-1} being recommended as optimal values for solid medium, respectively.[42]

Scale up from shake flask to laboratory bioreactor

k_La is a key parameter for scaling and optimization in mechanical mixing systems, where the rate of oxygen mass transfer between the gas and liquid phases is an essential phenomenon for process control.[43] Hence, k_La was chosen as the basic criterion for the scale-up procedure to the bioreactor level. The main goal of the scale-up process was to define the values of process conditions at the bioreactor level that will enable the same value of k_La established for shake flasks: namely to define the mixing speed that will provide the desired oxygen transfer from gas to a liquid phase.

Firstly, k_La was measured at different mixing speeds in the DSM medium at the bioreactor level (Table III). As expected, reducing the mixing speed also affects the reduction of the oxygen mass transfer rate. An increase in the stirrer speed from 100 to 400 rpm, causes an exponential increase in the k_La value. Such a result is in accordance with the literature data, since in the medium with 10 g L^{-1} of glucose at a specific air flow of 1 v.v.m, an increase in the value of k_La from 25.2 to 104.4 h^{-1} was detected when the mixing speed was increased from 300 to 600 rpm.[44] At higher mixing speeds the air bubbles break into small bubbles, which increases the gas-liquid interfacial surface to transfer the oxygen in the medium, thus increasing the k_La.[45]

TABLE III. Influence of mixing speed on the k_La values in DSM medium at bioreactor level

Mixing speed, rpm	100	200	300	400
k_La / h^{-1}	5.26±0.02	6.51±0.11	11.88±0.15	45.35±0.25
OTR / mmol m^{-3} h^{-1}	1.15	1.42	2.59	9.88

After applying regression analysis to experimental data obtained by the absorption method, the following empirical equation was developed to describe the relationship between the mixing speed N and $k_L a$:

$$k_L a = \exp(7.1\times10^{-3} N + 0.7) \quad (10)$$

Based on the obtained correlation it was calculated that at given conditions in a laboratory bioreactor containing DSM medium (33 °C and 0.3 v.v.m air flow rate) the mixing speed should be set to 452 rpm in order to achieve the required $k_L a$ value (45.35 h^{-1}).

Bioreactor cultivation

The success of the scale-up procedure was evaluated after the cultivation of *B. subtilis* NCIM 2063 at determined optimum conditions at the bioreactor level. It was concluded that, at the end of the cultivation period, the total number of viable cells in the bioreactor was 9.65±0.05 log (CFU mL^{-1}), which is 1.4 times more than the number of cells achieved in shake flasks (9.51±0.09 log (CFU mL^{-1}) under the same conditions. Growth kinetic and stoichiometric analysis lead to the same conclusion (Fig. 3, Table IV). After 24 h cultivation, the biomass concentration was higher in the bioreactor than in the shake flasks, although similar values of specific growth rate were recorded in both systems. The higher cell density at the end of cultivation in the bioreactor can be explained by better oxygen saturation of the medium, which is confirmed by a higher biomass yield on oxygen ($Y_{x/0}$) in the bioreactor (Table IV). Namely, in shake flasks, gas induction is based only on surface aeration. Initially, the substrate is saturated with air and the amount of oxygen is sufficient for microbe growth. After the exponential phase, a sharp drop in the oxygen concentration occurs in shake flasks. In the case of bioreactors, mixing and a constant supply of fresh air provide sufficient levels of oxygen, which can contribute to greater multiplication of cell mass, or lead to prolongation of the exponential phase.[46] This once again confirms that aeration and mixing play a very important role in the metabolic activity of microorganisms. Given that a satisfactory number of cells was achieved in the bioreactor at the end of the cultivation period, it is concluded that the scale-up process was successfully implemented, which created the basic condition for further scale-up to the semi-industrial level.

TABLE IV. Specific growth rate (μ_m), generation time (t_d), final biomass concentration (X) and biomass yield from oxygen consumption ($Y_{x/0}$) during shake flask and bioreactor cultivation of *B. subtilis* NCIM 2063

Cultivation	μ_m / h^{-1}	t_d / h	X / g L^{-1}	$Y_{x/0}$ / g g^{-1}
Bioreactor	0.44±0.08	1.57±0.58	7.24±0.00	0.81±0.00
Shake flask	0.41±0.03	1.71±0.26	5.6±0.51	0.71±0.31

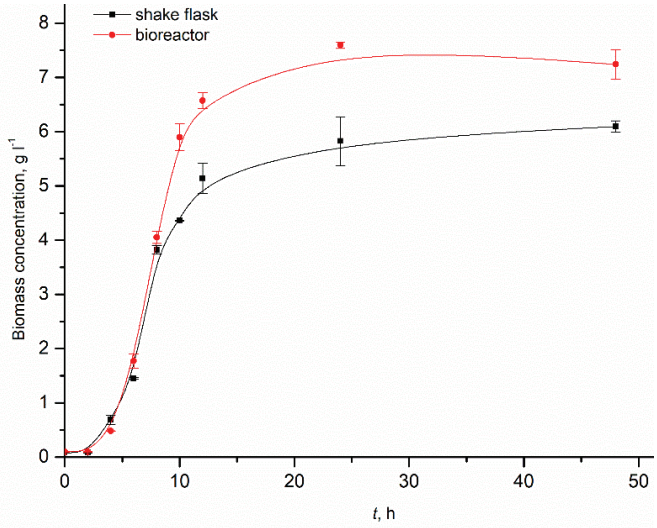

Fig. 3. *B. subtilis* NCIM 2063 growth kinetics at bioreactor and shake flask level at DSM medium containing 4.89 g L^{-1} glucose at bioreactor level under the optimum conditions: 33 °C and 452 rpm.

The success of the k_La-based scale-up process strategy has been shown earlier in the literature. k_La was used as a criterion for increasing the scale of phenyl acetyl carbinol production using the yeast *Saccharomyces cerevisiae*. In that research, the k_La value was first estimated by the absorption method in shake flasks, based on which appropriate correlations were developed. Similar k_La values and higher yield of the desired product were achieved in a 5 L bioreactor.[46] An analogous scale-up strategy was applied for the cultivation of *Corynebacterium glutamicum* and the production of lactic acid using adapted empirical models obtained by the sulfite method.[47] The optimal value of k_La (31 h^{-1}) was also the leading parameter for adjusting the mixing speed and air volume flow in order to obtain a quality *Azospirillum brasilense*-based product for pathogen biocontrol at the semi-industrial level.[18]

CONCLUSION

In this study, the conditions for batch cultivation of *B. subtilis* NCIM 2063 were optimized to maximize viability and sporulation. The individual and combined effects of k_La, temperature and glucose concentration were assessed and explained. Glucose and k_La have the greatest statistical significance (both as an individual and as a quadratic term) for the number of viable cells, followed by the interaction factor of these two terms, the individual temperature factor and the interaction of temperature and k_La. When it comes to the total number of spores, the concentration of glucose (individual and quadratic term), temperature, and the interaction of k_La and glucose have the greatest influence on this res-

ponse. Statistically significant quadratic models were developed with an insignificant lack of fit, which is confirmed by a good agreement between experimentally obtained and predicted data. Using Derringer's desirability function the following optimum conditions were proposed for a DSM medium: t = 33 °C, k_La = 50 mol m^{-3} h^{-1} and glucose concentration 4.89 g L^{-1}. Scale-up from shake flasks to a batch bioreactor was performed using k_La as a scale-up criterion. An empirical equation was developed to calculate the exact stirring speed needed to achieve the desired k_La. The success of the scale-up procedure was evaluated by bioreactor cultivation with additional analysis of kinetic and stoichiometric parameters. Given that a satisfactory number of cells has been achieved in the bioreactor and that the scale-up process was successfully implemented, a prerequisite is created to further scale up the process to semi-industrial and industrial levels in further research.

SUPPLEMENTARY MATERIAL

Additional data and information are available electronically at the pages of journal website: https://www.shd-pub.org.rs/index.php/JSCS/article/view/12350, or from the corresponding author on request.

Acknowledgment. Ministry of Science, Technological Development and Innovation, Republic of Serbia, Project no: 451-03-47/2023-01/200133

ИЗВОД

КУЛТИВАЦИЈА *Bacillus subtilis* NCIM 2063: МОДЕЛОВАЊЕ, ОПТИМИЗАЦИЈА И ПРОЦЕДУРА ПОВЕЋАЊА РАЗМЕРЕ

САНДРА СТАМЕНКОВИЋ СТОЈАНОВИЋ, ИВАНА КАРАБЕГОВИЋ, БОЈАНА ДАНИЛОВИЋ, СТОЈАН МАНЧИЋ и МИОДРАГ ЛАЗИЋ

Технолошки факултет у Лесковцу, Универзитет у Нишу, Булевар Ослобођења 124, 16000 Лесковац

Bacillus subtilis је непатогена, Грам-позитивна бактерија која спорулише и има изражену антимикробну и метаболичку активност, а самим тим и велики потенцијал за примену у различитим областима. Циљ овог рада био је одредити оптималне услове раста за *B. subtilis* NCIM 2063 и повећати размере процеса са ерленмајера на ниво биореактора. Критични параметри раста и ефекти њихове интеракције су изучавани применом Бокс–Бенкеновог (Box–Behnken) експерименталног дизајна и методе одзивних површина. Развијене једначине модела биле су статистики значајне. Током култивације у ерленмајерима са мешањем, глукозу треба додати у концентрацији до 5 g L^{-1} при концентрацији *OTR* од 10 mol m^{-3} h^{-1} и на 33 °C, како би се постигао максималан број ћелија и спора. За повећање размере процеса са нивоа ерленмајера на ниво биореактора k_La је коришћен као главни критеријум. Ефекат повећања размере утврђен је поређењем кинетике раста у ерленмајерима и у биореактору. Укупан број ћелија добијен у биореактору био је $4{,}57\times10^9$ CFU mL^{-1} што је1,41 пута више у одосу на број ћелија добијен у ерленмајеру, $3{,}24\times10^9$ CFU mL^{-1}, доказујући да је процедура повећања размере успешно спроведена.

(Примљено 7. априла, ревидирано 3. маја, прихваћено 8. јула 2023)

REFERENCES

1. S. Shahcheraghi, J. Ayatollahi, M. Lotfi, *Tropical J. Med. Res.* **18** (2015) 1 (http://dx.doi.org/10.4103/1119-0388.152530)
2. P. Garcia-Fraile, E. Menendez, R. Rivas, *AIMS Bioeng.* **2** (2015) 183 (http://dx.doi.org/10.3934/bioeng.2015.3.183)
3. J. Shafi, H. Tian, M. Ji, *Bioteh. Bioteh. Equip.* **31** (2017) 446 (http://dx.doi.org/10.1080/13102818.2017.1286950)
4. H. Hamdi, A. Hellal, *J. Serb. Chem. Soc.* **84** (2019) 679 (http://dx.doi.org/10.2298/JSC181204022H)
5. N. Akcan, B. Serin, F. Uyar, *Chem. Biochem. Eng. Q.* **26** (2012) 233 (https://hrcak.srce.hr/87357)
6. H. Wang, Y. Wang, R. Yang, *Appl. Microbiol. Biotechnol.* **101** (2017) 933 (http://dx.doi.org/10.1007/s00253-016-8080-9)
7. N. Božić, J. Ruiz, J. López-Santín, Z. Vujčić, *J. Serb. Chem. Soc.* **76** (2011) 965 (https://doi.org/10.2298/JSC101010098B)
8. A. Cagri-Mehmetoglu, S. Kusakli, M. van de Venter, *J. Dairy Sci.* **95** (2012) 3643 (https://dx.doi.org/10.3168/jds.2012-5385)
9. N. Haddad, X. Liu, S. Yang, B. Mu, *Protein Pept. Lett.* **15** (2008) 265 (https://doi.org/10.2174/092986609787049358)
10. V. K. Vaithyanathan, H. Cabana, V. K. Vaidyanathan, *Chem. Eng. J.* **419** (2021) 129966 (https://doi.org/10.1016/j.cej.2021.129966)
11. K. S. Ahmad, *Folia Microbiol. (Praha)* **65** (2020) 801 (https://doi.org/10.1007/s12223-020-00792-7)
12. H. Zhao, D. Shao, C. Jiang, J. Shi, Q. Li, Q. Huang, M. S. R. Rajoka, H. Yang, M. Jin, *Appl. Microbiol. Biotechnol.* **101** (2017) 5951 (http://dx.doi.org/10.1007/s12275-014-3354-3)
13. A. K. Das, V. Mandal, S. C. Mandal, *Phytochem. Anal.* **25** (2014) 1 (http://dx.doi.org/10.1002/pca.2465)
14. A.-I. Galaction, C. Oniscu, D. Cascaval, *Hem. Ind.* **57** (2003) 276 (http://dx.doi.org/10.2298/HEMIND0306276G)
15. S. Stamenković, V. Beškoski, I. Karabegović, M. Lazić, N. Nikolić, *Span. J. Agric. Res.* **16** (2018) e09R01 (http://dx.doi.org/10.5424/sjar/2018161-12117)
16. P. M. Doran, *Bioprocess engineering principles: Second edition*, Academic Press, London, 2013, ISBN 0-12-220855-2
17. F. Garcia-Ochoa, E. Gomez, *Biotechnol. Adv.* **27** (2009) 153 (http://dx.doi.org/10.1016/j.biotechadv.2008.10.006)
18. S. Suresh, V. C. Srivastava, I. M. Mishra, *Crit. Rev. Biotechnol.* **29** (2009) 255 (http://dx.doi.org/10.1002/jctb.2154)
19. M. A. Trujillo-Roldán, N. A. Valdez-Cruz, C. F. Gonzalez-Monterrubio, E. V. Acevedo--Sánchez, C. Martínez-Salinas, R. I. García-Cabrera, R. A. Gamboa-Suasnavart, L. D. Marín-Palacio, J. Villegas, A. Blancas-Cabrera, *Appl. Microbiol. Biotechnol.* **97** (2013) 9665 (http://dx.doi.org/10.1007/s00253-013-5199-9)
20. K. Meier, W. Klöckner, B. Bonhage, E. Antonov, L. Regestein, J. Büchs, *Biochem. Eng. J.* **109** (2016) 228 (http://dx.doi.org/10.1016/J.BEJ.2016.01.014)
21. Monteiro, J. J. Clemente, M. J. T. Carrondo, A. E. Cunha, *Adv. Microbiol.* **4** (2014) 444 (http://dx.doi.org/10.4236/aim.2014.48049)

22. M. B. Tavares, R. D. Souza, W. B. Luiz, R. C. M. Cavalcante, C. Casaroli, E. G. Martins, R. C. C. Ferreira, L. C. S. Ferreira, *Curr. Microbiol.* **66** (2013) 279 (http://dx.doi.org/10.1007/s00284-012-0269-2)
23. D. H. Green, P. R. Wakeley, A. Page, A. Barnes, L. Baccigalupi, E. Ricca, S. M. Cutting, *Appl .Environ. Microbiol.* **65** (1999) 4288 (https://doi.org/10.1128/AEM.65.9.4288-4291.1999)
24. M. Karava, F. Bracharz, J. Kabisch, *PLoS One* **14** (2019) e0219892 (https://doi.org/10.1371/journal.pone.0219892)
25. L. Li, J. Jin, H. Hu, I. F. Deveau, S. L. Foley, H. Chen, *J. Ind. Microbiol. Biotechnol.* **49** (2022) 14 (https://doi.org/ 10.1093/jimb/kuac014)
26. M. M. Nakano, F. M. Hulett, *FEMS Microbiol. Lett.* **157** (2006) 1 (http://dx.doi.org/10.1111/j.1574-6968.1997.tb12744.x)
27. S. Stamenkovic-Stojanovic, I. Karabegovic, V. Beskoski, N. Nikolic, M. Lazic, *Hem. Ind.* **73** (2019) 169 (http://dx.doi.org/10.2298/HEMIND190214014S)
28. S. M. Monteiro, J. J. Clemente, A. O. Henriques, R. J. Gomes, M. J. Carrondo, A. E. Cunha, *Biotechnol. Prog.* **21** (2005) 1026 (http://dx.doi.org/10.1021/bp050062z)
29. V. B. Veljković, S. Nikolić, M. L. Lazić, C. R. Engler, *Hem. Ind.* **49** (1995) 265 (https://www.researchgate.net/publication/259619801_Oxygen_transfer_in_flasks_shaken_on_orbital_shakers)
30. V. B. Veljković, *Fundamentals of biochemical engineering*, University of Niš, Leskovac, 1994, ISBN 86-82-367-01-07 (in Serbian)
31. D. Baş, İ. H. Boyacı, *J. Food Eng.* **78** (2007) 836 (http://dx.doi.org/10.1016/j.jfoodeng.2005.11.024)
32. R. Sen, K. S. Babu, *Proc. Biochem.* **40** (2005) 2531 (https://doi.org/10.1016/j.procbio.2004.11.004)
33. M. H. Sarrafzadeh, S. Schorr-Galindo, H.-J. La, H.-M. Oh, *J. Microbiol.* **52** (2014) 597 (http://dx.doi.org/10.1007/s12275-014-3547-9)
34. T. Khardziani, E. Kachlishvili, K. Sokhadze, V. Elisashvili, R. Weeks, M. L. Chikindas, V. Chistyakov, *Probiotics Antimicrob. Proteins* **9** (2017) 435 (http://dx.doi.org/10.1007/s12602-017-9303-9)
35. W. Abhyankar, A. Ter Beek, H. Dekker, R. Kort, S. Brul, C. G. de Koster, *Proteomics* **11** (2011) 4541 (http://dx.doi.org/10.1002/pmic.201100003)
36. N. Q. Anh, *PhD Thesis*, Universität Bayreuth, Bayreuth, 2010 (https://nbn-resolving.org/urn:nbn:de:bvb:703-opus-8418)
37. S.-W. Cheng, Y.-F. Wang, F.-F. Liu *Chem. Biochem. Eng. Q.* **25** (2011) 377 (http://silverstripe.fkit.hr/cabeq/assets/Uploads/Cabeq-2011-03-12.pdf)
38. J.-H. Cho, Y.-B. Kim, E.-K. Kim, *Korean J. Chem. Eng.* **26** (2009) 754 (http://dx.doi.org/10.1007/s11814-009-0126-6)
39. J. S. Eswari, M. Anand, C. Venkateswarlu, *Sãdhanã* **41** (2016) 55 (http://dx.doi.org/10.1007/s12046-015-0451-x)
40. K. Singh, K. Richa, H. Bose, L. Karthik, G. Kumar, K. V. Bhaskara Rao, *Appl. Biochem. Biotechnol.* **4** (2014) 591 (http://dx.doi.org/10.1007/s12010-008-8180-9)
41. L. F. Posada-Uribe, M. Romero-Tabarez, V. Villegas-Escobar, *Bioprocess Biosys. Eng.* **38** (2015) 1879 (https://doi.org/10.1007/s00449-015-1428-1)
42. S. W. Pryor, D. M. Gibson, A. G. Hay, J. M. Gossett, L. P. Walker, *Appl. Biochem. Biotechnol.* **143** (2007) 63 (https://doi.org/10.1007/s12010-007-0036-1)
43. R. Petříček, T. Moucha, F. J. Rejl, L. Valenz, J. Haidl, T. Čmelíková, *Int. J. Heat Mass Transf.* **124** (2018) 1117 (http://dx.doi.org/10.1016/j.ijheatmasstransfer.2018.04.045)

44. K. Limpaiboon, *Walailak J. Sci. Technol.* **10** (2013) 625 (https://wjst.wu.ac.th/index.php/wjst/article/view/472)
45. S. Suresh, V. C. Srivastava, I. M. Mishra, *J. Chem. Technol. Biotechnol.* **84** (2009) 1091 (http://dx.doi.org/10.1002/jctb.2154)
46. V. B. Shukla, U. Parasu Veera, P. R. Kulkarni, A. B. Pandit, *Biochem. Eng. J.* **8** (2001) 19 (http://dx.doi.org/10.1016/S1369-703X(00)00130-3)
47. J. M. Seletzky, U. Noak, J. Fricke, E. Welk, W. Eberhard, C. Knocke, J. Büchs, *Biotechnol. Bioeng.* **98** (2007) 800 (http://dx.doi.org/10.1002/bit.21359).

Journal of the Serbian Chemical Society
JSCS@tmf.bg.ac.rs • www.shd.org.rs/JSCS
J. Serb. Chem. Soc. *88* (11) S326–S327 (2023) *Supplementary material*

SUPPLEMENTARY MATERIAL TO

High cell density cultivation of *Bacillus subtilis* NCIM 2063: Modeling, optimization and a scale-up procedure

SANDRA STAMENKOVIĆ STOJANOVIĆ*, IVANA KARABEGOVIĆ, BOJANA DANILOVIĆ, STOJAN MANČIĆ and MIODRAG LAZIĆ

Faculty of Technology, University of Niš, Bulevar Oslobodjenja 124, 16000 Leskovac, Serbia

J. Serb. Chem. Soc. *88* (11) (2023) 1103–1117

Table S-I. Experimental (Exp.) and predicted (Pred.) values of the *B. subtilis* NCIM 2063 viable cell and spore count according to the BBD matrix

No.	Uncoded factor values			Dependent variables			
	Temperature °C (*A*)	*OTR*, mol $m^{-3}h^{-1}$ (*B*)	Initial glucose concentration, g l^{-1} (C)	Viable cell count log (CFU ml^{-1})		Spore count log (CFU ml^{-1})	
				Exp.	Pred.	Exp.	Pred
1	25.00	2.00	10.00	8.69±0.01	8.66	8.46±0.00	8.69
2	37.00	2.00	10.00	8.80±0.07	8.71	8.54±0.06	8.70
3	25.00	10.00	10.00	9.23±0.04	9.32	7.90±0.13	7.74
4	37.00	10.00	10.00	9.72±0.06	9.80	9.33±0.04	9.10
5	25.00	6.00	0.00	8.72±0.08	8.78	8.52±0.10	8.62
6	37.00	6.00	0.00	9.10±0.07	9.17	8.76±0.07	8.93
7	25.00	6.00	20.00	7.93±0.06	7.86	5.70±0.07	5.53
8	37.00	6.00	20.00	8.10±0.10	8.04	6.69±0.06	6.59
9	31.00	2.00	0.00	9.08±0.03	9.10	8.75±0.08	8.42
10	31.00	10.00	0.00	9.34±0.06	9.19	9.29±0.13	9.36
11	31.00	2.00	20.00	7.10±0.14	7.25	7.00±0.13	6.93
12	31.00	10.00	20.00	9.00±0.11	8.98	5.10±0.14	5.43
13	31.00	6.00	10.00	9.09±0.01	9.01	8.03±0.03	7.91
14	31.00	6.00	10.00	8.95±0.06	9.01	7.84±0.00	7.91
15	31.00	6.00	10.00	8.85±0.00	9.01	7.56±0.08	7.91
16	31.00	6.00	10.00	9.06±0.01	9.01	7.88±0.05	7.91
17	31.00	6.00	10.00	9.08±0.11	9.01	8.24±0.06	7.91

* Corresponding author. E-mail: sandra.stamenkovic@live.com

Table S-II. Criteria and the goals of the multicriteria optimization

Factors/Responses	Low level	High level	Significance	Criteria
Temperature, ^{o}C	25	37	3	minimize
OTR, mol $m^{-3}h^{-1}$	2	10	3	In range
Glucose concentration, g l^{-1}	0	20	3	In range
Number of viable cells, log (CFU ml^{-1})	7.1	9.72	5	Maximum
Spore count, log (CFU ml^{-1})	5.1	9.15	3	Maximum

Journal of the Serbian Chemical Society
JSCS-info@shd.org.rs • www.shd.org.rs/JSCS
J. Serb. Chem. Soc. *88* (11) 1119–1123 (2023)
JSCS–5684
Note
Published 11 November 2023

NOTE

Thermal investigation of material derived from the species *Apatura iris*

MARINA SIMOVIĆ PAVLOVIĆ[1]*, MAJA PAGNACCO[2], DIMITRIJE MARA[3], ALEKSANDRA RADULOVIĆ[3], BOJANA BOKIĆ[4], DARKO VASILJEVIĆ[4] and BRANKO KOLARIĆ[4,5]

[1]*Faculty of Mechanical Engineering, University of Belgrade, Kraljice Marije 16, Belgrade, Serbia,* [2]*Institute of Chemistry, Technology and Metallurgy, University of Belgrade, Njegoševa 12, Belgrade, Serbia,* [3]*Institute of General and Physical Chemistry, Studentski trg 12/V, Belgrade, Serbia,* [4]*Photonics Center, Institute of Physics, University of Belgrade, Pregrevica 118, Belgrade, Serbia and* [5]*Micro- and Nanophotonic Materials Group, University of Mons, Place du Parc 20, 7000 Mons, Belgium*

(Received 27 March, revised 20 April, accepted 21 July 2023)

Abstract: The material's size and shape influence its physical, chemical and mechanical properties. This study describes an investigation of natural photonic structure of the butterfly's wing, mainly composed of chitin. The effect of corrugations at the nanoscale on material's optical response is unambiguously revealed in the presented thermal measurements. Furthermore, the presented study shows the possibility of exploiting holography to monitor dynamics *in situ*.

Keywords: *Apatura iris* butterfly; biopolymer chitin; sensing dynamics *in situ*.

INTRODUCTION

Apatura iris butterfly's wing used for this study is shown in Fig. 1.[1–3] Butterfly wings are made of the biopolymer chitin,[4] with general formula $(C_8H_{13}O_5N)_n$. The chitin composition of different parts of the butterfly's body is described elsewhere.[5] The paper revealed that chitins from different parts are chemically very similar, but with significant differences in their surface morphologies.

In this study the surface morphology is characterized by JEOL JSM 6610 LV (Japan), scanning electron microscope (SEM) in conjunction with the energy dispersive spectroscopy (EDS) detector model X-Max large area analytical silicon drift connected with INCA Energy 350 Microanalysis (detection of elements $Z \geq 5$, detection limit: ~ 0.1 mas. %, resolution, 126 eV).

* Corresponding author. E-mail: simovicmarina99@gmail.com
https://doi.org/10.2298/JSC230327042P

Micro-elemental (EDS) analysis of *A. iris* butterfly's wing in two selected points, scale cell and the wing membrane, given in Fig. 2, showed the presence of carbon (C), oxygen (O) and nitrogen (N) originated from chitin. As it can be seen, the content of C, N and O slightly differs in scale cell and the wing membrane, indicating different chitin compositions in different surface structures. The presence of gold (Au) originates from the sample preparation for SEM/EDS analysis.

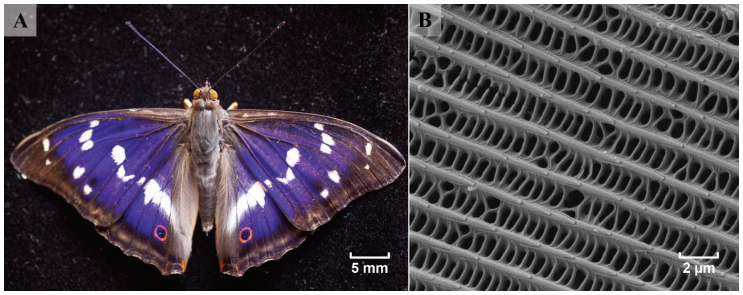

Fig. 1. *Apatura iris* butterfly: A) an optical image of the whole butterfly; B) SEM image of a ground scale of the wing.

Thermal camera "FLIR A65" (640×512 pixel, thermal resolution 50 mK, focal length 13 mm, field of view angle 45°×37°) is used to measure the temperature of the sample after the irradiation with laser. Later, holographic method will be used to characterize the interaction of the photonic structure with light.[6,7] A scheme of the holographic setup that is going to be used in the experiment is described elsewhere.[8] The setup will allow the simultaneous recording of deformation and temperature.

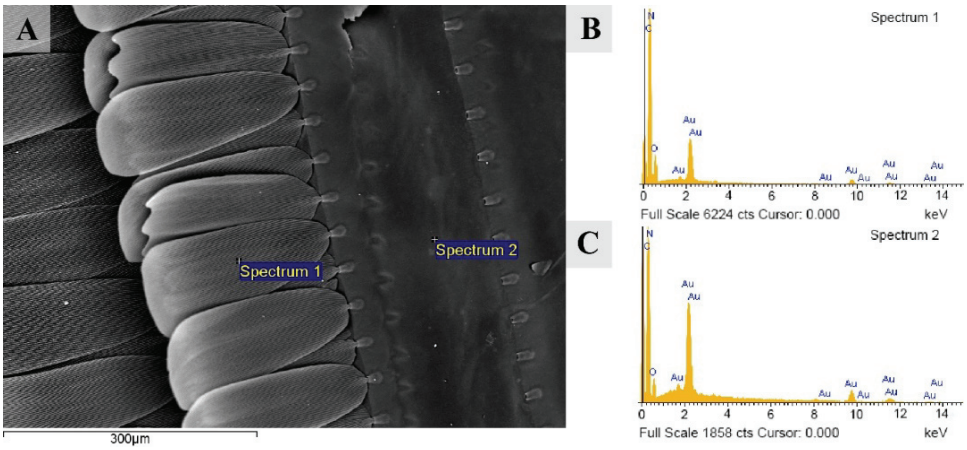

Fig. 2. A) SEM image of the scale cells and the wing membrane of *Apatura iris* butterfly's wing; B) EDS analysis of the wing at the scale cell (Spectrum 1); C) EDS analysis of the wing at the wing membrane (Spectrum 2).

RESULTS AND DISCUSSION

Six samples are individually irradiated by external lasers operating at four different wavelengths (450, 532, 660 and 980 nm) keeping the power and illuminated spot diameter constant at 1 mW and 1 mm, respectively. The thermal measurement is made over the period that includes the time before the start of heating (interaction with laser), during the heating itself, and after the irradiation stopped, more precisely the cooling of the sample.

The difference in temperature due to heating by laser at various wavelengths has been observed. The highest temperature is caused by the interaction with 450 nm light, while the lowest is recorded for the wavelength of 532 nm. However, the complete reversible cooling (reaching the initial state) has not been observed for the wavelengths of 450 and 980 nm. A complete return to the initial state is observed for the wavelengths of 532 and 660 nm.

Analyzing data in depth is vital to link thermal measurement with the reflectance spectrum[9] (Fig. 3A) and the heating/cooling process as a function of time. Fig. 3B is showing the change in temperature over time, as a function of wavelengths.

Finally, the thermal measurements match the reflectance pattern and the heating/cooling dynamics as a function of time. It is evident that the temperature maximum in Fig. 3B at 450 nm corresponds to the reflectance maximum. The maximum value recorded at 450 nm is followed by 660 nm, while the reflectance is at minimum around 532 nm.

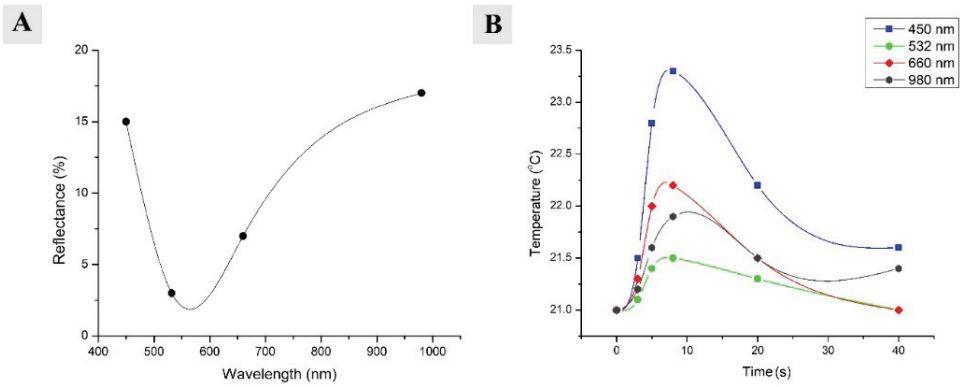

Fig. 3. A) *Apatura iris* reflectance spectrum; B) cooling dynamics as a function of time after the irradiation with four different wavelengths. The lasers have been switched on at 2nd s and switched off at 9th s in order to record heating/cooling dynamics. (Reflectance spectrum is taken from the reference 9).

The only observed discrepancy refers to the wavelength which does not belong to the visible part of the spectrum and for which completely different rules apply. The photon at 980 nm carries the energy that cannot cause any elec-

tronic transitions but can affect the vibrational one within the system as well as thermal management by vibrational relaxation.

The observed asymmetric heating/cooling response scales perfectly with the measured reflectance response.

CONCLUSION

This paper presents an investigation of *Apatura iris*'s natural photonic structures under the light irradiation at different wavelengths. The correlation between the reflectance at different wavelengths and thermal response is revealed.

Acknowledgements. B.K., D.V., and B.B. acknowledge funding provided by the Institute of Physics Belgrade, through the institutional funding by the Ministry of Education, Science and Technological Development of the Republic of Serbia. Additionally, B.K. acknowledges support from F.R.S.-FNRS. M.P. acknowledges support from the Ministry of Education, Science and Technological Development of the Republic of Serbia (Grant No. 451-03-47/2023--01/200026). D.M. and A.R. acknowledges support from Ministry of Science, Technological Development and Innovation of the Republic of Serbia Contract number: 451-03-47/2023-01/ /200051. All authors acknowledge the support of the Office of Naval Research Global through the Research Grant N62902-22-1-2024.

ИЗВОД

ТЕРМАЛНО ИСПИТИВАЊЕ МАТЕРИЈАЛА ИЗ ЛЕПТИРА *Apatura iris*

МАРИНА СИМОВИЋ ПАВЛОВИЋ[1], МАЈА ПАЊАКО[2], ДИМИТРИЈЕ МАРА[3], АЛЕКСАНДРА РАДУЛОВИЋ[3], БОЈАНА БОКИЋ[4], ДАРКО ВАСИЉЕВИЋ[4] и БРАНКО КОЛАРИЋ[4,5]

[1]Машински факултет – Универзитет у Београду, Краљице Марије 16, Београд, [2]Институт за хемију, технологију и металургију, Универзитет у Београду, Његошева 12, Београд, [3]Институт за општу и физичку хемију, Студентски трг 12/V, Београд, [4]Центар за фотонику, Институт за физику, Универзитет у Београду, Прегревица 118, Београд и [5] Micro- and Nanophotonic Materials Group, University of Mons, Place du Parc 20, 7000 Mons, Belgium

Облик и величина материјала утичу на његове физичке, хемијске и механичке особине. Ова студија описује проучавање природних фотонских структура, крила лептира која се претежно састоје од полимера хитина. Ефекат нано коругације на оптички одговор материјала је презентован кроз термална мерења. Такође је представљена могућност примене холографске методе за праћење динамике *in situ*.

(Примљено 27. марта, ревидирано 20. априла, прихваћено 21. јула 2023)

REFERENCES

1. S.R. Mouchet, P. Vukusic, *Adv. Insect Physiol.* **54** (2018) 1 (https://doi.org/10.1016/bs.aiip.2017.11.002)
2. D. Mara, B. Bokic, T. Verbiest, S. R. Mouchet, B. Kolaric, *Biomimetics* **7** (2022) 153 (https://doi.org/10.3390/biomimetics7040153)
3. Z. Han, L. Wu, Z. Qiu, H. Guan, L. Ren, *J. Bionic Eng.* **5** (2008) 14 (https://doi.org/10.1016/S1672-6529(08)60066-9)
4. H.I. Leertouwer, B. D. Wilts, D. G. Stavenga, *Opt. Express* **19** (2011) 24061 (https://doi.org/10.1364/OE.19.024061)

5. M. Kaya, B. Bitim, M. Mujtaba, T. Koyuncu, *Int. J. Biol. Macromol.* **81** (2015) 443 (https://doi.org/10.1016/j.ijbiomac.2015.08.021)
6. D. Pantelić, D. Grujić, D. Vasiljević, *J. Biomed. Opt.* **19** (2014) 127005 (https://doi.org/10.1117/1.JBO.19.12.127005)
7. J. Liu, W. Kuang, J. Liu, Z. Gao, S. Rohani, J. Gong, *J. Chem. Eng.* **438** (2022) 135554 (https://doi.org/10.1016/j.cej.2022.135554)
8. M. Simovic-Pavlovic, M.C. Pagnacco, D. Grujic, B. Bokic, D. Vasiljevic, S. Mouchet, T. Verbiest, B. Kolaric, *J. Vis. Exp.* (2022) e63676 (https://dx.doi.org/10.3791/63676)
9. D. Pantelić, S. Ćurčić, S. Savić-Šević, A. Korać, A. Kovačević, B. Ćurčić, B. Bokić, *Optics Express* **19** (2011) 5817 (https://opg.optica.org/oe/fulltext.cfm?uri=oe-19-7-5817#:~:text=https%3A//doi.org/10.1364/OE.19.005817).

Journal of the Serbian Chemical Society
JSCS-info@shd.org.rs • www.shd.org.rs/JSCS
J. Serb. Chem. Soc. *88* (11) 1125–1134 (2023)
JSCS–5685
Original scientific paper
Published 11 November 2023

Quantum-mechanical study of the electronic properties of $U_xPu_yO_z$ compounds formed during the recovery of spent nuclear fuel

ALEXANDER Y. GALASHEV*, ALEXEY S. VOROB'EV and YURI P. ZAIKOV

Institute of High Temperature Electrochemistry, Ural Branch, Russian Academy of Sciences, Yekaterinburg, Russia

(Received 13 February, revised 22 March, accepted 8 July 2023)

Abstract: A promising way to recover spent nuclear fuel (SNF) is the method of extracting transuranium compounds from molten salt, which makes it possible to obtain a partial separation between transuranium compounds and lanthanides. This work is devoted to the quantum mechanical study of changes in the structure, energy and electronic properties of the main SNF component, uranium dioxide, upon the removal of oxygen from the system. The influence of the considered properties on the substitution of uranium by plutonium is also studied at a ratio, of the number of plutonium atoms to uranium atoms, of 1:7 and 1:3. The removal of oxygen leads to a narrowing of the band gap up to the transition to a conductive state at a ratio of uranium to oxygen of 2:3. The band gap narrows and metallization sets in even when uranium is replaced by plutonium. A two-stage UO_2 metallization scheme based on lithium reduction and direct (electronic) reduction is proposed.

Keywords: geometric and band structures; oxides; plutoniuml; SNF recovery; spectrum of electronic states; uranium.

INTRODUCTION

The uranium–oxygen system seems to be an extremely complex system, the literature data on which are very contradictory.[1] There are reports in the literature about 14 types of oxides ranging from UO to UO_3. A number of uranium oxides have several crystalline modifications. Data on the physicochemical properties of these systems are of great importance, since stable compound UO_2 is a reactor fuel. The basis of ceramic nuclear fuel, *i.e.*, UO_2, has high corrosion, radiation and thermal stability. The high density of UO_2 provides a high concentration of fissile material. The production of electricity using a nuclear reactor does not emit greenhouse gases. Nuclear reactors have a very high energy density. Thus,

* Corresponding author. E-mail: alexander-galashev@yandex.ru
https://doi.org/10.2298/JSC230213038G

when one fuel pellet weighing 10 g is burned in a reactor, energy released is equivalent to the energy obtained by burning ~1300 kg of coal, ~1 m^3 of oil or ~150 m^3 of natural gas.[2] However, the low thermal conductivity of UO_2 leads to high temperature gradients, which limits the size of the products. In addition, the thermal conductivity of the fuel during its lifetime in the reactor is greatly reduced (up to 70 %).[3] Uranium oxides seem to be the most stable compounds of this element, which makes them suitable for storing uranium. Uranium oxides can act as intermediates in the production of other uranium compounds, such as fluorides.

The similar atomic weights and the largely similar atomic structure of uranium and plutonium create prerequisites for considering their effect on the near atomic environment to be practically identical. As a result, the same interaction potentials are used in molecular dynamics modeling of U and Pu.[4]

Electrical conductivity is the physical property that is determined by the electronic structure, has a feedback with it and affects the formation of a new phase. A change in electrical conductivity caused by any process can accelerate or slow down the development of this process. The reduction of uranium dioxide (UO_2) to uranium metal is reduced with the removal of oxygen from the system. The electrolytic reduction method involves the removal of oxygen from UO_2 by displacing uranium from this compound with lithium. The newly formed Li_2O compound enters the salt melt, where it decomposes into Li^+ and O^{2-}. During the electrolytic reduction of spent nuclear fuel (SNF), as a rule, U and Pu simultaneously deposited on the cathode. The U^{3+} reduction potential to metallic U^0 is only 0.34 eV higher than that of Pu^{3+}.[5] The subsequent separation of the alloy, consisting of U and Pu, requires additional operations.[6] In the field of pyroprocessing of SNF, liquid cadmium is applied to recover transuranics from molten salt and provide some degree of separations between transuranics and lanthanides. Analytical analysis using experimental data shows that in SNF recovery using a liquid Cd cathode, when both U and Pu are dissolved in cadmium, the highest Pu:U ratio is 8:1, and the lowest Pu:U ratio is 1:4.[7] Expectedly higher is the proportion of plutonium in binary (U–Pu) metallic fuel intended for fast reactors. In such a non-irradiated fuel, the Pu:U ratio approximately corresponds to a ratio of 1:3, while the proportion of Pu in the irradiated fuel increases significantly.[8] Hubbard corrected density functional theory (DFT+U), than study of the electronic and thermal properties of stoichiometric and hypostoichiometric phases of uranium dioxide was carried out by Kaloni *et al.*[9] It was shown that the removal of oxygen can affect the electronic and thermal transport properties of UO_2. In addition, such properties of hypostoichiometric UO_2 as electronic properties, electronic thermal conductivity, phonon dispersion and lattice thermal conductivity were calculated. A change in the electronic properties during SNF recovery can affect the rate of recovery and the completeness of this process.

Therefore, establishing the degree of electrical conductivity of the intermediate phases is important for controlling the mode of the SNF recovery process.

The purpose of this work is to study changes in the structural, energy and electronic properties of uranium dioxide systems, as well as uranium oxides containing plutonium, when the Pu:U ratio is 1:7 and 1:3, when oxygen atoms are removed from the system.

EXPERIMENTAL

These calculations were performed using the Siesta software package.[10] In the work, a study was made of the reduction of uranium dioxide, as well as the effect of the presence of plutonium on the structures energy and electronic properties of uranium oxides. Uranium dioxide was modeled by combining a 2×2×2 uranium FCC supercell (8 uranium atoms) and two cubic oxygen lattices (16 oxygen atoms). In what follows, we will represent the U_8O_{16} system as UO_2, and the U_8O_{12} system as U_2O_3. The structure of uranium dioxide after geometric optimization is shown in Fig. 1a. To simulate the reduction of uranium dioxide, two and four oxygen atoms were removed from the supercell; systems containing 14 and 12 oxygen atoms were considered. Fig. 1b shows the structure of U_2O_3, containing 8 uranium atoms and 12 oxygen atoms after geometric optimization. The introduction of plutonium is represented by the replacement of one or two U atoms in 2×2×2 uranium FCC supercell by Pu atoms. Thus, we considered systems with the Pu/U ratio in the uranium dioxide structure 1:7 (1 plutonium atom to 7 uranium atoms) and 1:3 (1 plutonium atom to 3 uranium atoms). The simulation was carried out using the LDA+U approximation,[11] the values of the parameters U_{eff} and J_{eff} for both uranium and plutonium atoms were taken to be 4.5 and 0.5 eV, respectively. In all systems considered by us, geometric optimization was carried out using the local density approximation in the CA form.[12] The dynamic relaxation of atoms continued until the change in the total energy of the system became less than 0.001 eV. In the *ab initio* calculations, the Born–Karman periodic boundary conditions were used. The density of the three-dimensional grid used to calculate the electron density was set using a cutoff energy of 550 Ry. The partial density electronic of states (PDOS) and band structures are often used to characterize the electronic properties of materials. The band structure was calculated in the L-Γ-X-U-K-Γ direction. The Brillouin zone was set by the Monkhorst-Pack method[13] using 5×5×5 *k*-points.

The binding energies of a uranium or plutonium atom with the rest of the compound (*i.e.*, compound without uranium or plutonium atom) were calculated according to the expression:

$$E_{bond}^{1U/1Pu} = -\frac{E_{Tot} - E_1 - E_{1A}}{N} \quad (1)$$

where E_{Tot} is the total energy of the system, E_1 is the total energy calculated for the system in the absence of a uranium or plutonium atom, E_{1A} is the energy calculated for a single uranium or plutonium atom, and N is the number of atoms in the system.

The energy of bonds between atoms in a compound:

$$E_{bond} = -\frac{E_{Tot} - N_O E_{1O} - N_U E_{1U} - N_{Pu} E_{1Pu}}{N} \quad (2)$$

where E_{1O}, E_{1Pu}, E_{1U} are the energies calculated for single oxygen, plutonium and uranium atoms, respectively, and N_O, N_{Pu}, N_U are the number of oxygen, plutonium and uranium atoms in the system, respectively.

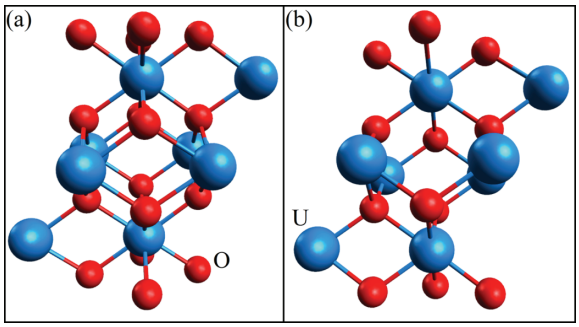

Fig. 1. Geometric structure of: a) UO_2 and b) U_2O_3 after geometric optimization.

RESULTS AND DISCUSSION

Table I represents the following system characteristics: the average binding energy between atoms in the entire system (E_b); the binding energy between the uranium atom and the rest of the system (E_b^{lU}); binding energy between a plutonium atom and the rest of the system (E_b^{lPu}); bond lengths between atoms of uranium and oxygen ($L_{(U–O)}$) and that of plutonium and oxygen ($L_{(Pu–O)}$). It can be seen that the replacement of uranium atoms in the UO_2 compound by plutonium atoms up to get ratios of plutonium to uranium (N_{Pu}/N_U) of 1:7 and 1:3 leads to a decrease in the binding energy E_b by 1.9 and 4.8 %, respectively. The removal of oxygen in the absence of a plutonium in the system leads to a gradual decrease in the binding energy E_b to 2.2 %. However, E_b behaves differently in the presence of plutonium. An increase in the number of oxygen vacancies similarly have affect on the values of E_b in systems with the ratio (N_{Pu}/N_U) of 1:7 and 1:3. In the hypothetical compound U_7PuO_{14} and $U_6Pu_2O_{14}$, the energy E_b increases by 0.3 and 2.5 %, respectively. However, after further withdrawal of oxygen, *i.e.*, in the U_7PuO_{12} and $U_6Pu_2O_{12}$ compounds, the energy E_b decreases. The calculation of the energies E_b^{lU} and E_b^{lPu} was carried out for 4 different uranium atoms; the table shows the average values of the calculated bond energies. In all considered cases, the energy E_b^{lU} decreases on removal of oxygen from the system. The largest drop in energy E_b^{lU} equal to 25.5 % is observed when 4 oxygen atoms are removed from the U_7PuO_{16} compound. At the same time, the bond energy E_b^{lPu} increases when oxygen is withdrawn from plutonium containing systems. Thus, when 4 oxygen atoms were removed from the U_7PuO_{16} and $U_6Pu_2O_{16}$ systems, the energy of E_b^{lPu} increased by 34.0 and 13.3 %, respectively.

The lengths of the U–U and Pu–U bonds in all the considered compounds are practically unchanged and are approximately equal to 3.81 and 3.79 Å, respectively. This agrees with the data of a small displacement of uranium atoms in hypostoichiometric UO_{2-x} compounds.[9] The U–O lengths upon replacement of one or two U atoms by Pu atoms in U_8O_y compounds decrease from 1.5 to 2.2 %

depending on the composition of the hypothetical compound. In all cases a slight decrease, from 0.1 to 1 % in the lengths, of the U–O bonds was found when 4 oxygen atoms were removed from the systems (UO_2, U_7PuO_{16} and $U_6Pu_2O_{16}$). While the Pu–O bond lengths during the transition from the U_7PuO_{16} and $U_6Pu_2O_{16}$ to U_7PuO_{12} and $U_6Pu_2O_{12}$ hypothetical compounds increase by 2.1 and 3.3 %, respectively.

TABLE I. Characteristics of systems $U_{8-x}Pu_xO_y$ (x and y is the number of plutonium and oxygen atoms in the system, respectively); E_b – bond energy of atoms in the system, E_b^{lU}, E_b^{lPu} – energy of bonds between 1 atom of uranium/plutonium with the rest of the system, $L_{(U\text{-}O)}$, $L_{(Pu\text{-}O)}$ – average bond lengths between uranium/plutonium and oxygen atoms

N_{Pu}	N_O	E_b / eV	E_b^{lU} / eV	E_b^{lPu} / eV	$L_{(U\text{-}O)}$ / Å	$L_{(Pu\text{-}O)}$ / Å
0	16	11.527	2.159	–	2.321	–
	14	11.406	2.113	–	2.314	–
	12	11.273	2.106	–	2.313	–
1	16	11.306	3.015	2.499	2.279	2.388
	14	11.345	2.515	3.240	2.279	2.426
	12	11.126	2.244	3.349	2.276	2.439
2	16	10.971	2.603	2.081	2.286	2.329
	14	11.248	2.492	2.280	2.278	2.369
	12	11.047	2.429	2.358	2.263	2.406

Fig. 2 shows the band structures of the considered systems, and Table II presents the electronic properties of the systems containing plutonium. The band gap obtained for uranium dioxide is 2.23 eV, which is slightly larger than the value of 2.19 eV obtained earlier.[14] The removal of two oxygen atoms from the UO_2 system leads to a narrowing of the band gap to 0.99 eV. If we continue to remove oxygen from the system in the same amount (*i.e.*, remove 2 more O atoms), then the system becomes conductive. The narrowing of the band gap and the transition to a conducting phase in hypostoichiometric uranium compounds are consistent with the data previously obtained.[9] Substitution of uranium by plutonium at ratios of N_{Pu}/N_U = 1:7 and 1:3 leads to metallization of the U_7PuO_{12}, $U_6Pu_2O_{16}$, $U_6Pu_2O_{14}$ and $U_6Pu_2O_{12}$ systems, while the U_7PuO_{16} and U_7PuO_{14} systems have semiconductor properties.

Fig. 3 shows the partial density of the electronic states for the UO_2, U_2O_3, U_7PuO_{12} and $U_6Pu_2O_{16}$ systems. It can be seen that the conductive properties in hypothetical compound U_2O_3 appear due to the interaction of the d and f orbitals of uranium with the p orbitals of oxygen. The Fermi level turns out to be slightly shifted into the conduction band of U_2O_3, and the width of the a band gap is ~0.1 eV. At the same time, in the PDOS spectra of U_7PuO_{12} and $U_6Pu_2O_{16}$, the valence band continuously passes into the conduction band. Moreover, conductivity appears in these compounds due to the interaction of 6d uranium orbitals with 5f plutonium orbitals and 5f uranium and plutonium orbitals with 2p oxygen orb-

itals, respectively. In the PDOS of the U_7PuO_{12} compound, a high bimodal peak related to the 5f electrons of uranium is in the valence band, while in the PDOS of the $U_6Pu_2O_{16}$ compound, a similarly shaped peak also related to the 5f electrons of uranium appears in the conduction band. For the three connections (UO_2, U_2O_3, $U_6Pu_2O_{16}$) shown in the figure in the PDOS spectrum, there are adjacent bands not wide enough to span the full range of electron energy levels. In the PDOS spectrum of U_7PuO_{16}, there are no such adjacent allowed bands. In other words, in this case the part of the spectrum that belongs to the valence band is continuous.

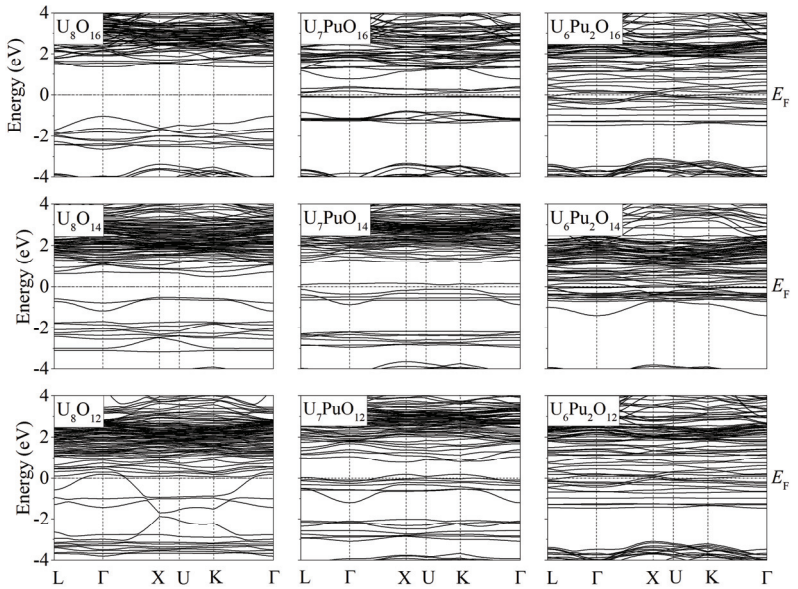

Fig. 2. Band structures obtained for compounds U_8O_{16}, U_8O_{14}, U_8O_{12}, U_7PuO_{16}, U_7PuO_{14}, U_7PuO_{12}, $U_6Pu_2O_{16}$, $U_6Pu_2O_{14}$ and $U_6Pu_2O_{12}$.

TABLE II. Conductivity characteristics of uranium oxide systems containing plutonium

Compound	Electronic properties	Band gap, eV	Compound	Electronic properties	Band gap, eV
U_7PuO_{16}	Semiconductor	0.07	$U_6Pu_2O_{16}$	Metal	–
U_7PuO_{14}	Semiconductor	0.21	$U_6Pu_2O_{14}$	Metal	–
U_7PuO_{12}	Metal	–	$U_6Pu_2O_{12}$	Metal	–

The presence of many different phases of non-stoichiometric actinide oxides (AO_x), complex structures and their tendency to form solid solutions make it extremely difficult to understand not only the structure, but also chemical composition. Nevertheless, the DFT+U calculations reflect the correct trend of the band gap depending on the oxidation state of the actinides.[15]

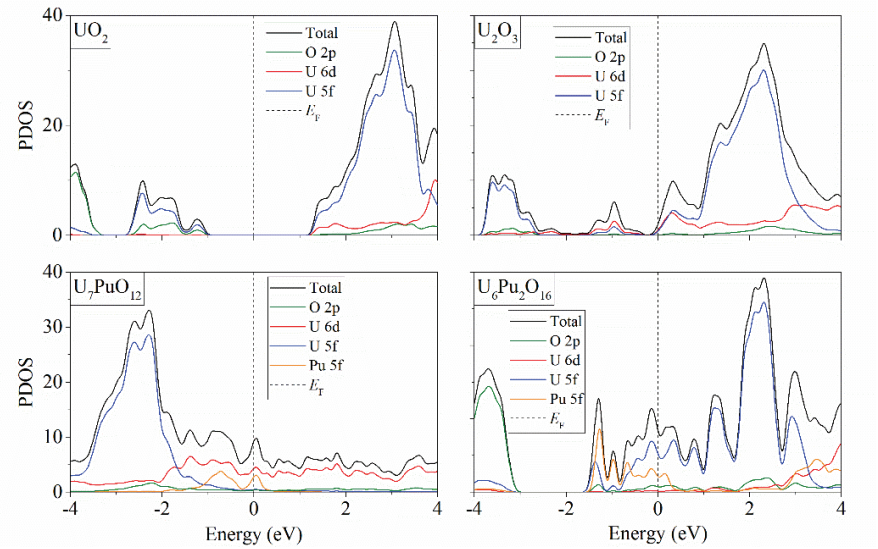

Fig. 3. Partial density of electronic states obtained for compounds UO_2, U_2O_3, U_7PuO_{12} and $U_6Pu_2O_{16}$.

The reduction of UO_2 to uranium metal in the molten salt of LiCl with the addition of Li_2O takes place in close contact with the cathode and is an electrochemical process. We now represent the process of reduction of UO_2 by chemical reactions. The presence of the electrical conductivity in the U_2O_3 phase allows us to understand more deeply the process of electrochemical pyrolysis that we consider. A small (~ 3 %) initial addition of Li_2O to the LiCl electrolyte leads to an imbalance between Li^+ and Cl^- in the salt melt and the creation of the necessary double charged layer near the surface of the UO_2 pellet after creating a certain electrical voltage (3.0–3.3 V) between the electrodes. In general, the decay of Li_2O can be represented as:

$$Li_2O \rightarrow 2Li^+ + O^{2-} \quad (3)$$

O^{2-} formed after the decay of Li_2O can quickly reach the anode, because O^{2-} are 2.2 times lighter than Cl^-. In addition, their electric charge is 2 times greater than that of Cl^-. Each O^{2-} gives out 2 electrons at the anode. The formed O atoms combine into O_2 molecules which form bubbles that rise and remove oxygen from the system.

To simplify, let us consider the SNF recovery process using pure UO_2 as an example. The first stage of the process mainly involves the external part (that is directly in contact with the electrolyte) of the UO_2 pellet. After the formation of a double electric layer between the surface of a highly polarized semiconductor (UO_2) and the near-surface part of an electrolyte (LiCl) strongly enriched with

Li^+, a strong local electric field arises and "pulls" oxygen ions from the surface of the semiconductor:

$$2UO_2 \rightarrow (U_2O_3)^{2+} + O^{2-} \quad (4)$$

In the near-surface region of the electrolyte, O^{2-} combines with two Li^+ to form an electrically neutral molecule Li_2O:

$$2Li^+ + O^{2-} \rightarrow Li_2O \quad (5)$$

The second stage of recovery begins with the electronically conductive metallized $(U_2O_3)^{2+}$ and with an excess of positive charge takes the missing electrons thus becomes electrically neutral, but the conducting substance:

$$(U_2O_3)^{2+} + 2e^- \rightarrow U_2O_3 \quad (6)$$

The continuation of the second stage of reduction is associated exclusively with the electrical conductivity of the intermediate U_2O_3 phase. The electrically conductive surface layer continues to receive electrons and U_2O_3 is reduced to the metallic uranium:

$$U_2O_3 + 6e^- \rightarrow 2U + 3O^{2-} \quad (7)$$

The mechanism for the reduction of UO_2 to metallic U presented here is supported by experimental facts, among which are the movement of the metallization front from the surface to the center of the pellet and the absence of lithium inside the pellet with a 98 % reduced metal U.[5–8] In addition, the reduction process actively occurs in a high-quality sintered UO_2 powder granule, but quickly fades if the spent fuel used for recovery is taken in the form of a conventional powder.

A significant increase in the electronic contribution for certain compositions of oxide nuclear fuel contributes to an increase in thermal conductivity.[9] We have shown that this conclusion is also valid in the presence of Pu in the fuel. Thus, the use of hypostoichiometric phases seems to be favorable for obtaining a fuel that is resistant to accidents.

CONCLUSION

In this work, based on quantum mechanical calculations, the partial reduction of uranium and uranium–plutonium oxides is studied. The change in the structure, energy, and electronic properties of these oxides was studied when uranium atoms were replaced by plutonium atoms up to the ratio of the number of atoms in the system N_{Pu}/N_U = 1:7 and 1:3. A decrease in the total bond energy in the UO_2 compound is shown when uranium is replaced by plutonium in the ratios N_{Pu}/N_U = 1:7 and 1:3. An increase in the bond energy between plutonium and the rest of the compound was revealed upon the removal of oxygen from the U_7PuO_{16} and $U_6Pu_2O_{16}$ systems. It is shown that the band gap narrows up to complete metallization of the compound when oxygen is removed from the UO_2

compound to the ratio N_U/N_O = 2:3. A transition to the conducting state of the UO_2 compound was revealed when uranium was replaced by plutonium in the ratios N_{Pu}/N_U = 1:3. A two-stage process of uranium metallization during its reduction in LiCl–Li_2O melt is proposed. We hope that this study will improve understanding of the SNF electrolytic reduction process and serve as a stimulus for its optimization.

Acknowledgements. The calculations were performed on a hybrid cluster-type computer "URAN" at the Institute of Mathematics and Mechanics, Ural Branch of the Russian Academy of Sciences with a peak performance of 216 Tflop/s and 1864 CPUs. The work is executed within the framework of the multipurpose program "Development of equipment, technologies and scientific research in the field of the use of atomic energy in the Russian Federation for the period up to 2024".

И З В О Д

КВАНТНО-МЕХАНИЧКА СТУДИЈА ЕЛЕКТРОНСКИХ ОСОБИНА $U_XPu_YO_Z$ ЈЕДИЊЕЊА ФОРМИРАНИХ ТОКОМ ОБНАВЉАЊА ИСТРОШЕНОГ НУКЛЕАРНОГ ГОРИВА

ALEXANDER Y. GALASHEV, ALEXEY S. VOROB'EV и YURI P. ZAIKOV

Institute of High Temperature Electrochemistry, Ural Branch, Russian Academy of Sciences, Yekaterinburg, Russia

Обећавајући начин за обнављање истрошеног нуклеарног горива (SNF) је метод екстракције трансуранских једињења из стопљене соли, што омогућава да се добије делимично раздвајање трансуранских једњења и лантанида. Овај рад је посвећен квантно механичкој студији промена у структури, енергији и електронским особинама главне SNF компоненте, уранијум диоксида, при уклањању кисеоника из система. Такође је студиран утицај проучаваних особина на однос броја плутонијумових атома према уранијумовим атомима 1:7 и 1:3. Уклањање кисеоника доводи до сужавања јаза између трака до преласка у проводно стање при односу уранијума и кисеоника од 2:3. Јаз између трака се сужава и долази до метализације чак и када се уранијум замени са плутонијумом. Предложена је двостепена шема метализације UO_2 заснована на редукцији литијумом и директној (електронској) редукцији.

(Примљено 13. фебруара, ревидирано 22. марта, прихваћено 8. јула 2023)

REFERENCES

1. E. Curti, D.A. Kulik, *J. Nucl. Mater.* **534** (2020) 152140 (https://doi.org/10.1016/j.jnucmat.2020.152140)
2. D. H. Hurley, A. El-Azab, M. S. Bryan, M. W. D. Cooper, C. A. Dennett, K. Gofryk, L. He, M. Khafizov, G. H. Lander, M. E. Manley, J. M. Mann, C. A. Marianetti, K. Rickert, F. A. Selim, M. R. Tonks, J. P. Wharry, *Chem. Rev.* **122** (2022) 3711 (https://doi.org/10.1021/acs.chemrev.1c00262)
3. C. Ronchi, M. Sheindlin, D. Staicu, M. Kinoshita, *J. Nucl. Mater.* **327** (2004) 58 (https://doi.org/10.1016/j.jnucmat.2004.01.018)
4. K. Govers, S. Lemehov, M. How, M. Verwerft, *J. Nucl. Mater.* **376** (2008) 66 (https://doi.org/10.1016/j.jnucmat.2008.01.023)

5. S. Kihara, Z. Yoshida, H. Aoiyagi, K. Maeda , O. Shirai , Y. Kitatsuji, Y. Yoshida, *Pure Appl. Chem.* **71** (1999) 1771 (https://doi.org/10.1351/pac199971091771)
6. A. Y. Galashev, *Int. J. Energy Res.* **46** (2022) 3891 (https://doi.org/10.1002/er.7458)
7. G. L. Fredrickson, T.-S. Yoo, *J. Nucl. Mater.* **508** (2018) 51 (https://doi.org/10.1016/j.jnucmat.2018.05.037)
8. A.Y. Galashev, *Int. J. Energy Res.* **45** (2021) 11459 (https://doi.org/10.1002/er.6267)
9. T. P. Kaloni, N. Onder, J. Pencer, E. Torres, *Ann. Nucl. Energy* **144** (2020) 107511 (https://doi.org/10.1016/j.anucene.2020.107511)
10. J. M. Soler, E. Artacho, J. D. Gale, A. García, J. Junquera, P. Ordejón, D. Sánchez-Portal, *J. Phys.: Condens. Matter* **14** (2002) 2745 (https://doi.org/10.1088/0953-8984/14/11/302)
11. S. L. Dudarev, G. A. Botton, S. Y. Savrasov, C. J. Humphreys, A. P. Sutton, *Phys. Rev., B* **57** (1998) 1505 (https://doi.org/10.1103/PhysRevB.57.1505)
12. J. P. Perdew, A. Zunger, *Phys. Rev., B* **23** (1981) 5048 (https://doi.org/10.1103/PhysRevB.23.5048)
13. H. J. Monkhorst, J. D. Pack, *Phys. Rev., B* **13** (1976) 5188 (https://doi.org/10.1103/PhysRevB.13.5188)
14. C. L. Dugan, G. G. Peterson, A. Mock, C. Young, J. M. Mann, M. Nastasi, M. Schubert, L. Wang, W.-N. Mei, I. Tanabe, P. A. Dowben, J. Petrosky, *Eur. Phys. J., B* **91** (2018) 67 (https://doi.org/10.1140/epjb/e2018-80489-x)
15. H. He, D. A. Andersson, D. D. Allred, K. D. Rector, *J. Phys. Chem., C* **117** (2013) 16540 (https://doi.org/10.1021/jp401149m).

Journal of the Serbian Chemical Society
JSCS-info@shd.org.rs • www.shd.org.rs/JSCS
J. Serb. Chem. Soc. *88* (11) 1135–1147 (2023)
JSCS–5686
Original scientific paper
Published 11 November 2023

Electrical conductivity of $GdCl_3$–LiCl and $GdCl_3$–LiCl-Gd_2O_3 molten systems

ELENA V. NIKOLAEVA*, IRINA D. ZAKIRYANOVA, ANDREY L. BOVET and IRAIDA V. KORZUN

Institute of High Temperature Electrochemistry, UB RAS, 620990 Yekaterinburg, Russia

(Received 31 January, revised 31 July, accepted 14 August 2023)

Abstract: The electrical conductivity of LiCl–$GdCl_3$ molten systems with the gadolinium chloride additions ranging from 0 to 23 mol % was measured depending on both the temperature and concentration of $GdCl_3$. The molar conductivity of the molten $GdCl_3$–LiCl system is calculated taking into account the assumption of additivity of the molar volume of the mixture. The obtained temperature dependencies can be approximated by Arrhenius-type equation. The effective activation energy, E_a, increased with the $GdCl_3$ content. The liquidus temperatures of the studied systems were determined by differential scanning calorimetry. The high-temperature Raman spectra of LiCl–$GdCl_3$ chloride melts were recorded. In addition, the conductivity of 0.77LiCl–0.23$GdCl_3$ molten system with 1 mol % of Gd_2O_3 was measured. The investigation demonstrates that the addition of gadolinium oxide results in a decrease of the conductivity of the chloride molten system and growth of its liquidus temperature.

Keywords: AC impedance; gadolinium chloride; liquidus temperature; Raman spectra.

INTRODUCTION

Gadolinium and its compounds are widely used in many areas of science and technology, such as nuclear power engineering, electronics, medicine. The unique magnetic properties of gadolinium allow it to be used for the production of laser materials. The high capability of neutron capturing makes it possible to use gadolinium compounds for controlling the operation of nuclear reactors.

The study of the electric transfer processes of molten mixtures of rare earth metal (RE) and alkali metal (M) chlorides is of interest in connection with the development of a number of scientific and technical problems related to the optimization of the processes of electrolytic production and refining of rare earth metals, use and regeneration of spent nuclear fuel (SNF).[1] For example, the pyro-

* Corresponding author. E-mail: E.Nikolaeva@ihte.uran.ru
https://doi.org/10.2298/JSC230131051N

chemical methods of SNF reprocessing are considered as promising options in the innovative nuclear fuel cycle.[2,3] The development of technologies requires knowledge of the electrochemical and thermodynamic properties of molten mixtures of rare earth and alkali metal halides. In industrial production, it is desirable to have an electrolyte with high electrical conductivity and low liquidus temperatures to reduce energy consumption. Lithium chloride has the highest electrical conductivity among alkali metal chlorides and a relatively low melting point. Thus, the main operations of the pyrochemical processing of SNF are supposed to be carried out using anhydrous technologies in molten LiCl and eutectic LiCl–KCl.[4]

The electrical conductivity of only certain mixtures of RE chlorides with lithium chloride has been experimentally studied: LiCl–$LaCl_3$,[5] LiCl–$PrCl_3$,[6] LiCl–$NdCl_3$[6] and LiCl–$SmCl_3$.[6] The conductivity of molten mixtures of $GdCl_3$ with NaCl and KCl were investigated.[7,8] Earlier we measured the conductivity of molten 0.515$GdCl_3$–0.485KCl[9] system and $GdCl_3$.[10] There is no available data on the conductivity of molten LiCl–$GdCl_3$ mixtures.

Zhou *et al*.[11] established the LiCl–$GdCl_3$ binary phase diagram based on the earlier results of differential thermal analysis and X-ray diffraction optimized using CALPHAD Thermo-Cal software. The authors[11] demonstrated that the phase diagram had a simple eutectic form. The eutectic point corresponds to the temperature of 678 K and a concentration of $GdCl_3$ of 45.2 mol %. The presence of Li_3GdCl_6 ternary compound with polymorphic transformation at 646 K and peritectoid decomposition at 660 K was identified in the solid phase.

The purpose of this work was to determine the specific conductivity of molten $GdCl_3$–LiCl systems containing up to 23 mol % $GdCl_3$. Based on the experimental data, the calculation of molar conductivity was carried out.

Lanthanide chlorides are known to be extremely hygroscopic. When the temperature rises, they react with their own crystallization water to form very stable oxychlorides, which can dissolve in RE chlorides when the latter are melted.[12] The presence of oxychlorides in molten $RECl_3$ in dissolved form or in the form of solid particles leads to a decrease in the electrical conductivity of the systems.[9,10] Therefore, another aim of this work was to study the effect of oxygen impurities on the electrical conductivity of $GdCl_3$–LiCl melts. To do this, the conductivity of 0.77LiCl–0.23$GdCl_3$ system containing 1 mol % of gadolinium oxide was investigated.

The liquidus temperatures were determined for all investigated chloride and oxide-chloride systems. In order to analyze the structural changes occurring in the chloride melt, the Raman spectra of homogeneous $GdCl_3$–LiCl chloride melts were obtained.

EXPERIMENTAL

Samples preparation

Lithium chloride (*puriss* grade, "Vekton," St. Petersburg, Russia) was heated in vacuum with a gradual increase in temperature to 673 K and melted in an argon atmosphere. The resulting melt was additionally purified by directional crystallization (zone melting). According to the DSC curve (thermal analyzer STA 449C Jupiter (NETZSCH)) of the purified LiCl, a single peak is observed, which corresponds to the salt melting (Fig. 1A), and its temperature position 880±1 K agrees with the available data for LiCl, T_m = 883±2 K.[13] The enthalpy change of melting (ΔH_m = 19.903 kJ/mol) also agrees well with the available data[13] (ΔH_m = = 19.83±0.2 kJ/mol).

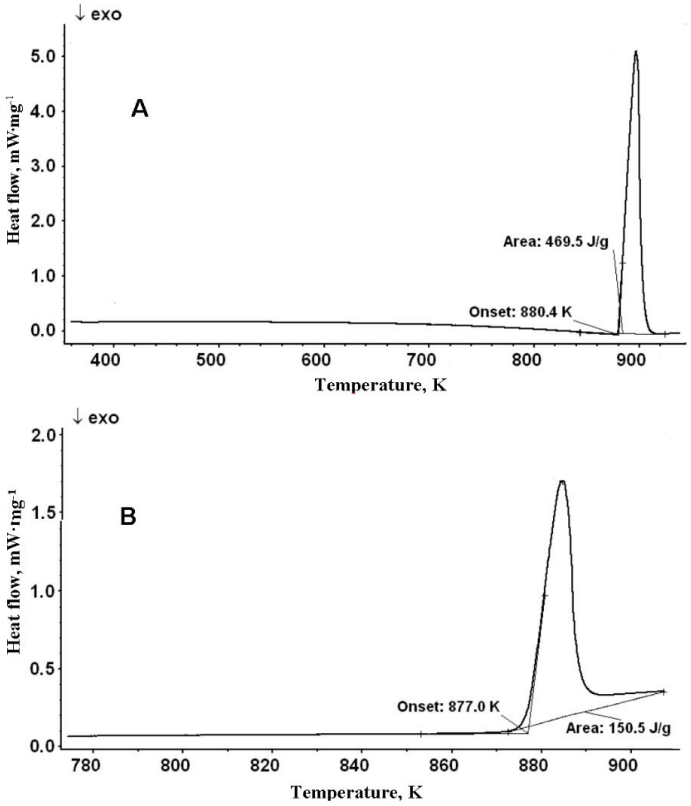

Fig 1. DSC curves for LiCl (A) and $GdCl_3$ (B).

Gadolinium chloride was prepared from gadolinium oxide (*puriss* grade, "Vekton," St. Petersburg, Russia) according to the well-known technique, a detailed description of which was given in literature.[10]

The quality of anhydrous $GdCl_3$ was investigated by a well-proven visual method for determining the transparency of a salt solution in distilled water. On the DSC curve (Fig.1B) of synthesized $GdCl_3$ one peak corresponding to the melting of the salt is observed, and its temperature position 877±1 K is consistent with the available data for $GdCl_3$.[14-17]

The Gd_2O_3 powder was dried at 973 K for 4 h. X-ray diffraction and Raman spectroscopy confirmed the monophasic nature of the obtained product.[10]

All the operations with the prepared reagents were carried out in a glove box in a dry nitrogen atmosphere.

Electrical conductivity measuring technique

The experiments to determine the electrical conductivity of the $GdCl_3$–LiCl melt were carried out in a cell with parallel platinum electrodes. The electrical conductivity was measured using a Z-1500J impedance meter, which allows the measurements to be carried out in the frequency range of alternating current from 1 to 1.5 MHz. The scheme of the experimental cell and the method of conducting the experiment are described in detail in the literature.[18]

The measuring set was calibrated in molten LiCl for which the explicit data on the conductivity within 917–1056 K are known.[5] The electrical conductivity measurements were performed at the temperatures above the liquidus temperature of each electrolyte composition. There were at least three consequential measurements in a series of experiments.

$GdCl_3$ was gradually added to molten LiCl in small portions without disturbing the gaseous atmosphere of the cell. After each addition, the system was kept at a certain temperature until the values of electrical resistance became stable. Only after this, the measurements of the temperature dependence of the electrical conductivity started. The concentration of $GdCl_3$ was determined after the experiment in a frozen float by the emission spectral analysis with inductively coupled plasma (Optima 4300 DV, "Perkin Elmer" USA).

Determination of liquidus temperature using differential scanning calorimetry

Liquidus temperatures were obtained by differential scanning calorimetry (DSC) using an STA 449C Jupiter® NETZSCH thermal analyser (Germany). The studies were carried out with a heating rate of 10 K/min in a high purity argon atmosphere in Pt–Rh crucibles. The uncertainty of the liquidus temperature values was less than 1 K. The liquidus temperature of each sample was determined during heating for the second measurement.[19]

High-temperature Raman spectra technique

Raman spectra of solid samples and melts were recorded using the Ava-Raman fiber-optic spectrometric complex (Avantes, the Netherlands), which includes a 50 mW laser source of monochromatic radiation with a wavelength of λ = 532 nm. When registering the spectra, an 180° optical scattering scheme was used. The device of a high-temperature optical prefix was described earlier.[19] Platinum crucible was used as a container; the experiment was carried out in an argon atmosphere.

RESULTS AND DISCUSSION

Liquidus temperature of LiCl–$GdCl_3$ system

DSC curves were obtained for LiCl–$GdCl_3$ systems containing up to 23 mol % of $GdCl_3$. As an example, Fig. 2 demonstrates the DSC and TG curves obtained for the 0.85LiCl–0.15$GdCl_3$ system. According to Zhou *et al.*[11] the temperatures of 647.7 and 664.3 K correspond to the temperatures of phase transitions in solid state. The solidus temperature is 680 K. The liquidus temperature for this composition is 819.3 K.

Liquidus temperatures for all the studied systems are given in Table I. Our data are in good agreement with the literature.[11]

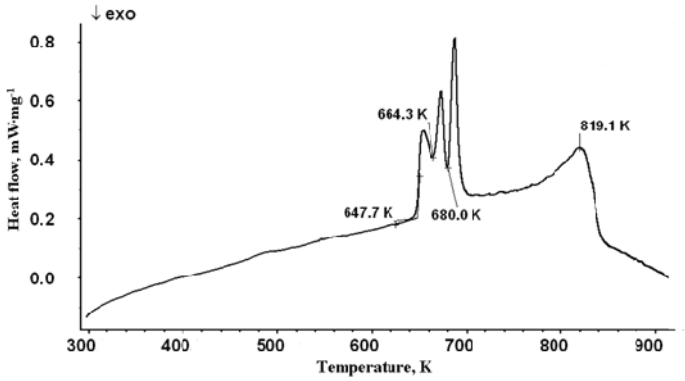

Fig. 2. DSC curve for the system 0.84LiCl–0.16$GdCl_3$.

Electrical conductivity of $GdCl_3$–LiCl molten systems

The temperature dependences of the specific electrical conductivity of the $GdCl_3$–LiCl molten systems containing up to 23 mol % of $GdCl_3$ were investigated in the range from the temperature above the liquidus temperature of each mixture up to 1073 K (for composition 0.23$GdCl_3$–0.77LiCl up to 1153 K). The obtained experimental data are shown in Fig. 3 together with the available data for LiCl.[5] It can be seen that the addition of $GdCl_3$ reduces the conductivity of the systems. The temperature dependences of the specific conductivity of LiCl–$GdCl_3$ melts were approximated by the linear equation:

$$\kappa = a + Bt \quad (1)$$

here κ is the specific conductivity, T – the temperature (K), a and b are constants. The coefficients of Eq. (1) are given in Table I.

TABLE I. Liquidus temperatures and coefficients in Eq. (1) for LiCl–$GdCl_3$ and LiCl–$GdCl_3$–Gd_2O_3 systems

System	T_{liq}	A	B	κ / S cm^{-1}		
	K	S cm^{-1}	S cm^{-1} K^{-1}	923 K	1023 K	1103 K
0.94LiCl–0.06$GdCl_3$	873	0.7125	0.00461	5.07	5.54	–
0.89LiCl–0.11$GdCl_3$	843	0.4292	0.00419	4.43	4.86	–
0.84LiCl–0.16$GdCl_3$	819	0.0691	0.00401	3.87	4.28	–
0.77LiCl–0.23$GdCl_3$	752	–0.1441	0.00356	3.16	3.51	3.79
[0.77LiCl–0.23$GdCl_3$]–Gd_2O_3 (1 mol %)	1090	0.9872	0.00243	–	–	3.67

Fig. 4 shows the isotherms of the normalized conductivity of the LiCl–$GdCl_3$ system containing from 0 to 23 mol % $GdCl_3$. It can be seen that the specific conductivity gradually decreases with an increase in the concentration of gadolinium chloride, deviating from additive magnitudes towards smaller values. Thus, at 1023 K, the addition of 20 mol % $GdCl_3$ reduces the specific conduct-

ivity of the system by almost 40 %. The largest changes in the conductivity of the system occur at low temperatures.

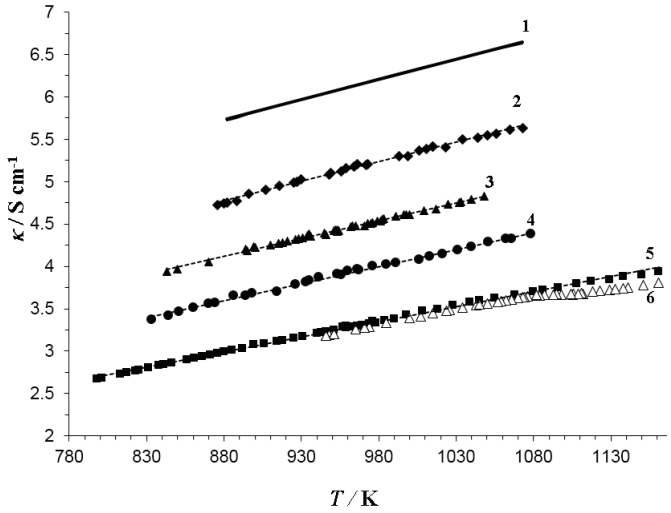

Fig. 3. Temperature dependence of the specific electrical conductivity of molten LiCl (1);[5] molten LiCl, containing $GdCl_3$ (mol %): 6 (2); 11 (3); 16 (4); 23 (5); 0.77LiCl–0.23$GdCl_3$ containing 1 mol % Gd_2O_3 (6).

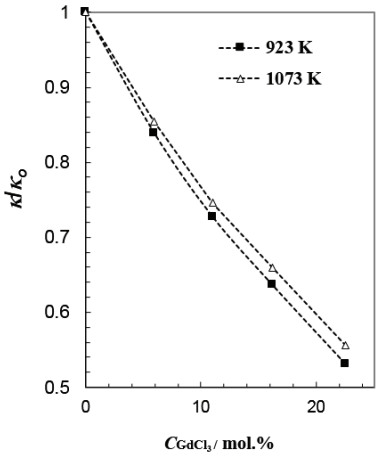

Fig 4. Isotherms of normalized electrical conductivity of LiCl–$GdCl_3$ molten system at different temperatures (κ_0 – specific conductivity of LiCl).

Molar conductivity of molten $GdCl_3$–LiCl mixtures

The specific conductivity is the conductivity of a single volume of liquid. It is the value directly measured in the experiment. For the purposes of further analysis, it has the disadvantage that a single volume of different liquids (melts) contains a different number of molecules of the studied substances and, thus, a direct comparison of specific conductivity does not quite correctly reflect the properties

of the compared melts. It is more correct to compare the molar conductivity, that is, the conductivity of one mol of each melt.

The molar conductivity (Λ) of LiCl–$GdCl_3$ melt can be calculated according to the equation:

$$\Lambda = \kappa V_m \quad (2)$$

where V_m is the molar volume.

Most mixtures of alkali and RE halides are formed with an increase in volume compared to its additive value.[20] Common to all systems is the effect of increasing deviations of the molar volume from the additive values as the size of the alkali metal cation increases.

Thus, according to the literature[5,20,21] for binary mixtures of RE chlorides with LiCl maximum the relative deviations of the additivity of the molar volume are less than 1 %. While when RE chlorides are mixed with cesium chlorides, this value can reach 4–5 %.

Therefore, the molar volume of the melt xLiCl–$y$$GdCl_3$ can be represented by the following expression:

$$V_m = x(M_1/d_1) + y(M_2/d_2) \quad (3)$$

where M_1 and d_1 are the molecular weight and density of the melt LiCl; M_2 and d_2 are the molecular weight and density of the melt $GdCl_3$ (extrapolated to the studied temperature range), x and y are the molar fractions of the corresponding melt components.

The values of molar electrical conductivity of LiCl–$GdCl_3$ melts calculated in this way are shown in Fig. 5 (curves 2–5) in coordinates ln $\Lambda \div 1/T$. In these coordinates, the values of molar conductivity can be approximated by the linear equation:

$$\ln \Lambda = A - E_A/(RT) \quad (4)$$

where A – constant; T is the absolute temperature (K); R – universal gas constant (J K^{-1} mol^{-1}); E_a is the activation energy of conductivity.

Fig. 5 also shows the molar conductivity values for LiCl (curve 1) and $GdCl_3$ (curve 6) melts calculated on the basis of the available data on specific conductivity [5,10] and density.[5,21] The values of the molar conductivity at 923 and 1023 K are given in Table II. The molar conductivity of LiCl is several times higher than of $GdCl_3$ whereas the activation energy of the $GdCl_3$ conductivity is 3 times higher than of LiCl. The addition of gadolinium chloride to molten LiCl reduces electrical conductivity of the systems. A slight increase in the activation energy can be noted with an increase in the concentration of $GdCl_3$ up to 23 mol %.

All isotherms of molar conductivity, both obtained by us for the $GdCl_3$–LiCl system and the available data for the $LaCl_3$–LiCl,[5] $PrCl_3$–LiCl,[6] $NdCl_3$–LiCl[6] and $SmCl_3$–LiCl[6] systems, have a similar layout. As the $RECl_3$ concentration increases, the molar conductivity of the LiCl–$RECl_3$ mixtures gradually dec-

reases, deviating from additivity towards lower values. The maximum deviations from additivity are achieved when the $RECl_3$ content in the melt is about 25 mol % and does not exceed 10–12 %. In this work, for the $GdCl_3$–LiCl system containing 23 mol % gadolinium chloride, the deviation of the molar conductivity from the additive values is 10 %.

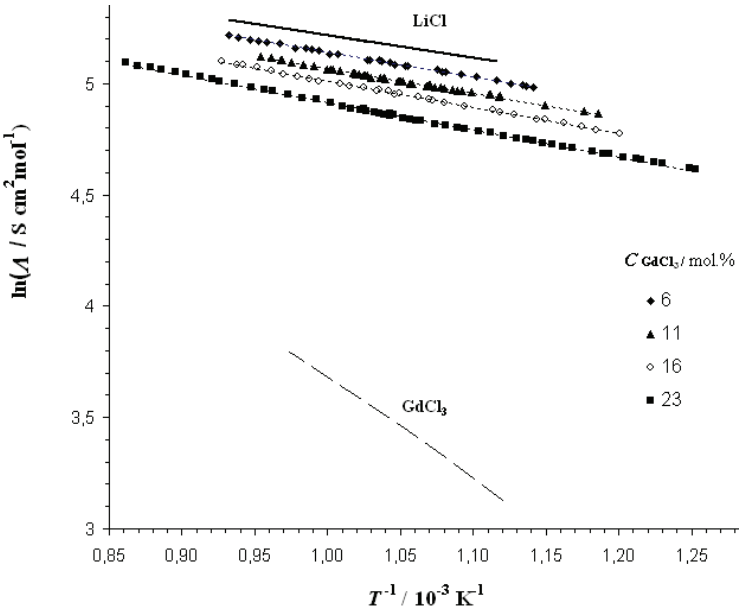

Fig. 5. Temperature dependence of the molar conductivity of molten LiCl;[5] $GdCl_3$;[10,21] LiCl containing 6, 11, 16 and 23 mol % of $GdCl_3$.

TABLE II. Coefficients of Eq. (3) for LiCl–$GdCl_3$ molten system

c_{GdCl_3} / mol %	Temperature range, K	A	E_a / kJ mol^{-1}	Λ / S cm^2 mol^{-1}	
				923 K	1023 K
0[5]	917–1056	6.2367	8.48	169.33	188.64
6	873–1070	6.2395	9.14	155.82	175.06
11	840–1045	6.1921	9.36	144.32	162.61
16	830–1063	6.1777	9.71	135.99	153.89
23	795–1158	6.1437	10.20	123.25	140.36
100[10,21]	893–1028	8.1969	37.55	27.35	43.62

In the $GdCl_3$–NaCl and $GdCl_3$–KCl systems, the molar conductivity isotherms show deeper minima. At $GdCl_3$ concentrations of 30–40 mol %, the deviation of molar conductivity from additive values reaches 30–50 %.[7]

The ionic potential of alkali metal cations is substantially lower than that of RE^{3+}. Therefore, RE^{3+} act as complexing agents, coordinating chlorine anions around themselves and displacing alkali metal cations into the second coordin-

ation sphere. When a small amount (on the order of magnitude of a few mol %) of $RECl_3$ is added to the MCl melt, strong 6-coordinate $GdCl_6^{3-}$ complexes are formed in the second coordination sphere of which there are alkali metal cations. This fact has been proven by many independent research methods. [22–25]

With an increase in the $RECl_3$ concentration, an increasing number of Cl^- are required for the formation of six-coordinated complexes. The theoretical limit is 25 mol % $RECl_3$ when all anions are coordinated around RE^{3+}. At higher $RECl_3$ concentrations, the melt structure becomes more complicated due to the inclusion of $RECl_6^{3-}$ octahedra in more complex ionic groups.

Analysis of the available data[5–10] shows that the conductivity of molten salt mixtures gradually decreases with the addition of RE chlorine anions to an alkali metal chloride, while the transfer numbers of chlorides decrease, since a lot of Cl^- bind to complexes and do not participate in the transfer of electricity.

The alkali metal cations are displaced into the second coordination sphere, the mobility of Na^+ and K^+ decreases slightly with increasing $RECl_3$ concentration[26] whereas in LiCl–$RECl_3$ mixtures, in the concentration range from 0 to 80 mol % $RECl_3$, the mobility of Li^+ decreases by half.[27] The ionic potential of Gd^{3+} is only 2.4 times greater than the ionic potential of Li^+,[28] so the counter-polarizing effect of three Li^+ can lead to strong distortions and dissociation of $GdCl_6^{3-}$ complexes. This can explain the fact that the deviations of molar conductivity of molten LiCl–$RECl_3$ mixtures from additive values are small.

Raman spectra of LiCl–$GdCl_3$ melts

In situ Raman spectroscopy has been used to obtain information about the structural features and characteristic vibrational frequencies of complex groupings in chloride melts containing lithium and gadolinium ions. Fig. 6 shows the Raman spectra of LiCl–$GdCl_3$ melts containing 0; 15; 25 mol. % $GdCl_3$. No vibrational bands are recorded in the LiCl melt (Fig. 6). This fact directly indicates the predominantly Coulomb type of interparticle interaction in this system and the absence of a stable complex structural groupings in it.[29,30] A band at 252 cm^{-1} was recorded in gadolinium-containing melts, which is attributed to the valence symmetric vibration of the complex grouping $GdCl_6^{3-}$. The increase in the normalized intensity of this vibrational band was noted with the growing content of gadolinium chloride in the melt (Fig. 6), which is associated with an increase in the concentration of such groupings.

The obtained results made it possible to explain the results of the study of the conductivity of these systems. Indeed, when gadolinium ions are introduced into the melt, part of the chlorides binds to the $GdCl_6^{3-}$ grouping, which leads to a decrease in their mobility, and, as a consequence, to a difficulty in electrical transfer and to an increase in the activation energy of this process.

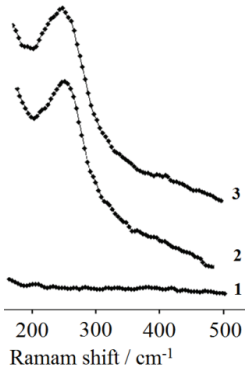

Fig 6. The Raman spectrum of the molten LiCl (1) and of the molten LiCl after the addition of $GdCl_3$ (mol %): 15 (2); 25 (3) at 898 K.

Conductivity and liquidus temperature of the $GdCl_3$–LiCl–Gd_2O_3 molten mixture

The temperature dependence of the electrical conductivity when introducing 1 mol % gadolinium oxide into the $0.23GdCl_3$–0.77LiCl system is shown in Fig. 3. Two sections with different slopes can be distinguished on the curve. The temperature at which the slope changes corresponds to the liquidus temperature of the system. Thus, the introduction of 1 mol % of gadolinium oxide leads to a significant increase in the liquidus temperature from 751 to 1090 K, which is obviously due to the low solubility of gadolinium oxide in the melt under study.

The section of the temperature dependence of the conductivity above the liquidus temperature was approximated by a linear equation of the form $\kappa = A + BT$, the coefficients of which are given in Table I. The decrease in the specific conductivity of the system $0.77GdCl_3$–$0.23LiCl$ after the addition of 1 mol % Gd_2O_3 in the range of 1093–1143 K is 3–4 %.

Gadolinium oxide is known[10] to react with gadolinium chloride, according to the reaction:

$$GdCl_3 + Gd_2O_3 \rightarrow 3GdOCl \quad (5)$$

The observed patterns of changes in the specific electrical conductivity of the $GdCl_3$–LiCl melt, when gadolinium oxide is added, can be explained by the formation of complex oxychloride groups when gadolinium oxychloride is dissolved in the liquid phase.

According to the results of studies of the local structure and ion dynamics in molten systems $0.5LiCl$–$0.5GdCl_3$, with a Gd_2O_3 concentration up to 2 mol % obtained by *ab initio* molecular dynamics and *in situ* Raman spectroscopy,[31] gadolinium oxide in the chloride melt dissociated to form [Gd_2OLi] groups, which were incorporated into the network-like structure of the original chloride melt.

CONCLUSIONS

The specific conductivity of the molten $GdCl_3$–LiCl system was investigated depending on the temperature and concentration of $GdCl_3$ up to 23 mol %.

A significant decrease of conductivity with the concentration of gadolinium chloride was shown. So at 923 K, the additive of 20 mol % $GdCl_3$ reduces the conductivity of the system by 40 %. An increase in the system temperature slightly slows down the decrease in the conductivity of the system with an increase in the concentration of $GdCl_3$.

The molar conductivity of the molten $GdCl_3$–LiCl system is calculated taking into account the assumption of additivity of the molar volume of the mixture. The temperature dependences of the molar conductivity were approximated by Arrhenius type equation. A slight increase in the activation energy of molar conductivity can be noted with an increase in the concentration of $GdCl_3$.

The spectral studies have shown that when gadolinium ions are introduced into the LiCl melt, part of the chlorine anions binds to the $GdCl_6^{3-}$ grouping. This leads to a decrease in their mobility, and, as a consequence, the difficulty of electrical transfer and an increase in the activation energy of this process.

The introduction of 1 mol % of gadolinium oxide to $GdCl_3$–LiCl melt leads to a significant increase in the liquidus temperature of the system and a decrease in conductivity. This can be explained by the formation of complex oxychloride groups during the dissolution of gadolinium oxide in the liquid phase.

Acknowledgements. We are grateful to V. N. Dokutovich for samples preparation. The emission spectral analysis and the XRD analysis were performed using the facilities of the Shared Access Centre “Composition of Compounds” (Institute of High Temperature Electrochemistry, Ural Branch of RAS).

И З В О Д

ПРОВОДЉИВОСТ РАСТОПА $GdCl_3$–LiCl И $GdCl_3$–LiCl–Gd_2O_3

ELENA V. NIKOLAEVA, IRINA D. ZAKIRYANOVA, ANDREY L. BOVET и IRAIDA V. KORZUN

Institute of High Temperature Electrochemistry, UB RAS, 620990 Yekaterinburg, Russia

Мерена је проводљивост растопа LiCl–$GdCl_3$ са додатком гадолинијум-хлорида у распону од 0 до 23 mol % при различитим температурама и концентрацијама $GdCl_3$. Моларна проводљивост растопа $GdCl_3$–LiCl је рачуната уз претпоставку адитивности моларне запремине смеше. Добијене температурне зависности се могу апроксимирати Аренијусовским типом једначине. Ефективна енергија активације, E_a, је расла са повећањем садржаја $GdCl_3$. Температуре ликвидуса испитиваних растопа су одређиване методом диференцијалне скенирајуће калориметрије. Снимљени су високо-температурни Рамanови спектри растопа LiCl–$GdCl_3$. Поред тога, измерена је проводљивост растопа 0,77LiCl–0,23$GdCl_3$ са 1 mol % Gd_2O_3. Испитивања су показала да додатак гадолинијум-оксида смањује електричну проводљивост хлоридних растопа и повећава њихову температуру ликвидуса.

(Примљено 31. јануара, ревидирано 31. јула, прихваћено 14. августа 2023)

REFERENCES

1. T. Koyama, M. Fujita, M. Iizuka, Y. Sumida, *Nucl. Technol*. **110** (1995) 357 (https://doi.org/10.13182/NT95-A35107)
2. J. J. Laidler, J. E. Battles, W. E. Miller, J. P. Ackerman, E. L. Carls, *Prog. Nucl. Energy* **31** (1997) 131 (https://doi.org/10.1016/0149-1970(96)00007-8)
3. C. E. Till, Y. I. Chang, in *Advances in Nuclear Science and Technology,* Vol. 20, J. Lewins, M. Becker, Eds., Springer, Boston, MA., 1988, pp.127–154 (https://doi.org/10.1007/978-1-4613-9925-4_3)
4. G.-Y. Kim, J. Jang, S. Paek, S.-J. Lee, *Sci. Tech. Nucl. Instal.* (2020) 2392489 (https://doi.org/10.1155/2020/2392489)
5. G. J. Janz, *J. Phys. Chem. Ref. Data* **17** (1988) 3 (https://srd.nist.gov/JPCRD/jpcrdS2Vol17.pdf)
6. Potapov, L. Rycerz, M. Gaune-Escard, in *Proceedingsof the International Symposium on Ionic Liquids*, 2003, Carry le Rouet, France, *International Symposium on Ionic Liquids in honour of Professor Marcelle Gaune-Escard*, Trondheim, Norway, 2003, p.469
7. K. Fukushima, M. Hayakawa, Y. Iwadate, *J. Alloys Comp.* **245** (1996) 66 (https://doi.org/10.1016/S0925-8388(96)02485-1)
8. Y. Shuyun, Y. Weiqian, Y. Yuntao, S. Yunfu, T. Dingxiang, *Chin. J. Appl. Chem*. **1** (1984) 21 (http://yyhx.ciac.jl.cn/EN/Y1984/V0/I1/21)
9. E. V. Nikolaeva, I. D. Zakir'yanova, A.L. Bovet, T. V. Sosnovtseva, *Rus. Metal. (Metally)* **8** (2020) 817 (https://doi.org/10.1134/S003602952008011X)
10. E. V. Nikolaeva, I. D. Zakiryanova, A. L. Bovet, *J. Electrochem. Soc.* **169** (2022) 036511 (https://doi.org/10.1149/1945-7111/ac5b37)
11. W. Zhou, Y.Wang, J. Zhang, M. Khafizovet, *J. Nucl. Mat.* **508** (2018) 40 (https://doi.org/10.1016/j.jnucmat.2018.05.030)
12. I. V. Korzun, I. D. Zakiryanova, E. V. Nikolaeva, *Rus. Metal. (Metally)* **3** (2018) 271 (https://doi.org/10.1134/s0036029518080104)
13. I. Barin, G. Platzky, *Thermochemical Data of Pure Substances*, 3rd ed., Wiley, 1995, p. 956 (ISBN 9780471188155)
14. I. Barin, F. Sauert, E. Schultze-Rhonhof, W. S. Sheng, *Thermochemical data of pure substances I*, VCH Verlagsgesellschaft, Weinheim/VCH Publishers, New York 1989, p. 753 (ISBN 9780895738660)
15. H. J. Seifert, *J. Therm. Anal. Calorim*. **82** (2005) 575 (https://doi.org/10.1007/s10973-005-6946-7)
16. L. Rycerz, M. Gaune-Escard, *J. Alloy Compd.* **450** (2008) 167 (https://doi.org/10.1016/j.jallcom.2006.12.096)
17. R. J. M. Konings, A. Kovacs, in *Handbook on physics and chemistry of rare earths*, Vol. 33, K.A. Gschneidner Jr., J.-C.G. Bünzli, V.K. Pecharsky, Eds., Springer, New York, 2003 pp. 147–247 (https://doi.org/10.1016/S0168-1273(02)33003-4)
18. E. V. Nikolaeva, I. D. Zakiryanova, A. L. Bovet, I. V. Korzun, *J. Electrochem. Soc.* **168** (2021) 016502 (https://doi.org/10.1149/1945-7111/abd64a)
19. L. Rycerz, *J. Therm Anal. Calorim.* **113** (2013) 231 (https://doi.org/10.1007/s10973-013-3097-0)
20. V. M. Minchenko, V. P. Stepanov, *Ionic melts: tensive and caloric properties*, IHTE UB RAS, Yekaterinburg, 2008, pp. 77–82 (http://www.ihte.uran.ru/?page_id=3817)

21. K. Cho, K. Irisawa, J. Mochinaga, T. Kuroda, *Electrochim. Acta* **17** (1972) 10 (https://doi.org/10.1016/0013-4686(72)85073-4)
22. H. Tatlipinar, Z. Akdeniz, G. Pastore, M. P. Tosi, *J. Phys. Condens. Matter.* **4** (1992) 8933 (https://doi.org/10.1088/0953-8984/4/46/001)
23. J. Mochinaga, M. Ikeda, K. Igarashi, K. Fukushima, Y. Iwadate, *J. Alloys Comp.* **193** (1993) 36 (https://doi.org/10.1016/0925-8388(93)90301-3)
24. G. N. Papatheodorou, S. N. Yannopoulos, in *NATO Science Series II, Molten Salts:From Fundamental to Applications*, M. Gaune-Escard, Ed., Kluwer Academic Publishers, Dordrecht, 2002, p. 47 (https://doi.org/10.1007/978-94-010-0458-9)
25. Y. Okamoto, H. Shiwaku, T. Yaita, S. Suzuki, M. Gaune-Escard, *J. Mol. Liq.* **187** (2013) 94 (https://doi.org/10.1016/j.molliq.2013.05.018)
26. M. Zabłocka-Malicka, W. Szczepaniak, *J. Mol. Liq.* **137** (2008) 36 (https://doi.org/10.1016/j.molliq.2007.03.004)
27. M. Zabłocka-Malicka, B. Ciechanowski, W. Szczepaniak, W. Gaweł, *Electrochim. Acta* **53** (2008) 2081 (https://doi.org/10.1016/j.electacta.2007.08.073)
28. R. D. Shannon, *Acta Cryst*. **32** (1976) 751 (http://dx.doi.org/10.1107/S0567739476001551)
29. D. Zakiryanov, *Comput. Theor. Chem.* **1210** (2022) 113646 (https://doi.org/10.1016/j.comptc.2022.113646)
30. S. A. Kirillov, *Rus. J. Electrochem.* **47** (2007) 901 (https://doi.org/10.1134/S1023193507080083)
31. I. D. Zakiryanova, D. O. Zakiryanov, P. O. Zakiryanov, *J. Mol. Liq.* **376** (2023) 121485 (https://doi.org/10.1016/j.molliq.2023.121485).

Journal of the Serbian Chemical Society
JSCS-info@shd.org.rs • www.shd.org.rs/JSCS
J. Serb. Chem. Soc. *88* (11) 1149–1160 (2023)
JSCS–5687
Original scientific paper
Published 11 November 2023

Copper leaching from the chalcopyrite-bearing MoS_2 concentrate by mixed chlorides solution

NARANGARAV TUMEN-ULZII* and BURMAA GUNCHIN

Institute of Chemistry and Chemical Technology, Mongolian Academy of Sciences, Ulaanbaatar 13330, Mongolia

(Received 24 January, revised 11 April, accepted 7 September 2023)

Abstract: In this study, the dissolution of copper sulfide minerals by the ferric ($FeCl_3$) and ferrous ($FeCl_2$) chloride leaching for upgrading the content of molybdenum disulfide (MoS_2) in a molybdenite concentrate was investigated. The effect of various parameters was studied on the copper dissolution behaviour from the concentrate. In this matter, the copper dissolution was reached 94.84 % under the optimized leaching conditions. The kinetics of copper dissolution from the concentrate was established using a shrinking core model (SCM), and the process was controlled by diffusion, with a corresponding activation energy of 18.63 kJ mol^{-1} at the temperature range of 343–373 K. The amount of copper in the leachate was tested by the inductively coupled plasma-optical emission spectrometer (ICP-OES) and the solid phase was studied by X-ray diffraction (XRD) and scanning electron microscope (SEM). Results of the experiments show that the content of MoS_2 in the solid residue was increased up to 88.59 % after the leaching.

Keywords: molybdenum disulfide; ferric/ferrous leaching; thermodynamic; kinetic models.

INTRODUCTION

The molybdenite concentrate contains the leading mineral of molybdenum disulfide (with formula MoS_2) <90 %, as well as numerous metals sulfide minerals, gangues in the form of oxides, and silicates.[1] The naturally occurring form of MoS_2 is a crucial solid lubricant for additives the purpose of which is to support withstanding of antiwear at extreme pressure, and it is used primarily for reducing friction in heavy conditions. The content of MoS_2 in the concentrate can be upgraded by a chemical refining approach that will be the background in order to obtain MoS_2 with a high purity of 98 %.[2] Furthermore, MoS_2 is a critical source of metal molybdenum and its other products manufacturing depends on its

* Corresponding author. E-mail: narangaravt@mas.ac.mn
https://doi.org/10.2298/JSC230114057T

purity.[3,4] Copper (Cu) commonly occurs in the form of the most abundant copper minerals such as chalcopyrite ($CuFeS_2$), covellite (CuS), and chalcocite (Cu_2S) in molybdenite concentrate.[5] The dissolution of undesired copper minerals in the concentrate, particularly $CuFeS_2$, which is one of the most complicated phases to dissolve in any liquid medium, requires a suitable technique within the field of the refining process.

We processed the molybdenite concentrate with sodium nitrate solution in a sulfuric acid medium to dissolve copper and iron from the concentrate by selectivity.[6] Due to this result, the MoS_2 content of 81.33–90.73 wt. % was reached after the leaching. The effectivity of the copper dissolution from the molybdenite concentrate using some oxidizing agents such as sulfuric acid and oxygen pressure,[7] and the leaching followed the sulfidation process has been reported by several researchers.[8] Moreover, Jennings *et al*. investigated the leaching mechanism of metals from the molybdenite concentrate with mixed chlorides $CaCl_2$–$CuCl_2$––$FeCl_3$ solution.[9] On this occasion, the extraction rate of Cu, Pb and Ca was up to 98, 98 and 79 %, respectively. In addition, the feasibility of refining the molybdenite concentrate has been demonstrated by the metal impurities removal from the concentrate *via* $NaNO_3$–HCl–HNO_3 solution.[10] Under the optimum conditions, molybdenum (Mo) content upgraded up to 59 % for 10 h of leaching.

For many years chloride-based techniques, particularly $FeCl_3$, have been applied to treat and extract various metals from sulfide minerals.[11] Commonly, ferric (Fe^{3+}) ion is a more effective oxidant with a redox potential of 0.77 mV in the acidic media, high metal solubility, and can be extracted more quickly than other oxidants.[12] $FeCl_3$ is often used as an oxidant for the oxidation of sulfur in copper sulfides by the leaching approach, and the efficiency is lower when an additional reagent is not included.[13,14] Therefore, the $FeCl_3$ solution in the presence of $FeCl_2$ was selected to dissolve copper from the molybdenite concentrate in this study.

The advantage of operating under $FeCl_2$ leaching is the significant increase in the boiling point of the lixiviant and H^+ activity. As well, the consumed leaching solution is an enhancement of the revival process where the $FeCl_2$ can be replaced by $FeCl_3$ by reaction with liquid chlorine, thus reprocessed for the treatment of unleached copper impurities. Even though the ferric and ferrous (Fe^{2+}) ions oxidation method is used widely for chalcopyrite dissolution,[15,16] this method has not been used for the leaching of copper from the molybdenite concentrate, particularly the combined process of them.

The present study experimentally investigated the novel process for the dissolution of copper from the concentrate using $FeCl_3$–$FeCl_2$ leaching to upgrade the MoS_2 content in the molybdenite concentrate, without breaking down its structure. The dissolution behaviour of copper from the concentrate was investigated at various intervals of leaching time and the shrinking core models were

used for the kinetic studies. Moreover, the value of Gibbs energy changes of copper dissolution has been estimated by thermodynamic analysis.

EXPERIMENTAL

Materials

In this study, the molybdenite concentrate from the "Erdenet" mining plant in Mongolia was used, with a particle size of less than 0.074 mm of about 91.03 % distribution. According to the chemical composition analyzed by ICP-OES, the main elements Mo, Cu, and iron (Fe) in the concentrate were 49.98, 1.89 and 2.69 %, respectively. Quartz (SiO_2) and sulfur (S) contents in the concentrate defined by chemical methods were 4.62 and 34.86 %, respectively. A peak with high intensity corresponding to Mo and S dominated, and low-intensity peaks of Cu, Fe, and silicon (Si) were exhibited in the initial sample of the molybdenite concentrate by SEM-EDS analysis (Fig. 1). Lixiviants as reagents of analytical grade containing $FeCl_3$ and $FeCl_2$, which were used, were prepared with distilled water in this experiment.

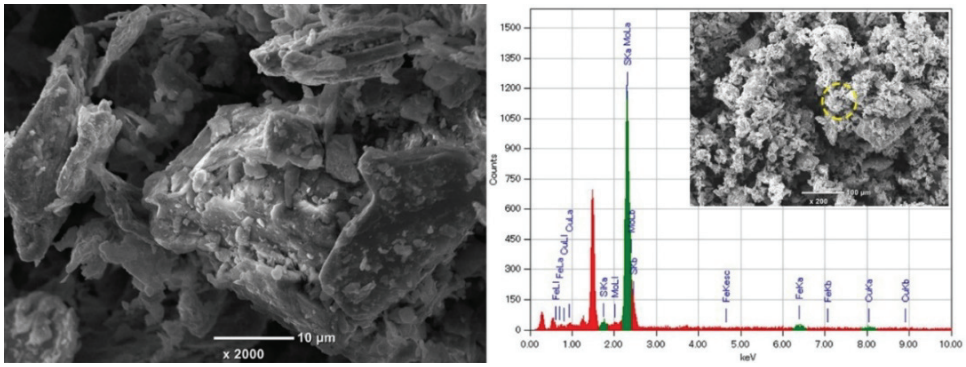

Fig. 1. SEM micrograph of the molybdenite concentrate.

Characterization

The chemical composition of the concentrate, obtained solid products, and solutions were identified by an inductively coupled plazma-optical emission spectrometer (ICP 7200, ICP-OES). The content of SiO_2 and S was determined by chemical gravimetric analysis. The X-ray diffractometer (XRD-7000, Shimadzu) and scanning electron microscopy with energy dispersive spectroscopy (SEM6000-EDS2300, JEOL) were performed to analyse the mineral and elemental composition of the concentrate and obtained solid products.

Experimental procedure

The leaching experiments were carried out in a round bottom glass reactor under solid to liquid ratio varied from 1:10 to 1:2.5, at the temperature range of 343–373 K for 30–240 min with a constant stirring speed of 300 rpm. 10 g of the concentrate was added into 100 mL leach solution containing $FeCl_3$ (10–30 %) in the presence of $FeCl_2$ (10-30 %). After completing the experiment, the leach liquor and solid residue were separated by filtration to determine the dissolution efficiency of the copper by ICP-OES analysis. Then, the characterization of solid residue was subjected to observation in XRD and SEM-EDS techniques.

Leaching kinetics

The copper leaching reaction is a heterogeneous process that occurs at the interface of solid and liquid phases. Therefore, the behaviour and mechanism of the dissolution can be explained by the SCM. According to SCM, the leaching process is considered generally to be controlled by the following steps:[17] surface chemical reaction (Eq. (1)), diffusion through the product layer, Eq. (2), or mixed models (Eq. (3)):

$$1-(1-\alpha)^{1/3} = k_c t \quad (1)$$

$$1-\frac{2}{3}\alpha-(1-\alpha)^{/3} = k_d t \quad (2)$$

$$[(1-\alpha)^{-1/3}-1]+\frac{1}{3}\ln(1-\alpha) = k_m t \quad (3)$$

where α is the fraction of copper dissolution; t is the leaching time, min; k_c, k_d and k_m are the apparent rate constants, min^{-1}.

Afterward, based on the Arrhenius equation, the activation energy (E_a) could be determined by plotting the ln k *versus* T^{-1}:

RESULTS AND DISCUSSION

Thermodynamic analysis

The thermodynamic analysis for defining the probability of reactions between the feed sample and leaching agent was performed using Gibbs energy change calculation (TABLE). HSC Chemistry 5 software was used to calculate the thermodynamic standard values for all compounds in the reaction at temperatures of 298.15–373.15 K.

TABLE I. The Gibbs energy change (kJ mol^{-1}) of the main chemical reactions[18] for copper dissolution at various temperatures

No.	Main chemical reaction	T / K				
		298.15	343.15	353.15	363.15	373.15
1	$CuFeS_2 + 3FeCl_3 = CuCl + 4FeCl_2 + 2S$	–130.90	–131.96	–132.20	–132.44	–132.67
2	$CuFeS_2 + 4FeCl_3 = CuCl_2 + 5FeCl_2 + 2S$	–154.29	–154.93	–155.08	–155.22	–155.36
3	$Cu_2S + 2FeCl_3 = 2CuCl + 2FeCl_2 + S$	–93.21	–94.43	–94.70	–94.98	–95.25
4	$CuS + 2FeCl_3 = CuCl_2 + 2FeCl_2 + S$	–56.50	–57.11	–57.24	–57.37	–57.51

In addition, the *Eh*–pH diagrams for Cu–Fe–S–H_2O and Cu–Fe–S–Cl–H_2O systems at 373 K within the pH range from 0 to 6 were constructed using HSC Chemistry 5 software data source, as shown in Fig. 2.

Copper in the molybdenite concentrate existed as copper sulfides and was dissolved by chloride leaching. The *Eh*–pH diagrams of the Cu–Fe–S–H_2O and Cu–Fe–S–Cl–H_2O systems are presented in Fig. 2a and b. As shown in Fig. 2a,

copper exists at a high potential (over 0.5 V_{SHE}) in the form of Cu^{2+}. Moreover, the pH range of the Cu^{2+} stable region is lower than 2.0. Hence, the dissolution of copper from the concentrate without the oxidizing agents is very complicated. Compared with the condition of the Cu–Fe–S–H_2O system,[19] the oxidation potential of Cu^{2+} is enhanced and copper can be transferred in the form of copper chloride into the solution with the presence of chloride at the pH value of less than 2.5 for the Cu–F—C–H_2O system, when the oxidation potential is between 0.5 and 1.5 V_{SHE}.

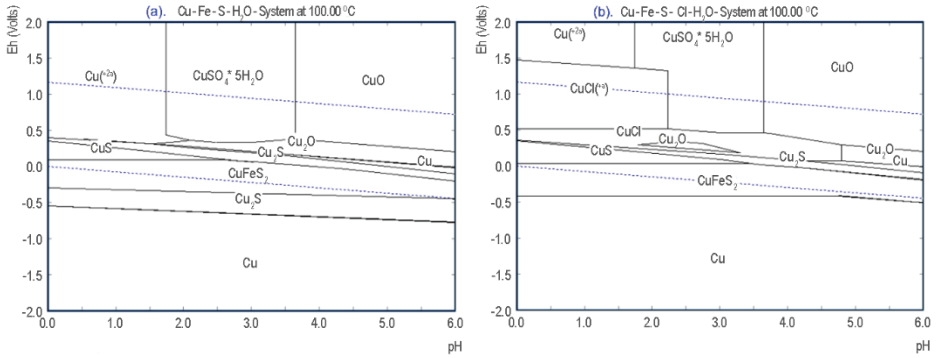

Fig. 2. *Eh*–pH diagram for the investigated systems.

Selection of leaching parameters on Cu dissolution

Effect of Fe(III) chloride concentration. The effect of the $FeCl_3$ concentration on the copper dissolution from the concentrate was examined, and the result is shown in Fig. 3. When the $FeCl_3$ concentration increased by 10 to 30 %, the copper dissolution was enhanced from 80.09 to 86.38 % after 60 min. With a further increase in leaching time, the dissolution level tends to be stable during the processes. Even though a suitable leaching time seems like a high yield in a short time of 60 min, it was selected for 240 min in the subsequent experiments to get more dissolution efficiency of copper. According to the experimental results, the $FeCl_3$ concentration was selected at 10 % in the following experiments.

In the reported work,[20] the efficiency of copper dissolution from the chalcopyrite concentrate was about 92 % when the $FeCl_3$ concentration was 100 g L^{-1} and the leaching time of 480 min at 95 °C in an acidic medium. However, when the $FeCl_3$ concentration increased higher, the leaching rate of copper gradually decreased during the process. Some researchers[21,22] have reported that the existing elemental sulfur at the surface of chalcopyrite, especially its concentrate, is due to the sulfur in the sulfides converted within the elementary form ($S^{2-} \rightarrow S$). That is because the oxidation product of sulfides is more probably the formation of elemental sulfur as stated in all reactions (1–4, Table I) in chloride media than sulfate.

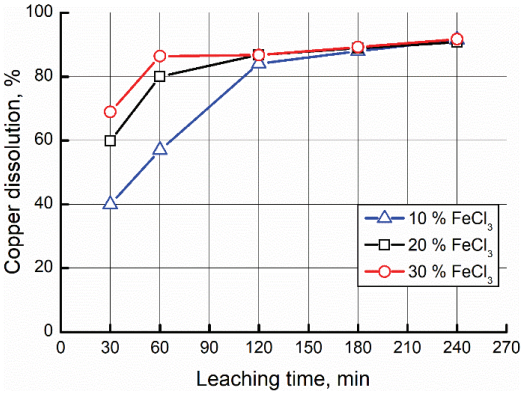

Fig. 3. Effect of the $FeCl_3$ concentration on the copper dissolution (1:10, 373 K, 20 % $FeCl_2$).

Effect of Fe(II) chloride concentration. The influence of $FeCl_2$ concentration was examined between 10 and 30 %, as shown in Fig. 4. The experimental results showed that the copper dissolution increased with an enhanced leaching time. Increasing the Fe^{2+} concentration in the solution affected significantly the copper dissolution. The copper dissolution yield increased from 72.35 to 94.38 % after 240 min, while the $FeCl_2$ concentration was increased from 10 to 30 %. Otherwise stated, it showed that the enhancement of $FeCl_2$ concentration positively affected the chalcopyrite leaching. Consequently, a $FeCl_2$ concentration of 30 % was chosen for the following experiments to enhance the copper leaching rate.

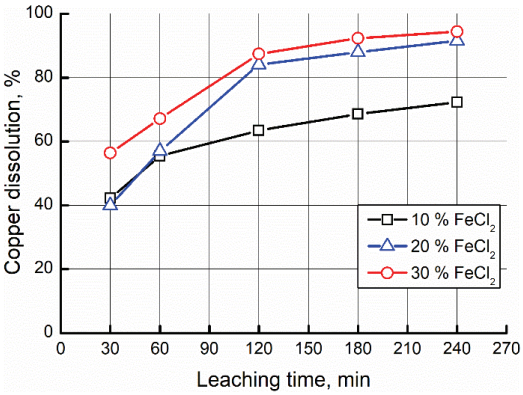

Fig. 4. Effect of the $FeCl_2$ concentration on the copper dissolution (1:10, 373 K, 10 % $FeCl_3$).

The $FeCl_3$ with additional $FeCl_2$ was used as an oxidant to improve the activity of H^+ and the boiling point of the leaching solution. At the same time, $FeCl_2$ can be oxidized to $FeCl_3$, which could be used for recycling to further leaching of each copper compound from the concentrate. These results indicate that Fe^{2+} is closely related to the copper dissolution. Moreover, Fe^{2+} enhances the kinetics of copper dissolution substantially compared to Fe^{3+}.[15]

Effect of solid to liquid (S:L) ratio. The leaching experiments were carried out using S:L ratios ranging from 1:2.5 to 1:10. The dependence between the Cu dissolution and phase ratio is represented in Fig. 6. As can be seen, the dissolution of copper was approximately 94.38 % at the S:L ratio of 1:10, when the S:L ratio decreased from 1:10 to 1:2.5, the copper dissolution gradually enhanced after leaching of 240 min. It was shown that a lower S:L ratio had a lesser probability of the reaction for copper dissolution in the short time between the concentrate and oxidants. Moreover, the another reason possible was that the increase in the S:L ratio enhances the medium diffusion of the solution and made the reaction more sufficient. Based on these results, the ratio of 1:10 was used for determining the other parameter.

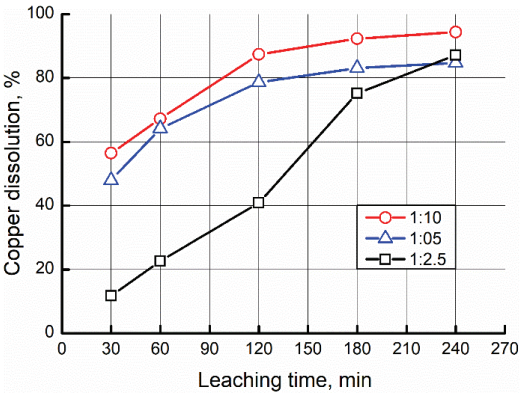

Fig. 6. Effect of the S:L ratio on the copper dissolution (373 K, 10 % $FeCl_3$, 30 % $FeCl_2$).

Effect of leaching temperature. The effect of temperature on the copper dissolution was studied at different temperatures of 343–373 K. As can be seen in Fig. 5, the copper dissolution rapidly proceeded up to 63.76–87.43 % at 120 min, and then enhanced remarkably to 78.70–94.38 % when the leaching time was over 120 min. In other words, it was observed that the temperature influence on

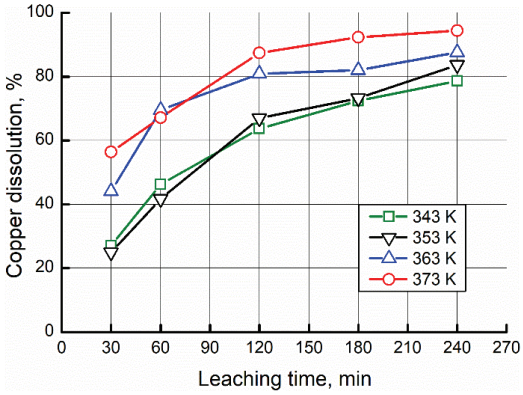

Fig. 5. Effect of the temperature on the copper dissolution (1:10, 10 % $FeCl_3$, 30 % $FeCl_2$).

the dissolution of copper diminished after 240 min. It indicates that the breakdown of chalcopyrite structure goes effectively at high-temperature values by $FeCl_3$–$FeCl_2$ for 240 min leaching. Therefore, it was concluded that the appropriate temperature was 373 K, which can be positively influenced by improving the Cu leaching kinetics.

Kinetics analysis

The dissolution efficiency of copper at varied temperatures was fitted by the SCM. The parameters of kinetic models (correlation coefficient, R^2 and rate constant, k) were obtained from the results plotted in a linear relationship according to Eqs. (1)–(3) as shown in Fig. 7. The results could be evaluated by the highest values of R^2 at various temperatures (Fig. 6). As shown in Fig. 7a–c, even though all correlation coefficients are over 0.93, the highest value is 0.99, it was confirmed that the leaching process of chalcopyrite from the concentrate in $FeCl_3$–$FeCl_2$ solution was controlled *via* the diffusion model (Fig. 7d) at the studied various temperatures.

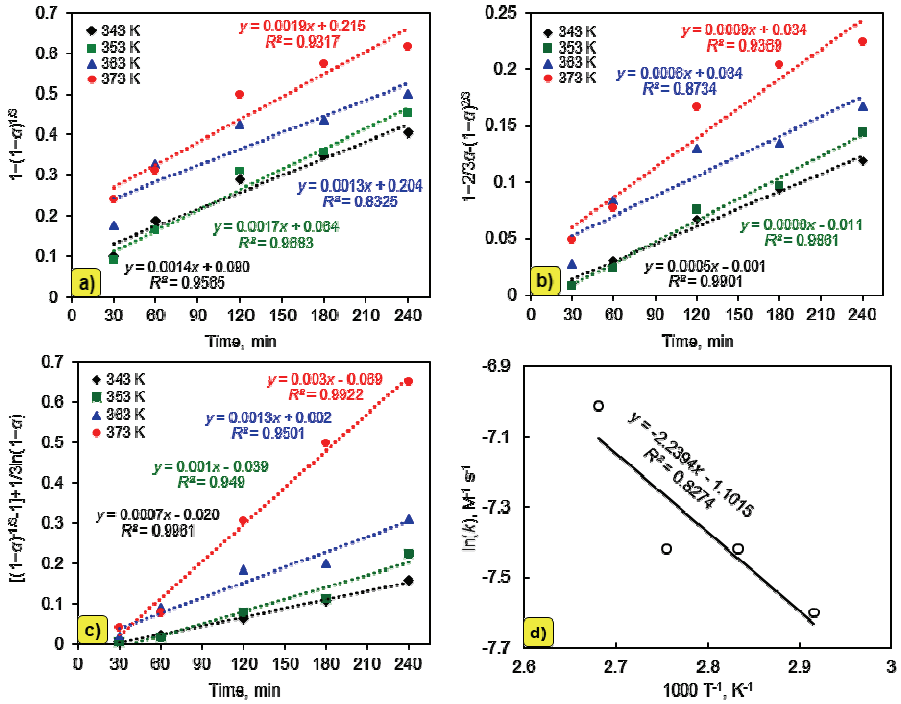

Fig. 7. a)–c) Plots of the models vs leaching time for Cu dissolution at different temperatures; d) Arrhenius plot based on the apparent rate constants calculated from a)–c).

The values of the activation energy of a reaction were calculated as 6.78, 18.62, and 48.93 kJ mol^{-1} for surface chemical reaction controlled, diffusion-

-controlled and mixed-controlled, respectively. The activation energy of the diffusion-controlled model is considered as lower than 20 kJ mol^{-1} because the temperature was a lower influence on the dissolution of copper. When the value of activation energy is generally more than 42 kJ mol^{-1}, the apparent constant rate is controlled by a chemical reaction. While the activation energy is between 20 and 42 kJ mol^{-1}, the rate-controlling step is expected for a mixed controlled system.[23] Thus, the activation energy obtained confirms that the copper leaching from the concentrate was followed by a diffusion-controlled model.

Leaching residue characterization

The leached residue was obtained with an experiment performed under the optimum conditions (leaching temperature of 373 K, $FeCl_3$ concentration of 10 %, $FeCl_2$ concentration of 30 %, solid to liquid ratio of 1:10, leaching time of 240 min, and kept the constant stirring speed of 300 rpm) were examined by XRD and SEM-EDS methods. The content of the elements in the residue was determined by ICP-OES and chemical methods where the main elements as Mo, S and undissolved Si were increased to 52.93, 35.66 and 2.48 %, respectively. In contrast, the amount of Cu and Fe were diminished to 0.12 and 1.77 %, respectively, which suggested that unreacted some chalcopyrite and pyrite particles remained in the residue during the chloride leaching. Moreover, the dissolution process's standard deviation (*SD*) was calculated by statistical analysis (TABLE) constructed within a 95 % confidence interval of repeated measurement ($n = 3$).

TABLE II. Statistical analysis of experimental results obtained under optimal conditions

n	Content of elements in the residue, %			Cu content in solution, %
	Mo	S	Fe	
1	52.93	35.66	1.76	1.80
2	52.99	35.62	1.77	1.78
3	52.86	35.71	1.79	1.80
Mean	52.93	35.66	1.77	1.79
SD	0.065	0.045	0.015	0.009

According to the results of the XRD pattern shown in Fig. 8, the main minerals in the molybdenite concentrate are MoS_2, $CuFeS_2$ and FeS_2 (Fig. 8a). But some copper minerals, CuS and Cu_2S with minor amounts are not detected due to the detection limit of the equipment. As it can be seen from the X-ray pattern of the residue (Fig. 8b), the main phase was MoS_2 except for that FeS_2 and SiO_2 particles have remained undissolved compounds for the $FeCl_3$-$FeCl_2$ leaching system.

The SEM-EDS analysis of the leaching residue after the $FeCl_3$–$FeCl_2$ leaching system is shown in Fig. . The intensity of energy peak corresponding to Cu in the residue was eliminated and the intensity of energy peaks related to Mo, S, Fe, and Si was increased after leaching. Fig. displays the EDS spectrum with

highlighted dominant peaks of Mo and S elements in the leaching residue, and it is obvious that chalcopyrite surfaces were effectively dissolved by $FeCl_3$–$FeCl_2$ leaching process. The results suggest that the high-grade molybdenite concentrate with a low amount of Cu could be produced by the combined chloride leaching.

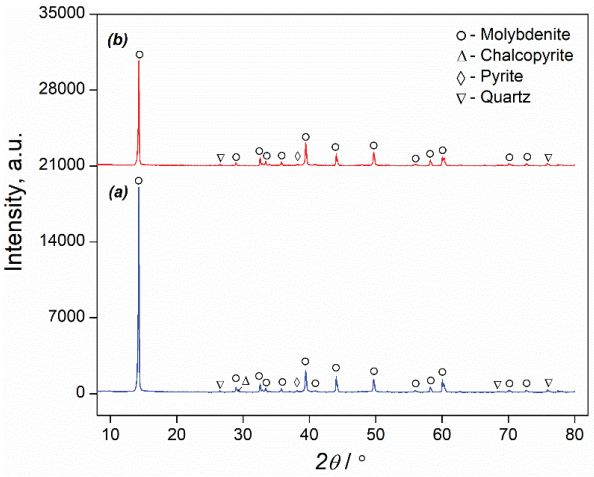

Fig. 8. X-ray diffraction analysis of the molybdenite concentrate (a) and solid residue (b).

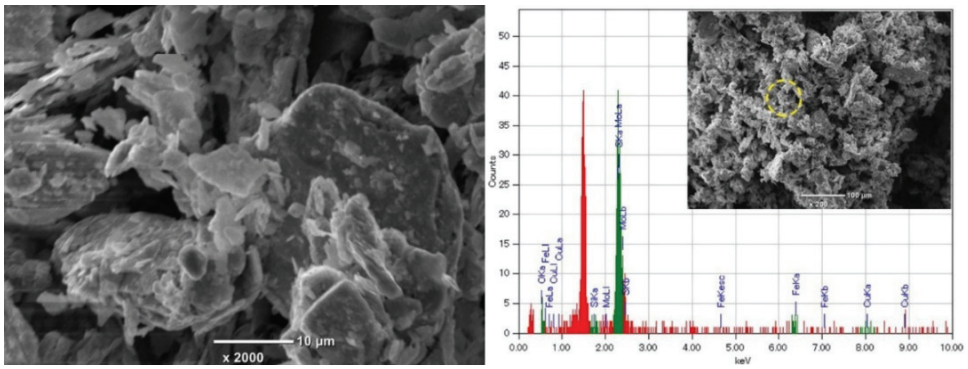

Fig. 9. SEM micrograph of the solid residue.

CONCLUSIONS

A novelty process to dissolve copper from the molybdenite concentrate has been effectively demonstrated by the combined Fe^{3+} and Fe^{2+} leaching methods. It was found that the copper dissolution increased with the $FeCl_2$ concentration, and the optimum leaching temperature was near the boiling point of the solution. When the amount of solid phase was comparatively lower, which made the diffusion more easy, thus an S:L ratio became superior for the copper leaching from the concentrate. The most efficient yield of copper was 94.83 %, obtained under

the following conditions: the temperature of 373 K, leaching time of 240 min, $FeCl_3$ concentration of 10 %, $FeCl_2$ concentration of 30 %, solid to liquid phase ratio at 1:10, and kept the constant stirring speed of 300 rpm. The result of the kinetic study using a shrinking core model suggested that the copper leaching process was controlled by the diffusion model with an activation energy of 18.62 kJ mol^{-1}. The characterization of the leached residues indicated that the copper sulfide minerals were almost completely dissolved in the $FeCl_3$–$FeCl_2$ combined solution and remained at 88.59 % MoS_2 aside from SiO_2 and FeS_2 in the residue. Therefore, it can be concluded that a Fe^{3+}/Fe^{2+} leaching system is an alternative approach for copper removal from the molybdenite concentrate. However, the novel process can solve the issue of copper leaching from the concentrate, but there are some obstacles to the recovery of iron and silica from leached residue.

Acknowledgement. This study was financially supported by the Mongolian Foundation for Science Technology through the Ministry of Education and Science of Mongolia under the project (2021–2023).

ИЗВОД

ИЗЛУЖИВАЊЕ БАКРА ИЗ КОНЦЕНТРАТА MoS_2 КОЈИ САДРЖИ ХАЛКОПИРИТ МЕШАНИМ РАСТВОРОМ ХЛОРИДА

NARANGARAV TUMEN-ULZII и BURMAA GUNCHIN

Institute of Chemistry and Chemical Technology, Mongolian Academy of Sciences, Ulaanbaatar 13330, Mongolia

У овом раду испитивано је излуживање бакар сулфида испирањем фери- и феро--хлоридом ради повећања садржаја молибден-дисулфида (MoS_2) у концентрату молибденита. Проучаван је утицај различитих параметара на понашање растварања бакра из концентрата. У овом случају, под оптималним условима лужења постигнуто је излуживање бакра од 94,84 %. Кинетика растварања бакра из концентрата је утврђена коришћењем модела скупљајућег језгра (SCM), а процес је контролисан дифузијом, са енергијом активације од 18,63 kJ mol^{-1} у температурном опсегу 343–373 K. Проценат бакра у процедној води је тестиран индуктивно спрегнутим плазма-оптичким емисионим спектрометром (ICP-OES), а чврста фаза је проучавана рендгенском дифракцијом (KSRD) и скенирајућим електронским микроскопом (SEM). Резултати експеримената показују да је садржај MoS_2 у чврстом остатку повећан до 88,59 % након испирања.

(Примљено 24. јануара, ревидирано 11. априла, прихваћено 7. септембра 2023)

REFERENCES

1. C. K. Gupta, *Chemical Metallurgy, Principles and Practice*, WILEY-VCH Verlag GmbH & Co. KGaA, Weinheim, 2003 (ISBN: 3-527-30376-6)
2. A. R. Lansdown, *Molybdenum Disulfide Lubrication*, Elsevier, Swansea, 1999 (ISBN: 0-444-50032-4)
3. O. Samy, A. El Moutaouakil, *Energies* **14** (2021) 1 (https://doi.org/10.3390/en14154586)
4. D. Gupta, V. Chauhan, R. Kumar, *Inorg. Chem. Commun.* **121** (2020) 108200 (https://doi.org/10.1016/j.inoche.2020.108200)

5. E. L. R. Chiluiza, P. N. Donoso, *J. Mex. Chem. Soc.* **60** (2016) 238 (ISSN: 1870-249X)
6. N. Tumen-Ulzii, A. Batnasan, B. Gunchin, *Miner. Eng.* **185** (2022) 107715 (https://doi.org/10.1016/j.mineng.2022.107715)
7. R. Padilla, C. Opazo, M. C. Ruiz, *Metall. Mater. Trans., B* **46** (2015) 30 (https://doi.org/10.1007/s11663-014-0171-3)
8. R. Padilla, H. Letelier, M. C. Ruiz, *Hydrometallurgy* **137** (2013) 78 (https://doi.org/10.1016/j.hydromet.2013.05.012)
9. H. L. Jennings, P.H., Stanley, R.W. Ames, in *Proceedings of Second Int. Symp. Hydrometall.* New York (AIME), 1973, pp. 868–883
10. D. Guo, L. Fu, S. Wang, L. Zhang, J. Peng, *Chem. Pap.* **72** (2018) 2997 (https://doi.org/10.1007/s11696-018-0544-1)
11. A. A. Baba, K. I. Ayinla, F. A. Adekola, M. K. Ghosh, O. S. Ayanda, R. B. Bale, A. R. Sheik, S. R. Pradhan, *Int. J. Min. Eng. Miner. Process.* **1** (2012) 1 (https://doi.org/10.5923/j.mining.20120101.01)
12. M. Nicol, H. Miki, L. Velásquez-Yévenes, *Hydrometallurgy* **103** (2010) 86 (https://doi.org/10.1016/j.hydromet.2010.03.003)
13. Y. Li, F. Wang, B. Yang, J. Wu, & Y. Tian, *J. Sustain. Metall.* **6** (2020) 419 (https://doi.org/10.1007/s40831-020-00284-5)
14. N. T. Phuong Thao, S. Tsuji, S. Jeon, I. Park, C. B. Tabelin, M. Ito, N. Hiroyoshi, *Hydrometallurgy* **194** (2020) 105299 (https://doi.org/10.1016/j.hydromet.2020.105299)
15. N. Hiroyoshi, H. Miki, T. Hirajima, M. Tsunekawa, *Hydrometallurgy* **60** (2001) 185 (https://doi.org/10.1016/S0304-386X(00)00155-9)
16. J. Lu, D. Dreisinger, *Miner. Eng*. **45** (2013) 185 (https://doi.org/10.1016/j.mineng.2013.03.007)
17. O. Levenspiel, *Electrochemical Reaction Engineering*, John Willey & Sons, New York, 1999, (ISBN: 0-471-25424-X)
18. T. Agacayak, M. T. O. A. Ahmed, *Acta Chem. Iasi* **28** (2020) 82 (https://doi.org/10.2478/achi-2020-0006)
19. E. M. Córdoba, J. A. Muñoz, M. L. Blázquez, F. González, A. Ballester, *Hydrometallurgy* **93** (2008) 81 (https://doi.org/10.1016/j.hydromet.2008.04.015)
20. Y. Turkmen, E. Kaya, *J. Ore Dress.* **11** (2009) 16
21. M. E. Taboada, P. C. Hernández, A. P. Padilla, N. E. Jamett, T. A. Graber, *Metals* **11** (2021) 866 (https://doi.org/10.3390/met11060866)
22. T. Hidalgo, L. Kuhar, A. Beinlich, A. Putnis, *Hydrometallurgy* **188** (2019) 140 (https://doi.org/10.1016/j.hydromet.2019.06.009)
23. T. Havlík, *Hydrometallurgy, Principles and Application*, CRC Press, Boca Raton, FL, 2008 (ISBN: 978-1-84569-461-6).

Journal of the Serbian Chemical Society
JSCS@tmf.bg.ac.rs • www.shd.org.rs/JSCS
J. Serb. Chem. Soc. *88* (11) 1161–1173 (2023)
JSCS–5688
Original scientific paper
Published 11 Novembar 2023

Health risk assessment of potentially harmful substances from fly ashes generated by coal and coal waste combustion

JOVANA Z. BUHA MARKOVIĆ[1]*, ANA D. MARINKOVIĆ[1], JASMINA Z. SAVIĆ[1], ALEKSANDAR D. KRSTIĆ[1], ANDRIJA B. SAVIĆ[1] and MIRJANA Đ. RISTIĆ[2#]

[1]*University of Belgrade, Vinča Institute of Nuclear Sciences - National Institute of the Republic of Serbia, Belgrade, Serbia and* [2]*University of Belgrade, Faculty of Technology and Metallurgy, Karnegijeva 4, Belgrade, Serbia*

(Received 30 December 2022, revised 24 July, accepted 3 August 2023)

Abstract: Lignite and coal waste used as feed fuels in thermal power plants (TPPs) and semi-industrial fluidized bed boiler (FBB), as well as their representative fly ashes (FAs), were examined. Fly ashes were compared employing anions and cations content in correspondent water extracts, trace elements and polycyclic aromatic hydrocarbon concentrations, as well as health risk assessments of substances known to be of concern for public health. Fluoride and sulfate contents in water extracted FAs are far below the legislation limits for waste, classifying all investigated FAs as non-hazardous. Among investigated trace elements, Cd content is the lowest, while Mn content is the highest. The highest enrichment ratios are noticed for As, Pb, Hg, Cu, V and Cr. The results indicate that total PAHs content is elevated in FA from the combustion of coal waste (AFB), with fluoranthene prevailing. The cancer risk of As and the non-cancer risk of As and Ni in some FAs surpass their respective permissible limits. The incremental lifetime cancer risk of an adult population indicates a potential PAHs risk in AFB, whereas all other fly ashes are within safe limits.

Keywords: coal ashes; leaching; trace elements; PAHs; carcinogenic risk; total hazard impact.

INTRODUCTION

Despite limited coal supplies, its consumption in Europe is expected to rise due to the uncertainty of the energy sector, so therefore many EU countries extended the life of coal-fired power plants.[1,2] The choice of the appropriate coal as a feed fuel for particular combustion systems relies on coal characteristics, such as its moisture, ash content and gross calorific value.[3] Fluidized bed com-

* Corresponding author. E-mail: jbuha@vin.bg.ac.rs
# Serbian Chemical Society member.
https://doi.org/10.2298/JSC220130048M

bustion is regarded as an environmentally friendly way of producing energy from low grade coals, due to continuous operation and low NO_x and SO_2 emissions.[4,5]

Coal is the dominant energy source in Serbia, with over 7 billion tons of estimated lignite reserves. Annually, the Electric Power Industry (EPI) of Serbia produces around 560, 2010 and 7878 GW h in thermal power plants (TPPs) Kolubara A, Kostolac B and Nikola Tesla A, respectively, which brings to the generation of 0.25, 0.61 and 2.08 Mt fly ash, accordingly.[6] Since lignite with particle sizes lower than 10 mm cannot be used further in thermal power plant boilers, it is considered waste. However, coal waste might have a significant energy perspective and can be used as a feed fuel in other combustion technologies, such as fluidized bed combustion.[4] In these circumstances, coal waste originating from the Kolubara basin, discarded as waste in TPP Kolubara A, was tested as a feed fuel in a semi-industrial FBB with a thermal power of up to 500 kW.

Most studies have shown that potentially harmful trace elements emitted during coal combustion are distributed in bottom ash, fly ash particles of different parameters and flue gases so that they can reach soil and water.[7] Content of heavy metals salts, such as chlorides or sulfates, affect leaching mechanisms of potentially harmful compounds in FAs.[8,9] Ca and Mg are the most dominant cations in fly ash water leachates, while anions primarily include sulfates, carbonates and fluorides.[10] Furthermore, anions and cations content were determined to complement the scarce literature data considering water extracted FAs.

In addition, persistent organic compounds, such as polycyclic aromatic hydrocarbons (PAHs), represent significant environmental pollutants generated during coal combustion.[11] The US Environmental Protection Agency (US EPA) regulated 16 priority PAHs due to their harmful effects on people and the environment.[12] Physicochemical properties of PAHs and, consequently, their environmental fate depends on their structure and number of fused aromatic rings.[13] PAHs are usually classified into low molecular weight (LMW), medium molecular weight (MMW) and high molecular weight (HMW). As the molecular weight of a particular PAH increases, its carcinogenicity rises, while its acute toxicity decreases.[14] The fate and partitioning of toxic elements and PAHs in coal combustion by-products depends on the used feed fuel, combustion temperature, burner type and structure.[10] Therefore, a thorough analysis of the used coals and produced FAs is necessary to optimize combustion processes in terms of environmental and health issues.[15] Intake of potentially toxic substances by humans can be through three pathways, *i.e.*, ingestion, inhalation and dermal contact. Model of human exposure (adults and children) to potentially harmful substances is developed by the US EPA guidelines.[16]

In this study, feed coals and FAs from TPPs Kolubara A (TPKb), Kostolac B (TPKs) and Nikola Tesla A (TPNT), as well as coal waste and FA from semi-

-industrial FBB were investigated. This paper characterizes and compares different coals based on proximate and ultimate analysis, along with trace element concentrations, and analyzes corresponding fly ashes, determining their particle size diameters, trace elements and PAHs content, as well as anions and cations content in fly ash water leachates. The aim of this study was to perform a human health risk assessments of potentially harmful substances in fly ashes by estimating the carcinogenic and non-cancer risk for trace elements and the incremental life cancer risk of seven carcinogenic PAHs associated with different exposure routes.

EXPERIMENTAL

A sampling of coals and fly ashes

A sampling of coals from TPP Kolubara A (CKb), TPP Kostolac B (CKs), TPP Nikola Tesla A (CNT) and coal waste from a fluidized bed boiler (CFB) was done according to the standard method.[17] The same method was used for the collection of coal fly ashes from TPKb (AKb), TPKs (AKs), TPNT (ANT) and from the cyclone of FBB (AFB). The samples were prepared and stored in a glass container at a dark place under a temperature below 15 °C.[18,19]

Granulometric analysis of fly ashes

The granulometric analysis of investigated fly ashes was performed using a set of sieves with round hole diameters of 90, 200, 500 and 1000 μm.[20]

Proximate and ultimate analysis of coals

The proximate analysis of investigated coals was done by LECO TGA 701 according to a standard test method.[21] The ultimate analysis was performed by a LECO CHN 628 Series with a Sulfur add-on module.[22-24]

Determination of anions and cations by ion chromatography

5 g of each FA was mixed with 50 mL of deionized water in an IKA KS130 orbital shaker (800 rpm) for 180 min. Obtained extracts were filtered and further used to determine cations and anions by ion chromatograph Dionex. The details are given in the Supplementary material.

Determination of trace elements in coals and FAs

Extraction of 18 elements (As, Be, Cd, Co, Cr, Cs, Cu, Ga, Ge, Hg, Mn, Mo, Ni, Pb, Sb, Sr, U, V) was done by sequential extraction.[25] Trace elements concentrations were determined by the inductively coupled plasma mass spectrometry (ICP-MS) using an Agilent 7500ce instrument equipped with Octopole Reaction System in FullQuant mode. The details about ICP-MS measurements are described in the Supplementary material. Each element's total concentration is the sum of its six representative fractions.

PAHs analysis

The extraction of 16 priority PAHs (naphthalene, Nap; acenaphthylene, Acy; acenaphthene, Ace; fluorene, Flu; phenanthrene, Phe; anthracene, Ant; fluoranthene, Fla; pyrene, Pyr; benzo[*a*]anthracene, BaA; chrysene, Chry; benzo[*b*]fluoranthene, BbF; benzo[*k*]fluoranthene, BkF; benzo[*a*]pyrene, BaP; dibenzo[*a*,*h*]anthracene, DahA; benzo[*g*,*h*,*i*]perylene, BghiP and indeno[1,2,3-*cd*]pyrene, IP) from fly ashes was done according to literature.[26] The prepared

extracts were analyzed by HPLC/DAD. The details are explained in the Supplementary material to this paper.

Enrichment ratios (ERs) of trace elements

The ER of a particular trace element was calculated as a quotient of its concentration in ash and correspondent coal. ER higher than 1 indicates trace elements enhancement in ash compared to the corresponding feed fuel.

Human health assessment for trace elements and PAHs from FAs

The human health assessment associated with trace elements and PAHs found in FAs was performed for adults and children.

Human health assessment comprises the calculation of total risk indexes (*R*) for carcinogenic substances (As^{cc}, Cd^{cc}, Cr^{cc}, Co^{cc}, Ni^{cc}), as well as total hazard indexes (*HI*) for non-carcinogenic substances (As^{ncc}, Pb, Hg, Cd^{ncc}, Cr^{ncc}, Co^{ncc}, Ni^{ncc} and Cu). Total *R* and *HI* were calculated for each element by the following equations:

$$R = D_{ig} \times SF_{ig} + D_{ih} \times SF_{ih} + D_{d} \times SF_{d} \quad (1)$$

$$HI = D_{ig}/RF_{ig} + D_{ih}/RF_{ih} + D_{d}/RF_{d} \quad (2)$$

D_i / mg kg^{-1} day^{-1} is the daily intake dose, SF_i / kg day mg^{-1} is the corresponding carcinogenicity slope factor and RF_i / mg kg^{-1} day^{-1} is the reference dose for each exposure route i, where i stands for ingestion (ig), inhalation (ih) or dermal contact (d). Parameters used to calculate D_i are given in Supplementary material (Table S-I, a, and S-II), and the toxicity values for RF_i and SF_i are in Table S-III.[27,28]

Generally, a risk less than 10^{-6} can be ignored; a carcinogenic risk in the range of 10^{-6} to 10^{-4} is acceptable or tolerable, while a risk exceeding 10^{-4} is considered unacceptable for any element. If *HI* is higher than 1, negative health effects are probable.

The incremental lifetime cancer risk (*ILCR*) was estimated as the sum of 7 carcinogenic PAHs (BaA, Chry, BbF, BkF, DahA, BghIP and IP) for three exposure routes. $ILCR \leq 10^{-6}$ generally denotes virtual safety, $10^{-6} < ILCR < 10^{-4}$ indicates potential risk, while $ILCR > 10^{-4}$ represents a high risk.

The health assessment calculations for PAHs and their parameter values are shown in Supplementary material (Table S-I, b, and S-II).

RESULTS AND DISCUSSION

Proximate and ultimate analysis

The fuels used in four combustion facilities were examined by proximate and ultimate analysis and the results on air dried basis are shown in Table I. Compared to coal waste, all feed fuels from TPPs have better properties as a combustion feedstock due to lower ash content, as well as higher volatile matter, carbon content and heating value.[29] Because high volatile matter can be associated with spontaneous combustion (particularly with low-rank coals such as lignite), knowing the volatile content of the coal simplifies transportation and handling. The total sulfur of CKs is fourfold higher than other coal samples. CKb, CNT and CFB originate from the same basin (Kolubara), while CKs derive from the Kostolac basin. The combustible sulfur proportion of CFB (36 %) is substantially lower than for other coals from the Kolubara basin (62–69 %).[30]

TABLE I. Proximate and ultimate analysis of lignite from TPPs Kolubara A (CKb), Kostolac B (CKs) and Nikola Tesla A (CNT) and coal waste from FBB (CFB)

Parameter	CKb	CKs	CNT	CFB
Content, % (proximate analysis)				
Total moisture[a]	42.94	40.34	48.90	36.74
Inherent moisture[b]	6.04	8.18	7.14	7.04
Ash	37.21	36.29	36.86	61.85
Coke	61.55	60.56	57.31	77.43
Combustible	61.79	63.71	63.14	38.15
Volatile	38.45	39.44	42.69	22.57
C-fix	23.34	24.27	20.45	15.58
Heating value, MJ kg^{-1}				
High	16.56	16.56	16.41	10.16
Low	15.75	15.62	15.60	9.75
Content, % (ultimate analysis)				
Carbon	41.26	41.64	38.80	24.81
Hydrogen	3.74	3.78	3.74	1.96
Total sulfur	0.64	2.76	0.55	0.66
Combustible sulfur	0.43	1.91	0.34	0.26
Nitrogen	0.58	0.67	0.44	0.34
Oxygen	16.77	15.65	19.92	10.78

[a]As-received; [b]as determined. All other data are given on a dry basis

Granulometric analysis

Ash particle size is an important parameter since finer ashes provide a greater surface area for the sorption of harmful substances.[31] The granulometric analysis results are shown in Fig. 1. AKb mainly comprises finer particles with diameters less than 90 μm (64.61 %), while AFB has the highest yield in the F3 fraction (92.96 %). FAs from TPPs have mean particle diameters ranging from 126 to 131 μm, while for AFB, it is 341 μm. The variations of FAs particle size are affected by combustion system characteristics, burning temperatures, used feed fuels, as well as the system treatment of the gaseous effluents.[32]

Anions and cations content in water extracted fly ashes

Fig. 2 depicts the leaching of anions and cations in water extracted FAs. Among determined cations, calcium prevails with concentrations ranging from 2.06 (in ANT) to 5.32 mg/g (in AKs). It is in line with the literature since calcium salts easily dissolve.[33] Potassium is the most dominant in AKb with a concentration of 3.38 mg/g, which is more than tenfold higher than in other FAs. Sulfates are the most abundant among the other anions, ranging from 2.32 (in ANT) to 10.32 mg/g (in AKs), whereas chlorides, phosphates and nitrates are undetected. Fluorides vary from 0.10 (in AKs) to 0.18 mg/g (in AKb). Most of the fluorides in FA are insoluble, while the water-soluble form of fluoride mainly originates from NaF and KF.[34]

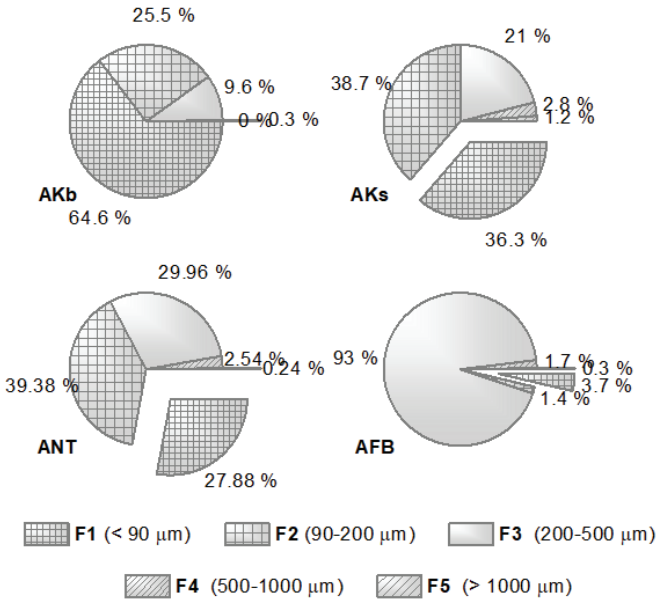

Fig. 1. Granulometric analysis of fly ashes from TPPs Kolubara A (AKb), Kostolac B (AKs), Nikola Tesla A (ANT) and from fluidized bed boiler (AFB).

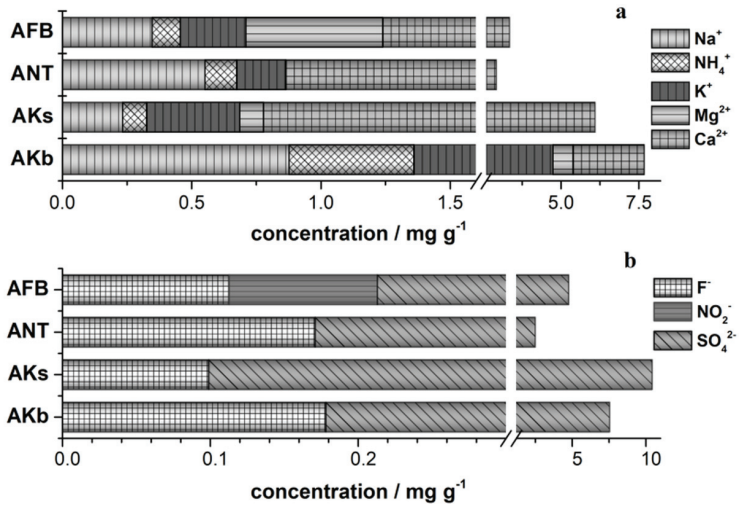

Fig. 2. Leaching of cations (a) and anions (b) in water extracted fly ashes from TPPs Kolubara A (AKb), Kostolac B (AKs), Nikola Tesla A (ANT) and from fluidized bed boiler (AFB).

All water extracted FAs can be regarded as non-hazardous waste since fluoride and sulfate contents are far below upper legislation limit values for waste classification given in Table S-IV of the Supplementary material.

The concentration of trace elements in coals and representative FAs; enrichment ratios (ERs)

Fig. S-1 and Table S-I of the Supplementary material show the overall trace elements concentrations in feed coals and their corresponding fly ashes. CFB has the lowest overall trace element content among all the investigated feed coals (256.72 mg/kg). Trace element concentrations in coals are the highest for Mn (up to 209.63 mg/kg), while decreased content for Hg and Ge is observed (Fig. S-1, a and b). Trace element contents in FAs vary from the lowest values for Cd (up to 0.76 mg/kg in AKs) to the highest content for Mn, ranging from 210.48 mg/kg in AFB to 607.29 mg/kg in AKb (Fig. S-1, c and d). Finer TPP ashes have elevated trace element concentrations compared with AFB due to higher concentrations in corresponding feed fuels and larger surface area of ash particles.[35] Furthermore, the reason for significantly lower concentrations of As, Co, Cs and Hg in AFB compared with other FAs from TPPs can be higher combustion temperatures in TPPs. It is known that higher combustion temperatures can imply enhanced trace element concentrations in flue gases which can further easily condensate on fly ash particles.[36] In contrast, Cu, Ga, Ge and Sb contents in AFB are not the lowest of all FAs, which is consistent with the literature where these trace elements do not show a significant correlation with ash particle diameters.[31]

The enrichment ratios (*ER*) are presented in Fig. 3. As (from 13.58 to 18.60), Pb (from 6.55 to 8.85), Hg (from 2.97 to 5.68), Cu (from 4.08 to 6.13), V (from 3.14 to 5.45), and Cr (from 2.60 to 5.04) have the highest *ER* values. These elements are enhanced in FAs due to their vaporization during coal combustion and subsequent condensation on the fly ash particles.[37] At relatively low temperatures, arsenic easily forms volatile compounds.[38] In addition, Pb related to organic matters volatilizes at around 850 °C, while Hg may react with flue gas components and form oxidized mercury in a wide temperature range.[39] Other elements, such as Be, Co, Ni, U, Sb and Sr, have lower ERs because they are correlated with less volatile minerals.[5]

PAHs content in investigated FAs

Fig. 4a shows the distributions of LMW, MMW and HMW PAHs. The total PAH content and the concentration of 10 PAHs defined in Serbian legislation for soil are presented in Fig. 4b. The total PAHs content varies from 278.95 (ANT) to 32548.66 ng/g (AFB), which is consistent with PAHs ranges for FAs found in the literature.[40] The MMW PAHs are the most abundant in AKb (68.25 %) and AFB (70.03 %), while LMW PAHs prevail in AKs (75.23 %) and ANT (67.28 %). Among examined FAs, AFB and AKb contain the highest fluoranthene content, while AKs and ANT have the highest fluorene concentration (Table S-I, b). These findings are in accordance with literature revealing Fla and Flu as the most abundant PAHs due to incomplete combustion of fossil fuels.[26] The content of 10

PAHs is in the range from 124.13 (ANT) to 23075.48 ng/g (AFB), which is lower than permissible limits in Serbian soil guidance (Table S-IV).[41]

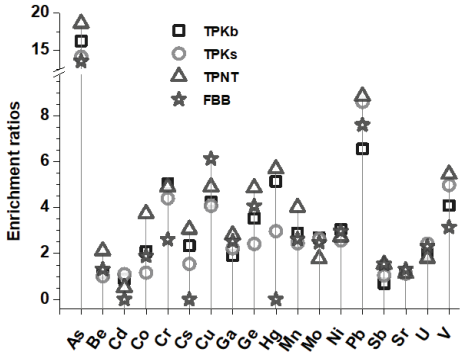

Fig. 3. Enrichment ratios for TPPs Kolubara A (TPKb), Kostolac B (TPKs), Nikola Tesla A (TPNT) and fluidized bed boiler (FBB).

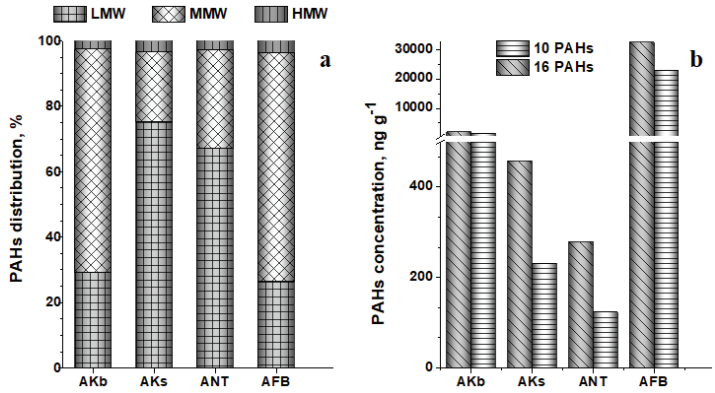

Fig. 4. Distribution of PAHs according to molecular weight (a); the overall and 10 PAHs content (b); fly ashes from TPPs Kolubara A (AKb), Kostolac B (AKs), Nikola Tesla A (ANT) and fluidized bed boiler (AFB).

Health impact for potentially toxic trace elements and PAHs from FAs

Risk indices, as well as total hazard indices for children and adults, are presented in Table II. The non-cancer risks for children demonstrate that Ni values in AKb, AKs and ANT, as well as As for all FAs, exceed the acceptable limit. Furthermore, *HI*s for adults are higher than safe values for As in AKb, AKs and ANT (Table II). Hazard indices for Cd^{ncc}, Co^{ncc}, Cu, Hg and Pb are about two orders lower than the regulatory level.[42] To acquire better insight into the health impact of each FAs, the overall *HIs*, as well as the overall *Rs*, are determined as the sum of *HI* or *R* for all investigated elements, respectively. The estimated overall *HI* is the highest for AKb (7.15 for children and 2.15 for adults). Trace elements hazard quotients (HQ_{ig}, HQ_{ih} and HQ_d) and risk indices (R_{ig}, R_{ih} and R_d) for three exposure routes are shown in Table S-V, a and b. The dominant

exposure routes for the non-cancer risk are dermal contact for As^{ncc}, Cd^{ncc}, Ni^{ncc} and Cu, and ingestion for Co^{ncc}, Cr^{ncc}, Hg and Pb.

TABLE II. Trace elements cancer risk (*R*) and total hazard impact (*HI*); PAHs total risk (*ILCR*) for fly ashes from TPPs Kolubara A (AKb), Kostolac B (AKs) and Nikola Tesla A (ANT) and from fluidized bed boiler (AFB)

Target group	Element	Fly ash origin			
		AKb	AKs	ANT	AFB
		R, carcinogenic elements			
Children	As	1.81×10^{-4}	1.51×10^{-4}	1.61×10^{-4}	4.82×10^{-5}
	Cd	2.87×10^{-17}	4.92×10^{-17}	1.70×10^{-17}	–
	Co	1.55×10^{-9}	1.11×10^{-9}	2.13×10^{-9}	6.79×10^{-10}
	Cr	4.25×10^{-11}	3.25×10^{-11}	4.93×10^{-11}	2.91×10^{-11}
	Ni	1.24×10^{-10}	1.14×10^{-10}	1.05×10^{-10}	8.08×10^{-11}
Overall R		1.81×10^{-4}	1.51×10^{-4}	1.61×10^{-4}	4.82×10^{-5}
Adults	As	2.51×10^{-4}	2.09×10^{-4}	2.23×10^{-4}	6.69×10^{-5}
	Cd	4.49×10^{-17}	7.69×10^{-17}	2.66×10^{-17}	–
	Co	2.42×10^{-9}	1.74×10^{-9}	3.33×10^{-9}	1.06×10^{-9}
	Cr	6.65×10^{-11}	5.08×10^{-11}	7.71×10^{-11}	4.54×10^{-11}
	Ni	2.26×10^{-9}	2.08×10^{-9}	1.91×10^{-9}	1.47×10^{-9}
Overall R		2.51×10^{-4}	2.09×10^{-4}	2.23×10^{-4}	6.69×10^{-5}
		HI, non-carcinogenic elements			
Children	As	4.68	3.90	4.16	1.25
	Cd	8.71×10^{-4}	1.49×10^{-3}	5.16×10^{-4}	–
	Co	7.66×10^{-3}	5.51×10^{-3}	1.06×10^{-2}	3.36×10^{-3}
	Cr	9.71×10^{-1}	7.41×10^{-1}	1.13	6.64×10^{-1}
	Cu	9.56×10^{-2}	1.96×10^{-1}	1.11×10^{-1}	1.57×10^{-1}
	Hg	1.02×10^{-1}	6.61×10^{-2}	1.23×10^{-1}	2.80×10^{-2}
	Ni	1.18	1.09	1.00	7.73×10^{-1}
	Pb	1.11×10^{-1}	1.20×10^{-1}	1.41×10^{-1}	7.91×10^{-2}
Overall *HI*		7.15	6.13	6.68	2.95
Adults	As	1.30	1.08	1.16	3.47×10^{-1}
	Cd	3.12×10^{-4}	5.35×10^{-4}	1.85×10^{-4}	–
	Co	5.86×10^{-4}	4.21×10^{-4}	8.07×10^{-4}	2.57×10^{-4}
	Cr	2.32×10^{-1}	1.77×10^{-1}	2.69×10^{-1}	1.59×10^{-1}
	Cu	3.85×10^{-2}	7.88×10^{-2}	4.46×10^{-2}	6.33×10^{-2}
	Hg	2.43×10^{-2}	1.58×10^{-2}	2.93×10^{-2}	6.69×10^{-3}
	Ni	5.32×10^{-1}	4.90×10^{-1}	4.50×10^{-1}	3.47×10^{-1}
		HI, non-carcinogenic elements			
Adults	Pb	2.41×10^{-2}	2.60×10^{-2}	3.06×10^{-2}	1.71×10^{-2}
Overall *HI*		2.15	1.87	1.98	9.40×10^{-1}
		ILCR, PAHs			
Children		1.32×10^{-7}	2.12×10^{-8}	1.65×10^{-7}	6.05×10^{-6}
Adults		4.29×10^{-7}	6.91×10^{-8}	5.40×10^{-7}	1.98×10^{-5}

AFB displays the lowest total risk index (4.82×10^{-5} for children and 6.69×10^{-5} for adults). The calculated total risk indices decrease in the following order: $As^{cc}>Co^{cc}>Ni^{cc}>Cr^{cc}>Cd^{cc}$ (Table II). Total cancer risk of As (up to 2.51×10^{-4} in AKb) exceed the safe limits, while Co^{cc}, Ni^{cc}, Cr^{cc} and Cd^{cc} risk values are far below permissible limit values. The arsenic content should be thoroughly monitored and controlled. The most dominant exposure route among carcinogenic substances is the inhalation for Co^{cc}, Ni^{cc}, Cr^{cc} and Cd^{cc}, while for As^{cc}, it is dermal contact (Table S-V, a and b).

Three exposure routes were used, both for children and adults, to determine human health issues caused by PAHs. Table II demonstrates that only AFB for adults indicates a potential risk for PAHs, while all other FAs are within safe limits. The literature provides health assessments of PAHs for various soil types, while there is a lack of information regarding health assessments of PAHs from FAs generated during coal combustion.[43]

CONCLUSIONS

Potassium is the most dominant among cations (AKb), while sulfates have the highest content in all FAs among anions. Investigated FAs can be considered non-hazardous since fluorides and sulfates content are far below legislation limits for waste classification. The ERs are the highest for As, Pb, Cu, V, Hg and Cr. Among all investigated FAs, the highest concentration of Fla was noticed in AKb and AFB, while Flu concentrations are maximal in AKs and ANT. Health calculations associated with trace elements and PAHs in FAs lead to some general conclusions:

- The obtained results for non-cancer risk show that Ni in AKb and AKs and ANT, as well as As for all FAs, exceed the permissible limit for children, while HIs for adults are higher than safe values for As in AKb, AKs and ANT.
- As exceeds the safe limit for cancer risk in all FAs, apart for AFB.
- PAHs potential risks for adults (except for AFB) are within safe values.

Due to the lack of information on anions and cations analysis in water extracted FAs, as well as health risks related with exposure to PAHs and trace elements, this research could contribute to the current state of knowledge for health issues associated with fly ash disposal.

SUPPLEMENTARY MATERIAL

Additional data and information are available electronically at the pages of journal website: https://www.shd-pub.org.rs/index.php/JSCS/article/view/12208, or from the corresponding author on request.

Acknowledgement. This work was supported by the Ministry of Science, Technological Development and Innovation of the Republic of Serbia; grant number 451-03-47/2023-01/ /200017.

ИЗВОД

ПРОЦЕНА РИЗИКА ЗА ПОТЕНЦИЈАЛНО ОПАСНЕ СУПСТАНЦЕ ИЗ ЛЕТЕЋИХ ПЕПЕЛА ДОБИЈЕНИХ САГОРЕВАЊЕМ УГЉА И ОТПАДНОГ УГЉА

ЈОВАНА З. БУХА МАРКОВИЋ[1], АНА Д. МАРИНКОВИЋ[1], ЈАСМИНА З. САВИЋ[1], АЛЕКСАНДАР Д. КРСТИЋ[1], АНДРИЈА Б. САВИЋ[1] и МИРЈАНА Ђ. РИСТИЋ[2]

[1]Универзитет у Београду, Институт за нукларне науке Винча – Институт од националног значаја за Републику Србију, Београд и [2]Универзитет у Београду, Технолошко–металуршки факултет, Карнегијева 4, Београд

У овом раду, испитивана су горива (лигнит и отпадни угаљ) која се користе у термоелектранама и полуиндустријском постројењу са флуидизованим слојем, као и летећи пепели добијени њиховим сагоревањем. Летећи пепели су упоређени на основу: садржаја анјона и катјона у њиховим воденим екстрактима, концентрације елемената у траговима и полицикличних ароматичних угљоводоника (PAH), као и процене здравственог ризика који потиче од претходно поменутих потенцијално опасних супстанци. Садржај флуорида и сулфата у воденим екстрактима летећих пепела далеко је испод законски дозвољених граница за отпад, на основу чега се могу сврстати у безопасне. Од испитиваних елемената у траговима, садржај Cd је најнижи, док је концентрација Mn највиша. Највеће обогаћење пепела у односу на одговарајући угаљ, примећено је за As, Pb, Hg, Cu, V и Cr. На основу добијених резултата показано је да је укупни садржај PAH највећи за летећи пепео добијен сагоревањем отпадног угља. Међу испитиваним PAH, највишу концентрацију има флуорантен. Ризици који потичу од арсена (међу канцерогеним елементима), као и арсена и никла (међу неканцерогеним елементима), премашују дозвољене граничне вредности. Вредност процењеног ризика од рака код одрасле популације у случају PAH, показује да за летећи пепео добијен сагоревањем отпадног угља постоји потенцијални ризик, док су вредности за остале пепеле унутар дозвољених граница.

(Примљено 30. децембра 2022, ревидирано 24. јула, прихваћено 3. августа 2023)

REFERENCES

1. *Coal information: overview*, International Energy Agency, Paris, 2019
2. *Added value from coal*, https://euracoal.eu/info/coal-industry-across-europe/added-value/(accessed December 08, 2022)
3. I. Obernberger, G. Thek, *Biomass Bioenergy* **27** (2004) 653 (https://doi.org/10.1016/j.biombioe.2003.07.006)
4. B. S. Repić, M. J. Paprika, M. R. Mladenović, S. Đ. Nemoda, A. M. Erić, D. V. Dakić, in *Proceedings of International Conference "Power Plants 2018"*, 2018, Zlatibor, Serbia, Institute of Agricultural Economics, Belgrade, pp. 318–329
5. S. Singh, L. C. Ram, R. E. Masto, S. K. Verma, *Int. J. Coal Geol.* **87** (2011) 112 (https://doi.org/10.1016/j.coal.2011.05.006)
6. *Technical report*, Electric Power Industry of Serbia, 2018
7. D. Saha, D. Chatterjee, S. Chakravarty, T. Roychowdhury, *Nat. Resour. Res.* **28** (2019) 1505 (https://doi.org/10.1007/s11053-019-09451-2)
8. F. Jiao, L. Zhang, Z. Dong, T. Namioka, N. Yamada, Y. Ninomiya, *Fuel Process. Technol.* **152** (2016) 108 (https://doi.org/10.1016/j.fuproc.2016.06.013)
9. A. Tasić, I. Sredović Ignjatović, L. Ignjatović, M. Ilić, M. Antić, *J. Serb. Chem. Soc.* **81** (2016) 1081 (https://doi.org/10.2298/jsc160307038t)

10. H.P. Jambhulkar, S.M.S. Shaikh, S.M. Kumar, *Chemosphere* **213** (2018) 333 (https://doi.org/10.1016/j.chemosphere.2018.09.045)
11. J. Han, Y. Liang, B. Zhao, Y. Wang, F. Xing, L. Qin, *Environ. Pollut.* **251** (2019) 312 (https://doi.org/10.1016/j.envpol.2019.05.022)
12. *Priority pollutant list*, https://www.epa.gov/sites/production/files/2015-09/documents/priority-pollutant-list-epa.pdf (accessed November 23, 2022)
13. S. K. Sahu, R. C. Bhangare, P. Y. Ajmal, S. Sharma, G. G. Pandit, V. D. Puranik, *Microchem. J.* **92** (2009) 92 (https://doi.org/10.1016/j.microc.2009.02.003)
14. K. Ravindra, R. Sokhi, R. Van Grieken, *Atmos. Environ.* **42** (2008) 2895 (https://doi.org/10.1016/j.atmosenv.2007.12.010)
15. N. Wang, X. Sun, Q. Zhao, Y. Yang, P. Wang, *J. Hazard. Mater.* **396** (2020) 122725 (https://doi.org/10.1016/j.jhazmat.2020.122725)
16. *Human health evaluation manual (part A), risk assessment guidance for superfund*, Office of Emergency and Remedial Response, Washington, DC, 1989
17. ASTM D346-90: *Standard practice for collection and preparation of coke samples for laboratory analysis* (1998)
18. ASTM D2013-07: *Standard practice for preparing coal samples for analysis* (2007)
19. S. Lacorte, F. Bono-Blay, M. Cortina-Puig, in: *Comprehensive Sampling and Sample Preparation*. J. Pawliszyn, Ed., Academic Press, Oxford, 2012, pp. 65–84
20. ISO 1953:1994: *Hard Coals - Size Analysis* (1994)
21. ASTM D7582-12: *Standard test methods for proximate analysis of coal and coke by macro thermogravimetric analysis* (2012)
22. ASTM D5373-14: *Standard test methods for determination of carbon, hydrogen and nitrogen in analysis samples of coal and carbon in analysis samples of coal and coke* (2014)
23. ASTM D5016-08: *Standard test method for total sulfur in coal and coke combustion residues using a high-temperature tube furnace combustion method with infrared absorption* (2008)
24. ASTM D3176-09: *Standard practice for ultimate analysis of coal and coke* (2009)
25. R. E. Masto, E. Sarkar, J. George, K. Jyoti, P. Dutta, L. C. Ram, *Fuel Process. Technol.* **132** (2015) 139 (https://doi.org/10.1016/j.fuproc.2014.12.036)
26. J. Z. Buha-Marković, A. D. Marinković, S. Đ. Nemoda, J. Z. Savić, *Environ. Pollut.* **266** (2020) 115282 (https://doi.org/10.1016/j.envpol.2020.115282)
27. *Integrated Risk Information System*, US EPA, 2005 (http://www.epa.gov/iris)
28. *Exposure factors handbook: 2011 edition*, National Center for Environmental Assessment, Office of Research and Development, Washington, DC, 2011
29. S. Chakravarty, A. Mohanty, A. Banerjee, R. Tripathy, G. K. Mandal, M. R. Basariya, M. Sharma, *Fuel* **150** (2015) 96 (https://doi.org/10.1016/j.fuel.2015.02.015)
30. C.-L. Chou, *Int. J. Coal Geol.* **100** (2012) 1 (https://doi.org/10.1016/j.coal.2012.05.009)
31. N. Koukouzas, C. Ketikidis, G. Itskos, *Fuel Process. Technol.* **92** (2011) 441 (https://doi.org/10.1016/j.fuproc.2010.10.007)
32. R. Barbosa, D. Dias, N. Lapa, H. Lopes, B. Mendes, *Fuel Process. Technol.* **109** (2013) 124 (https://doi.org/10.1016/j.fuproc.2012.09.048)
33. M. Izquierdo, X. Querol, *Int. J. Coal Geol.* **94** (2012) 54 (https://doi.org/10.1016/j.coal.2011.10.006)
34. G. Wang, Z. Luo, J. Zhang, Y. Zhao, *Minerals* **5** (2015) 863 (https://doi.org/10.3390/min5040530)

35. E. Loginova, D. S. Volkov, P. M. F. van de Wouw, M. V. A. Florea, H. J. H. Brouwers, *J. Clean. Prod.* **207** (2019) 866 (https://doi.org/10.1016/j.jclepro.2018.10.022)
36. G. Chen, Y. Sun, Q. Wang, B. Yan, Z. Cheng, W. Ma, *Fuel* **240** (2019) 31 https://doi.org/10.1016/j.fuel.2018.11.131.
37. J. W. Kaakinen, R. M. Jorden, M. H. Lawasani, R. E. West, *Environ. Sci. Technol.* **9** (1975) 862 (https://doi.org/10.1021/es60107a012)
38. S. K. Verma, R. E. Masto, S. Gautam, D. P. Choudhury, L. C. Ram, S. K. Maiti, S. Maity, *Fuel* **162** (2015) 138 (https://doi.org/10.1016/j.fuel.2015.09.005)
39. S. Zhao, Y. Duan, Y. Li, M. Liu, J. Lu, Y. Ding, X. Gu, J. Tao, M. Du, *Fuel* **214** (2018) 597 (https://doi.org/10.1016/j.fuel.2017.09.093)
40. S. Liu, Y. Wang, Z. Zhang, Z. Li, C. Chen, T. Guo, Y. Mei, J. Dong, *J. Electrostat.* **96** (2018) 144 (https://doi.org/10.1016/j.elstat.2018.10.012)
41. *Regulation on the systematic monitoring program of soil quality, indicators for assessing the risk of soil degradation, and methodology for remediation programs developing*, Government of the Republic of Serbia, 2018 (in Serbian)
42. *Supplemental guidance for developing soil screening levels for superfund sites*, Washington, DC, 2002
43. Y. Chen, J. Zhang, F. Zhang, X. Liu, M. Zhou, *Ecotoxicol. Environ. Saf.* **156** (2018) 383 (https://doi.org/10.1016/j.ecoenv.2018.03.020).

Journal of the Serbian Chemical Society
JSCS@tmf.bg.ac.rs • www.shd.org.rs/JSCS
J. Serb. Chem. Soc. *88* (11) S328–S337 (2023) *Supplementary material*

SUPPLEMENTARY MATERIAL TO

Health risk assessment of potentially harmful substances from fly ashes generated by coal and coal waste combustion

JOVANA Z. BUHA MARKOVIĆ[1]*, ANA D. MARINKOVIĆ[1], JASMINA Z. SAVIĆ[1], ALEKSANDAR D. KRSTIĆ[1], ANDRIJA B. SAVIĆ[1] and MIRJANA Đ. RISTIĆ[2]

[1]*University of Belgrade, Vinča Institute of Nuclear Sciences - National Institute of the Republic of Serbia, Belgrade, Serbia and* [2]*University of Belgrade, Faculty of Technology and Metallurgy, Karnegijeva 4, Belgrade, Serbia*

J. Serb. Chem. Soc. *88* (11) (2023) 1161–1173

DETERMINATIONS OF ANIONS AND CATIONS BY ION CHROMATOGRAPHY

Cations (sodium, potassium, magnesium, calcium, and ammonium ions) in aqueous extracts of ash samples were determined by ion chromatograph Dionex with a conductivity detector and Dionex IonPack CS12 (4×250 mm) column with pre-column CG12 (10-32) (4×50 mm). The mobile phase contained 0.02 M methane sulfonic acid (flow rate of 0.7 mL min^{-1}).

Anions (sulphates, Su; nitrates, NA; nitrites, NI; phosphates, Ph; chlorides, Ch and fluorides, Fl) were determined by ion chromatograph Dionex with a conductivity detector and Dionex IonPack AS14 (4×250 mm) column with pre-column AG14 (4×50 mm). The mobile phase contained 0.5 mM $NaHCO_3$ and 2 mM Na_2CO_3 (flow rate of 0.9 mL min^{-1}). The injection volume for cations and anions determination was 20 μL.

ICP-MS ANALYSIS

The measurements of every subsample were done in 3 replicates. ICP-MS was calibrated using Agilent Multi-Element Calibration Standards (standards 2, 3 and 4) with six standard solutions. Standard solutions and blanks were prepared in 2 % HNO_3. A tuning solution containing 1 μg/L Li, Mg, Co, Y, Ce and Tl (Agilent) was used for the instrument optimization. The limits of detection of measured elements were: As 0.015, Be 0.046, Cd 0.002, Co 0.001, Cr 0.015, Cs 0.01, Cu 0.005, Ga 0.007, Ge 0.006, Hg 0.01, Mn 0.098, Mo 0.07, Ni 0.022, Pb 0.005, Sb 0.01, Sr 0.163, U 0.005, V 0.001(all in μg/L). Quality control was performed using the certified reference material SLRS-5 (River water reference

* Corresponding author. E-mail: jbuha@vin.bg.ac.rs

material for trace metals, National Research Council of Canada). Accuracy was in the range of 88 – 112 %.

HPLC ANALYSIS

A Thermo Fisher Scientific Dionex UltiMate 3000 HPLC system with a diode array detector (DAD) and Envirosep-PP 125×2 mm column, with particle size 5 μm (Phenomenex) was used. A portion of 5 g of coal, coal waste, or ash was mixed with 50 mL of hexane:acetone mixture (1:1, v/v). PAHs extraction lasted 70 min, and was carried out by Grant XUB ultrasonic bath, Grant Instruments (Cambridge) Ltd, UK. After that, the mixture of ash samples with solvents was filtered through Whatman No. 44 filter paper, and ash was washed out several times with a total of 20 mL of acetone: hexane mixture (1:1). Then, the extract was transferred quantitatively into separating funnel; deionized water was added, and after shaking extract was divided into two layers: the upper hexane layer and downer polar layer (acetone-water). The downer layer was removed from the separating funnel. The hexane layer was dried with anhydrous Na_2SO_4 and concentrated up to 1 mL by a vacuum rotary evaporator (Heidolph Instruments GmbH, Germany). After that, the concentrated extract was evaporated to dryness in a nitrogen stream; 0.5 mL of acetonitrile was added and filtered by 0.22 μm nylon syringe filter ESF-NY-13-022 of 13 mm (Kinesis) before further PAHs analysis. The procedure was done in triplicate to check the reproducibility of extraction.

HUMAN HEALTH ASSESSMENT

The dose received through each of the three pathways was calculated by the following equations:

$$Dig = C \times \frac{IRig \times EF \times ED \times CF_1}{BW \times AT} \quad (1)$$

$$Dih = C \times \frac{IRih \times EF \times ED}{PEF \times BW \times AT} \quad (2)$$

$$Dd = C \times \frac{SA \times SL \times ABS \times EF \times ED \times CF_1}{BW \times AT} \quad (3)$$

C/ mg kg^{-1} - concentration of each representative metal in fly ash samples (given in Table S-I, a). Values for all other parameters used in health assessment calculations are presented in Table S-II.

TABLE S-I, a. Concentration of elements in fly ash samples (*C*/ mg kg^{-1})

Elements content- *C*/ mg kg^{-1}				
Element	AKb	AKs	ANT	AFB
As	63.26	52.78	56.26	16.87
Pb	23.17	24.95	29.44	16.47
Hg	1.65	1.075	1.99	0.46
Cd	0.44	0.76	0.26	/
Cr	158.02	120.58	183.09	107.98
Co	13.96	10.04	19.24	6.12
Ni	107.19	98.89	90.79	70.02
Cu	59.32	121.45	68.75	97.50

TABLE S-I, b. Individual PAHs concentration in fly ash samples (*C*/ ng kg^{-1})

PAHs content - *C*/ ng kg^{-1}					
PAHs	Abbreviation	AKb	AKs	ANT	AFB
Naphthalene	Nap	23.54	10.88	7.33	21.80
Acenaphthylene	Acy	2.77	49.36	38.05	745.23
Acenaphthene	Ace	6.56	8.29	3.25	104.70
Fluorene	Flu	150.06	144.76	92.01	1576.70
Phenanthrene	Phe	385.87	129.26	44.90	4993.90
Anthracene	Ant	17.20	1.87	2.14	1159.98
Fluoranthene	Fla	795.89	55.31	50.24	9509.68
Pyrene	Pyr	410.35	13.01	14.17	6999.46
Benzo[a]anthracene	BaA	84.37	20.39	15.32	3838.38
Chrysene	Chry	77.25	8.89	4.09	2445.81
Benzo[b]fluoranthene	BbF	25.05	0.00	1.39	491.95
Benzo[k]fluoranthene	BkF	4.32	7.61	1.33	53.56
Benzo[a]pyrene	BaP	5.59	0.00	21.06	338.25
Dibenzo[a,h]anthracene	DahA	0.04	0.00	0.00	25.29
Benzo[g,h,i]perylene	BghIP	10.66	3.54	1.49	115.92
Indeno[1,2,3-cd]pyrene	IP	4.51	0.46	0.17	128.05

TABLE S-II. Parameters used for risk assessment of trace elements and PAHs

Parameter, unit	**Abbr.**[ref]	**Children**	**Adults**
Body weight, kg	BW[2,3]	18.6	80
Exposure frequency, day year^{-1}	*EF*	350	350
Exposure duration, year	*ED*	6	30
Dust ingestion rate, mg day^{-1}	*IR*ig[2,3,5]	200	50
Inhalation rate, m^3 day^{-1}	*IR*ih[2,3]	41.76	56.16
Dermal exposure area, cm^2	*SA*[2]	2625	6475
Dermal adsorption factor (for elements)	*ABS*[6,9]	As (0.03), Pb (0.006), Hg (0.05), Cd (0.14), Cr and Co (0.001), Cu (0.1), Ni (0.35)	
Skin-soil adherence factor	*SL*[2]	1.2	0.98
Dermal adherence factor, mg cm^{-2}	*AF*[4]	0.2	0.07
Dermal adsorption factor (for PAHs), unitless	*ABS*[4,8]	0.13	0.13
Averaging time (for elements), year	*AT*[4,5]	6* 70**	30* 70*
Averaging lifespan (for PAHs), day	*AT*[9]	25550	25550
Particle emission factor, m^3 kg^{-1}	*PEF*[6]	6.8×10^8	6.8×10^8
Unit conversation factor, unitless	CF_1	10^{-6}	10^{-6}
Carcinogenic slope factor ih, kg day mg^{-1}	*CSF*ih[7]	3.85	3.85
Carcinogenic slope factor ig, kg day mg^{-1}	*CSF*ig[7]	7.30	7.30
Carcinogenic slope factor d, kg day mg^{-1}	*CSF*d[7]	25.00	25.00

*for non-carcinogenic, AT=ED, 6×365=2190 days for children and 30×365=10950 days for adults, ** for carcinogenic effect, 70×365=25550 days

TABLE S-III. Cancer slope factors (SF_i/ kg day mg^{-1}) for carcinogenic elements and Reference dose factors (RF_i/ mg kg^{-1} day^{-1}) for non-carcinogenic elements, for three exposure routes

Element	SF_{ig}	SF_{ih}	SF_d
Cancer Slope factor - SF_i/ kg day mg^{-1}			
As	1.5	3.66	15
Cd	/	/	6.3
Cr	/	/	42
Co	/	/	9.8
Ni	/	/	0.84
Reference dose - RF_i/ mg kg^{-1} day^{-1}			
As	3×10^{-4}	1.23×10^{-4}	3×10^{-4}
Pb	3.5×10^{-3}	5.25×10^{-3}	3.5×10^{-3}
Hg	3×10^{-4}	3×10^{-4}	8.6×10^{-5}
Cd	2×10^{-2}	1.6×10^{-2}	5.71×10^{-6}
Cr	3×10^{-4}	6×10^{-5}	3×10^{-5}
Co	2×10^{-2}	1.6×10^{-2}	5.71×10^{-6}
Ni	2×10^{-2}	5.4×10^{-3}	2×10^{-2}
Cu	4×10^{-2}	1.2×10^{-2}	4×10^{-2}

The *ILCR* were calculated for ingestion, inhalation and dermal route using the following equations:[1]

$$ILCRig = \frac{C_s \times \left(CSFig \times \sqrt{\left(\frac{BW}{70} \right)} \right) \times IRig \times EF \times ED}{BW \times AT \times 10^6} \quad (4)$$

$$ILCRih = \frac{C_s \times \left(CSFih \times \sqrt{\left(\frac{BW}{70} \right)} \right) \times IRih \times EF \times ED}{BW \times AT \times PEF} \quad (5)$$

$$ILCRd = \frac{Cs \times \left(CSFd \times \sqrt{\left(\frac{BW}{70} \right)} \right) \times SA \times AF \times ABS \times EF \times ED}{BW \times AT \times 10^6} \quad (6)$$

Health assessment calculations, according to literature data, are given in Table S-II.[2-9]

Concentrations of all 16 PAHs are shown in Table S-I, b, while Cs represent sum of converted PAHs concentrations for 7 CarPAHs based on toxic equivalents of BaP using the toxic equivalency factor in ng g^{-1}.[7]

TABLE S-IV. Literature data and permissible limits for anions and cations, trace elements and PAHs leaching

Analytes	C/ mg kg^{-1}	Data description,[reference]
	Anions and cations	
F^-	10 - 500	Limit values for waste classification,[11]
SO_4^{2-}	1000-50000	
Na^+	189.92	Leaching from class F FA,[12]
NH_4^+	9.0-12.20	Leaching from Australian FAs,[13]
K^+	181.7	Leaching from class F FA,[12]
Ca^{2+}	42.32-52.42	Leaching from class F FA and Serbian FA,[12,14]
Mg^{2+}	2042.3	Leaching from class F FA,[12]
	Trace elements	
As	29-55	Legislation limits for metals in soil,[15,16]
Be	1.1-30	
Cd	0.8-2	
Co	9-240	
Cr	100-380	
Cu	36-190	
Hg	0.3-10	
Ni	35-210	
Pb	85-530	
Mo	3-200	
U	42-250	
	PAHs	
10 PAHs	1-40	Legislation limits for PAHs in soil,[15]

TABLE S-V. a. Risk indices (R_{ig}, R_{ih} and R_d) and hazard quotients (HQ_{ig}, HQ_{ih} and HQ_d) for three exposure routes for fly ashes from TPPs Kolubara (AKb) and Kostolac (AKs)

AKb

	Children			Adults		
Element	R_{ig}*	R_d	R_{ih}	R_{ig}	R_d	R_{ih}
As^{cc}	8.39×10^{-5}	9.67×10^{-5}	1.07×10^{-8}	2.44×10^{-5}	2.26×10^{-4}	1.68×10^{-8}
Cd^{cc}	0.00	0.00	2.87×10^{-17}	0.00	0.00	4.49×10^{-17}
Cr^{cc}	0.00	0.00	4.25×10^{-11}	0.00	0.00	6.65×10^{-11}
Co^{cc}	0.00	0.00	1.55×10^{-9}	0.00	0.00	2.42×10^{-9}
Ni^{cc}	0.00	0.00	1.24×10^{-10}	0.00	0.00	2.26×10^{-9}
Element	HQ_{ig}*	HQ_d	HQ_{ih}	HQ_{ig}	HQ_d	HQ_{ih}
As^{ncc}	2.17	2.51	2.78×10^{-5}	1.26×10^{-1}	1.17	8.70×10^{-6}
Pb	6.83×10^{-2}	4.30×10^{-2}	8.73×10^{-7}	3.97×10^{-3}	2.01×10^{-2}	2.73×10^{-7}
Hg	5.68×10^{-2}	4.47×10^{-2}	2.54×10^{-6}	3.30×10^{-3}	2.10×10^{-2}	7.93×10^{-7}
Cd^{ncc}	2.29×10^{-4}	6.31×10^{-4}	1.03×10^{-5}	1.33×10^{-5}	2.96×10^{-4}	3.21×10^{-6}
Cr^{ncc}	5.43×10^{-1}	4.28×10^{-1}	6.95×10^{-4}	3.16×10^{-2}	2.00×10^{-1}	2.17×10^{-4}
Co^{ncc}	7.20×10^{-3}	1.42×10^{-4}	3.23×10^{-4}	4.18×10^{-4}	6.64×10^{-5}	1.01×10^{-4}
Ni^{ncc}	5.53×10^{-2}	1.13	7.07×10^{-7}	3.21×10^{-3}	5.28×10^{-1}	2.21×10^{-7}
Cu	1.53×10^{-2}	8.03×10^{-2}	1.96×10^{-7}	8.89×10^{-4}	3.76×10^{-2}	6.12×10^{-8}

AKs

	Children			Adults		
Element	R_{ig}	R_d	R_{ih}	R_{ig}	R_d	R_{ih}
As^{cc}	7.00×10^{-5}	8.07×10^{-5}	8.95×10^{-9}	2.03×10^{-5}	1.89×10^{-4}	1.40×10^{-8}
Cd^{cc}	0.00	0.00	4.92×10^{-17}	0.00	0.00	7.69×10^{-17}
Cr^{cc}	0.00	0.00	3.25×10^{-11}	0.00	0.00	5.08×10^{-11}
Co^{cc}	0.00	0.00	1.11×10^{-9}	0.00	0.00	1.74×10^{-9}
Ni^{cc}	0.00	0.00	1.14×10^{-10}	0.00	0.00	2.08×10^{-9}
Element	HQ_{ig}	HQ_d	HQ_{ih}	HQ_{ig}	HQ_d	HQ_{ih}
As^{ncc}	1.81	2.09	2.32×10^{-5}	1.05×10^{-1}	9.79×10^{-1}	7.26×10^{-6}
Pb	7.35×10^{-2}	4.63×10^{-2}	9.40×10^{-7}	4.27×10^{-3}	2.17×10^{-2}	2.94×10^{-7}
Hg	3.70×10^{-2}	2.91×10^{-2}	1.65×10^{-6}	2.15×10^{-3}	1.36×10^{-2}	5.16×10^{-7}
Cd^{ncc}	3.93×10^{-4}	1.08×10^{-3}	1.76×10^{-5}	2.28×10^{-5}	5.07×10^{-4}	5.50×10^{-6}
Cr^{ncc}	4.14×10^{-1}	3.26×10^{-1}	5.30×10^{-4}	2.41×10^{-2}	1.53×10^{-1}	1.66×10^{-4}
Co^{ncc}	5.18×10^{-3}	1.02×10^{-4}	2.32×10^{-4}	3.01×10^{-4}	4.77×10^{-5}	7.25×10^{-5}
Ni^{ncc}	5.10×10^{-2}	1.04×10	6.52×10^{-7}	2.96×10^{-3}	4.88×10^{-1}	2.04×10^{-7}
Cu	3.13×10^{-2}	1.64×10^{-1}	4.01×10^{-7}	1.82×10^{-3}	7.70×10^{-2}	1.25×10^{-7}

* Cancer risk (R) and hazard quotient (HQ) are unitless parameters

TABLE S-V. b. Risk indices (R_{ig}, R_{ih} and R_d) and hazard quotients (HQ_{ig}, HQ_{ih} and HQ_d) for three exposure routes for fly ashes from TPP Nikola Tesla (ANT) and fluidized bed boiler (AFB)

ANT

	Children			Adults		
Element	R_{ig}*	R_d	R_{ih}	R_{ig}	R_d	R_{ih}
As^{cc}	7.46×10^{-5}	8.60×10^{-5}	9.54×10^{-9}	2.17×10^{-5}	2.01×10-04	1.49×10-08
Cd^{cc}	0.00	0.00	1.70×10^{-17}	0.00	0.00	2.66×10-17
Cr^{cc}	0.00	0.00	4.93×10^{-11}	0.00	0.00	7.71×10-11
Co^{cc}	0.00	0.00	2.13×10^{-9}	0.00	0.00	3.33×10-09
Ni^{cc}	0.00	0.00	1.05×10^{-10}	0.00	0.00	1.91×10-09
Element	HQ_{ig}*	HQ_d	HQ_{ih}	HQ_{ig}	HQ_d	HQ_{ih}
As^{ncc}	1.93	2.23	2.47×10^{-5}	1.12×10^{-1}	1.04	7.74×10^{-6}
Pb	8.67×10^{-2}	5.46×10^{-2}	1.11×10^{-6}	5.04×10^{-3}	2.56×10^{-2}	3.47×10^{-7}
Hg	6.86×10^{-2}	5.40×10^{-2}	3.06×10^{-6}	3.99×10^{-3}	2.53×10^{-2}	9.57×10^{-7}
Cd^{ncc}	1.36×10^{-4}	3.74×10^{-4}	6.09×10^{-6}	7.89×10^{-6}	1.75×10^{-4}	1.90×10^{-6}
Cr^{ncc}	6.29×10^{-1}	4.96×10^{-1}	8.05×10^{-4}	3.66×10^{-2}	2.32×10^{-1}	2.52×10^{-4}
Co^{ncc}	9.92×10^{-3}	1.95×10^{-4}	4.45×10^{-4}	5.77×10^{-4}	9.15×10^{-5}	1.39×10^{-4}
Ni^{ncc}	4.68×10^{-2}	9.56×10^{-1}	5.99×10^{-7}	2.72×10^{-3}	4.48×10^{-1}	1.87×10^{-7}
Cu	1.77×10^{-2}	9.30×10^{-2}	2.27×10^{-7}	1.03×10^{-3}	4.36×10^{-2}	7.09×10-8

AFB

	Children			Adults		
Element	R_{ig}	R_d	R_{ih}	R_{ig}	R_d	R_{ih}
As^{cc}	2.24×10^{-5}	2.58×10^{-5}	2.86×10^{-9}	6.50×10^{-6}	6.04×10^{-5}	4.47×10^{-9}
Cd^{cc}	0.00	0.00	0.00	0.00	0.00	0.00
Cr^{cc}	0.00	0.00	2.91×10^{-11}	0.00	0.00	4.54×10^{-11}
Co^{cc}	0.00	0.00	6.79×10^{-10}	0.00	0.00	1.06×10^{-9}
Ni^{cc}	0.00	0.00	8.08×10^{-11}	0.00	0.00	1.47×10^{-9}
Element	HQ_{ig}	HQ_d	HQ_{ih}	HQ_{ig}	HQ_d	HQ_{ih}
As^{ncc}	5.80×10^{-1}	6.68×10^{-1}	7.42×10^{-6}	3.37×10^{-2}	3.13×10^{-1}	2.32×10^{-6}
Pb	4.85×10^{-2}	3.06×10^{-2}	6.21×10^{-7}	2.82×10^{-3}	1.43×10^{-2}	1.94×10^{-7}
Hg	1.57×10^{-2}	1.23×10^{-2}	7.00×10^{-7}	9.11×10^{-4}	5.78×10^{-3}	2.19×10^{-7}
Cd^{ncc}	/	/	/	/	/	/
Cr^{ncc}	3.71×10^{-1}	2.92×10^{-1}	4.75×10^{-4}	2.16×10^{-2}	1.37×10^{-1}	1.48×10^{-4}
Co^{ncc}	3.16×10^{-3}	6.21×10^{-5}	1.41×10^{-4}	1.83×10^{-4}	2.91×10^{-5}	4.42×10^{-5}
Ni^{ncc}	3.61×10^{-2}	7.37×10^{-1}	4.62×10^{-7}	2.10×10^{-3}	3.45×10^{-1}	1.44×10^{-7}
Cu	2.51×10^{-2}	1.32×10^{-1}	3.22×10^{-7}	1.46×10^{-3}	6.18×10^{-2}	1.01×10^{-7}

* Cancer risk (R) and hazard quotient (HQ) are unitless parameters

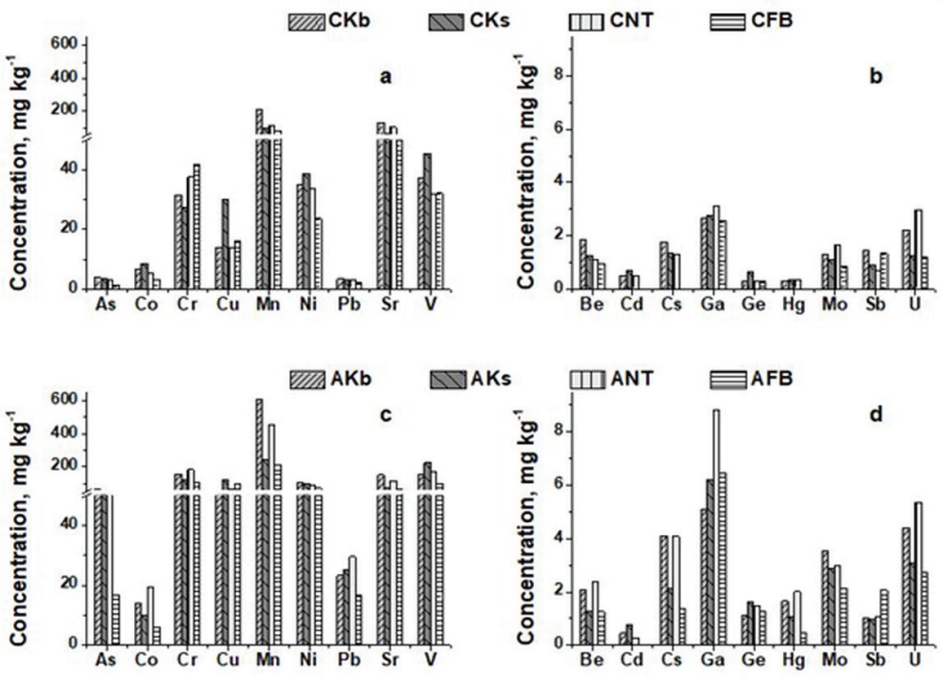

Fig. S-1. As, Co, Cr, Cu, Mn, Ni, Pb, Sr and V content in coals (a) and in fly ash samples (c); Be, Cd, Cs, Ga, Ge, Hg, Mo, Sb, U in coals (b) and in fly ash samples (d)

REFERENCES

1. Y. Chen, J. Zhang, F. Zhang, X. Liu, M. Zhou, *Ecotoxicol. Environ. Saf.* **156** (2018) 383 (https://doi.org/10.1016/j.ecoenv.2018.03.020)
2. *Exposure factors handbook: 2011 edition*, National Center for Environmental Assessment, Office of Research and Development, Washington D.C., 2011
3. *Exposure factors handbook*, National Center for Environmental Assessment; Office of Research and Development, Washington, 1997
4. Supplemental guidance for developing soil screening levels for superfund sites, Washington D.C., 2002
5. Human health evaluation manual (part A), risk assessment guidance for superfund, Office of Emergency and Remedial Response, Washington D.C., 1989
6. E. De Miguel, I. Iribarren, E. Chacón, A. Ordoñez, S. Charlesworth, *Chemosphere* **66** (2007) 505 (https://doi.org/10.1016/j.chemosphere.2006.05.065)
7. Peng C., Chen W. Liao, X. Wang, M. Ouyang, Z. Jiao, W. Bai Y, *Environmental Polution* **159** (2011) 802 (https://doi.org/10.1016/j.envpol.2010.11.003)
8. Federal Contaminated site risk assessment in Canada: Toxicological References values, Canada, Health, 2004
9. Chen Y., Zhang, J., Zhang F., Liu X., Zhou M., *Ecotoxicology and Environmental Safety* **156 (**2018**)** 383 (https://doi.org/10.1016/j.ecoenv.2018.03.020)
10. I.C. Nisbet, P.K. LaGoy, Regul. Toxicol. Pharm. 16 (1992) 290 (https://doi.org/10.1016/0273-2300(92)90009-X)

11. European Council Decision of 19 December 2002 establishing criteria and procedures for the acceptance of waste at landfills pursuant to Article 16 of and Annex II to Directive 1999/31/EC, 2002
12. A. Kim, G. Kazonich, M. Dahlberg, *Environ. Sci. Technol.* **37** (2003) 4507 (https://doi.org/10.1021/es0263691)
13. S.M. Pathan, L.A.G. Aylmore, T.D. Colmer, *Soil Res.* **40** (2002) 1201 (https://doi.org/10.1071/SR02019)
14. R. Krgović, J. Trifković, D. Milojković-Opsenica, D. Manojlović, J. Mutić, *Sci. World J.* **2014** (2014) (https://doi.org/10.1155/2014/212506)
15. R. Pöykiö, K. Manskinen, H. Nurmesniemi, O. Dahl, *Energy Explor. Exploit.* **29** (2011) 217 (https://doi.org/10.1260/0144-5987.29.3.217)
16. Regulation on the systematic monitoring program of soil quality, indicators for assessing the risk of soil degradation, and methodology for remediation programs developing, Government of the Republic of Serbia, 2018 (in Serbian).

Journal of the Serbian Chemical Society
JSCS@tmf.bg.ac.rs • www.shd.org.rs/JSCS
J. Serb. Chem. Soc. *88* (11) 1175–1188 (2023)
JSCS–5689
Original scientific paper
Published 11 November 2023

Read this first! How to prepare a manuscript for submission to a chemical science journal

ANJA DEKANSKI[1] and ALEKSANDAR DEKANSKI[2]*#

[1]*Karolinska Institute, Department of Physiology and Pharmacology, Solnavägen 9, Solna, Sweden and* [2]*University of Belgrade, Institute of Chemistry, Technology and Metallurgy, Department of Electrochemistry, Njegoševa 12, Belgrade, Serbia*

(Received 5 May, revised 23 June, accepted 31 August 2023)

Abstract: In addition to the subject-matter theoretical knowledge acquired during undergraduate and especially postgraduate studies future young scientists must also acquire the accompanying academic skills. This skillset will enable them to plan and conduct their research in accordance with the scientific method, but also to present the results of that research in suitable forms. No result and no new knowledge derived from research is valuable in itself, as long as it is not presented to the scientific community and society as a whole. This dissemination is most often done through the peer-reviewed publishing in scientific journals. Hence, acquiring the skill of writing scientific publications must be an integral part of education, *e.g.*, part of the acquired academic skills. However, that is not currently the case in all scientific environments and a significant number of (young) scientists and researchers do not possess all the necessary knowledge and skills to write academic articles, especially when it comes to the standardized format and technical preparations. This skill-gap often results in a significant number of submitted papers to be rejected or sent back for resubmission even before they reach the Editor's desk. In an effort to provide an academic-writing-skill resource for young academics in the field of chemistry, this article points out the general principles of a well-written and prepared paper, indicates the most common errors and omissions, and suggests ways to prevent them. In addition, the article considers the current state of academic skills in less developed scientific environments, with Serbia as an example, and some of the causes of such a state.

Keywords: academic skills; postgraduate education; publish or perish; 12 golden rules; IUPAC recommendations and nomenclature.

* Corresponding author. E-mail: dekanski@ihtm.bg.ac.rs
# Serbian Chemical Society member.
https://doi.org/10.2298/JSC230505055D

INTRODUCTION

The number of scientific journals and thus the number of published papers has increased enormously in recent years. According to PublishingState.com[1] more than 30,000 journals were published in 2021, and the number continues to increase by about 5 -7 % per year. In 2021 SCIMAGOJR recognized 27,399 journals, while their number in 1999 was 16,978.[2] They published 4,941,761 papers in 2021, while in 1996 just 1,153,167 papers were published.[3] The number of submitted papers is probably several times higher than that. The reasons for this expansion lie in several prevalent changes, the largest of which is the technological development in the recent years. The number of researchers, and therefore research, increased greatly due to the availability of information and literature, but also to new methods, new instruments, and analysis techniques.[4] This technological progress has made it possible for scientific research, from the most basic and simple to the complex, long-lasting and demanding kind, to become available to many more researchers. Therefore, bearing in mind that the results and new knowledge obtained through research are non-traceable until they are made publicly available, the number of scientific papers to be published has increased tremendously.

PUBLISH OR PERISH – A PUSH FOR SPEED BEFORE QUALITY

Digital publishing, electronic communication between authors and journals and other innovations with digital platforms made the submission process easier, faster and more accessible.[5] Parallelly, publishing papers and doing so frequently is a powerful, often the only, tool to gain and maintain a position in the scientific community. With the advent of digital technologies and the growing pressure to publish, there has been a significant increase in the number of published scientific results. This expansion can be attributed to several factors.[6] A larger number of published research papers means that the scientist and their institution are successful, worthy of funding for their research and that they deserve attention from the academic community.[7] The number of publications is often the most important measure of success and competence. Increasingly, it is also the basic criterion when selecting candidates for employment, promotion or obtaining a leadership role, for example.[8] Scientists who publish less often and dedicate themselves to other academic activities (teaching, applied research, *etc*.) may therefore be at a disadvantage, either when applying for grants for their research, or for positions in the educational system.[9] Thus, the phrase *Publish or perish*, uttered by Coolidge back in 1932, became a harsh truth.[10]

And what has the expansion in the publication of scientific papers brought about? One thing is certain – many new technologies, new products, new materials, and new drugs are largely the result of that expansion. We have found or are well on our way to finding the technological sides of the solutions to many of

today's challenges, such as energy, global warming, environmental protection, communicable diseases, *etc*.[11] We have made communication easier and more efficient, we have achieved new efficient ways of trading and much more.

However, this expansion has another side. As result of the *Publish or perish* challenge, authors under pressure to publish as much as possible may end up neglecting the quality of their research or may not have the time to present their research in a quality way.[12,13] Besides a number of issues with poorly communicated or poorly conducted research, a common side-effect is to overwhelm the publishers with poorly written, poorly technically prepared, and not infrequently papers with almost inconsiderable results and conclusions. Sometimes, papers that possess some substantial and valuable knowledge are not published because of being poorly written or not adhering to the standards and instructions set by the journals they are submitted to. This can occur due to various reasons, such as lack of writing skills, unfamiliarity with the specific journal's guidelines, or limited resources for professional editing. Such papers often end up in the waste-basket even before they reach the Editor, or are desktop rejected because the Editors do not even want to consider such articles. At best, they will be published in journals of low influence, bad reputation and visibility, and sometimes even in predatory ones.

WHAT IS THE CURRENT STATE?

As an illustration of the current state of challenges with article volumes arriving to editors, we take the data on the number of papers submitted and taken into consideration in the Journal of the Serbian Chemical Society (JSCS) from 2011 to 2022. Namely, in that period 16,185 manuscripts were submitted to the journal), and only 2785 of them (or 17.21 %) were accepted for consideration, and 1505 (9.30 %) were published. The number of submitted articles here includes those which were repeated submissions of the same manuscript several times. The authors were informed that their article is not prepared in accordance with the Instructions for Authors, or did not meet the minimum requirements, primarily in technical preparation.

A more detailed analysis of data for a period of a little longer than a year (March 2015 to July 2016) on submitted papers in the same journal showed that there is a "significant difference between local (in this case—Serbian) and external submissions".[14] Fig. 1 shows the distribution of papers submitted, received in the procedure and published in the indicated period, according to the countries of origin of the authors.

All the above data show that the number of "articles that were published in the journal is only the tip of the huge iceberg of all submitted manuscripts".[14] Likewise, the data clearly show that the journal submissions are constantly filled with manuscripts that are not prepared according to the Instructions for Authors

and/or do not contain all the required information. This also means that the technical editors have to spend a lot of time on checking such manuscripts, and pointing out the omissions that need to be corrected. Moreover, it is sometimes necessary to perform this procedure several times for the same manuscript, because many authors resubmit the text without making the necessary corrections.[14]

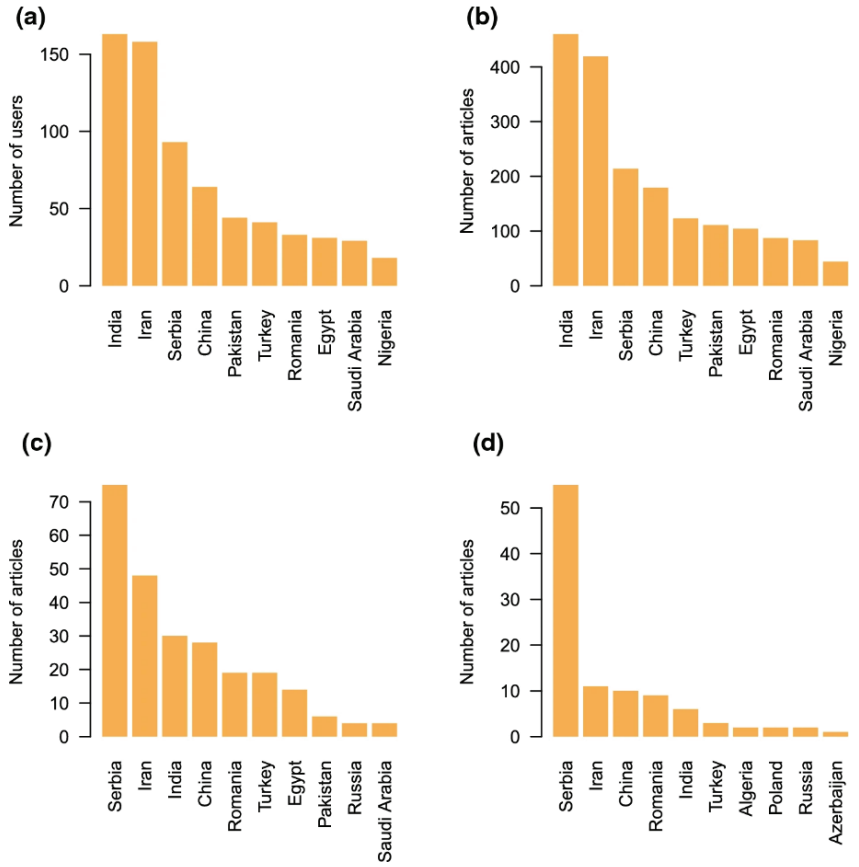

Fig. 1. Distribution of country of origin for: a) all corresponding authors of submitted papers (users), b) all submitted manuscripts, c) All manuscripts accepted for consideration (subject to peer review) and d) published manuscripts.[14] Permissions under Attribution 4.0 International (CC BY 4.0).

One of the authors of this article himself has been a part of the JSCS Editorial team for years. As he had insight into each of the 16,185 manuscripts submitted in the previous 12 years, taking into account the data presented,[14] he believes that it can be assumed that a large number of authors either does not read the Instructions for Authors before starting to prepare the manuscript, or ignores its requirements.

Why is it so? There are probably many reasons, but it has been shown, for example, that young researchers and authors from Serbia[15] feel a lack of education in acquiring academic skills, among which is the presentation of scientific results, including writing a scientific paper. After a seminar on peer review,[16] which can be seen as putting scientific writing skills to use on someone else's work, the participants were asked to fill out a survey. One of the questions was whether a course on writing and peer review of scientific papers should be introduced in doctoral studies. The vast majority of those who filled out the questionnaire, 94 % of them, stated that it was desirable, of which almost 40 % said it was necessary, Fig. 2.[15]

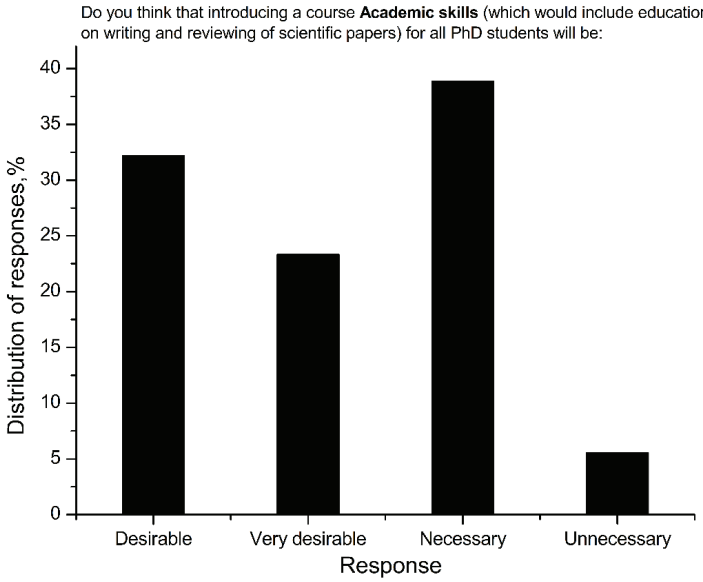

Fig. 2. The peer review seminar's participants opinion on the introduction of a course on writing and reviewing scientific papers in doctoral studies.[15,16] Permissions under Attribution 4.0 International (CC BY 4.0).

By reviewing the curricula of master's and doctoral studies at faculties covering the field of chemistry and similar sciences at universities in Serbia, it was established that there are often no courses on acquiring academic skills. When such or similar courses exist, too little space is devoted to writing scientific papers, with contents often remaining on generic theory without acquiring the skill-set (Table S-III of the Supplementary material to this paper). Based on the results of the JSCS case study,[14] it can be assumed that such courses in "external" countries (in the case of this study these were primarily India, Iran, Pakistan, China, Turkey,...) are rare or of low quality. Based on the author's extensive experience in the Editorial Boards of several international journals, it is sug-

gested that there exists a negative correlation between the number of papers rejected or returned for corrections and resubmission for technical reasons, and the level of academic skills acquired through undergraduate and postgraduate education. However, it is important to note that this conclusion is drawn primarily from personal experience and lacks quantifiable data to support it. The number of manuscripts in academic research is increasing, particularly from authors who come from education programs that do not prioritize the development of "soft academic skills" such as writing, peer-reviewing and scientific communication. This lack of emphasis on these skills can have a significant impact on the quality and effectiveness of the manuscripts produced. Of course, this claim is not based on exact data, but primarily based on the personal experience of the author of the paper. Finally, many other possible factors, such as cognitive abilities, motivation or self-efficacy, not analysed here, may influence the acquisition of academic skills.

On the other hand, although there are many publications, papers, books, guides and even video tutorials on how to write and publish a scientific paper, *i.e.*, present scientific results (only a few are listed here),[17–27] they modestly refer to the technical preparation of the manuscript, which, as concluded here, is a fairly common reason for the manuscript not even being considered for publication.

In any case, it can be stated that the number of submissions that are returned or rejected for technical reasons is too large. Hence, it is necessary to show the authors that the preparation and form of the manuscript are as important as its content. Editorial offices do not want to waste time and resources, neither theirs nor those of the reviewers who need to evaluate such works. How to do this?

HOW TO IMPROVE THE PRESENT STATE?

As is previously alluded, academic skill education is the supposed best way to inform and train the authors. The necessity of such education in some academic communities is clearly established,[15] and it certainly exists in environments where that segment of education is neglected or does not exist at all.

The "obligation" of senior researchers to pass on their experiences and knowledge to their young collaborators should not be neglected either. Young researchers should have the help of their mentors and supervisors while writing their first paper. They must be guided on the standards and principles of good paper writing practice and on the importance of clear presentation of results, including making illustrations and creating tables. On the other hand, there must be no hesitation in asking more experienced colleagues for help or suggestions whenever younger ones encounter doubts or unknowns.

In an effort to contribute to the dissemination of good writing practice, the rest of this article gives some of the general principles that should be followed

when writing a scientific paper including a dozen examples on how they are often neglected. The examples are limited to the fields of chemistry and related fields, but those principles are generally valid for all fields of science, with the specificities that these sciences have.

12 GOLDEN RULES OF A WELL-WRITTEN PAPER

Firstly, as the sub-heading notes, this section focuses on rules of a well--written paper, not a good paper. In order for a scientific paper to be said to be good we would have to evaluate the scientific content and conclusions, their scope, relevance and scientific methods. Still, a good publication also requires good writing to be able to communicate its findings. The following "12 golden rules" contain what should be kept in mind before and while writing a scientific publication.

1. Read the Instructions for Authors carefully and in detail

Each publisher and/or journal has its own standards for the final appearance of the publication. In order to apply these standards, Instructions for authors are created, which contain detailed requirements that authors must adhere to when writing manuscripts. Those instructions are sometimes very extensive and detailed from the author's point of view, but the authors are expected to comply with them. The detailedness of the Instructions is most often the result of explicitly pointing out some of the general "rules" of writing a paper to the authors and these make up the rest of these 12 golden rules.

2. The title and keywords must be composed wisely

The title of the publication should describe the content of the research that will be presented as succinctly as possible. Terms such as investigation, analysis, presentation or similar, are often redundant. Titles which are too broad or too long, in which the reader has to work hard to discern what the content of the article is, have weaker chances of being read. On the other hand, it is often recommended that the title contains exact names, for example the material that is the subject of the research, geographical names, or the location to which the research refers, *etc.*

Keywords and words from the title are, as a rule, the most important and sometimes the only terms on the basis of which databases (such as SCOPUS or Web of Science) are searched, so repeating terms from the title as keywords does not help and should be avoided.

3. An abstract is a publication in itself

The abstract is what the reader will read first to decide whether to read the complete work as well. In order to ensure the effectiveness and clarity of a research paper or report, it is crucial that the abstract section is concise and provides a clear understanding of the purpose, methodology and findings of the research.

This section should not be overly extensive, as it may overwhelm the reader and dilute the main points being conveyed. Instead, it should focus on presenting a comprehensive overview of what, why and how something was researched, as well as the knowledge gained from the research. That is why it must not contain extensive details about procedures, experiments, used methods or techniques, *etc*. The abstract is often most useful if there is one line on the general background and one line on the exact research question of the paper at the beginning. The rest can be a combination of summarizing findings and conclusions while emphasizing the most impactful ones.

4. The Introduction explains the motives and objectives of the research

Based on the presentation of current knowledge, through an adequate review of the literature, the introduction should clearly show the reasons and aims of the research presented in the paper. The literature review must not be too extensive, but also not incomplete from the point of view of the research objective. Usually up to 20 literature citations are sufficient, which will clearly show the previous knowledge, including several review papers in which this knowledge is systematically presented. The aim of the research should be explicitly commented on: whether it was achieved, what new findings were obtained, whether and to what extent they are in line with the previous ones. As a general guideline, it is useful to refer to the Creating A Research Space (CARS) model on writing introductions.[28,29] The model underlines this balance between presenting the current state in the field and building a space for your research question within it.

5. Experiments performed should be described to be reproducible

Experiments, measurements and analyses must be described in the Experimental part of the paper in such a way that anyone should be able to reproduce the results. The procedure, materials and equipment used must be described in detail. Experimental protocols should be listed chronologically, leaving no room for confusion when repeating them. This section of the paper should not contain any experimental data. If the protocols are well-established, it is acceptable to cite previous publications which describe them in detail.

6. Do not clutter the paper with unnecessary results

Almost every research produces a large number of results, but there is no need to present them all in the paper. Authors often clutter their manuscripts with lots of tables and figures, long descriptions or unnecessary data. It should be limited only to those results that will directly support the discussion and conclusions, without repeating similar ones or presenting irrelevant or less important ones unless they directly confirm reliability of the findings. For example, there is no need to show all the spectra recorded during the research, or to list the details of the spectral data, but only representative and key ones. If, however, it is

deemed important (especially for readers engaged in close research), such data should be presented in the Additional Material or deposited in some repository, and the main body of the paper should only refer to them.

7. Tables, figures and equations must be clear without reading the text of the manuscript

When looking at a table or figure, reading the figure legend and the accompanying footnote (if any), their content must be completely clear and understandable, without reading the text. For example, the comparisons shown, and the abbreviations used should be stated clearly. Of course, how the presented data were obtained, how it is interpreted and what conclusions the data led to, should be commented in the manuscript.

Besides these general rules, there are a few more technical ones. One, there is no need to show the data presented in the form of a table again as a figure and *vice versa*. Two, the axes on the diagrams should have a range that is not greater than the range of the plotted data. It is unnecessary to write the data values directly on the figure; instead, they can be read from the axes. Three, the resolution of the illustrations, the chosen font, and its size, as well as the thickness of the lines on them, must be such that what is shown can be clearly seen and read.

The colours of illustrations (diagrams and graphics) should be chosen carefully, as a rule no more than three colours (if the number of displayed data is large, patterns and/or shades of the same colours should be used). Animations and photo processing are not permitted, except to increase clarity and/or contrast.

Finally, tables, illustrations and equations should be numbered according to the order of appearance in the text, and they should be referred to in the text (before their appearance) by stating their number, without using designators such as above, below, next, following, *etc*.

8. Values of physical quantities should be stated clearly, along with units

Either in text, picture or in table, numerical values of physical quantities must always be listed with the name of the quantity (or the appropriate symbol) and the unit in which they are expressed. When naming quantities and/or using their symbols, IUPAC recommendations and nomenclature[30,31] should be followed, and SI units[32,33] should be used (except when this is not possible for justified reasons). In general, unless otherwise required in the Instructions for Authors of a particular journal, the designation of physical quantities (symbols) must be in italic, whereas the units and indexes (except for indexes having the meaning of physical quantities) are in upright letters. In graphs and tables, a slash should be used to separate the designation of a physical quantity from the unit, for example: p / kPa, T_0 / K, t / h, ln (j / mA cm^{-2}). If the full name of a physical quantity is unavoidable, it should be given in upright letters and separated from

the unit by a comma, for example: Pressure, kPa; Temperature, K; Current density, mA cm^{-2}.

9. The results and discussion should be concise and easy to read

Whether they are presented in separate chapters in the paper, or together, the presentation of the results and their discussion should not recount the data already presented in the tables and illustrations. Through short and clear paragraphs, no longer than 5–6 sentences, the conclusions to which the results have led, which new findings have been obtained, and how they relate to current knowledge and literature data should be highlighted. The reader should not be overwhelmed with unnecessary details, long comments, and information without essential importance to understand the interpretation of the obtained data. For each presented data that leads to a unique conclusion, their logical connection, cause-and-effect relationship, or mutual dependence should be explained.

10.Any retrieved Information must be cited

Every literary data, including those obtained in personal communication, must be listed in the references. On the other hand, the list of references must not contain any citation that is not referred to in the manuscript. If sentences or parts of the text are taken in their entirety, they must be placed in quotation marks, along with references to the source. For tables or illustrations taken from the literature, it must be checked whether they are protected by copyright, and if they are, permission to use them must be sought.

When creating a list of references, it is mandatory to follow the format required by the journal to which the manuscript is submitted.

11.The point is in the Conclusions

As already mentioned, the Abstract and Conclusions must make it completely clear to the reader what the article contains. This should be considered when compiling the content of the Conclusions. There is no need to summarize what has been said in the rest of the paper. The conclusion should briefly re-state the main objective of the project and give clear answers to the questions indicated in the Introduction; why and how the research was conducted and what new knowledge resulted from the research. After reading the paper, the reader must not ask the question: Okay, so what? Therefore, the findings must be related back to the larger context of the research and the field.

Speculations and conjectures are inadmissible, assumptions must be clearly supported by facts, and claims must be based only on presented results.

12.The Acknowledgement must not be forgotten

Although this does not affect whether the article is well written or whether its content is of high quality, it is necessary to acknowledge all those who

contributed to the research being carried out and the paper being written. These are primarily funds, organizations and/or institutions that financed the research, but also colleagues or collaborators, apart from co-authors, who helped with advice, discussions, or consultations, perhaps provided some instruments, or even made some measurements during the research.

In addition, at the end of the manuscript, it is desirable to attach statements on conflict of interest, informed consent and on human and animal ethical treatment, if applicable.

EXAMPLES OF BAD PRACTICE

Based on the long-term experience of the author of the article, several specific examples of bad practice and the most common mistakes made by authors during chemistry manuscript preparation are listed in the Supplementary material.

CONCLUSION

The current state of scientific publication is witnessing a rise in the quantity of submitted articles for review which can overwhelm the editorial process. Based on a few exact data, it can be concluded that there is a need for systematic education of young researchers and scientists in acquiring academic skills (primarily during postgraduate studies), with special attention to writing and reviewing scientific publications. A higher level of academic skills enables clear communication of the scientific findings and increase the chances of publication which is the most valued out of research in the current evaluations systems in many institutions. In an effort to contribute to a higher level of general knowledge on the principles of academic writing, the second part of the article shows the basic principles that should be followed for a scientific paper to be well written, along with several examples of the most common mistakes and ways to overcome them.

SUPPLEMENTARY MATERIAL

Additional data and information are available electronically at the pages of journal website: https://www.shd-pub.org.rs/index.php/JSCS/article/view/12376, or from the corresponding author on request.

PUBLISHING REMARKS

This article was published as a preprint on May 19, 2023, on https://www.preprints.org/; paper ID: 74034; https://doi.org/10.20944/preprints202305.1443.v1

ИЗВОД

ПРВО ПРОЧИТАЈТЕ ОВО!
КАКО ПРИПРЕМИТИ РУКОПИС ЗА ПОДНОШЕЊЕ У ХЕМИЈСКИ НАУЧНИ ЧАСОПИС

АЊА ДЕКАНСКИ[1] и АЛЕКСАНДАР ДЕКАНСКИ[2]

[1]*Karolinska Institute, Department of Physiology and Pharmacology, Solnavägen 9, Solna, Sweden и* [2]*Универзитет у Београду, Институт за хемију, технологију и металургију, Центар за електрохемију, Његошева 12, Београд*

Поред теоријских знања стечених током основних, а посебно последипломских студија будући млади научници морају да стекну и пратеће академске вештине. Ове вештине ће им омогућити да планирају и спроводе истраживања у складу са научним методом, али и да резултате тог истраживања представе у одговарајућим облицима. Ниједан резултат и никаква нова сазнања која произилазе из истраживања нису драгоцена сама по себи, све док се не презентују научној заједници и друштву у целини. То се најчешће врши објављивањем рецензираних чланака у научним часописима. Зато стицање вештине писања научних публикација мора бити саставни део образовања, односно део стечених академских вештина. Међутим, тренутно то није случај у свим научним срединама и значајан број (посебно младих) научника и истраживача не поседује сва потребна знања и вештине за писање академских чланака, посебно када су у питању стандарди форме рукописа и техничке припреме. Овај недостатак у вештинама често доводи до тога да значајан број предатих радова буде одбијен или послат на поновно подношење чак и пре него што стигну до уредничког стола. У настојању да младим академцима у овој области пружи помоћ при академском писању, овај чланак указује на општа начела добро написаног и припремљеног рада (са тежиштем на област хемије), указује на најчешће грешке и пропусте и предлаже начине за њихово спречавање. Поред тога, у чланку се разматра тренутно стање поседовања академских вештина у, пре свега, мање развијеним научним срединама, као и узроци таквог стања. Резултати анкетирања показују да у Србији, и поред тога што на докторским студијама многих факултета из области хемији постоје курсеви (често као изборни предмети) на којим би се наведене академске вештине могле стећи, значајан број младих научника сматра да их не поседује на жељеном и потребном нивоу.

(Примљено 5. маја, ревидирано 23. јуна, прихваћено 31. августа 2023)

REFERENCES

1. *How Many Academic Journals are There in the World?*, https://publishingstate.com/how-many-academic-journals-are-there-in-the-world/2021/ (accessed: October 31, 2022)
2. *SJR : Scientific Journal Rankings*, https://www.scimagojr.com/journalrank.php (accessed: October 31, 2022)
3. *SJR – International Science Ranking*, https://www.scimagojr.com/countryrank.php (accessed: October 31, 2022)
4. *Reducing the time from basic research to innovation in the chemical sciences,* A Workshop Report to the Chemical Sciences Roundtable, The National Academies Press, Washington DC, 2003 (https://doi.org/10.17226/10676)
5. L. Brown, R. Griffiths, M. Rascoff, K. Guthrie, *J. Electron. Publ.* **10** (2007) (https://doi.org/10.3998/3336451.0010.301)
6. M. Nentwich, *Poiesis und Prax.* **3** (2005) 181 (https://doi.org/10.1007/S10202-004-0071-8)
7. M. Kozlov, *Nature* **613** (2023) 225 (https://doi.org/10.1038/D41586-022-04577-5)

8. C. D. Kelly, M. D. Jennions, *Trends Ecol. Evol.* **21** (2006) 167 (https://doi.org/10.1016/J.TREE.2006.01.005)
9. M. R. Shen, E. Tzioumis, E. Andersen, K. Wouk, R. McCall, W. Li, S. Girdler, E. Malloy, *Acad. Med.* **97** (2022) 444 (https://doi.org/10.1097/ACM.0000000000004563)
10. H. J. Coolidge, *Archibald Cary Coolidge, life and letters*, Houghton Mifflin Company, Boston, MA, 1932 (http://catalog.hathitrust.org/api/volumes/oclc/2530584.html)
11. J. H. Grossman, P. P. Reid, R. P. Morgan, *J. Technol. Transf.* **26** (2001) 143 (https://doi.org/10.1023/A:1007848631448)
12. H. Aguinis, C. Cummings, R. S. Ramani, T. G. Cummings, *Acad. Manage. Perspect.* **34** (2020) 135 (https://doi.org/10.5465/AMP.2017.0193)
13. P. Rzymski, M. Nowicki, G. E. Mullin, A. Abraham, E. Rodríguez-Román, M. B. Petzold, A. Bendau, K. K. Sahu, A. Ather, A. F. Naviaux, P. Janne, M. Gourdin, J. R. Delanghe, H. D. Ochs, J. E. Talmadge, M. Garg, M. R. Hamblin, & N. Rezaei, *Int. Immunopharmacol.* **86** (2020) 106711 (https://doi.org/10.1016/J.INTIMP.2020.106711)
14. M. J. Mrowinski, A. Fronczak, P. Fronczak, O. Nedic, A. Dekanski, *Scientometrics* **125** (2020) 115 (https://doi.org/10.1007/S11192-020-03619-X)
15. I. Drvenica, A. Dekanski, N. Bućevac, I. Umeljić, O. Nedić, *Hem. Ind.* **73** (2019) 275 (https://doi.org/10.2298/HEMIND191020029D)
16. *Održan seminar o recenziranju u Narodnoj biblioteci – CPN*, https://www.cpn.edu.rs/odrzan-seminar-o-recenziranju-u-narodnoj-biblioteka/?script=lat (accessed: January 17, 2023) (in Serbian)
17. *How to Write a Research Paper: A Step-By-Step Guide*, Grammarly Blog, https://www.grammarly.com/blog/how-to-write-a-research-paper/?gclid=CjwKCAiAzp6eBhByEiwA_gGq5N-uF3vL5wEqTKopDXLpK3_0t6Xvonj2U9MnfTfsz8THZdVWCdnP_hoCgxEQAvD_BwE&gclsrc=aw.ds (accessed: January 22, 2023)
18. J. H. Shubrook, J. Kase, M. Norris, *Int. J. Sports Phys. Ther.* **7** (2012) 512 (https://doi.org/10.1016/j.osfp.2010.06.004)
19. *How to write a scientific paper* – YouTube, https://www.youtube.com/watch?v=Vky9PDKx5KU&ab_channel=GlobalHealthwithGregMartin (accessed: January 18, 2023)
20. Z. Popović, *Kako napisati i objaviti naučno delo*, Akademska misao i Institut za fiziku Beogradskog univerziteta, Beograd, 2014 (in Serbian)
21. A. Dekanski, *J. Serbian Chem. Soc.* **79** (2014) 1561 (https://doi.org/10.2298/JSC140610066D)
22. F. Ecarnot, M. F. Seronde, R. Chopard, F. Schiele, N. Meneveau, *Eur. Geriatr. Med.* **6** (2015) 573 (https://doi.org/10.1016/J.EURGER.2015.08.005)
23. S. M. Richardson, F. Bella, V. Mougel, J. V. Milić, *J. Mater. Chem., A* **9** (2021) 18674 (https://doi.org/10.1039/D1TA90183D)
24. F. A. Maiorana, H. F. Mayer, *Eur. J. Plast. Surg.* **41** (2018) 489 (https://doi.org/10.1007/S00238-018-1418-Z)
25. P. Kukołowicz, *Polish J. Med. Phys. Eng.* **23** (2017) 1 (https://doi.org/10.1515/PJMPE-2017-0001)
26. J. Faber, *Dental Press J. Orthod.* **22** (2017) 113 (https://doi.org/10.1590/2177-6709.22.5.113-117.SAR)
27. *How To Write A Chemistry Research Paper? All Details*, https://www.rasayanika.com/2021/05/06/how-to-write-a-chemistry-research-paper-all-details/ (accessed: January 18, 2023)

28. S. Abdullah, *EFL J.* **1** (2016) 1 (https://doi.org/10.21462/EFLJ.V1I1.1)
29. J. Swales, *"Create a Research Space" (CARS) Model of Research Introductions*. in *Writing about writing : a college reader*, E. Wardle, D. P. Downs, Eds., Bedford/St. Martin's, Boston, MA, 2014, pp. 12–15 (https://vdoc.pub/documents/writing-about-writing-a-college-reader-1mb5686j3i9o)
30. *IUPAC Recommendations Archives – International Union of Pure and Applied Chemistry*, https://iupac.org/tag/iupac-recommendations/ (accessed: February 14, 2023)
31. A. D. Mc Naught, A. Wilkinson, *IUPAC* (2012) 1670 (https://doi.org/10.1351/goldbook)
32. *SI Brochure – BIPM*, https://www.bipm.org/en/publications/si-brochure (accessed: February 18, 2023)
33. *Essentials of the SI: Base & derived units*, https://physics.nist.gov/cuu/Units/units.html (accessed: February 22, 2023).

Journal of the Serbian Chemical Society
JSCS@tmf.bg.ac.rs • www.shd.org.rs/JSCS
J. Serb. Chem. Soc. *88* (11) S338–S345 (2023) *Supplementary material*

SUPPLEMENTARY MATERIAL TO

Read this first! How to prepare a manuscript for submission to a chemical science journal

ANJA DEKANSKI[1] and ALEKSANDAR DEKANSKI[2]*#

[1]*Karolinska Institute, Department of Physiology and Pharmacology, Solnavägen 9, Solna, Sweden and* [2]*University of Belgrade, Institute of Chemistry, Technology and Metallurgy, Department of Electrochemistry, Njegoševa 12, Belgrade, Serbia*

J. Serb. Chem. Soc. *88* (11) (2023) 1175–1188

EXAMPLES OF THE MOST COMMON OMISSIONS AND ERRORS IN THE TECHNICAL PREPARATION OF MANUSCRIPTS

All Figures and Tables in this Supplemental Material are based on real ones found in submitted manuscripts to several different journals, but the data in them has been changed and some of them modified to highlight the mistakes made. Since they do not represent real results, the sources are not cited.

TITLE AND KEYWORDS

An example of a title which is too long and extensive, where almost all words are repeated as keywords, is shown in Figure 1. A much clearer and shorter title can be: **Trace and selective determination of chobalt(II)**, with the keywords: *Cathodic adsorptive stripping voltammetry; water and salt samples; presence of pyrogallol red*.

* Corresponding author. E-mail: dekanski@ihtm.bg.ac.rs

Trace and selective determination of cobalt(II) in water and salt samples using cathodic adsorptive stripping voltammetry in the presence of Pyrogallol Red

Keywords: adsorptive cathodic stripping voltammetry; Pyrogallol Red; Co(II) determination.

Figure S-1. Poorly created title and wrong choice of keywords

ILLUSTRATIONS

Figure S-2 shows a completely unclear and useless illustration. As the names and units shown on the axes are missing, the reader cannot know what is shown in the figure. Even reading of figure caption can't help with that. Two sets of data are shown, (a) and (b), but without a legend it is not clear which data refer to which set.

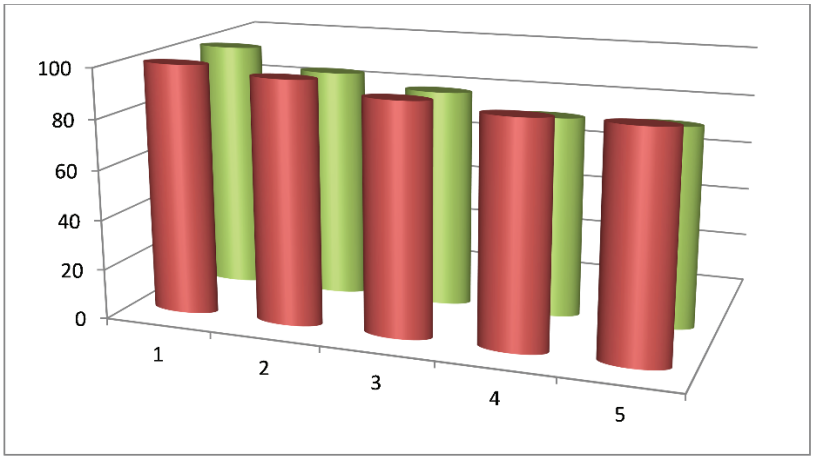

Figure 3. Durability and reusability of (a) KN and (b) SKN coatings

Figure S-2. Unclear and useless illustration

An example of poorly selected ranges of presented data and unclear axis names is illustrated in Figure S-3a. It should look like in Figure 3b. A very common mistake is the one made in naming the y-axis on this graph: logarithmic quantities must always be displayed together with its units, because, for example, it is not the same whether the current density whose logarithmic values are presented, are expressed in A dm^{-2} or in mA cm^{-2}. It is similar with the name of the x-axis, without unit of time the presented results do not make sense.

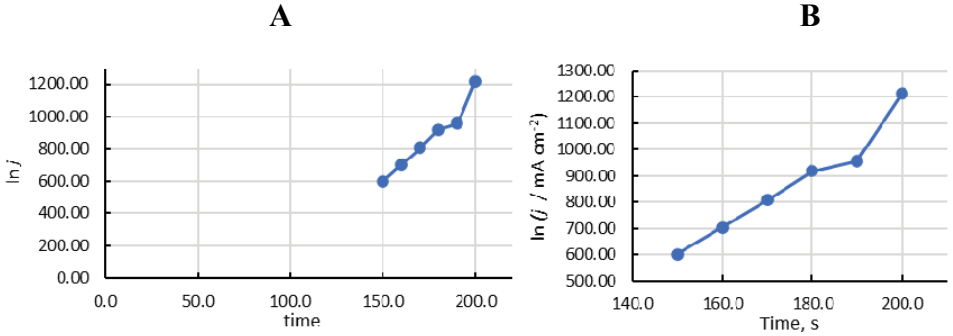

Figure S-3. A – wrong and B – right presentation of the same results

Probably the most common mistakes in articles from chemistry and related fields is the presentation of thermogravimetric analysis (TGA) data. Figure 4 shows three graphs that illustrate those errors[1,2]. Although these Figures are probably clear to anyone who is even the least familiar with TGA, science implies precise and clear communication, so the *y*-axes on the graphs are not correct. In Figure 4A, the name of the *y*-axis is Weight (%), although percent is not a unit of weight. It is obvious that the relative mass loss of the sample during heating is shown on that axis. It would be most accurate if, instead, the mass of the sample, which decreases during heating, is presented on the axis. If it was decided to be a relative change expressed in percentages, the name of the axis should have been: Mass loss, %, with range from 100 to 0 %, not from 0 to 100 %, as it is wrongly shown in Figure 4B a. An alternative is for the axis range to remain from 0 to 100 %, but the axis name to be: Residual mass loss, % or even very precise: $((m\text{-}m_t / m)100)$ / %, where m is starting mass of sample and m_t mass of sample at temperature t / °C. Analogously, the *y*-axis in Figure 4B b should be, for example: d (Mass loss) dt^{-1} / % $°C^{-1}$ or $(d(m\text{-}m_t / m)100)$ dt^{-1} / % $°C^{-1}$. In addition, *x*-axis in all figures would be more correct to write as t / °C or Temperature, °C.

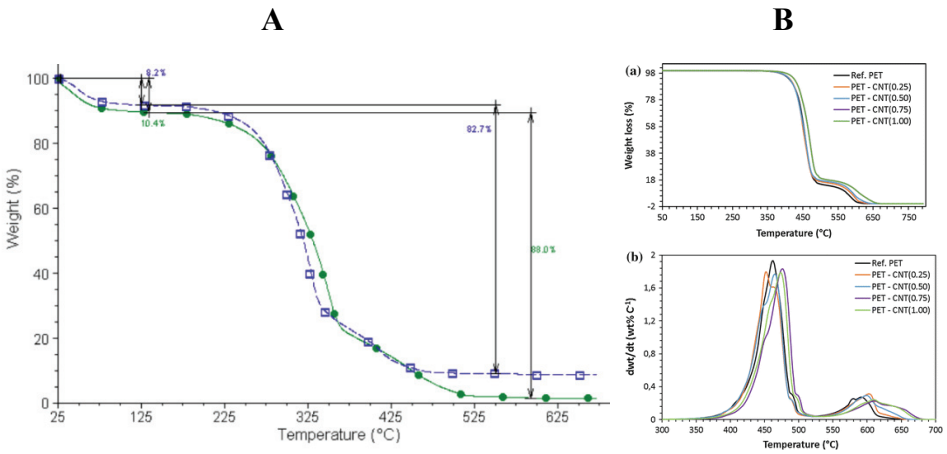

Figure S-4. Examples of poorly named axes on TGA plots

Although electronic publishing made it possible for lower quality and resolution and different formats of illustrations (compared to publishing on paper) to be acceptable, it is necessary that they meet a certain minimum. Figure S-5 shows the same figure in different resolutions. Figure S-5A is .gif format illustration with the resolution of 100 dpi, while Figure S-5B is in .tif format and resolution of 600 dpi. In addition, on the first one, the font size is insufficient for the data from the figure to be easily and clearly read.

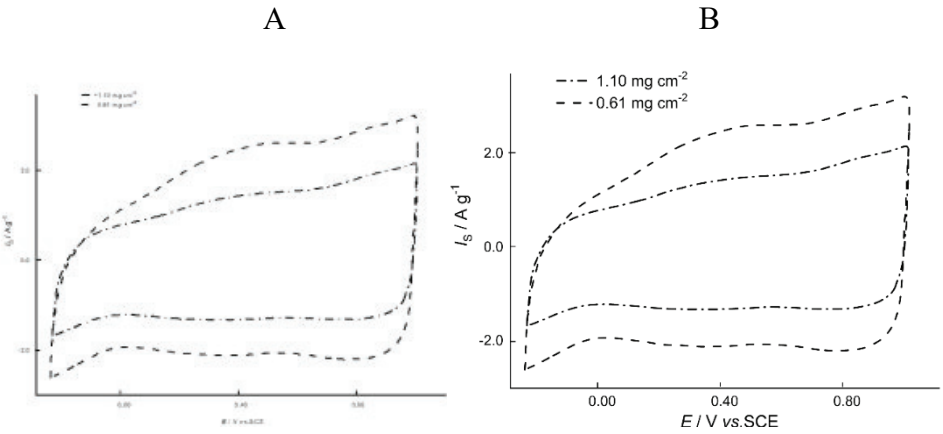

Figure S-5. The same illustration prepared A - poor and B - good

TABLES

Several omissions were illustrated in Table S-I:

1. In all columns, except for the column titled Plasticizer, all values are equal, so the tabular presentation is completely unnecessary. The table can be

replaced with only one sentence in the text, which would list all reactants and their quantities, except for Plasticizer, which should be stated as present in Exp. 18, instead 0.4 l of RA was added in Exp. 19, and 0.4 l of ESO was added in Exp. 20.

2. Although it would probably be clear to the reader that the numerical quantities shown in the table refer to the quantities and volumes of reactants, the names of the columns are misleading. Starch, plasticizer, 15% H_2O_2, catalyst and hydroquinone are not physical quantities and cannot have any numerical value. These are their masses or volumes, so the column headings should be as, for example, in Table S-II.

3. In table caption it is stated that the reaction conditions are also shown, but there is no such data, the table only contains the quantities of reactants. Therefore, the title of the table should be as in Table S-II

Table S-I. Quantities of reactants and reaction conditions used in experiments

Sample	Starch, [kg]	Plasticizer, [l]		15% H_2O_2, [l]	Catalyst, [kg]		Quinone, [kg]
Exp 18	200	-		20	Cu citrate	0.03	0.4
Exp 19	200	RA	0.4	20	Cu citrate	0.03	0.4
Exp 20	200	ESO	0.4	20	Cu citrate	0.03	0.4

Table S-II. Quantities of reactants used in the experiments

Sample	Mass, kg			Volume, l	
	Starch	Catalyst (Cu-citrate)	Quinone	Plasticizer	10 % H_2O_2
Exp 18	200	0.03	0.4	-	20
Exp 19	200	0.03	0.4	0.4 RA	20
Exp 20	200	0.03	0.4	0.4 ESO	20

MANUSCRIPT PREPARATION

A drastic example of ignoring or not reading the Instructions for Authors and not knowing the elementary principles of good writing of a scientific article is illustrated in Figure S-6.

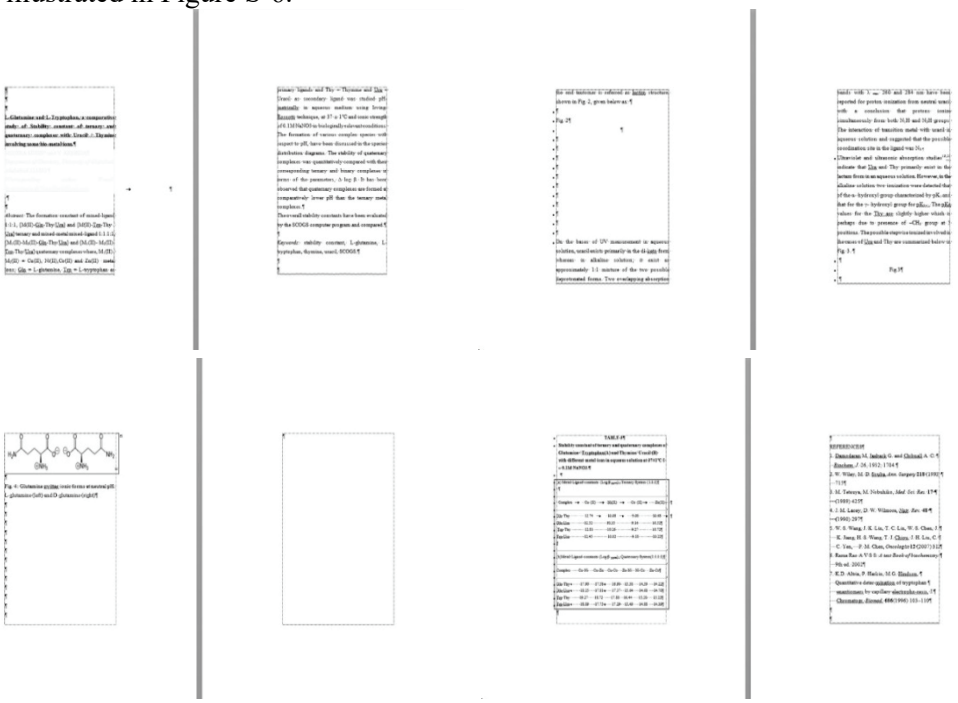

Figure S-6. Screenshots of eight pages of a manuscript submitted for publication in a scientific journal

There are so many errors on the presented 8 pages that it is difficult even to count them. From clearly wrong margins, through unnecessary blank pages and the use of consecutive spaces and new lines to format text and tables, to an incorrectly and inconsistently formatted reference list. For such a new submission, one can expect nothing more than desktop rejection, even without reading the article itself.

ACQUIRING ACADEMIC SKILLS AT FACULTIES IN THE FIELD OF CHEMISTRY AND CHEMISTRY-RELATED FIELDS IN SERBIA

Table S-III provides an overview of the courses for acquiring academic skills at doctoral studies at faculties in the field of chemistry and related sciences in Serbia. The data were taken from the official websites of higher education institutions, and the links to them are listed in the table.

Table S-III. Courses of academic skills in doctoral studies at faculties in the field of chemistry and related sciences in Serbia

Faculty	Course name	URL
Faculty of Chemistry, University of Belgrade	Writing and publishing scientific papers, compulsory	https://www.chem.bg.ac.rs/predmeti/773A2-en.html,
Faculty of Technology and Metallurgy, University of Belgrade	Methodology of scientific research, elective	http://www.tmf.bg.ac.rs/en/fis/karton_predmeta/22DMNIR#gsc.tab=0
Faculty of Pharmacy, University of Belgrade	Methodology and ethics in scientific research, 1st year, compulsory Communication and presentation skills, 2nd year, compulsory	http://www.pharmacy.bg.ac.rs/files/DAS/2021/Table%20of%20subjects.pdf
Faculty of Physical Chemistry University of Belgrade	There is no course, but the study description states that students will be able to: "Communicate the achieved results at scientific conferences, publish them in renowned scientific journals, register them as patents"	https://www.ffh.bg.ac.rs/%D0%BE%D0%BF%D1%88%D1%82%D0%B5-%D0%B8%D0%BD%D1%84%D0%BE%D1%80%D0%BC%D0%B0%D1%86%D0%B8%D1%98%D0%B5-3/
Faculty of Agriculture, University of Belgrade	Methods of scientific research work, compulsory or elective, depending on the module.	https://agrif.bg.ac.rs/sr/studije/doktorske-akademske-studije
Technical Faculty in Bor, University of Belgrade	It does not exist as a compulsory course, the list of elective courses is not available	https://www.tfbor.bg.ac.rs/files/doc/studijski-programi/TI/2019/das_ti_nastavni_plan.pdf
Faculty of Sciences, University of Novi Sad	Scientific research work, compulsory	https://www.pmf.uns.ac.rs/en/studies/study-programs/phd-in-chemistry/
Faculty of Technology, University of Novi Sad	Methodology in scientific research, compulsory	https://www.tf.uns.ac.rs/en/studies/doctoral-academic-studies.html
Faculty of Agriculture, University of Novi Sad	Methods of scientific work, compulsory	http://polj.uns.ac.rs/sites/default/files/upload/DAS%20Agronomija%202021_1.pdf
Faculty of Pharmacy, University Business Academy, Novi Sad	Methodology and ethics in scientific research, compulsory Writing a scientific paper, compulsory	https://faculty-pharmacy.com/program/doktorske-akademske-studije/
Faculty of Sciences, University of Kragujevac	Methodology of scientific research work in chemistry, compulsory	https://www.pmf.kg.ac.rs/pub/f653e65df59d87b1b5bccff88397ad99_12072016_115210/dokproghemija.pdf
Faculty of Sciences, University of Niš	Does not exist	http://wpresspmf.pmf.ni.ac.rs/?page_id=4066&lang=en

Faculty of Technology, Leskovac University of Niš	Methodology of scientific research work, elective Presentation of scientific results, elective	https://www.tf.ni.ac.rs/studiranje/doktorske-akademske-studije/predmeti-das/
Faculty of Sciences, University of Priština	Methodology of scientific research work in chemistry, elective	https://www.pmf.pr.ac.rs/doktorske/hemija
Faculty of Technical Sciences, University of Priština	Methodology of scientific research work, compulsory	https://ftn.pr.ac.rs/wp-content/uploads/2022/05/Nastavni_plan_tehnolosko_inzinjerstvo_DAS.pdf